

SC09

How to Design Fiber Optic Sensors That Work: Basic Technology, Main Problems, Pitfalls, and Potential Solutions

John P. Dakin

Univ. of Southampton

Photonics East

18-22 September, 1999

Hynes Convention Center

Boston, Massachusetts

Wednesday, 22-Sep-1999

8:30 am to 12:30 pm

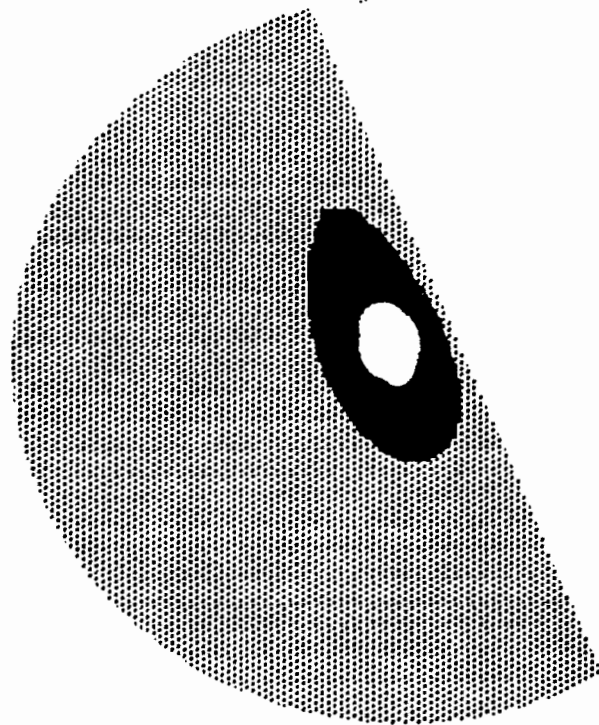
Room: 208



SPIE-The International Society for Optical Engineering

SPIE • P.O. Box 10 • Bellingham, WA 98227-0010

OPTICAL FIBER SENSORS
JOHN DAKIN & BRIAN CULSHAW



ARTEC HOUSE

ISBN 0-89006-317-6

Vol 1

ISBN 0-89006-376-1

Vol 2

NOTE : NEW VOLS III & IV NOW AVAILABLE

Summary of lecture topics

- **Overview of optical fibre sensor types**
(Classified according to operating principles)
- **Difference between intrinsic and extrinsic sensors**
- **Intensity-based sensors**
- **Spectrally-encoded sensors**
- **Propagation-time-encoded sensors**
- **Interferometric sensors**
- **Discussion of how to avoid problems and make practical sensors**
- **Multiplexed and distributed sensors**

Summary of lecture & discussion topics (Case studies)

- **Remote spectroscopy**
(Transmission, scattering & reflectance, fluorescence, Raman, colorimetry etc.)
- **Gas sensors**
- **Liquid-phase sensors**
(Egs. pH, O₂, impurities; mainly in aqueous media)
- **Particle sensing and sizing**
- **Flow sensing**
- **Sensing of pressure**
- **Sensing of strain**
- **Sensing of temperature (including distributed sensing)**
- **Multi-phase analysis (eg, bubble sensing)**

What are the most usual problems with a bad sensor?

- **Sensor responds to the quantity to be measured, but also to many other things**
- **It doesn't have a stable & reproducible response**
- **Strong sensitivity to perturbation of leads**
- **There are changes in signal as light source ages, or if it is changed for a new one.**
- **There is crosstalk from adjacent sensors**
- **Design is not practical for a real engineering environment, or is not a cost-effective design**
- **The sensor is not reliable**

What should a real sensor do?

- **Respond to a quantity to be measured**
- **Have a stable & reproducible response**
(Linearity useful but not essential)
- **Have no response to other parameters**
(Some response is OK, if easily corrected for)
- **Have no sensitivity to perturbation of leads**
- **Have no change in signal if light source ages**
- **Have no crosstalk from adjacent sensors**
- **Have a practical & cost effective design**

Principal mechanisms for optical fibre sensors

- (i) Propagation delay**
- (ii) Transmission loss**
- (iii) Backscatter intensity (OTDR)**
- (iv) Backscatter Polarisation (POTDR)**
- (v) Fluorescence**
- (vi) Raman scattering**
- (vii) Brillouin scattering**
- (viii) Non-linear interaction (eg Raman gain)**

BASIC FIBRE SENSOR TYPES

Fibre as Sensing Element (Intrinsic)

- Propagation Delay
- Transmission (Intensity)
- Transmission (Spectrum)
- Transmission (modal power distribution)
- Back-scatter (OTDR)
- Polarisation
- Light generation in fibre

Fibre-compatible Sensors (Extrinsic)

- Light-Collecting
- Intensity-modulation
- Reflective
- Light-scattering
- Spectral Filtering
- Energy-Transition
- Polarisation

Evanescent Field Sensors

- Unclad Fibre
- Reactive fibre cladding
- Polished half coupler
- Integrated optics
- Plasmon Resonance

INTENSITY-BASED OPTICAL FIBER SENSORS

John P Dakin

Optoelectronics Research Centre, University of Southampton, Highfield, Southampton,
SO17 1BJ, United Kingdom.

ABSTRACT

This tutorial reviews the many ways in which optical fibers may be used to sense physical or chemical parameters, either as intrinsic sensors, where the fiber itself acts as the sensing element, or in extrinsic sensors, where the fiber acts in its normal communication role, to carry light to and from an external optical sensor. Because there are now very many variations of optical fiber sensor, it is necessary when reviewing applications to concentrate on a selection of important principles and methods and describe a few practical sensor types in more detail. This short course will consider only intensity-based sensors, where the total optical power received on a detector is the important factor, rather than parameters such as optical phase or polarisation, which are important in interferometers. Other courses in the series will consider other types of sensor, such as interferometric types and very specific types such as fiber gyros. In order to provide a structured course, there will inevitably be a little overlap in content with the introductory course by E. Udd and the Bragg grating course by A. Kersey. However, viewing some aspects of new technology from different perspectives is often a desirable feature. A far more detailed account of all types of fiber sensors is given in the textbooks mentioned in the bibliography. The course attendee will gain maximum benefit from using these short lecture notes in conjunction with these more extensive volumes.

INTRODUCTION

Optical fibers are widely used in long distance trunk telecommunications systems and their use in shorter distance applications is growing rapidly. For communications systems, it is desirable to utilise a cable having transmission properties which are insensitive to environmental changes. Intrinsic fiber sensors, in contrast, rely on deliberately configuring the optical system to be sensitive to external influences on the fiber or cable. This involves the arrangement of the fiber cable, its associated light source, the optical receiver and the chosen signal processing scheme so as to maximise (and detect) a change in transmission properties which is characteristic of the parameter to be sensed. This may be carried out either by using specialty-sensitive cables or by interrogating them in a manner intended to highlight small changes in transmission. The resulting changes in transmission are then used as a measure of the external environment

An extrinsic fiber sensor usually uses normal fiber (preferably with environmentally-insensitive cable) and merely employs this fiber as a light-guiding medium to transport light to and from more conventional optical sensors. This sensor, in response to an external physical parameter, modifies the light couples from the input fiber into the return fiber. Such a sensor may, however, still be affected by small changes in cable properties, unless particular care is taken with the design. This aspect of cable-induced errors in both forms of sensor is a very important practical consideration. In a good sensor design, care will be taken to avoid significant sensitivity to undesirable losses in

the optical network, such as could occur due to fiber bending or due to connector variations.

The research area of fiber optic sensors is a fruitful one for original thought, as there is both a large number of physical parameters which may be sensed, and also a multitude of ways in which the parameter may modulate the optical transmission. However, in order to make a successful sensor, the normal principles of good instrument design must be adhered to (ie. low crosstalk to undesirable parameters, good signal to noise ratio and repeatable and reliable operation) and the sensor must be cost effective for the intended application. Many of the successful commercial applications of such sensors are in niche market areas, which rely on the inherent advantages of optical sensors over more conventional electrically-based sensors. The advantages include the following :-

- (i) Intrinsic freedom from Electromagnetic Interference (EMI), lightning strike, etc
- (ii) Intrinsic safety in hazardous (explosive vapour) environments (provided optical signal power is low, which is almost invariably the case).
- (iii) High electrical isolation, enabling their use for high voltage and medical applications and for data collection from points at different electrical potential. Freedom from problems of electrical short circuit and open circuit.
- (iv) Excellent resistance to chemical corrosion (eg. saltwater, acid, alkali etc.)
- (v) Passive operation. Therefore no electronics or power required at remote sensing point.
- (vi) May be used in high temperature areas where electronic systems would not survive.
- (vii) Optical fibers are small, light and relatively cheap.
- (viii) May be used for distributed sensors of extreme length, due to the low losses achievable in optical fibers.
- (ix) Fibers have excellent resistance to chemicals and can be used in highly corrosive environments.
- (x) Where optically-based data transmission is already envisaged, optical-fiber-compatible sensors may make additional optical/ electrical interfaces redundant.
- (xi) Optical sensing can provide a very rapid response in many applications, as changes in optical transmission can occur very rapidly and be detected almost instantly.

When the use of optical signal cables becomes more common, it is likely that optical transducers will start to find more general applications, even in areas where the above intrinsic advantages are not a major consideration. The ability to sense, communicate and multiplex signals within an optical network is an important attribute, which will lead to their greater application.

THE OPTICAL FIBER AS A SENSOR (Intrinsic Sensors)

The intrinsic optical fiber sensor takes advantage of measurable changes in transmission characteristics of the fiber itself. The principal parameters of interest are :-

- (i) The propagation time of light in the fiber (proportional to the length and inversely proportional to the velocity of light)
- (ii) The optical power transmitted by the fiber (either the total power or the spectral variations in transmission).
- (iii) The distribution of optical power between the various modes of propagation. (This can be measured from either the near- or far-field waveguide mode patterns at the end of the fiber).
- (iv) The state of polarisation of the transmitted energy through the fiber (or back-scattered energy from the fiber).
- (v) The light scattered from within the fiber core material.
- (vi) Light generation in the fiber due to physical interactions (eg. scintillation or Cerenkov radiation).

The more important of these aspects will be covered in the lecture and in the attached copies of the view-foils, which will be enlarged upon in the lecture. Table 1 summarises the various sensor types, and helps to classify sensors according to their mode of operation.

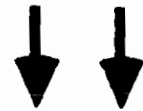
BIBLIOGRAPHY

1. Optical Fiber Sensors, Vol I, II, III & IV, Edited by J.P. Dakin and B. Culshaw. Published by Artech House, Boston, London.
(ISBN 0-89006-317-6, 0-89006-376-1, 0-89006-932-8, 0-89006-940-9)
2. SPIE video tutorial courses on optical fiber sensors: Organised by E Udd.
3. SPIE critical review CR 44 "Distributed fibre optic sensors", J P Dakin.

LIGHT SOURCE



DETECTOR



INTRINSIC SENSOR

LIGHT SOURCE



DETECTOR

SENSOR



EXTRINSIC SENSOR

LIGHT SOURCE



CORE

OPTICAL
FIELD
STRENGTH

INTERACTION
REGION

DETECTOR

EVANESCENT FIELD SENSOR

(UNCLAD FIBRE TYPE)

SCHEMATIC OF SIMPLE INTENSITY-
BASED SENSOR SYSTEMS.

EVANESCENT FIELD SENSORS

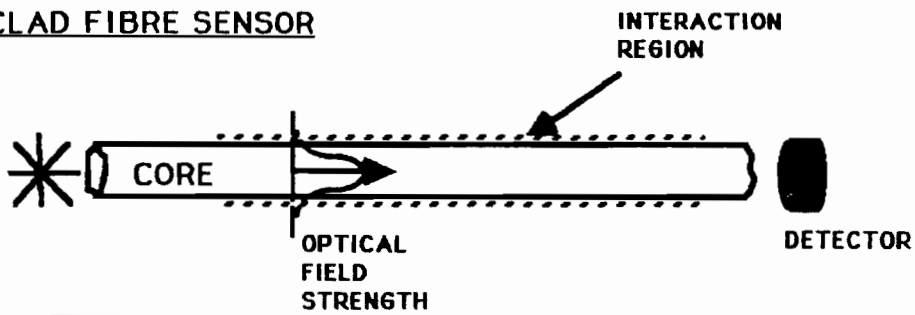
Evanescent field sensors have some of the characteristics of **intrinsic** sensors and **extrinsic** types. As with intrinsic sensors, the light is guided by the fibre (or by an optical waveguide attached to the fibre) in the sensing region, but, in the case of evanescent field sensors, a portion of the optical energy travels outside the physical limits of the waveguide material. In the lateral direction, the field decays away rapidly with distance from the waveguide, so this is termed evanescent field behaviour. Because there is light energy outside the guide material, it is possible for this light to interact with (eg. be absorbed, scattered, excite fluorescence) the surrounding material. Thus, the evanescent field sensor can detect the optical properties of a fluid in which it is immersed simply by measuring the light transmitted through the fibre. Unfortunately, because the evanescent field region is very thin (typically less than 1 micron thick), this type of sensor is very prone to surface contamination. Also, the evanescent field penetration depends strongly on the refractive index of the surrounding material (and hence on temperature) and on whether the guide is bent or not, so is very sensitive to the operational environment.

Instead of immersing the evanescent field sensor directly into a solution to be monitored, it can be coated with an active layer, such as a polymer or a vitreous sol-gel coating. This coating can be made sensitive to desired chemicals by incorporating (immobilising) an indicator chemical into it. Provided the layer is semi-permeable, chemicals can diffuse in from the surroundings and change the optical transmission of the indicator material.

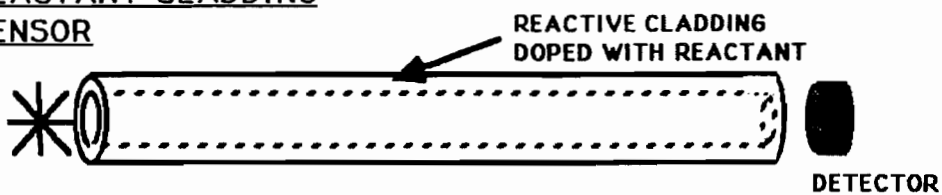
A further variation is to coat the light guide with a thin metal layer, which can enhance the field in the evanescent region by a mechanism called plasmon resonance, which, as the name implies, involves excitation of the "electron-gas" present within all metallic conductors. This plasmon resonance mechanism can give greatly improved sensitivity to any absorption in the evanescent field region, and still allows indicator layers to be coated on as before.

Because of the ease of contamination and the environmental sensitivity of evanescent sensors, they are usually better suited to qualitative testing for chemicals, rather than a means of performing quantitative chemical or spectral analysis of fluids in which they are immersed. Nonetheless, they can be a very sensitive means of detecting trace quantities of chemicals, provided they are designed and used with care.

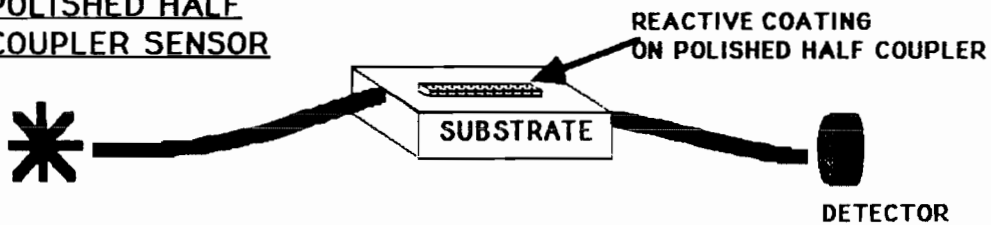
UNCLAD FIBRE SENSOR



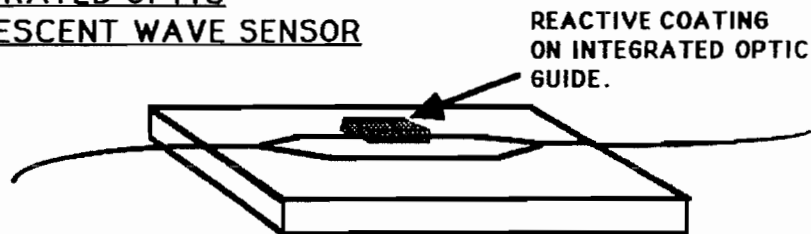
REACTANT CLADDING SENSOR



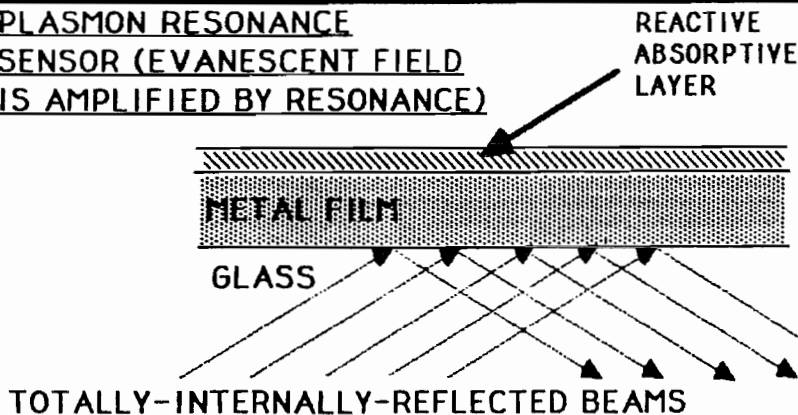
POLISHED HALF COUPLER SENSOR



INTEGRATED OPTIC EVANESCENT WAVE SENSOR



PLASMON RESONANCE SENSOR (EVANESCENT FIELD IS AMPLIFIED BY RESONANCE)



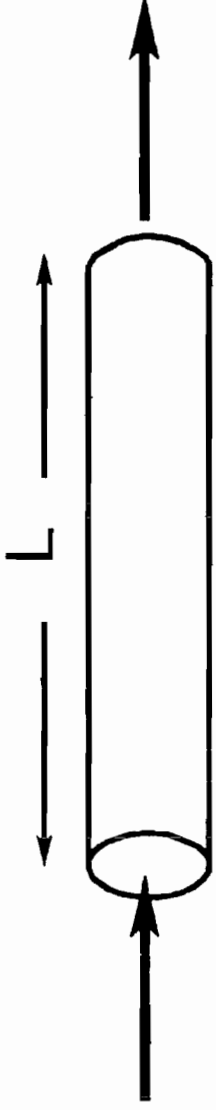
EVANESCENT FIELD SENSORS

PROPAGATION-DELAY SENSORS

These sensors allow the monitoring of physical or chemical effects by examining the time light takes to travel through the sensing element. This element is usually the fibre itself. Its length can change if it is mechanically strained (delay changes arise due to change in physical length or due to refractive index changes arising from the strain) or if it changes temperature. If the fibre is very long, it is possible to examine small changes in the arrival time of a short optical pulse that has travelled through it. However, because of the extremely high velocity of light, it is difficult to perform such a measurement with high precision. An alternative way is to modulate the light source at a very high frequency (typically 500MHz to few Ghz) and observe phase changes in the modulation envelope caused by optical delay changes.

By far the most precise method of monitoring, however, is to launch a continuous light wave through a sensor (eg a length of fibre) and examine the changes in optical phase due to the external influence. As the wavelength of light is of the order of 1 micron (ie 1 micrometre), and phase changes of the order of one millionth of a complete fringe can be observed, then fibre length changes of the order of 1 in 10^{13} of a 10 metre section can be observed. This represents an extremely sensitive method that forms the basis of optical fibre hydrophones (where pressure changes the dimensions of a hydrophone element incorporating the fibre, and hence changes the fibre length) and magnetometers (where a magnetic material attached to a fibre changes its length under the influence of the magnetic field).

Although possible with good design, it is a quite complex procedure to observe static strain with such a sensor, as it is difficult to separate length changes due to strain or due to thermal effects. Fortunately, for acoustic sensing, it is desired to monitor alternating pressure changes, which are converted to alternating strain fields in the fibre sensor. Because of the high frequency nature of these, compared to the slow changes of temperature in a fibre, it is relatively easy to separate out the acoustically-induced changes simply by high-pass electrical filtering of the output of the sensor.



Optical Time Delay = Ln/c

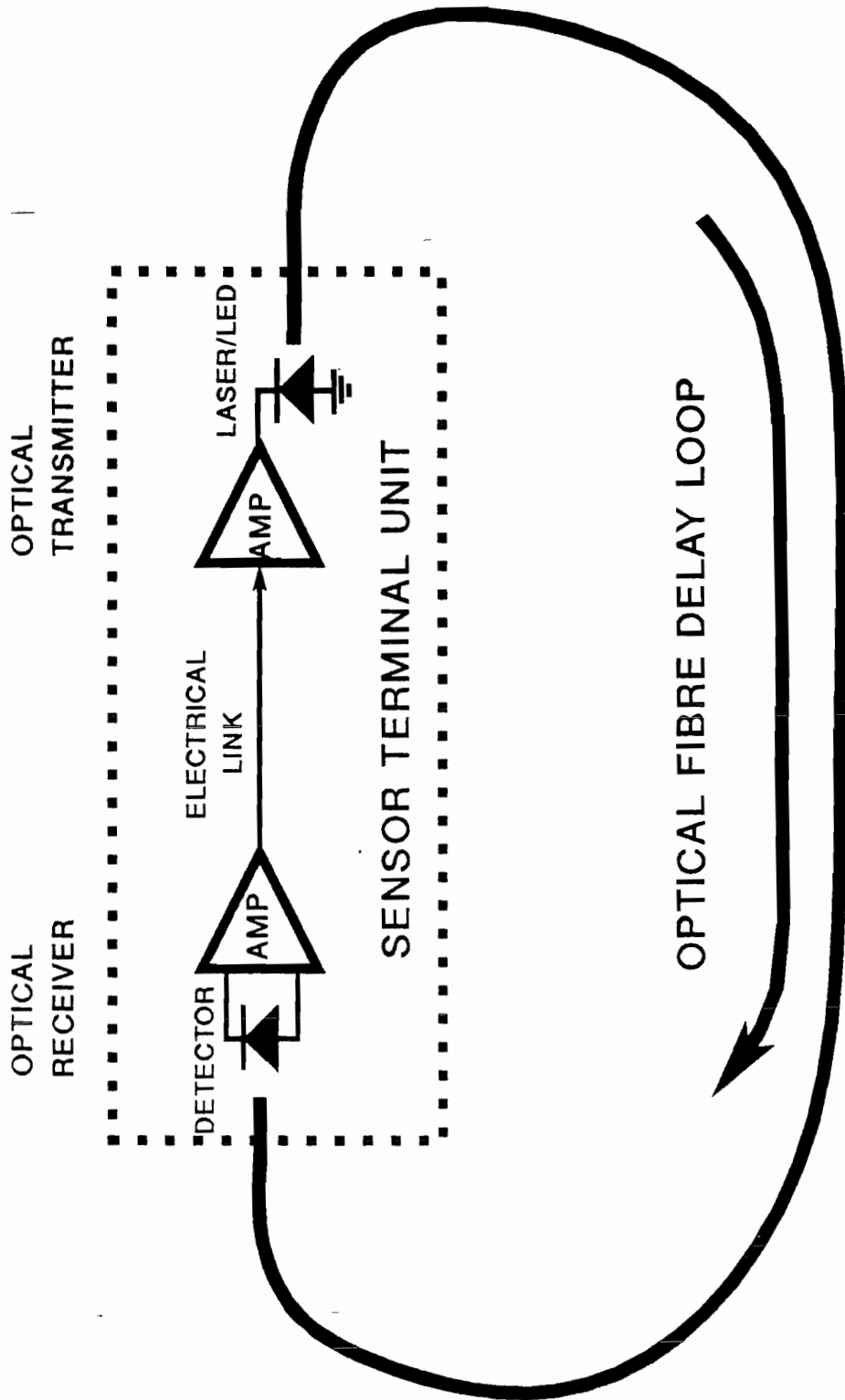
Phase Shift = $\frac{2\pi \cdot L}{\text{Guide Wavelength}}$

Temp. response: $L \cdot n = f(\text{temp})$

Strain response: $L \cdot n = f(\text{strain})$

The optical time delay sensor has a high sensitivity in interferometric mode, but care must be taken to track the fringe order. The sensor can be monitored with amplitude modulated signals, but care is again needed to separate the responses to temperature and strain.

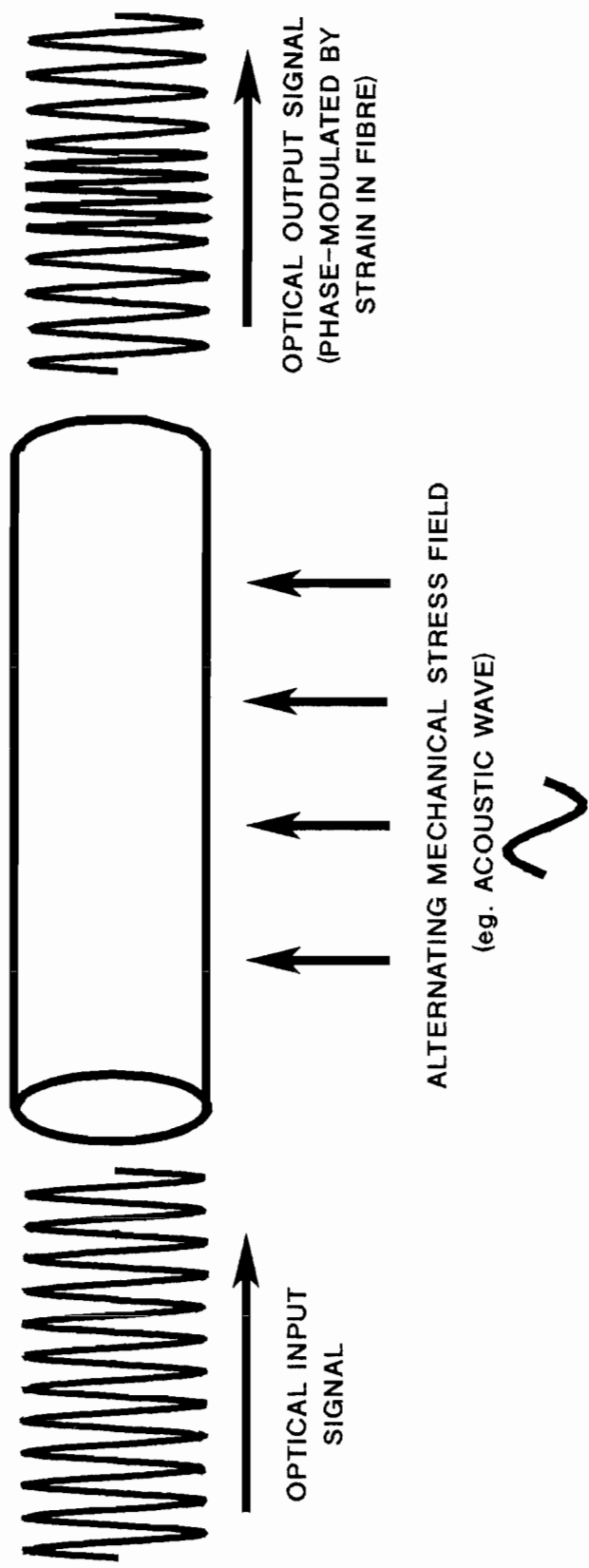
The Propagation-Delay Sensor



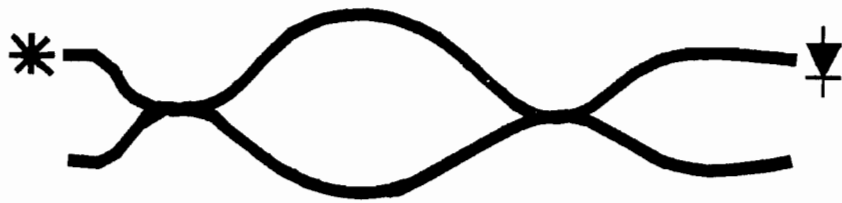
SCHEMATIC OF FIBRE OPTIC LOOP OSCILLATOR

(OSCILLATION FREQUENCY DEPENDS ON SUM OF OPTICAL AND ELECTRICAL DELAYS. THUS, CAN SENSE STRAIN IN FIBRE LOOP)

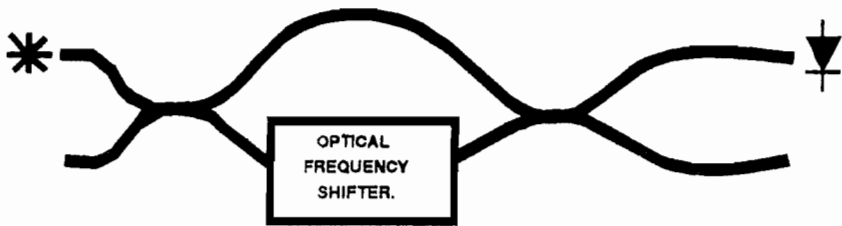
(METHOD AFTER JOHNSON & ULRICH)



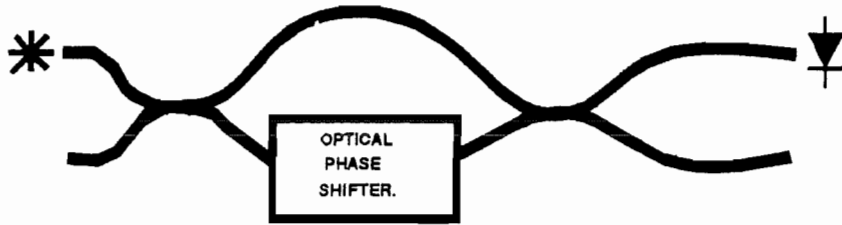
SCHEMATIC ILLUSTRATION OF THE PHASE MODULATION OF LIGHT BY AN ACOUSTIC WAVE ACTING ON A FIBRE.



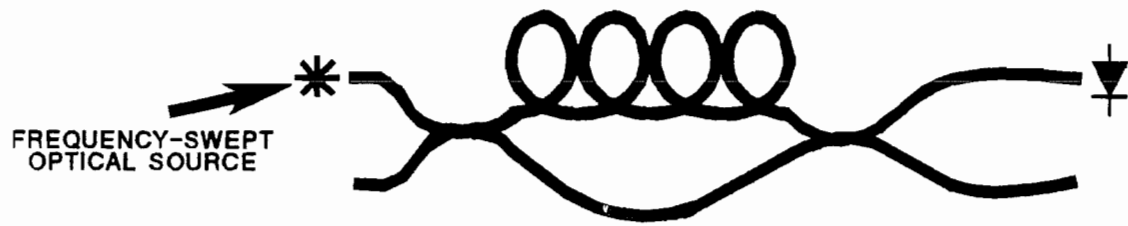
HOMODYNE SENSOR SYSTEM (MACH-ZEHNDER)



HETERODYNE SENSOR SYSTEM.

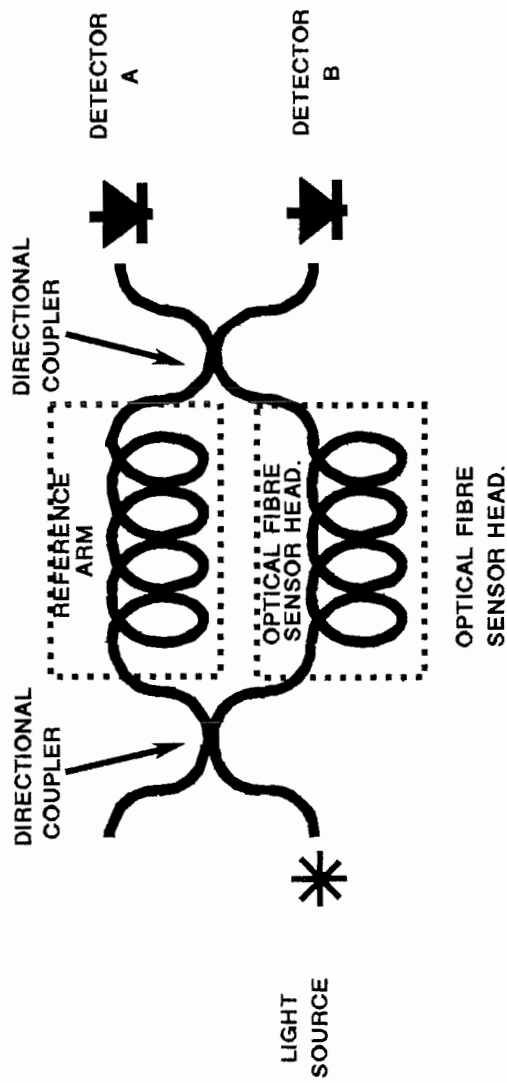


PHASE-GENERATED-CARRIER SENSOR SYSTEM



FREQUENCY-MODULATED CARRIER WAVE (FMCW) SYSTEM

BASIC TYPES OF COHERENT SENSOR PROCESSING SCHEMES



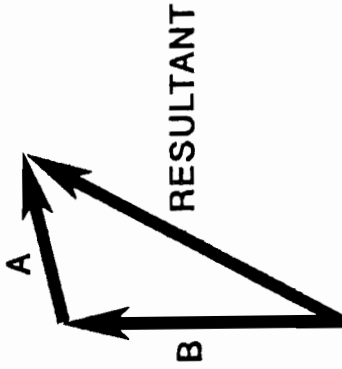
**SCHEMATIC OF MACH-ZEHNDER INTERFEROMETER
FOR SENSING OF ACOUSTIC SIGNALS**

**(BALANCED PATH VERSION, FOR DIFFERENTIAL SENSING)
NOTE THAT THE SENSOR WILL SENSE PRESSURE GRADIENT,
UNLESS ONE COIL IS SHIELDED FROM ACOUSTIC SIGNALS.
BECAUSE OF WELL-BALANCED CONFIGURATION, SOURCE
PHASE NOISE IS NOT A PROBLEM AND SHORT COHERENCE
LENGTH SOURCES ARE PERMITTED.**

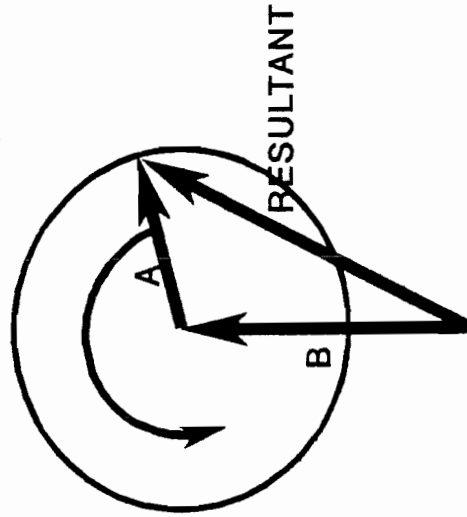
RESULTANT



HOMODYNE
(IN PHASE)



HOMODYNE
(OUT OF PHASE)



HETERODYNE

(PHASE VARYING LINEARLY
WITH TIME, IN THE ABSENCE
OF ADDITIONAL PHASE
MODULATION BY MEASURAND

COMPARISON OF HOMODYNE AND HETERODYNE DETECTION
SCHEMES, BY MEANS OF PHASOR DIAGRAMS.

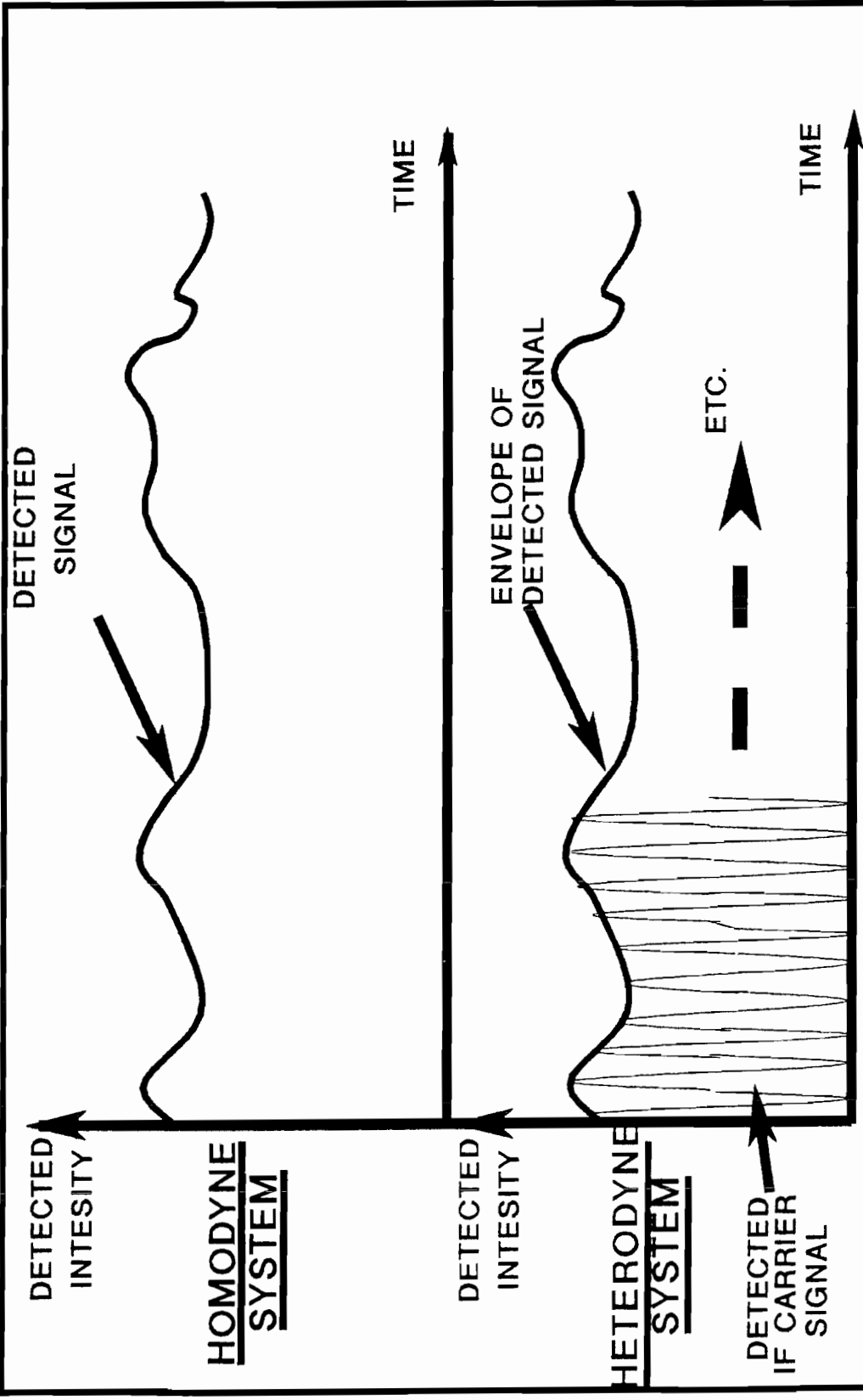
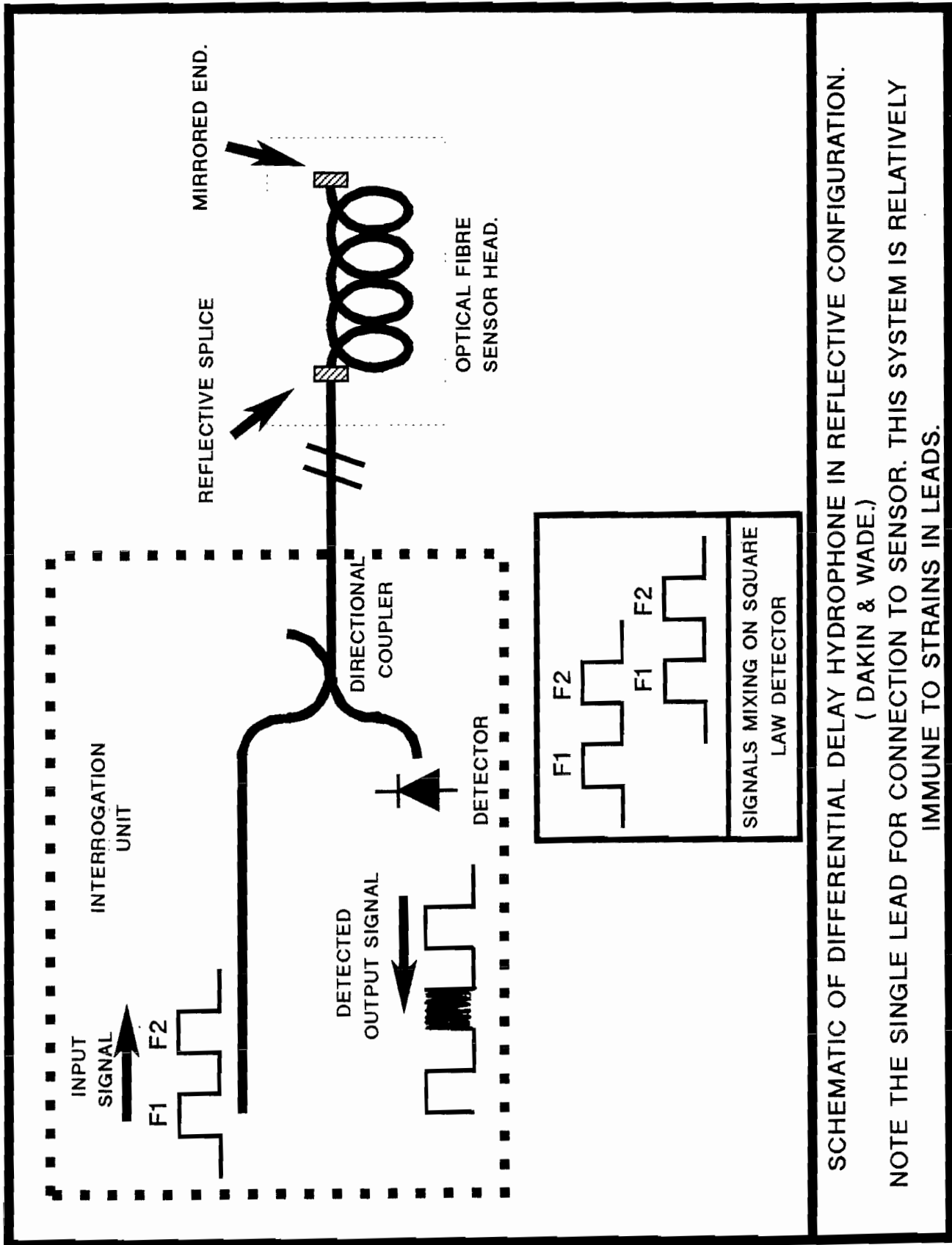


ILLUSTRATION OF THE ADVANTAGES OF HETERODYNE PROCESSING WHEN SIGNAL AMPLITUDE FADES. (eg. WHEN POLARISATION FADING OCCURS.)

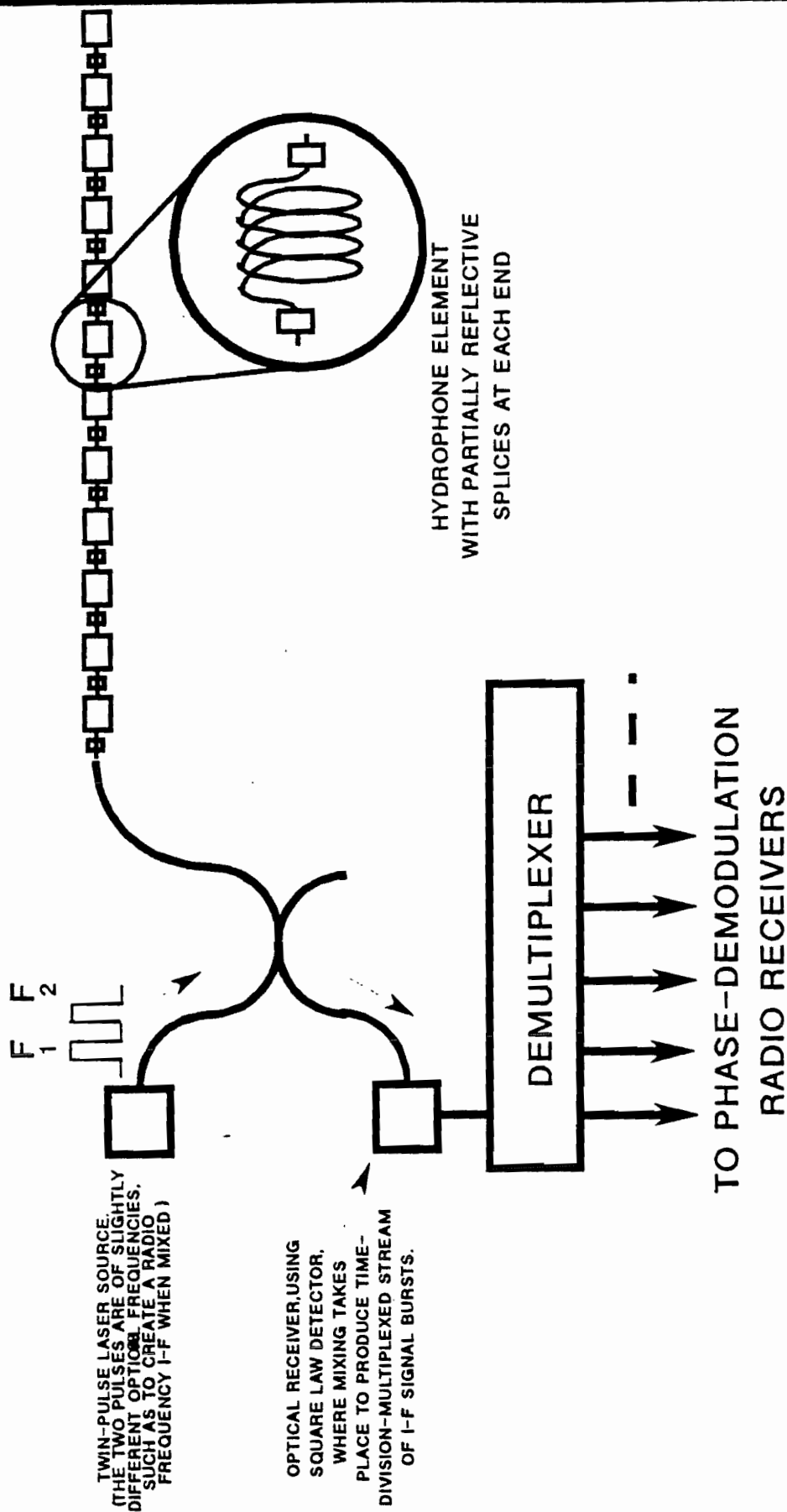
THE ONLY SIGNAL DISTORTION ON THE INTERMEDIATE FREQUENCY CARRIER SIGNAL IS THAT OF ENVELOPE MODULATION. BY WELL-KNOWN PRINCIPLES OF FM RADIO SYSTEMS, THE EFFECT OF SLOW AMPLITUDE MODULATION ON A HIGH FREQUENCY FM SIGNAL IS MUCH LESS SERIOUS THAN WITH AN AM SIGNAL IN TERMS OF S/N RATIO.



SCHEMATIC OF DIFFERENTIAL DELAY HYDROPHONE IN REFLECTIVE CONFIGURATION.

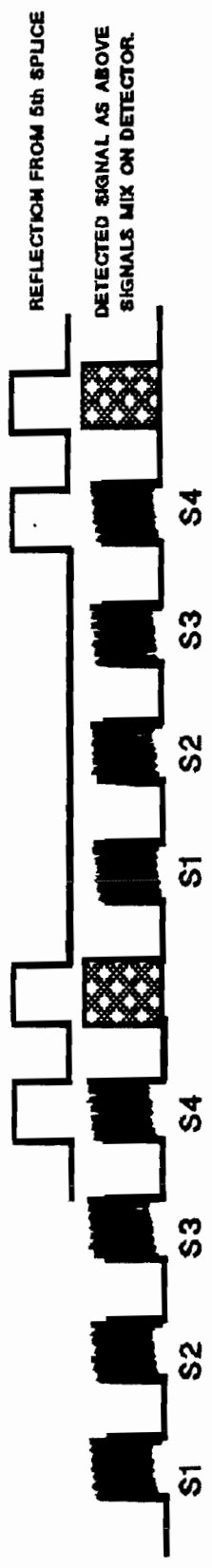
(DAKIN & WADE.)

NOTE THE SINGLE LEAD FOR CONNECTION TO SENSOR. THIS SYSTEM IS RELATIVELY IMMUNE TO STRAINS IN LEADS.



SCHEMATIC OF PLESSEY MULTIMPLEXED HYDROPHONE CONCEPT, USING DIFFERENTIAL DELAY HETERODYNING (DAKIN, WADE, HENNING, LAMB)

F1 F2 LAUNCHED OPTICAL PULSE TRAIN
 (i.e. REPEATED SEQUENCE OF PULSE PAIRS AT TWO DIFFERENT OPTICAL FREQUENCIES)



**TIMING DIAGRAM OF SIGNALS FROM A 4-ELEMENT
 HYDROPHONE ARRAY, AS IN PREVIOUS DIAGRAM.**

**(SYSTEM OF DAKIN AND WADE, FORMERLY OF
 PLESSEY Co. Ltd)**

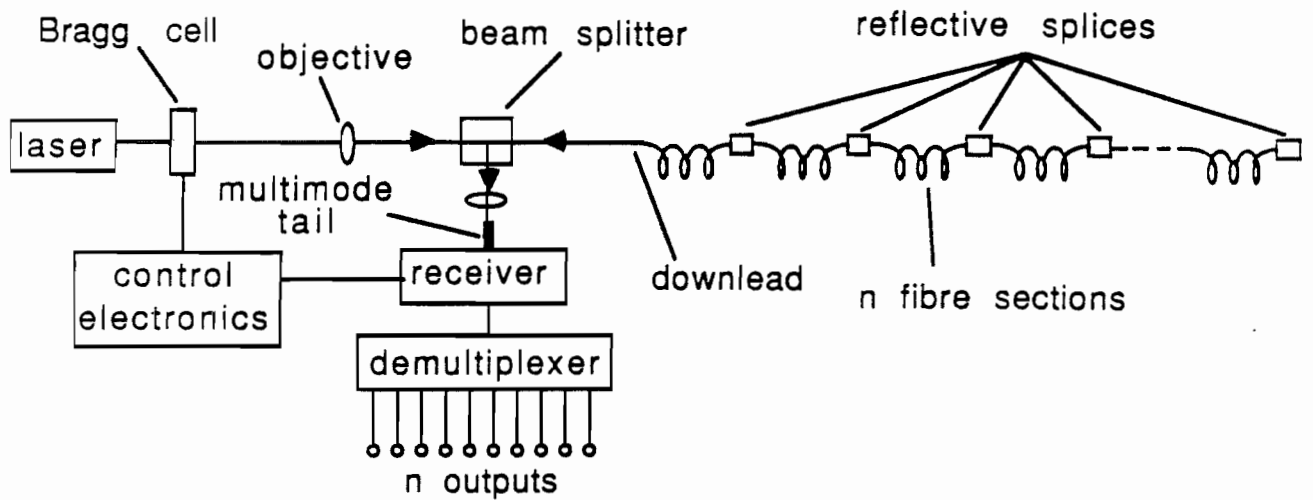
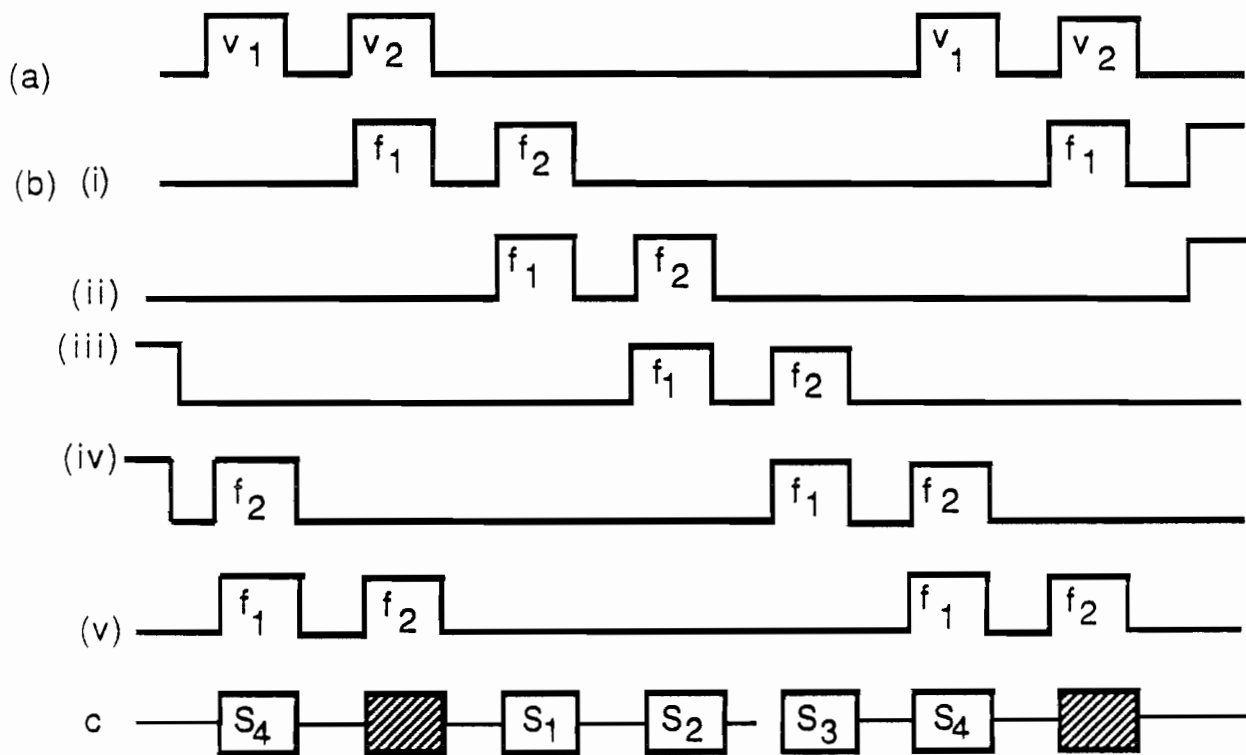


FIG 3a DIAGRAM OF OPTICAL FIBRE HYDROPHONE ARRAY

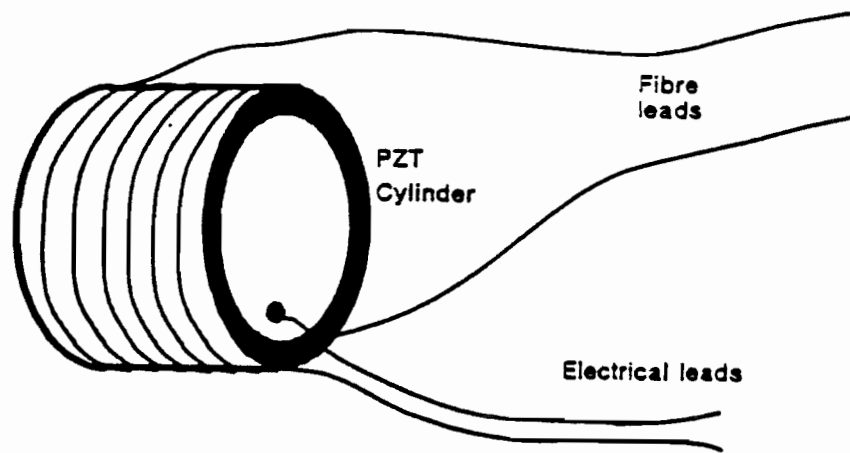


- (a) Input to Bragg cell
- (b) Reflections from end of :
 - (i) Download
 - (ii) 1st sensor
 - (iii) 2nd sensor
 - (iv) 3rd sensor
 - (v) 4th sensor
- (c) Output from photodiode

FIG 3b TIMING DIAGRAM FOR A FOUR - ELEMENT ARRAY

Optical fibre phase modulators

It is useful to be able to change the phase of light travelling in a monomode optical fibre, as the device can then be coupled efficiently to an optical fibre sensing network using low loss splices or connectors. The simplest and most common means of achieving this is to use a piezo-electric (PZT) ring transducer, with the fibre wound around it (and usually bonded to it with epoxy).



Schematic of piezoelectric fibre phase modulator

When the PZT is driven by an electrical drive frequency it expands and contracts, causing the fibre to also expand and contract with it. The length changes in the fibre cause the effective optical path length through the coil of fibre to change, partly as a result of the physical length increase/decrease and secondly as a result of changes in the propagation velocity in the fibre as its refractive index changes due to expansion/contraction.

(Unfortunately, the effect of the refractive index change is of opposite sign to that of the physical length change, so this reduces the total optical path length modulation) The resulting changes in optical path length modulate the time of propagation of light through the device, and hence the phase of light emerging from it. In order to cause phase modulation of 180° or more, as typically desired in a phase modulator, it is usually necessary to have several tens of metres of fibre on the PZT ring and use drive voltages of several tens or hundreds of volts. Because of the high mechanical stiffness and density of the PZT material, the transducer can be driven more easily at mechanical resonance, which means sinusoidal modulation is more readily achieved. For some applications, such as linear frequency shifting, it would be desirable to drive the PZT with a linear electrical ramp, but this must eventually reach a voltage drive limit and must have a return to zero. This requires a "sawtooth" drive signal. However, it is much more difficult to achieve a fast "flyback" signal across a device of high capacitance and this form of signal will normally excite numerous modes of mechanical resonance or "ringing" of the crystal. However, success with sawtooth drive signals has been achieved by embedding such a fibre modulator in acoustically-absorbing putty and servo-controlling the electrically-induced dimensional changes by using a small attached strain monitor (another small PZT sensor) and controlling the mechanical response to the desired "sawtooth" response using an electronic feedback control circuit.

Integrated-optic phase shifters

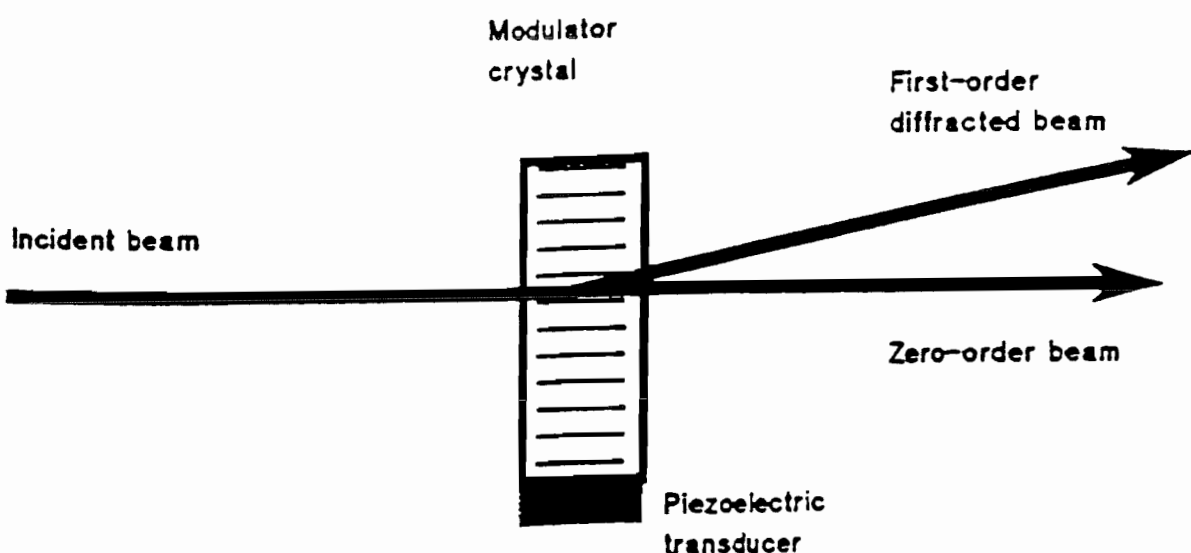
These are constructed using the Pockels effect, as discussed above. The phase of light of one particular polarisation is controlled by application of a high field across an integrated optic light guide. Because of the small width of the light guide (few μm) the frequency response is extremely high (typically hundreds of Mhz, even with simple electrode design), it is only necessary to apply a few volts to the crystal and mechanical resonances are avoided because of rapid acoustic energy dissipation into the bulk of the electro-optic crystal. The disadvantage is the strong polarisation

sensitivity and the additional losses (typically $\sim 3\text{dB}$) on coupling to optical fibres. However, if optical amplifiers can be afforded, the latter objection is less of a problem.

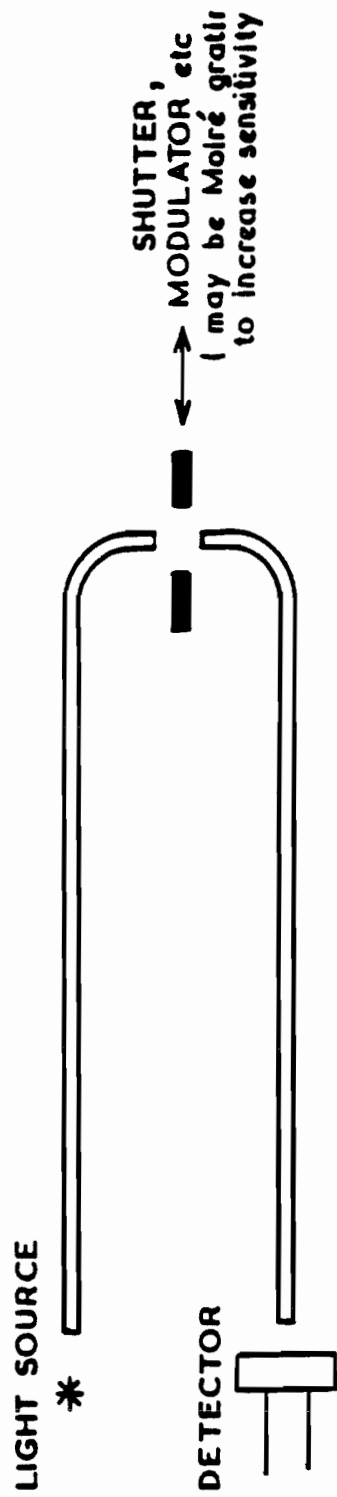
The Bragg cell acousto-optic modulator

The Bragg cell operates by diffraction of an optical beam passing through an optically-dense crystal (typically lead molybdate or gallium arsenide) or glass material. The diffraction is caused by the light passing through a region of optical density changes in the material, the latter being induced by a travelling acoustic wave. The acoustic wave is generated by a thin piezoelectric transducer bonded to the crystal. This transducer element is driven by a radio-frequency signal to generate the desired high-frequency (short wavelength) acoustic signal. With electrical drive powers of typically 1 W, it is possible to produce diffraction efficiencies of 50% or higher, with energy being lost from the transmitted or zero-order optical beam into the diffracted beam. In addition to suffering a small deflection (typically a few degrees) the diffracted beam is frequency shifted from the original input beam by an amount equal to the frequency of the RF drive signal. The device is therefore very useful in optical heterodyne systems, as it can generate optical signals with controlled differences in their frequency, which can later be caused to interfere on a detector to regenerate the difference frequency by a non-linear^{*} mixing process. The device can also be used as an optical deflector, modulator or switch, by controlling the frequency (varies deflection angle) or power level (varies diffraction efficiency, ie power in diffracted beam) of the RF drive signal.

* An optical detector gives a photocurrent proportional to the intensity of the light, which is proportional to the square of the electric field intensity of the incident light

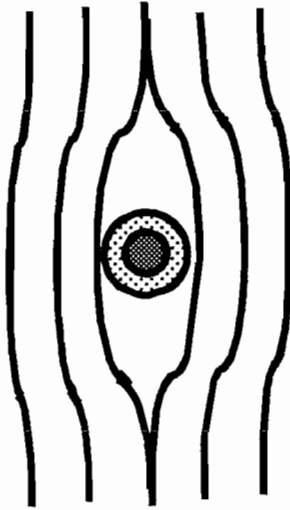


Schematic of Bragg cell, showing incident beam, transmitted (ie. zero-order) beam and first-order diffracted beam. (The latter is frequency shifted by the applied RF signal)

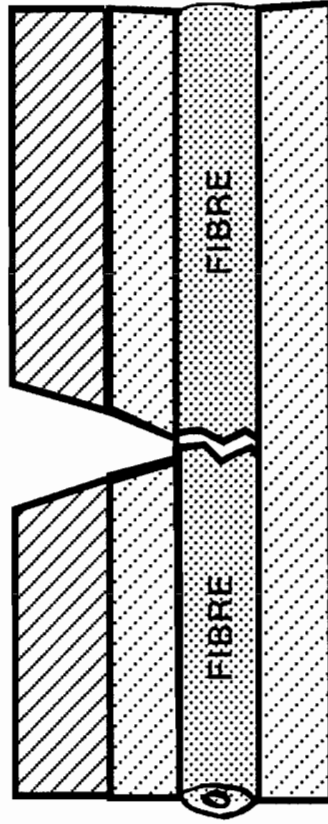


BASIC BEAM INTERRUPTION SENSOR

FIBRES IN LAMINATES FOR SMART SKINS.



SCHEMATIC OF OPTICAL FIBRE IN A LAMINATED STRUCTURE.



**FIBRE BROKEN BY A CRACK IN THE LAMINATE.
(NOTE: IT IS NOT NORMALLY NECESSARY TO HAVE SUCH A SEVERE FAULT, AND EXTERNALLY-INVISIBLE DEFECTS IN THE LAMINATE MAY GIVE RISE TO FIBRE BREAKAGE AT THE WEAKENED POINT.)**

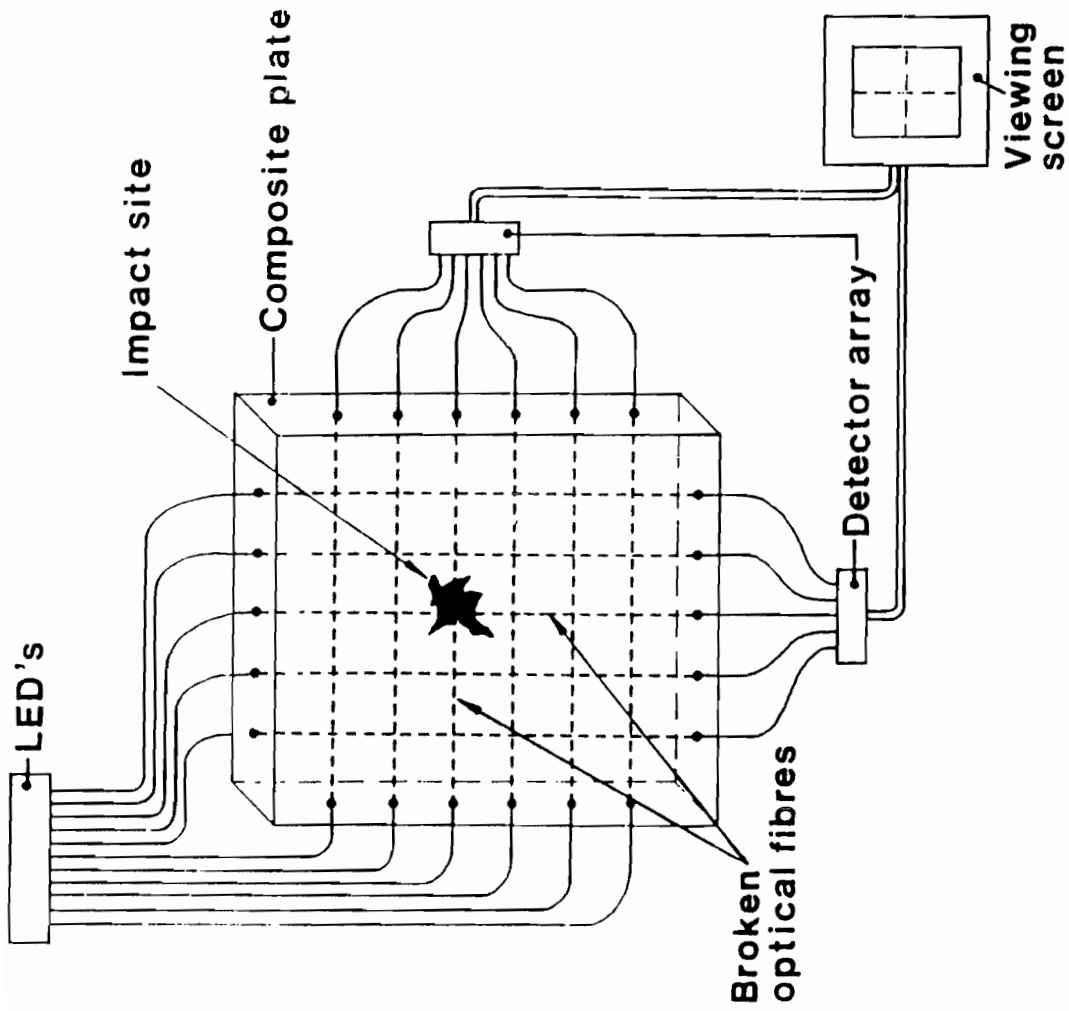
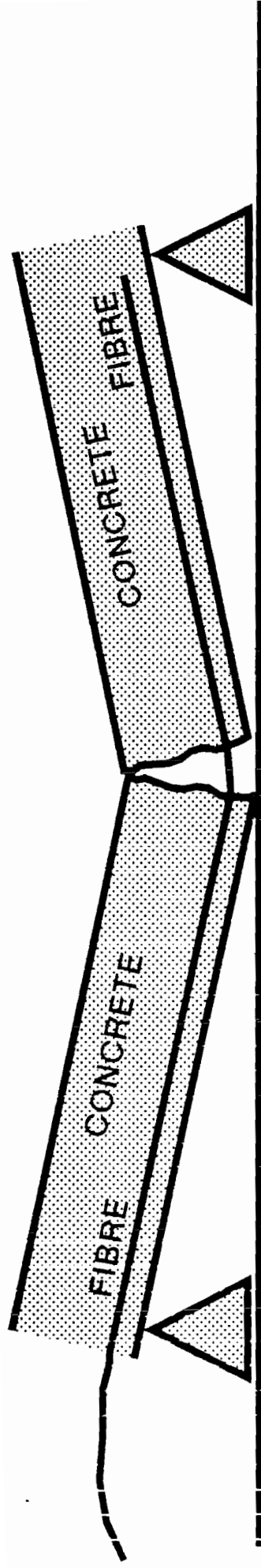


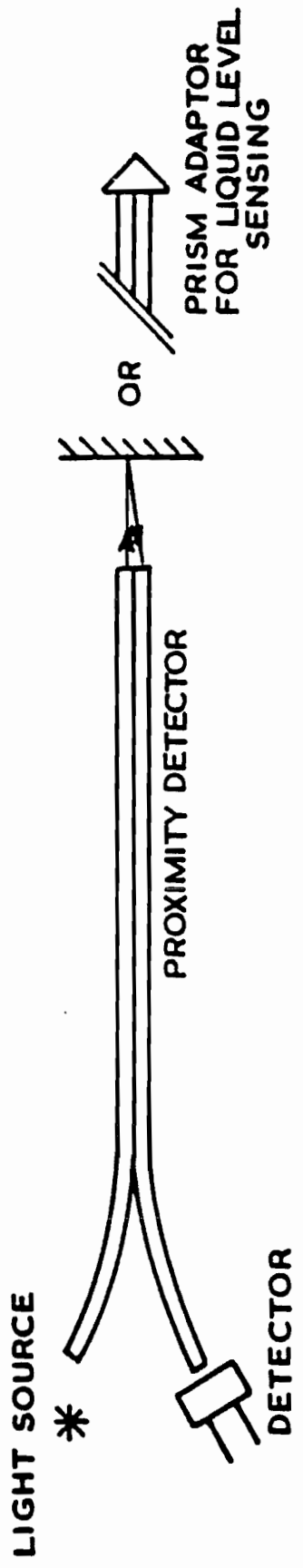
Fig. 19.11 Schematic diagram of an optical fiber system showing the location of impact damage in a composite structure.

THIS DRAWING IS REPRODUCED WITH THANKS FROM
 "OPTICAL FIBER SENSORS" PUBLISHED BY ARTECH HOUSE.
 EDITORS: J P DAKIN, B CULSHAW.
 DIAGRAM TAKEN FROM CHAPTER BY A J A BRUINSMA, T M J JONGELING



PROBLEMS WITH CRACK DETECTION IN CONCRETE BEAMS

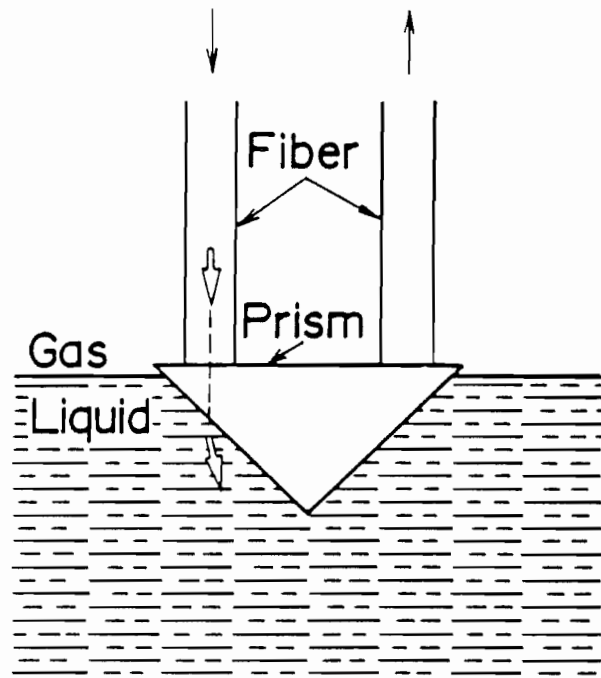
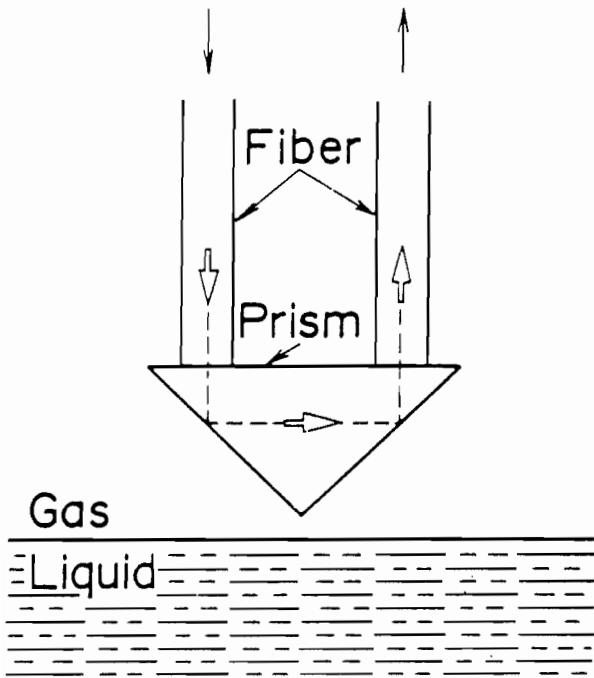
(Fibre has less adhesion to concrete and can pull out)



BASIC REFLECTIVE SENSOR
 (single fibre may be used with directional couplers)

Light source (High level) Detector (High level)

Light source (Low level) Detector (Low level)



Principle of operation of a liquid-level sensor with a prism attached to the two optical fibers (Delta Controls Ltd., U.K., technical leaflet, liquid-level switches, 850 series).

THIS DRAWING IS REPRODUCED WITH THANKS FROM
"OPTICAL FIBER SENSORS" PUBLISHED BY ARTECH HOUSE.
EDITORS: J P DAKIN, B CULSHAW.
DIAGRAM TAKEN FROM CHAPTER BY K. KYUMA

MICROBEND SENSORS

Microbend sensors are intrinsic sensors which take advantage of the loss in optical fibres when they are bent. The word microbend is used because gradual bends, ie. bends of large radius (greater than 50mm), cause very little loss in a fibre (otherwise they would not find the extensive uses that they have in communications!), whereas sharp "kinks" of small bending radius can cause high losses even if present over very short lengths.

The losses in the fibre are due to conversion of energy in guided fibre-core modes to cladding modes, which are then usually lost by absorption or scattering in the fibre sheathing material. In the case of monomode fibres, the mechanism is relatively simple, as there is only one guided mode (strictly two, if polarisation effects are taken into account) to be coupled out, and the extent of coupling, and hence the loss, can be uniquely determined by the degree of bending.

In the case of the multimode fibres, more commonly used with such sensors, the situation is much more complex. Firstly, bending causes mode conversion, in particular coupling of lower order modes (associated with rays in the core which travel at a small angle to the fibre axis) to higher order ones (associated with rays travelling at larger angles to the axis) and eventually to cladding modes. This "chain" of events, coupling energy from low order modes, via higher order ones, to radiation ones depends in a complex way on not only how the fibre is bent but also on which modes were initially present in the fibre in the section immediately preceding the bend. Because of the latter aspects, it is extremely difficult to derive quantitative information from microbend sensors, particularly if several are cascaded along the length of a single fibre, as then the condition of each one will affect the response of subsequent ones.

Multimode microbend sensors have a particularly strong response if they cause the fibre to be periodically bent with a particular spatial period which corresponds to the "zig-zag" period associated with the highest order rays that the fibre will guide. These highest order rays are those striking the core cladding interface at the normal Snell's law critical angle associated with total internal reflection. Thus, a strong response can be achieved by pressing the fibre between corrugated plates, with offset corrugations (or plates covered with parallel metal pins) which will periodically deform the fibre with the appropriate spatial period (usually around 1 to 2 mm, for typical multimode fibres) to ensure strong mode coupling. Under these conditions, very high losses can be induced in the fibre with a few microns lateral displacement. However, the response is highly non-linear and care must be

taken to avoid the possibility of exceeding the long-term mechanical bend limitations of the fibre. Clearly with polymer coatings, slow mechanical creep will be a problem.

Probably the most practical qualitative microbend sensor is the distributed cable version, first devised by Dr Alan Harmer at Battelle labs, Geneva. This consists of an optical fibre which is helically wound with a thin fibre thread, before being sheathed within an outer polymer tube. The spatial period of the helically wound fibre is designed to correspond with the mode-coupling length. When the outer tube is compressed from opposite sides, the fibre is deformed to cause high loss. This assembly finds most use as a cable to sense, in an on/off manner the presence of lateral force or weight. Applications are detection of the pressure due to a human foot (eg for safety mats or intruder detection) or that due to trapping of objects in a sliding door or window (eg lift door, car window, sun-roof, etc)

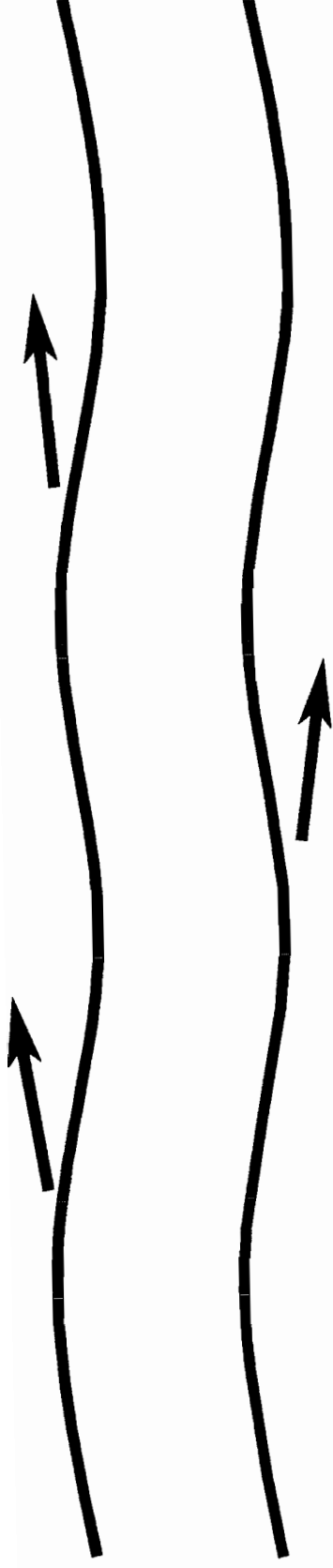
OTHER INTRINSIC FIBRE-LOSS BASED SENSORS

The following pages will illustrate the microbend sensor, plus a number of other loss-based fibre sensors.

The oil sensor of D Pitt, shown in the simple schematic, relied initially on the scattering loss due to oil droplets adhering to the outside of an unclad optical fibre. It was effective at sensing oil in water, but proved difficult to clean for re-use. It was subsequently superceded by the more comple (extrinsic) sensor shown in the "pump-room" in the diagram. This relied on monitoring scattered light from oil droplets, and only used fibres for delivery and collection of light. This was one of the most commercially successful fibre sensors made so far, having been installed in numerous sea-going oil tankers.

The oil sensor shown in the later diagram used a fibre clad with a low-index silicone polymer, which adsorbed oil, changing both its refractive index and attenuation. This evanescent field sensor was proposed by Nishizawa, of Nippon Sheet Glass, Japan, for oil sensing in groundwater.

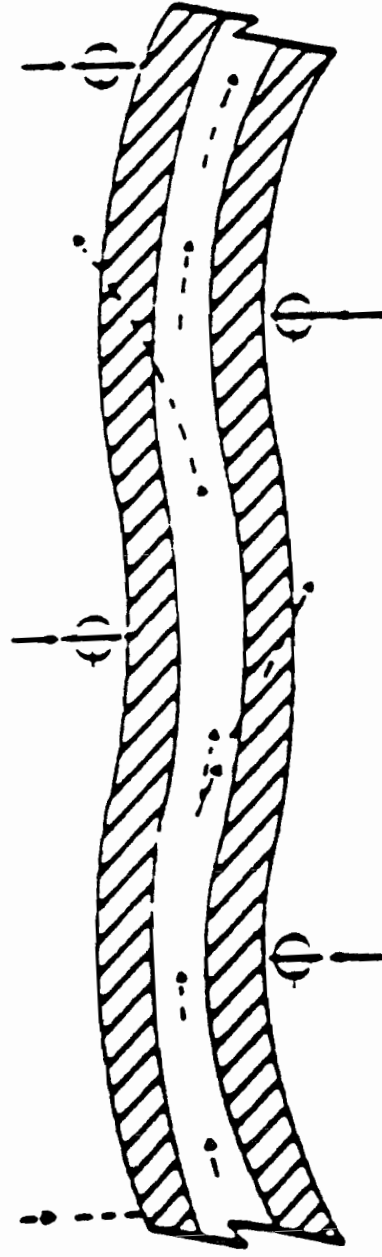
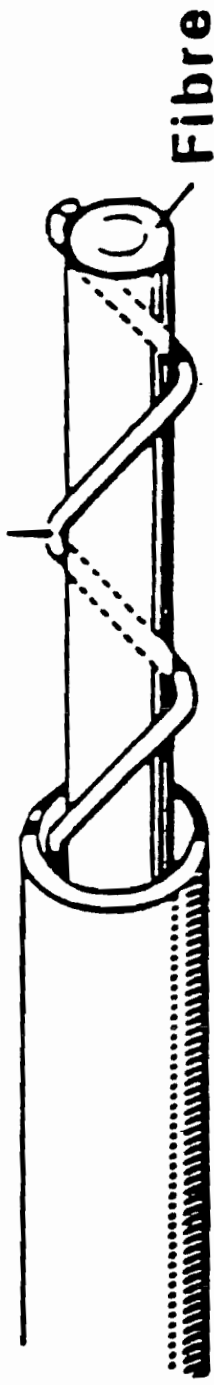
Another attractive loss-based intrinsic sensor is the radiation dosimeter, in which the attenuation of the fibre is increased by ionising radiation. Silica fibres are suitable for high radiation level detection, whereas lead-glass fibres have a better response at lower levels. In all cases, however, the losses exhibit a time or dose-rate dependence and reduce gradually after thermal annealing, even at room temperature.



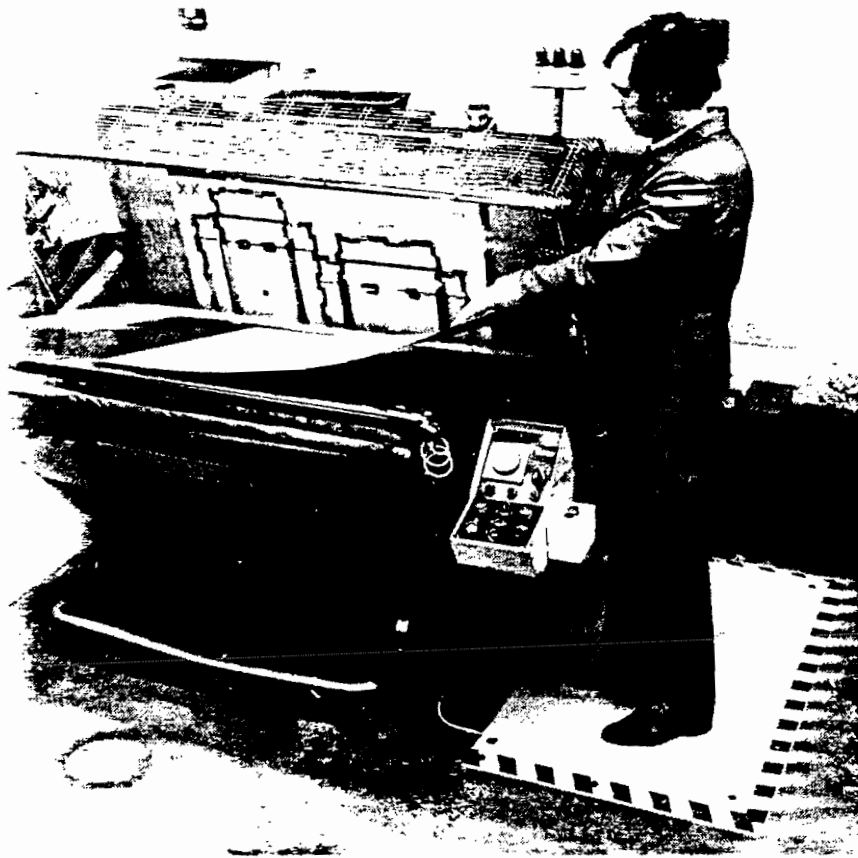
Fibre microbend sensor

(Light is lost by radiation of energy at bends)

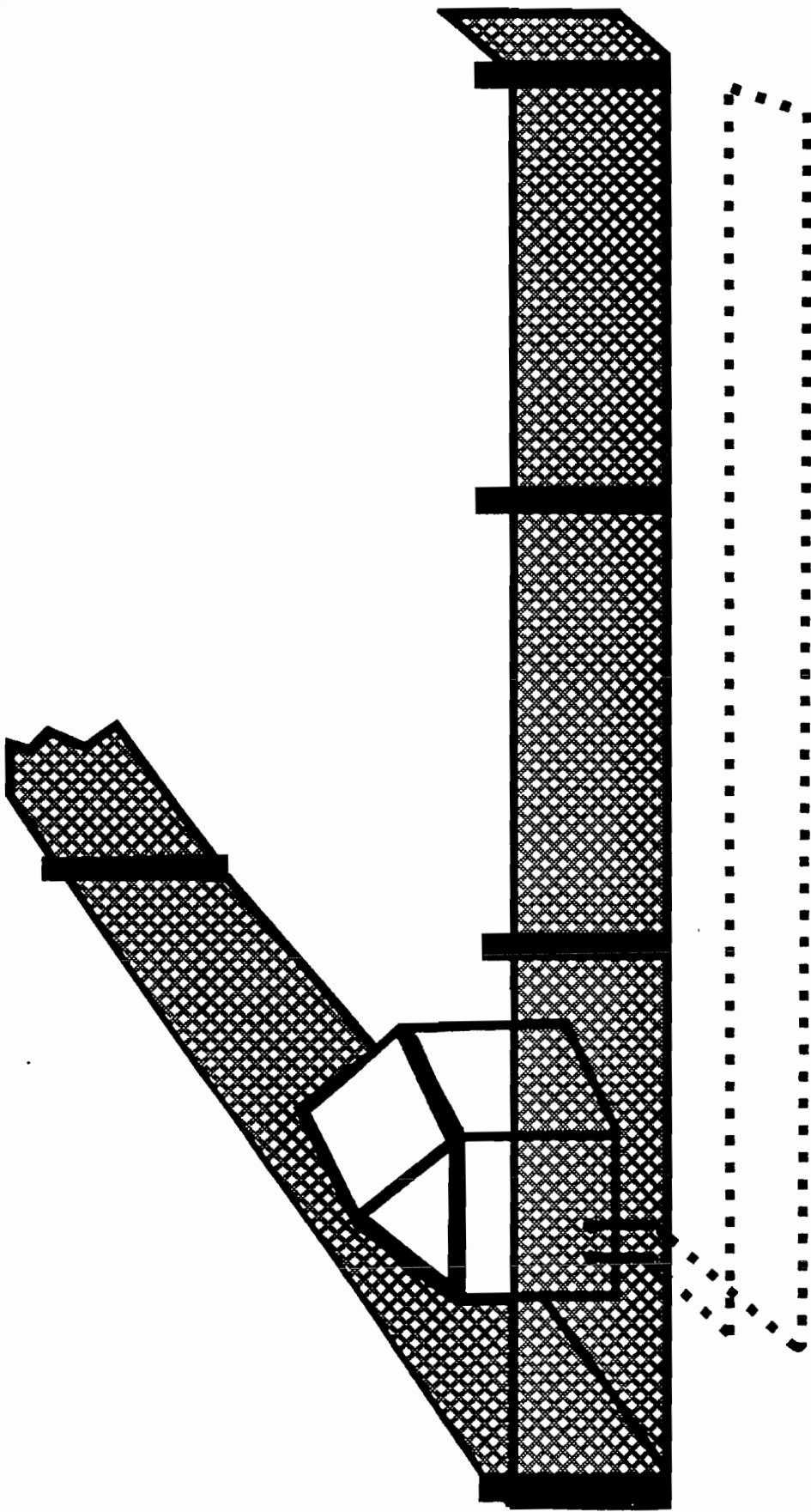
Spiral



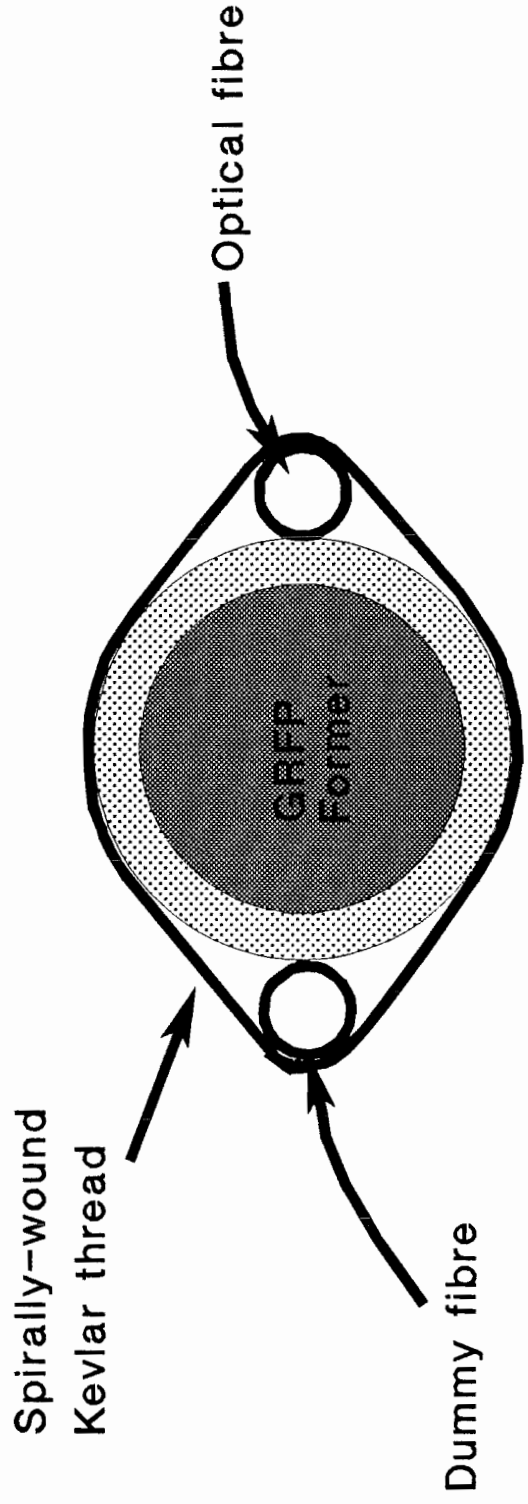
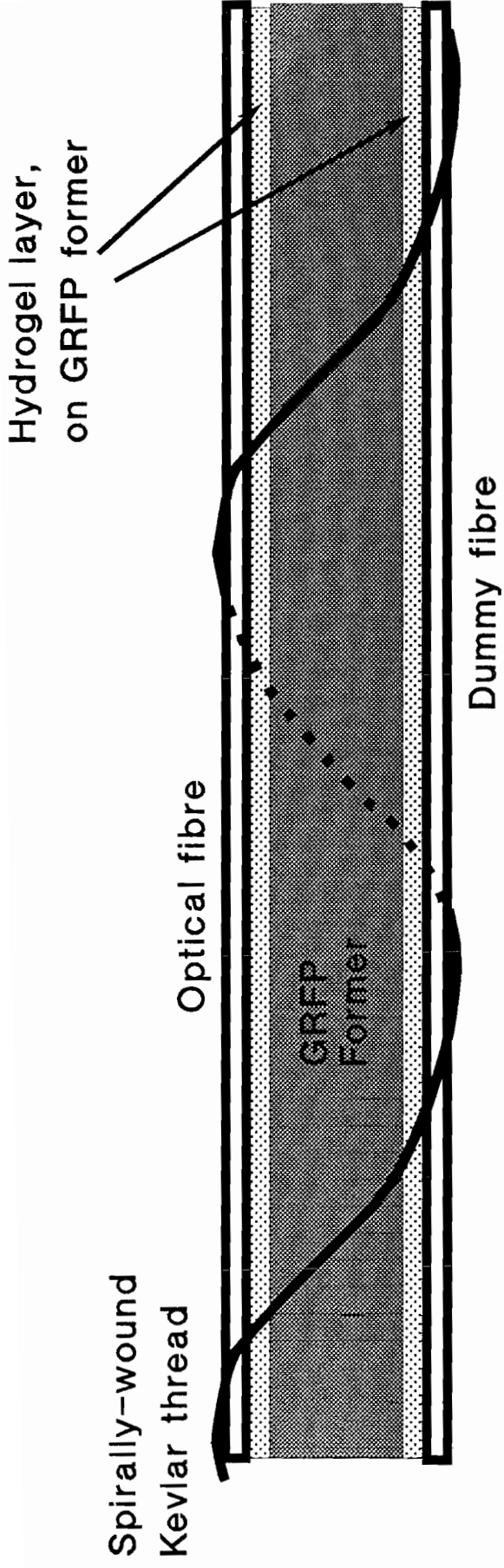
Principle of the pressure-sensing cable, using microbend sensor. (Courtesy Herga Electric, U.K.)

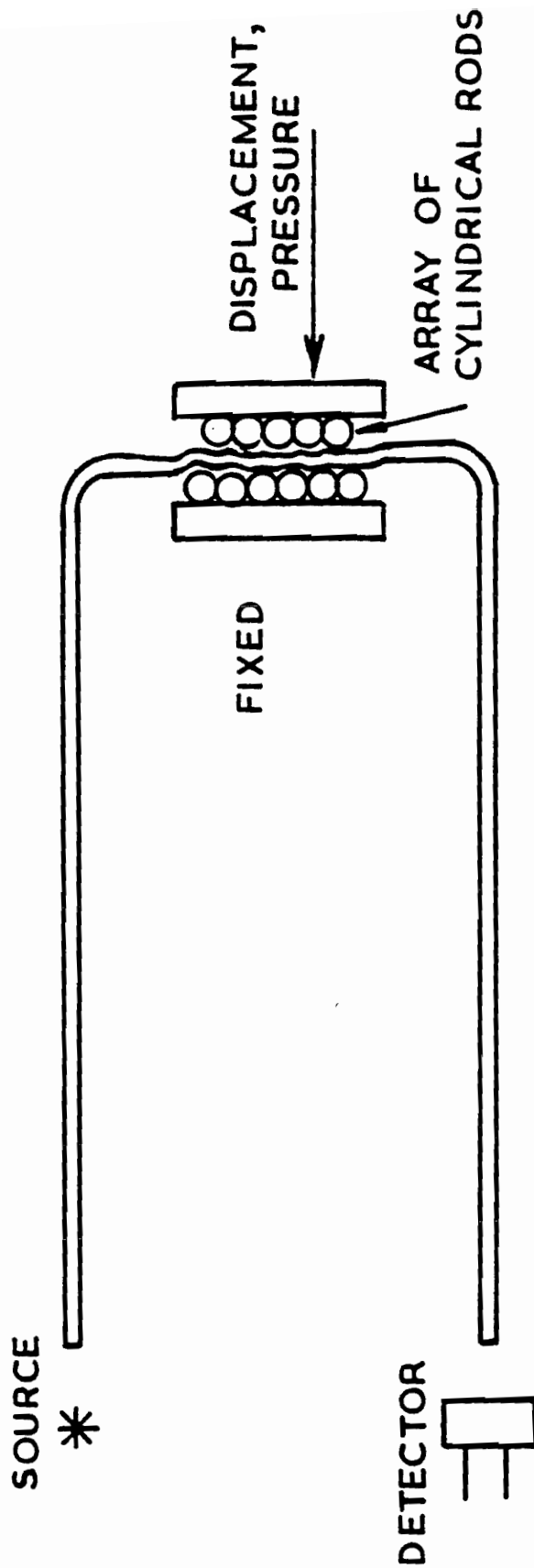


A pressure-sensing mat for machine guarding (Herga Electric Ltd., U.K.).



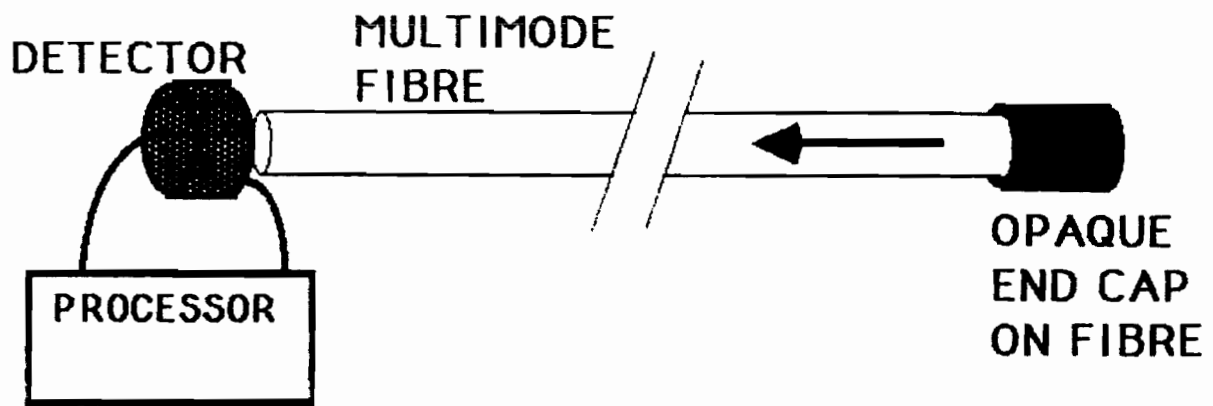
**SCHEMATIC OF APPLICATION OF
FIBRE-OPTIC INTRUDER DETECTOR
SYSTEM BURIED IN GROUND**





FIBRE TRANSMISSION MODULATION SENSOR
'RIPPLE COUPLER'

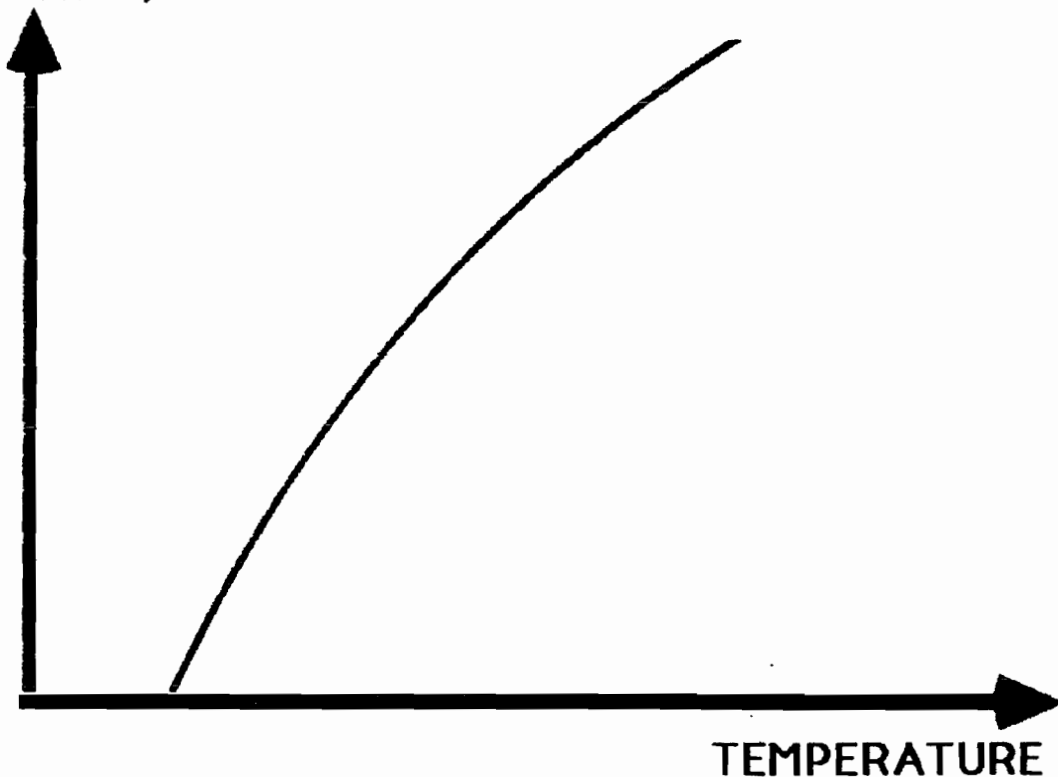
(AFTER J.M. FIELDS J. ACOUSTIC SOC. AMER. 167 (.1984) 816



SCHEMATIC ILLUSTRATION OF SENSOR

(DETECTION SYSTEM MAY ALSO TAKE RATIO OF SIGNALS IN TWO WAVELENGTH BANDS, IF DESIRED.)

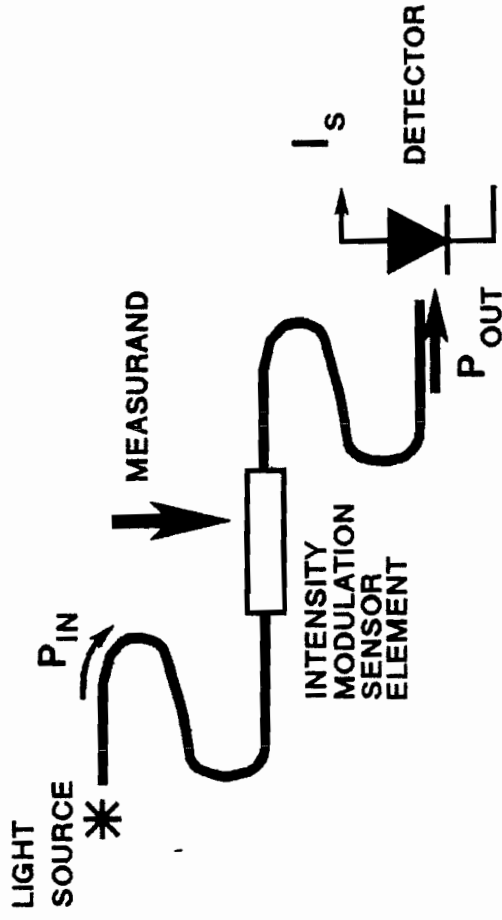
LOG (DETECTED SIGNAL INTENSITY)



PYROMETRIC TEMPERATURE SENSOR (DAKIN & KAHN 1976)

(SENSOR COLLECTS NEAR-INFRA RADIATION FROM INSIDE SURFACE OF HEATED OPAQUE END CAP ON FIBRE).

SIGNAL TO NOISE RATIO OF INTENSITY BASED SENSORS



Fractional change in signal in modulator in response to measurand = Δ

Mean optical signal intensity = P_0

Modulated component of optical signal = $P_0 \Delta$

Modulated component of detected signal = $P_0 \Delta R$ } (R= Detector Responsivity)

Mean detected signal = $\bar{I}_s = P_0 R$

Photon noise current at detector = $\sqrt{2q \bar{I}_s B}$

(q= electronic charge, \bar{I}_s = mean detector current, B = bandwidth)

$$\text{Signal to noise ratio} = \frac{P_0 \Delta R}{\sqrt{2q P_0 R B}} = \Delta \sqrt{\frac{P_0 R}{2q B}}$$

NOTE: Analysis assumes photon-noise-limited performance, the usual condition for simple low-speed sensor systems.

PROBLEMS WITH SIMPLE INTENSITY-BASED SENSORS, AND MEANS OF IMPROVEMENT BY SENSOR REFERENCING

The use of intensity based sensors is very attractive because of the ease of measuring the intensity (eg. from the detected photocurrent in a silicon photodiode). However, simply measuring the output intensity from a single fibre containing a sensor can lead to a number of sources of error/uncertainty in the state of the sensor. The following factors can affect the output signal and hence cause errors in the observed sensor reading.

- (i) Light source variations
- (ii) Fibre lead and connector variations
- (iii) Variations in detector response
- (iv) Detector / preamplifier noise

In practice, the noise and variations in response of the optical receiver are not usually a major problem when using silicon detectors at low frequency. However, changes in light source intensity and in the transmission of optical fibres and connectors can be very significant.

In order to resolve the above problems, it is usually necessary, when making a quantitative measurement, to **reference** the sensor. This involves providing a reference optical signal which has not been changed by the measurand in the same manner as the sensing signal. The problems of simple intensity sensors and methods of referencing them are shown in the following overheads.

The simplest method of referencing is based on the provision of more than one fibre path from the light source, leading to two separate detectors, with the sensing section included in only one of the paths. The signals are then ratioed. More complex systems are possible, with routing of signals via separate paths using couplers or fibre switches. Alternatively, fibre paths of different length can be used to separate signals from a pulsed source. Here the separation occurs in the time domain, according to the propagation delay each signal has experienced in its separate optical path.

A particularly attractive method is to use spectral encoding in the sensor, where the sensor head provides an optical filtering function. Then, at the receiver, the relative signal strength at two or more optical wavelengths is monitored. If the sensor can filter out just one narrow spectral band, having a central wavelength dependent on the measurand, then this is even more attractive, as this wavelength can then be monitored almost independently of the optical power level or intensity.

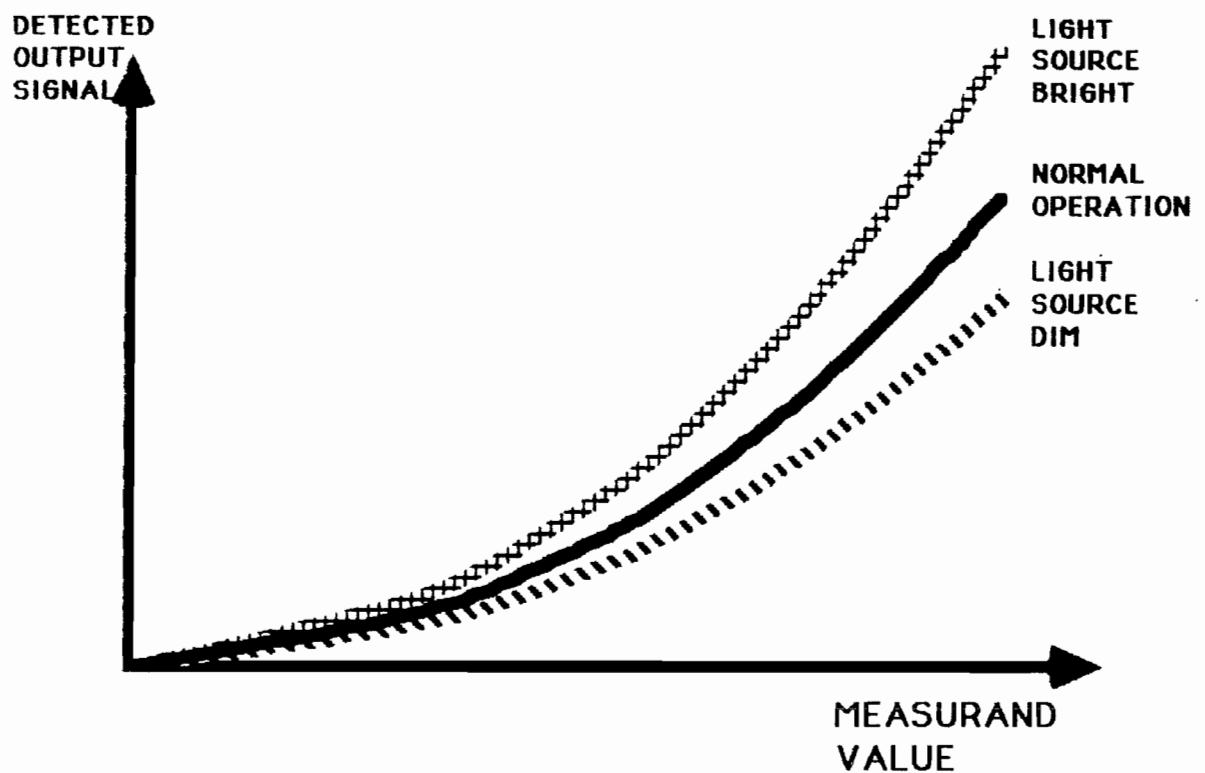


ILLUSTRATION OF THE PROBLEMS ASSOCIATED WITH SIMPLE INTENSITY BASED SENSORS.
(SIMILAR PROBLEMS ARISE IF CONNECTOR OR FIBRE LOSSES CHANGE, INSTEAD OF LIGHT SOURCE OUTPUT)

12.3.1 Balanced bridge (Culshaw, 1983; Culshaw *et al.*, 1984)

The configuration of the balanced bridge system is illustrated in Fig. 12.11. Two separate LED light sources provide light to the sensing head

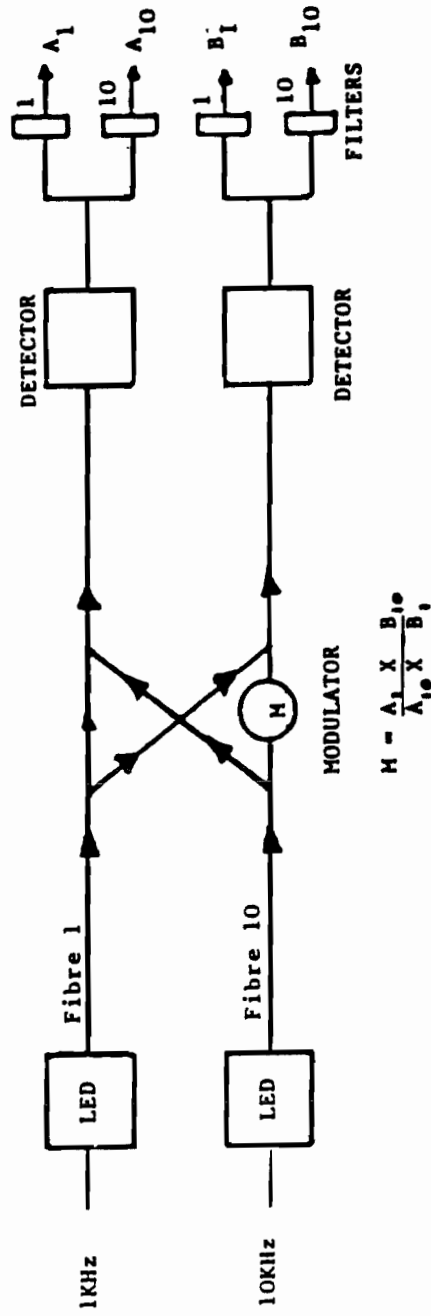


Fig. 12.11 Single-wavelength referencing using balanced bridge arrangement.

THIS DRAWING IS REPRODUCED WITH THANKS FROM "OPTICAL FIBER SENSORS", PUBLISHED BY ARTECH HOUSE.
 EDITORS: J P DAKIN, B CULSHAW.
 DIAGRAM TAKEN FROM CHAPTER BY B E JONES, R MEDLOCK, R SPOONCER

DUAL-FIBRE REFERENCING

(POOR IF MICROBENDING EFFECTS, SURFACE

CONTAMINATION

OR SPLITTER/COUPLER VARIATIONS

AFFECTING MEASUREMENT & REFERENCE

PATHS TO DIFFERING DEGREES.)

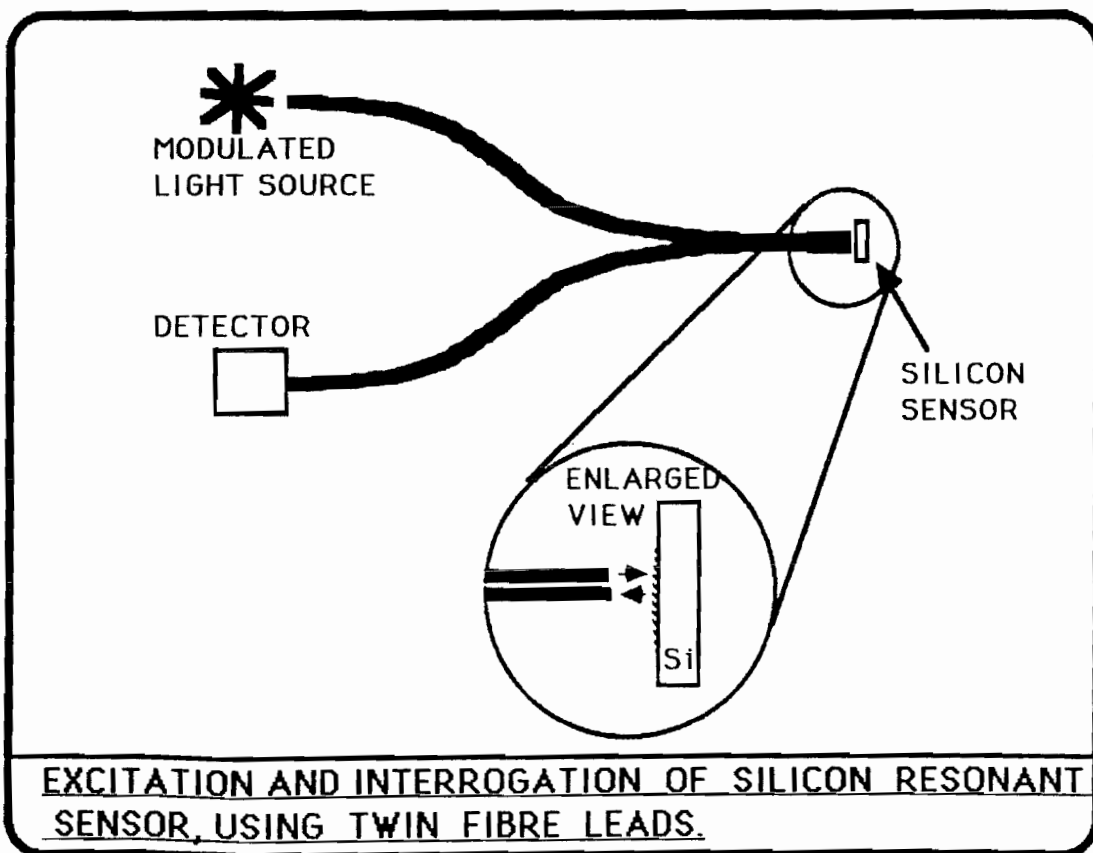
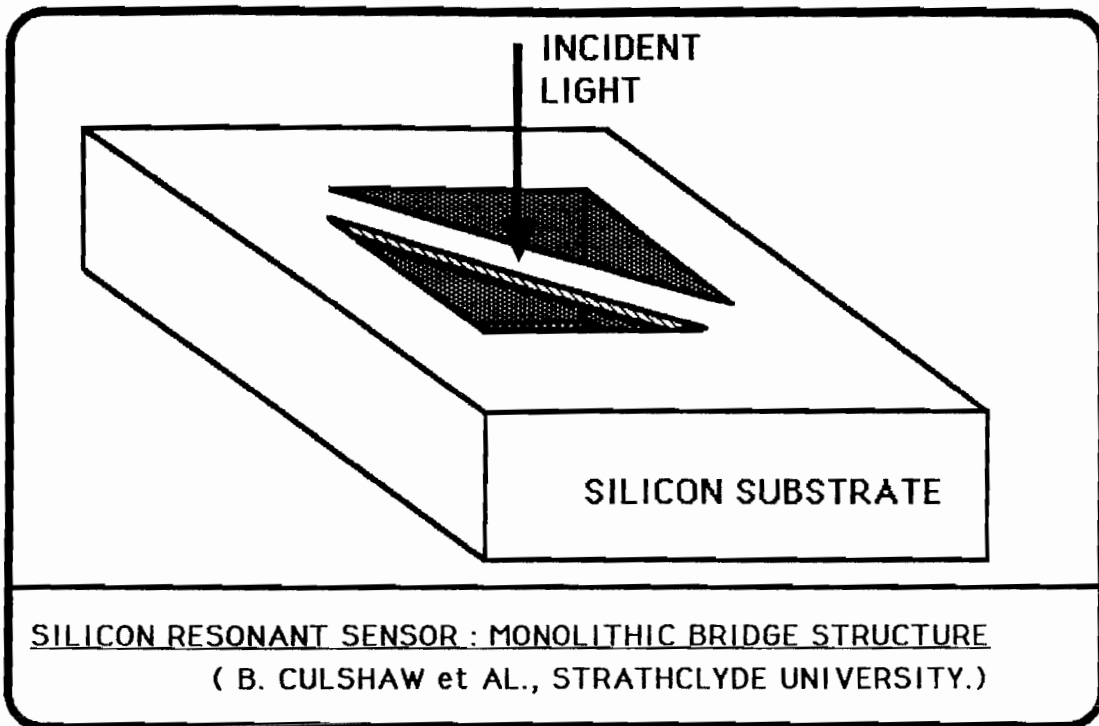
SILICON RESONANT SENSORS

Silicon resonant sensors are commonly used in industry, and usually rely on monitoring the mechanical resonant frequency of a silicon micro-resonator. The resonator structure is typically a cantilever, tuning fork, micro-bridge or similar structure that is excited by some electromechanical actuator (eg piezo-electric, electrostatic, electrostrictive effect).

It is possible to make optically-driven versions of these sensors (see next page). These are similar mechanical structures (a silicon bridge device is shown in the diagram) which are driven into mechanical motion by illumination with a modulated optical beam from a laser. Several effects can contribute to the driving force, but the most common is that of a simple heat engine: the cyclic heating of one side of a cantilever causes the illuminated face to expand and contract relative to the dark side, and this causes a bending moment which excites the mechanical oscillation. The mechanical Q factor of such structures is very high, so very little force is needed to create significant deflection of such a tiny element at the resonant frequency.

The structure can easily be configured to make the resonant frequency respond to changes in temperature, strain, pressure, etc., in the same manner as routinely done with traditional electrical types.

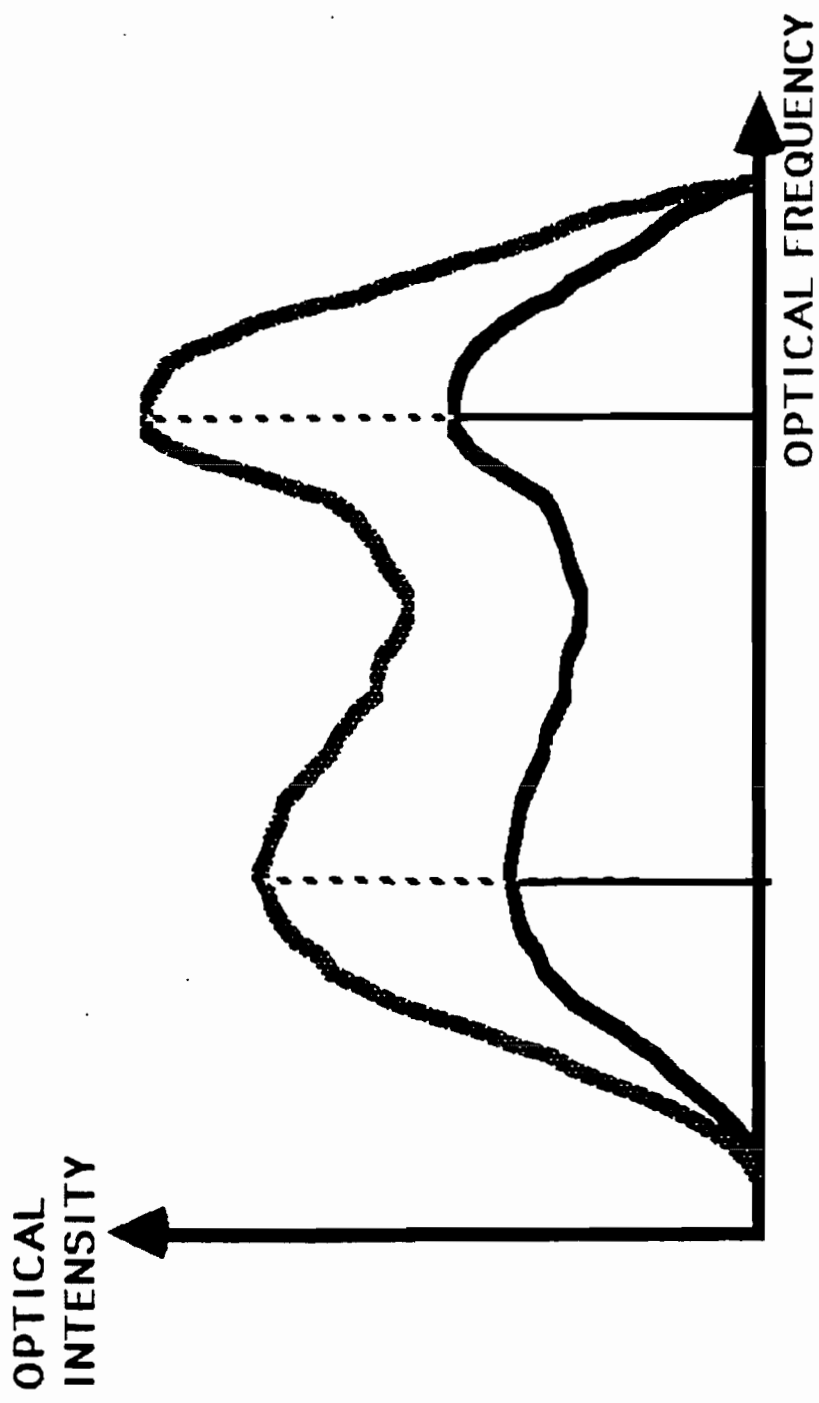
In order to interrogate the sensor, the frequency of the exciting beam can be changed to observe the resonance and the mechanical response can be determined from the changes in optical intensity or phase as the tiny beam deflects.



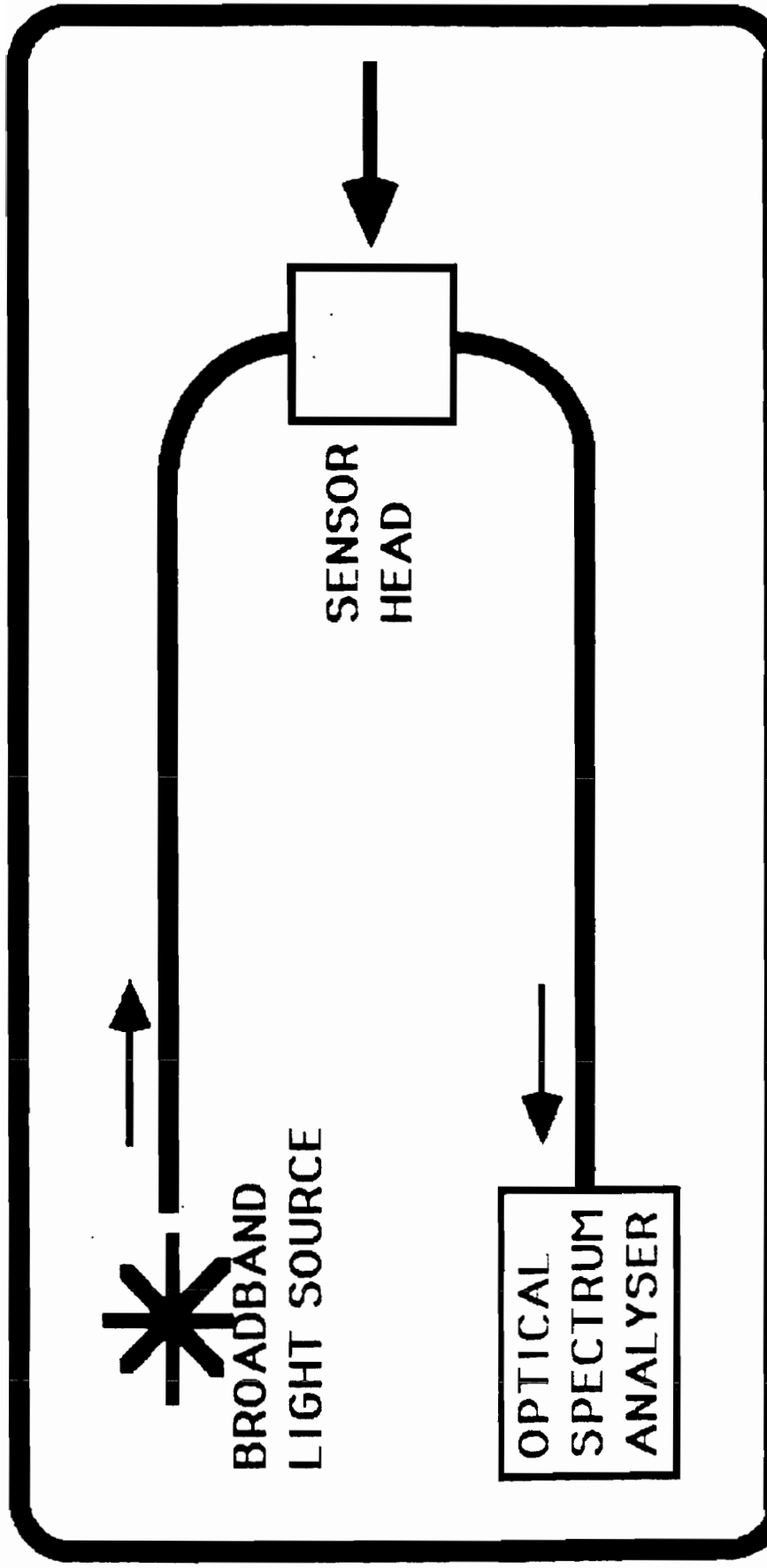
**ANALOGUE TWO - WAVELENGTH -
REFERENCED SYSTEMS**

(RATIO $P_{\lambda 1} / P_{\lambda 2}$ DEPENDS ON

MEASURAND)



DUAL-FREQUENCY (DUAL-WAVELENGTH) REFERENCING.
NOTE. THE OUTPUT IS THE RATIO OF THE DETECTED OPTICAL
INTENSITY AT THE TWO OPTICAL FREQUENCIES(WAVELENGTHS)]
THIS RATIO IS UNCHANGED IF THE LOSSES ARE THE SAME AT EACH.



SCHEMATIC OF SPECTRAL-FILTERING
SENSOR CONCEPT.

DETECTED
OUTPUT
SIGNAL

[F_1 IS SIGNAL FOR FIRST MEASURAND VALUE]
[F_2 IS SIGNAL FOR SECOND MEASURAND VALUE]

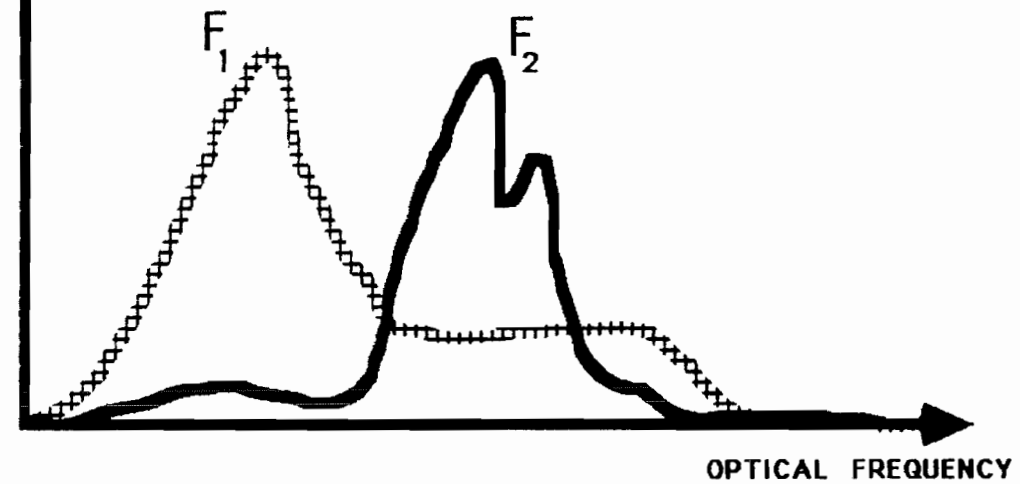


ILLUSTRATION OF THE BASIC CONCEPT
OF A SPECTRAL FILTERING SENSOR

ANALOGUE SPECTRAL FILTERING SYSTEMS:

**(NARROW-BAND FILTERED OUTPUT WITH CENTRE
WAVELENGTH DEPENDENT ON MEASURAND)**

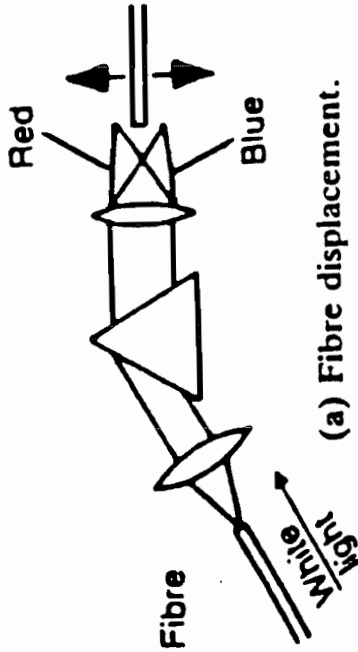
E.G. * ROTATING-GRATING SHAFT-ANGLE ENCODER

*** ZONE-PLATE TRANSLATIONAL-POSITION
ENCODER**

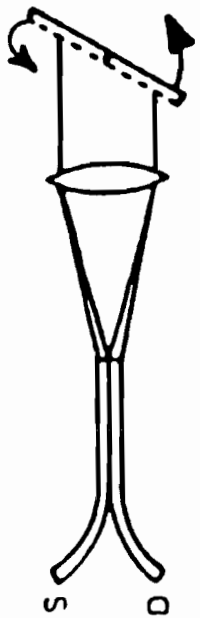
*** CHRISTIANSEN FILTER TEMPERATURE SENSOR**

*** GRADED INTERFERENCE FILTER DISPLACEMENT
SENSOR**

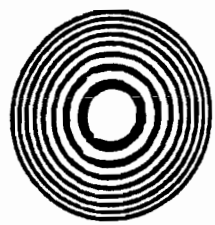
WAVELENGTH-BASED SENSORS.



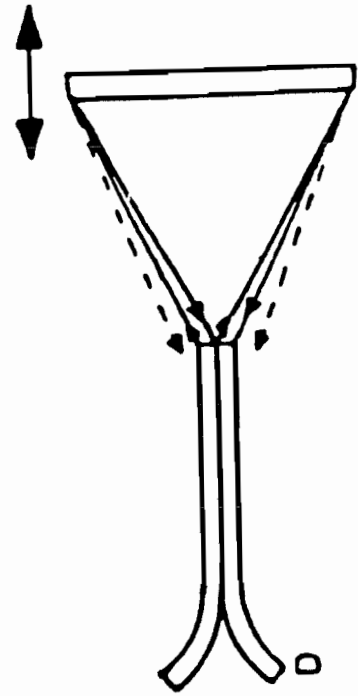
(a) Fibre displacement.



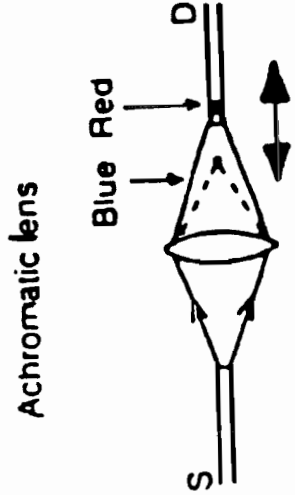
(b) Grating rotation.



Zone plate

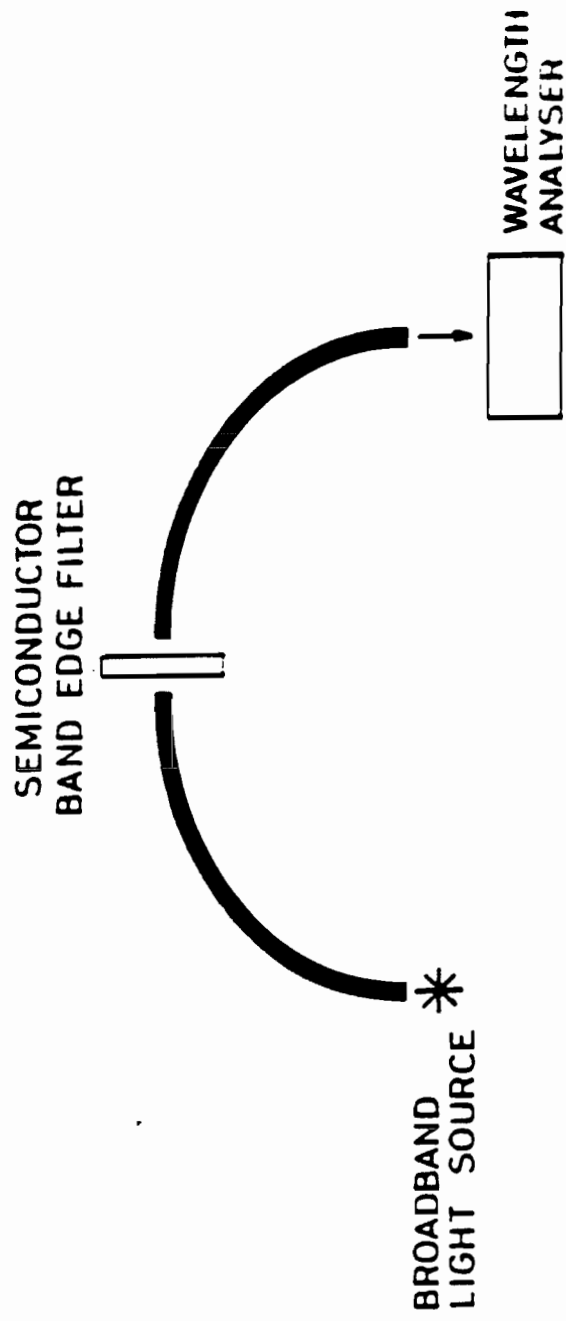


(c) Zone plate displacement.



(d) Achromatic lens and fibre displacement.

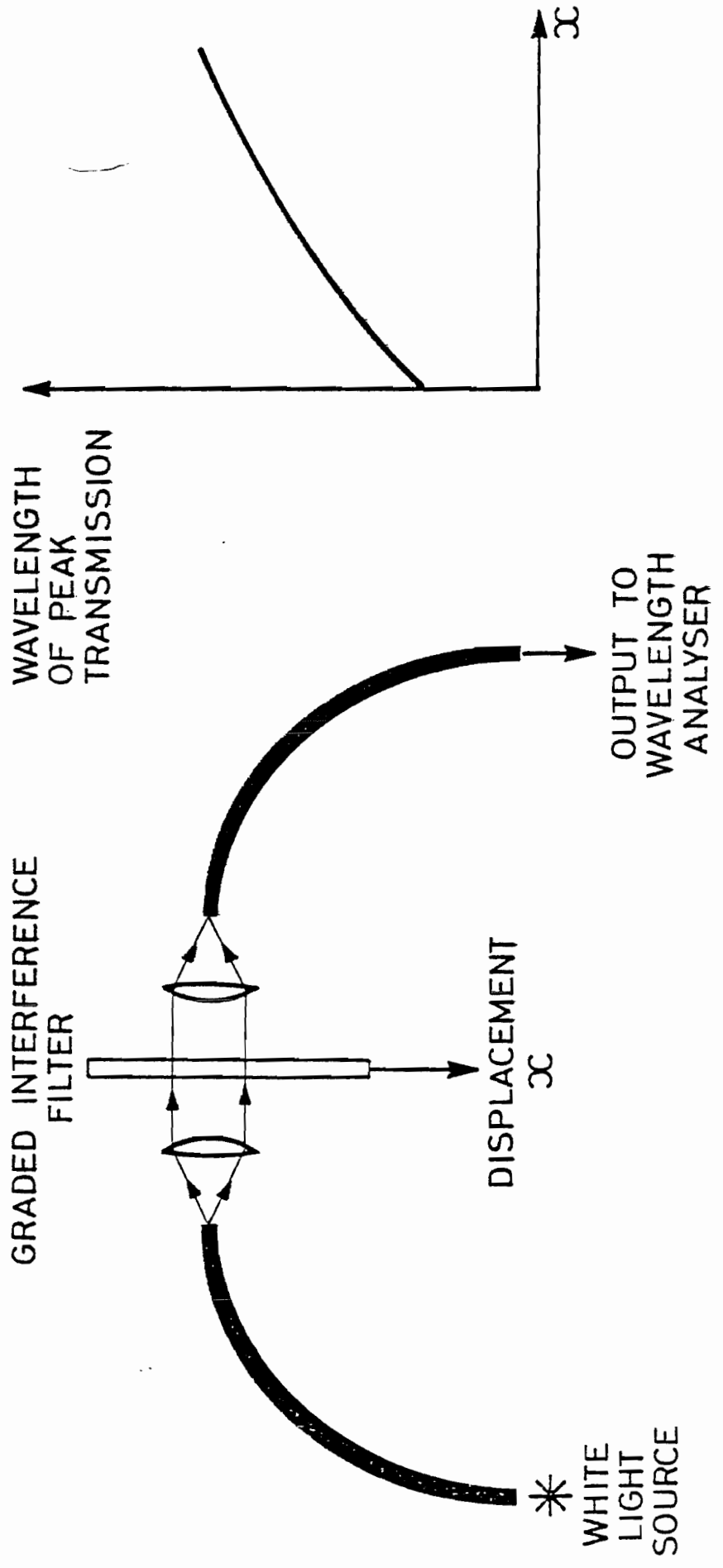
THIS DRAWING IS REPRODUCED WITH THANKS FROM "OPTICAL FIBER SENSORS", PUBLISHED BY ARTECH HOUSE. EDITORS: J P DAKIN, B CULSHAW. DIAGRAM TAKEN FROM CHAPTER BY B E JONES, R MEDLOCK, R SPONCER



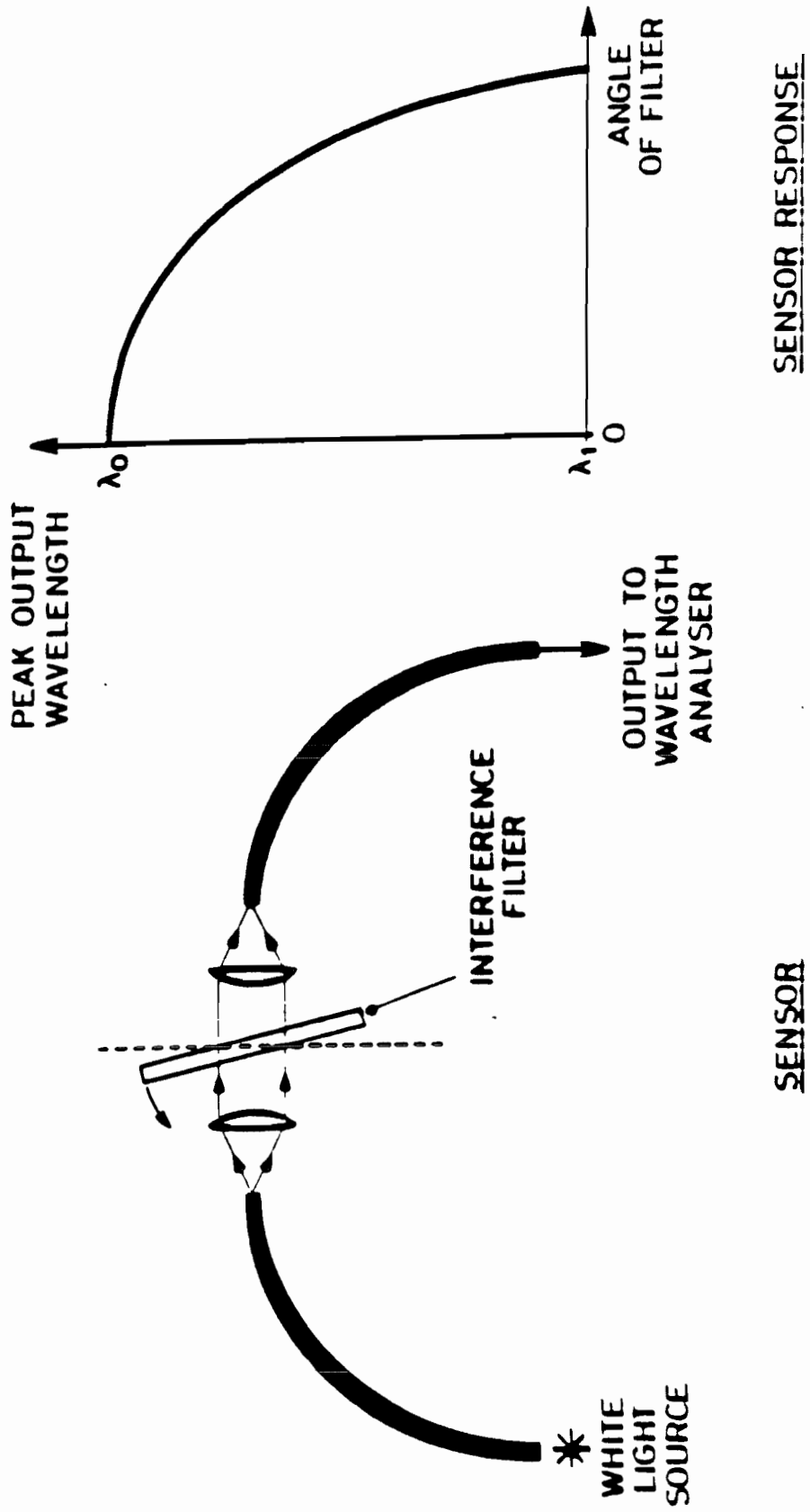
SPECTRAL FILTERING TEMPERATURE SENSOR
USING SEMICONDUCTOR BAND EDGE FILTER

(SAASKI & SKAUGSET)

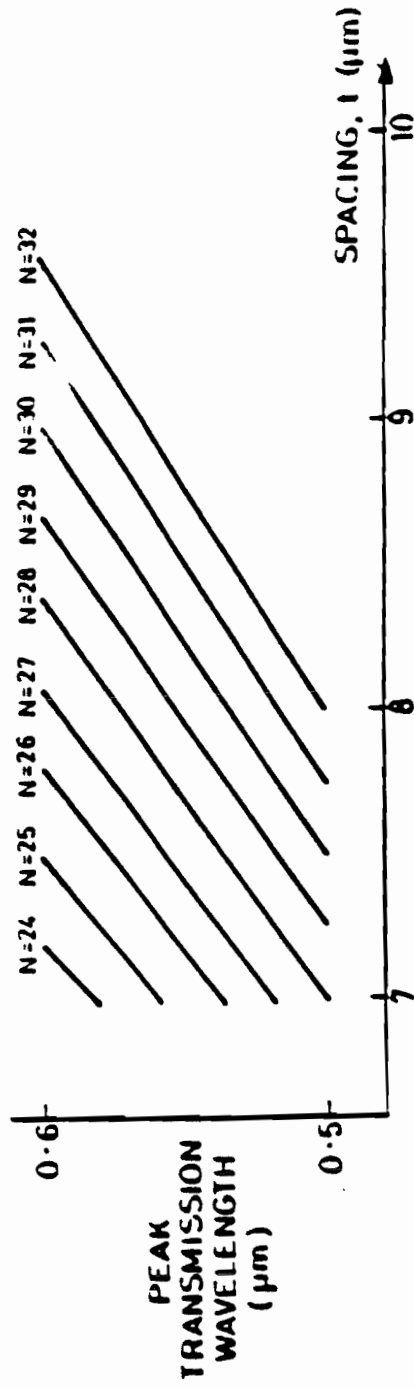
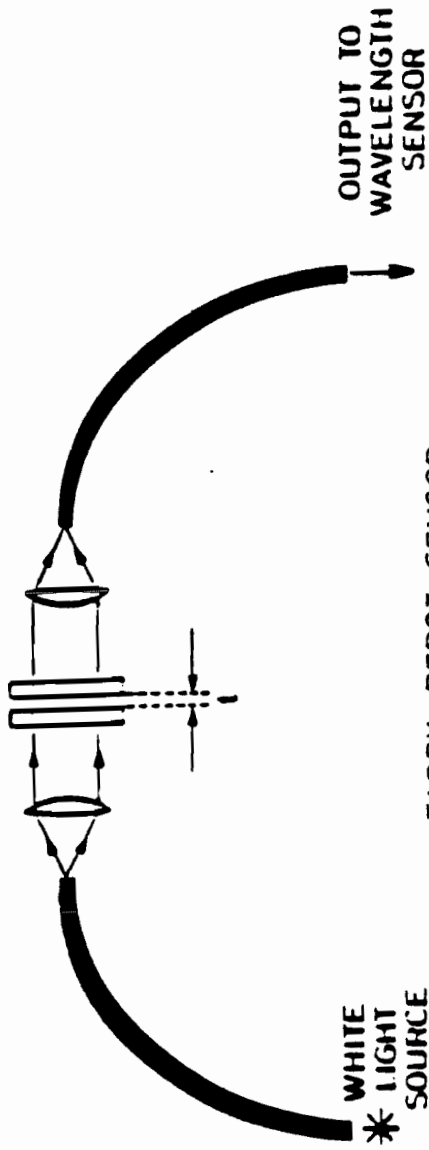
(ALTERNATIVELY MAY USE LIQUID CRYSTAL FILTER AFTER JOHNSON & ROZZELL)



DISPLACEMENT SENSOR USING GRADED INTERFERENCE FILTER



SENSOR USING ROTATING INTERFERENCE FILTER



FABRY - PEROT SENSOR (GLEN, MOREY & SNITZER, NASA CR-159468)

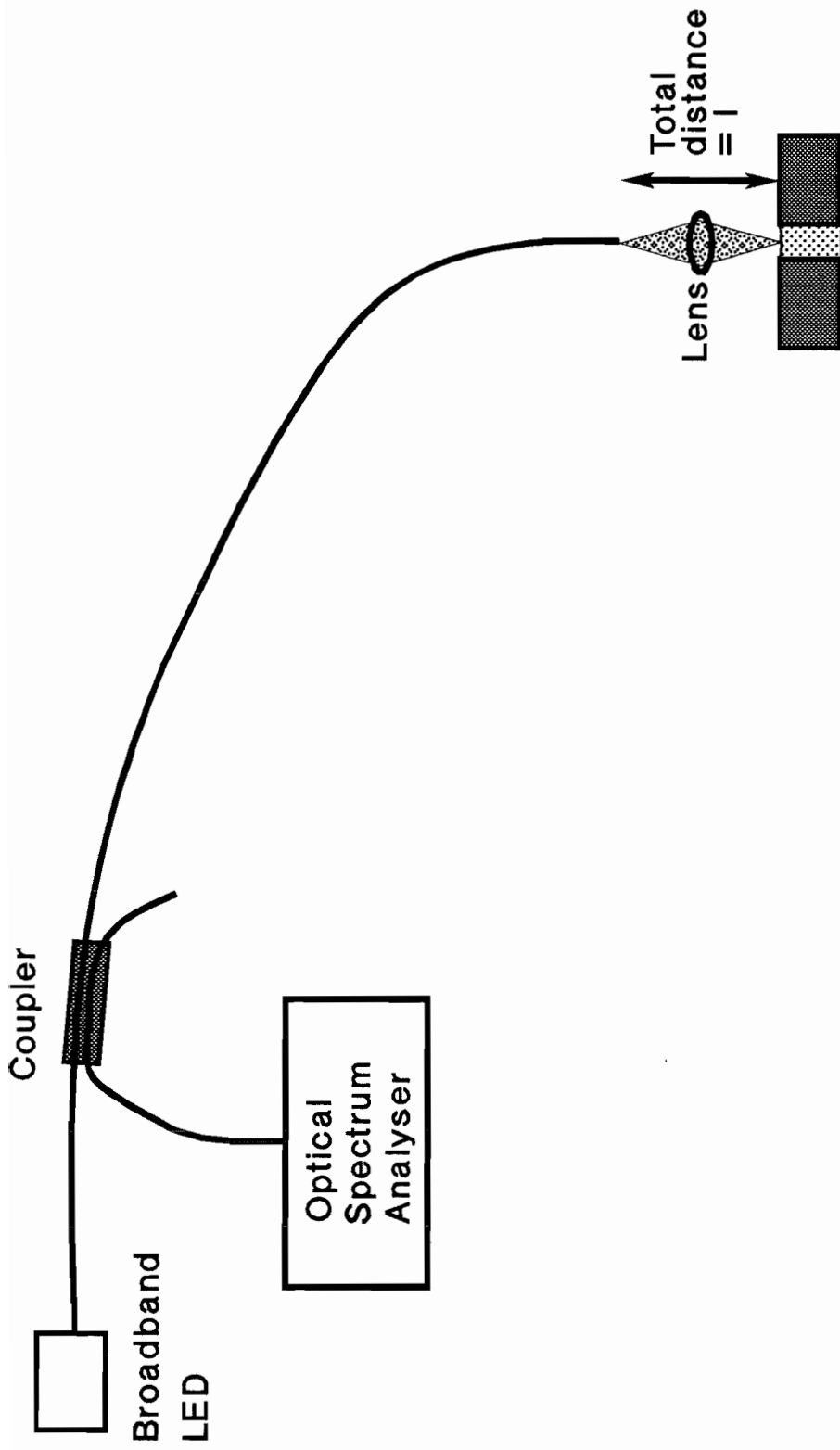
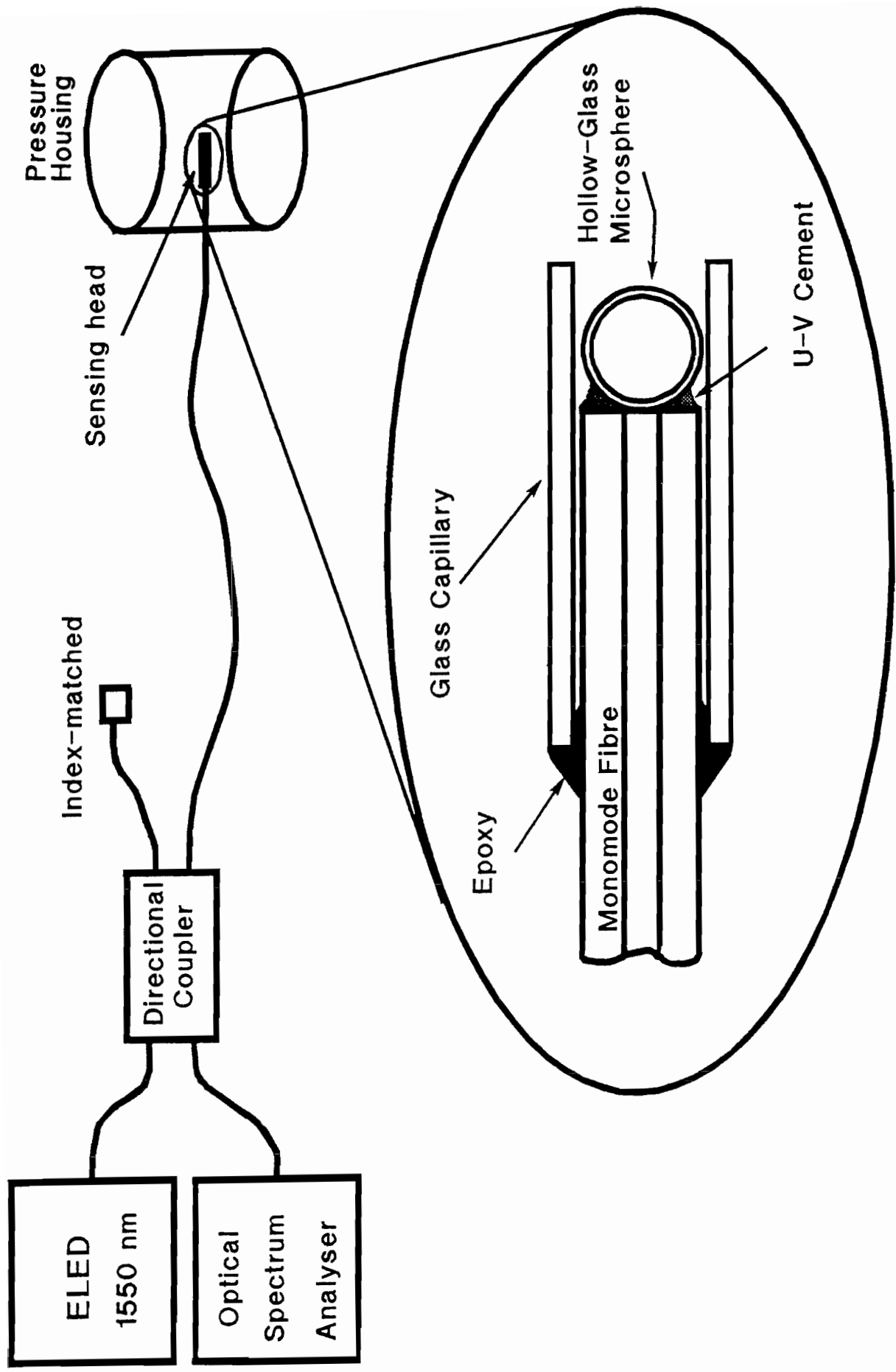


Fig 2. Arrangement for distance monitoring, using spectral analysis



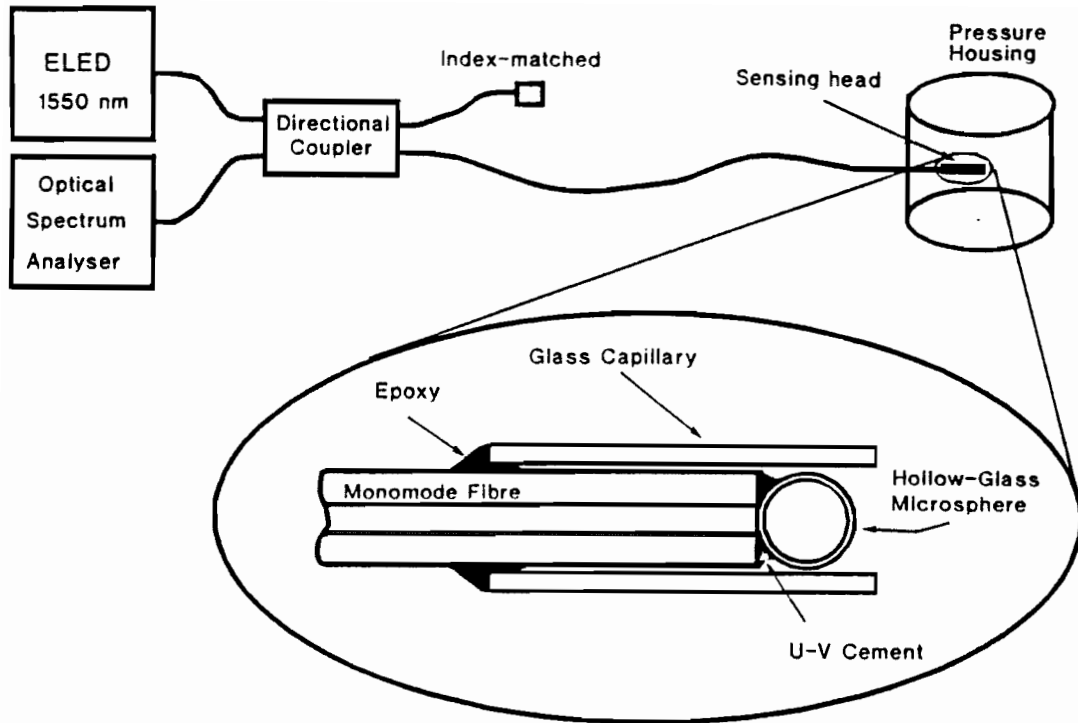


Fig 1. Schematic of the hollow-glass microsphere pressure sensor

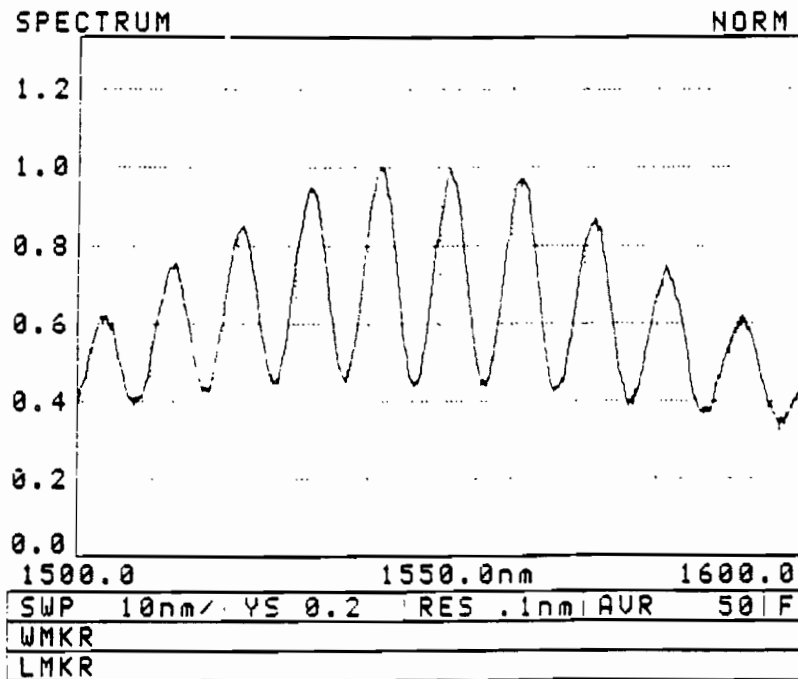


Fig.2 Reflected spectrum from sensing probe

Wavelength shift of maxima due to application of pressure:

$$\Delta \lambda = \frac{\lambda}{d} \frac{\delta d}{\delta P} \Delta P$$

Diameter change due to pressure-induced strain in hollow sphere:

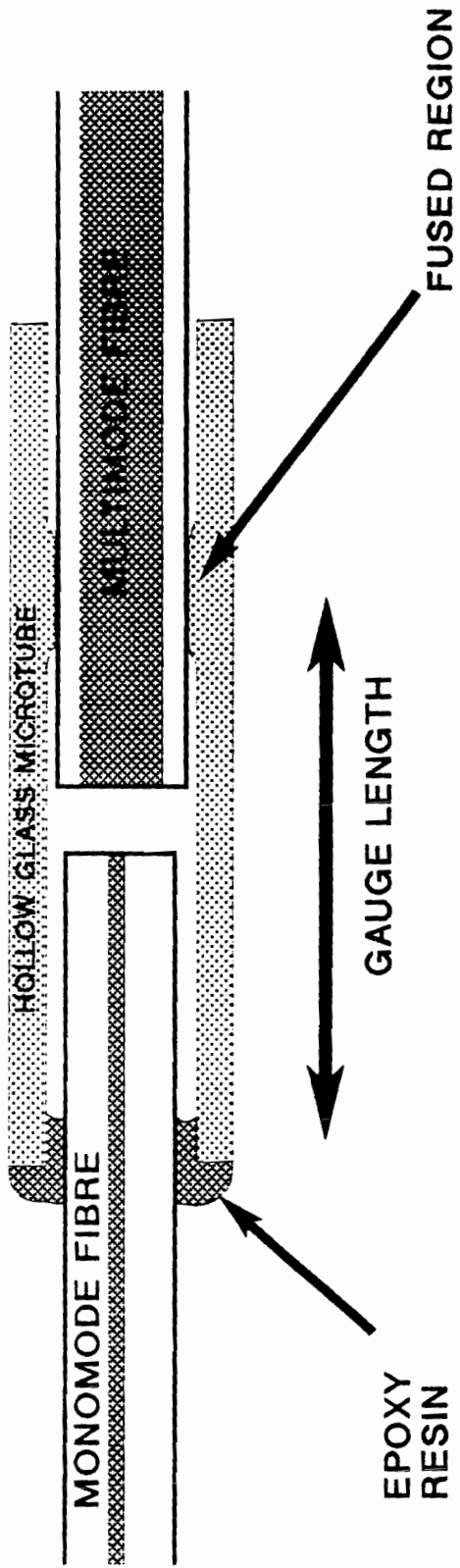
$$\Delta d = - \frac{P d^2 (1 - \nu)}{4 Y t}$$

ν = Poisson ratio, Y = Young's modulus, t = sphere wall thickness.

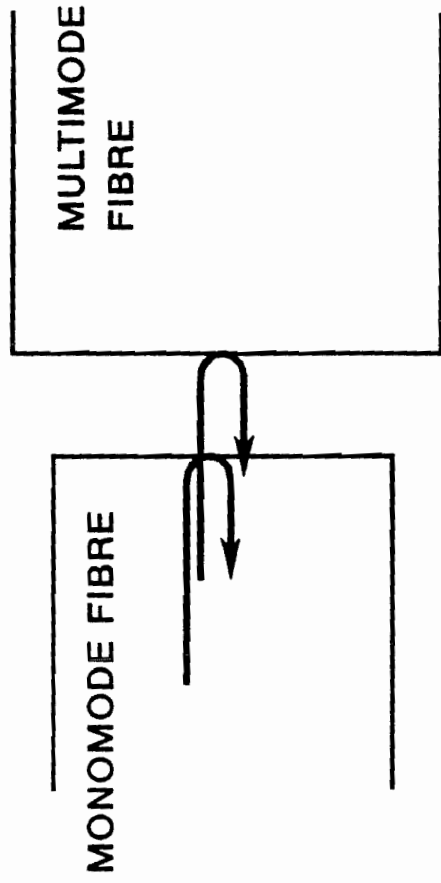
Wavelength shift of maxima due to pressure and temperature:

$$\Delta \lambda = - \frac{\lambda d (1 - \nu)}{4 Y t} \Delta P$$

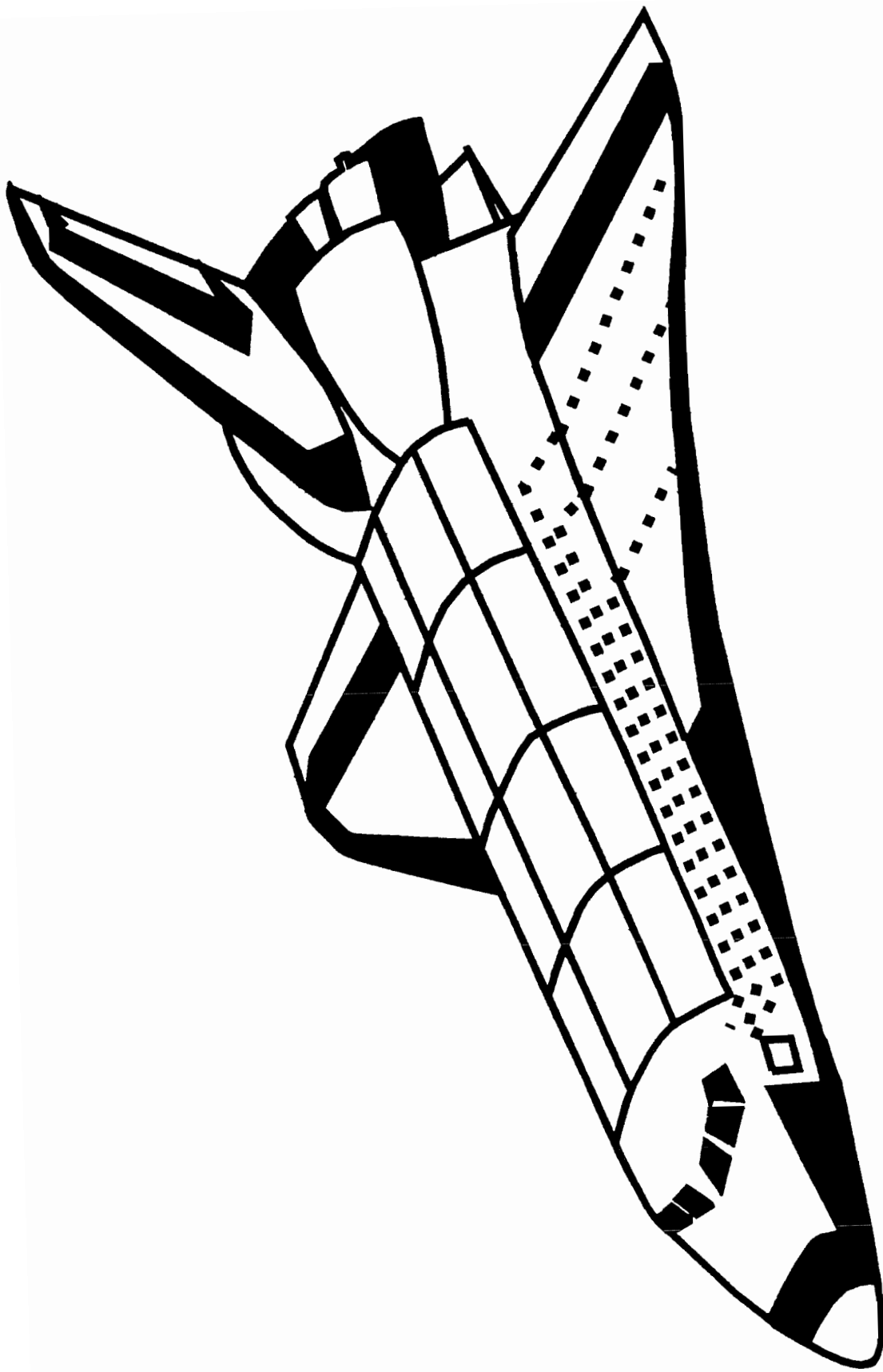
$$\Delta \lambda = \frac{\lambda}{d} \frac{\delta d}{\delta T} \Delta T$$



FIBRE SENSOR OF CLAUS et AL, VIRGINIA TECH, USA.



SCHEMATIC OF INTERFERING LIGHT BEAMS REFLECTED FROM EACH FIBRE END SURFACE.



**SCHEMATIC OF SMART SKINS CONCEPT FOR
MONITORING OUTER SURFACE STRUCTURES
OF AEROSPACE AND OTHER VEHICLES.**

FIBRE GRATING SENSORS

Fibre grating sensors use optically-written structures in the light-guiding core of the optical fibre, which act as very narrow band optical filters. These have a very narrow band reflection spectrum (typically 0.1 to 1nm bandwidth) and usually have a peak back-reflection between 5% and 100% . In transmission, they have a similar bandwidth, but act as blocking filters over a similar narrow band.

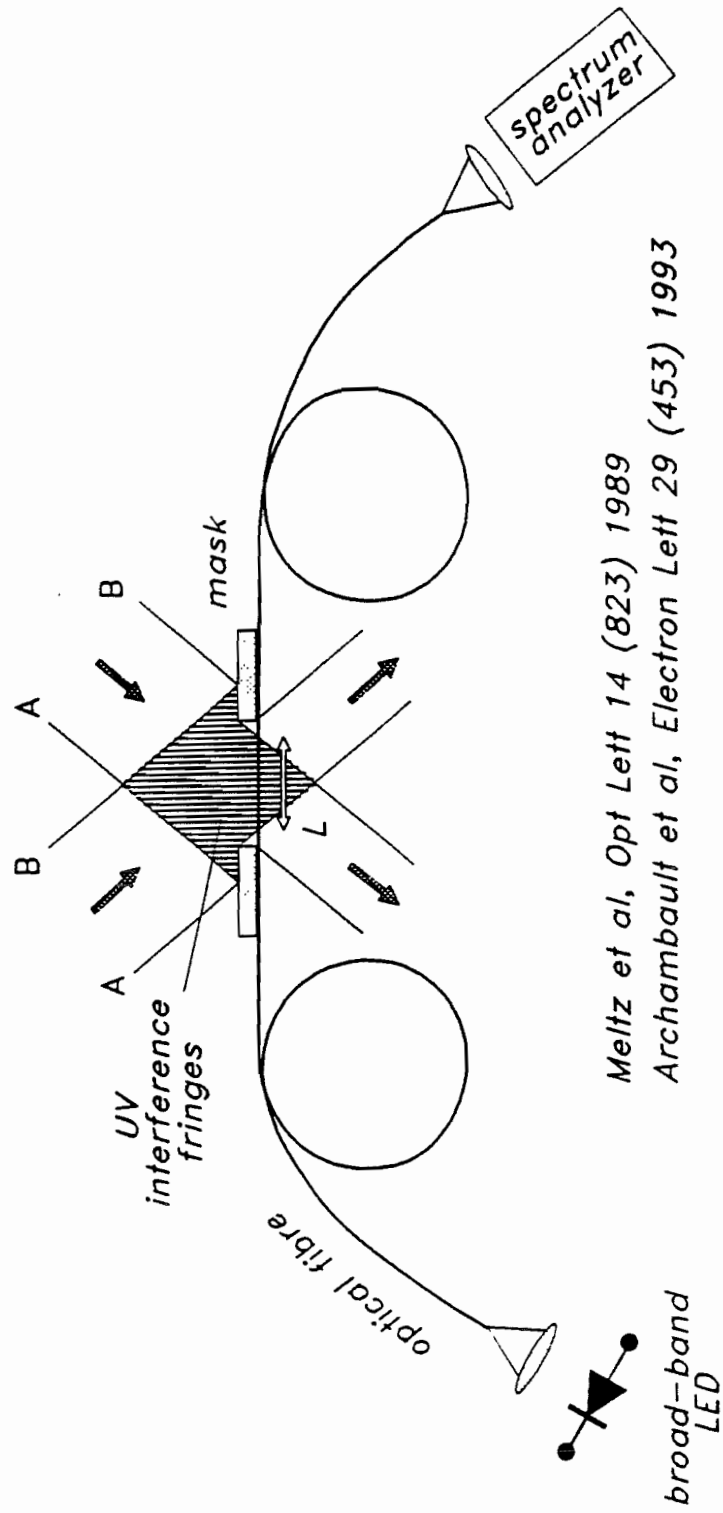
The grating consists of a short region of fibre (typically 1 to 10 mm) where the refractive index of the fibre core has been modified to have a periodic variation as a function of distance in the longitudinal (ie. axial) direction. This variation is achieved by lateral illumination of a fibre with two converging beams of ultraviolet light, either using optical convergence of two separate beams (see next page).

[NOTE: It is now more common to create two such beams by diffraction of a single beam in a phase mask]

The beams interfere to give fringes with the desired spatial variation of optical intensity and this gives rise to a corresponding refractive index variation in the fibre as a result of a photo-refractive effect. This effect is small, yet significant in germania-doped silica fibres, as the periodic small refractive index variations build up coherently to cause significant reflection of light at the Bragg wavelength, ie the wavelength at which each low-intensity reflected wavelet from each undulation in refractive index adds coherently to all the others from other parts of the grating. It is this need for constructive addition of back-reflected wavelets that gives rise to the narrowband filtering effect; the longer the grating, the narrower the filter and the more efficient the reflection for a given index change.

The in-fibre grating is an excellent sensing element as it is tiny, and can be configured to sense both thermal and strain influences, and is even being considered as the basis for optical hydrophones. Although optically written, the gratings will withstand elevated temperatures of several hundred degrees C, but of course, the wavelength varies with temperature when heated or cooled.

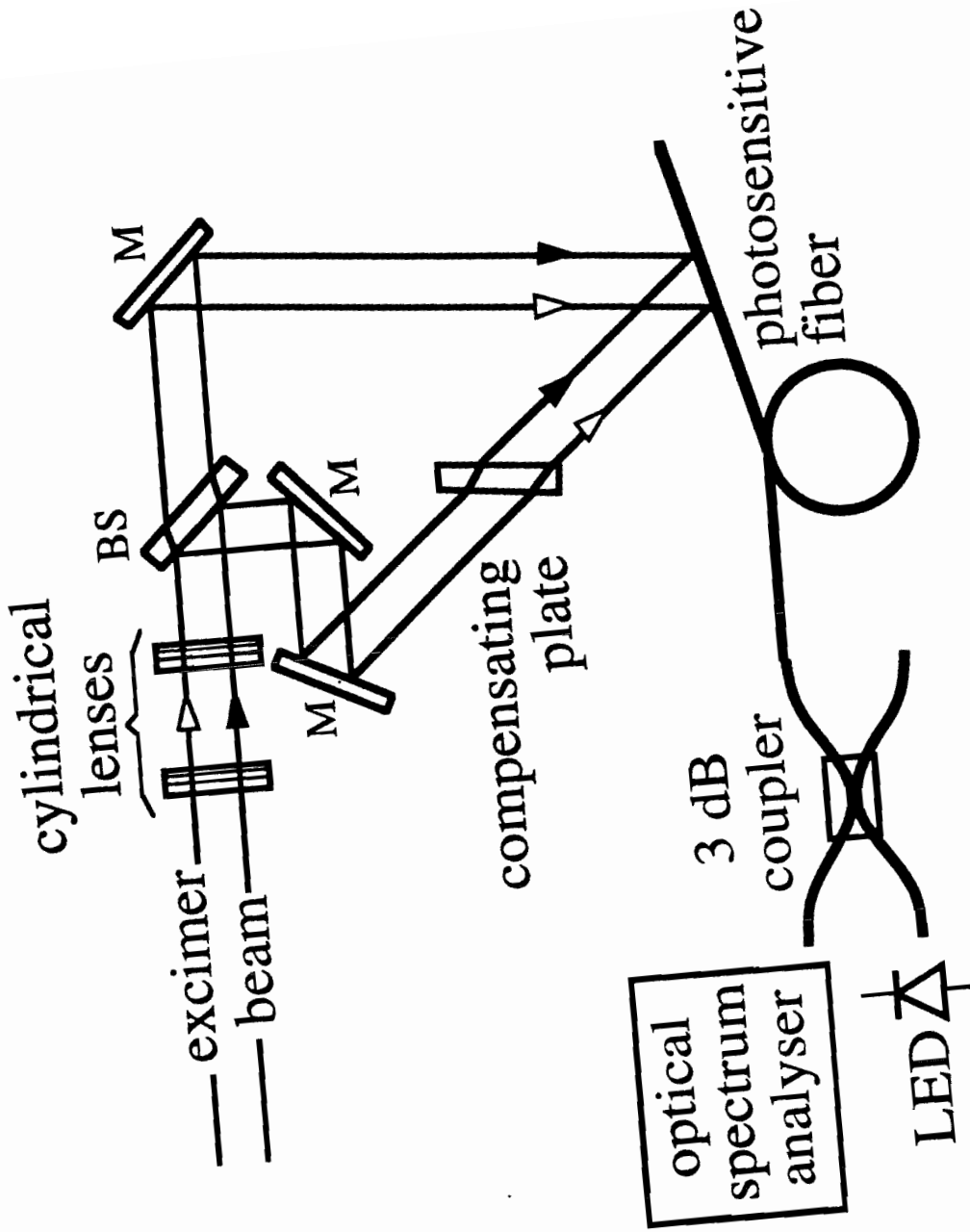
Interferometric Inscription of Fibre Gratings by UV laser light



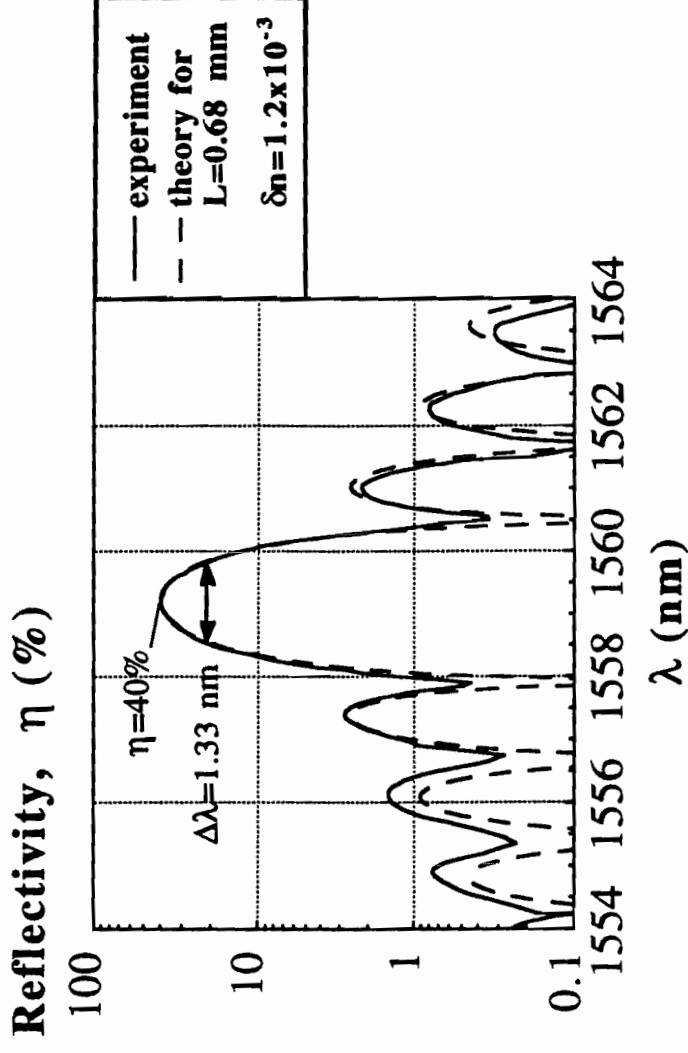
Meltz et al, Opt Lett 14 (823) 1989

Archambault et al, Electron Lett 29 (453) 1993

Experimental setup



Reflection spectrum of short Type I grating showing side lobes (experiment + theory)



- longer grating \rightarrow higher η , lower $\Delta\lambda$
- larger $\delta n \rightarrow$ higher η , higher $\Delta\lambda$

PHOTOREFRACTIVE FIBRE GRATING

Effect of temperature, T

$$\frac{\Delta \lambda_g}{\lambda_g} = (\alpha + \xi) \Delta T$$

λ_g = peak grating reflection wavelength

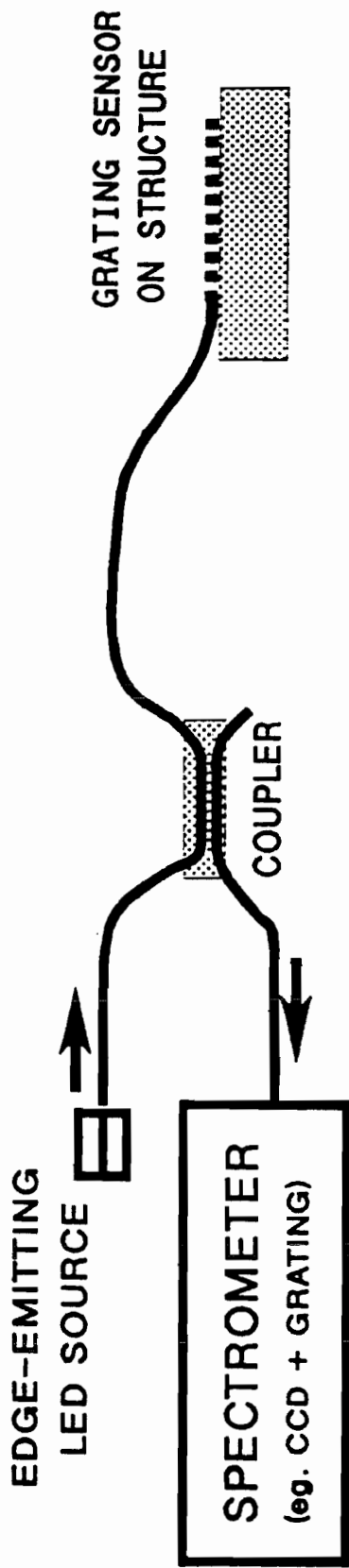
α = thermooptic coefficient

ξ = thermal expansion coefficient

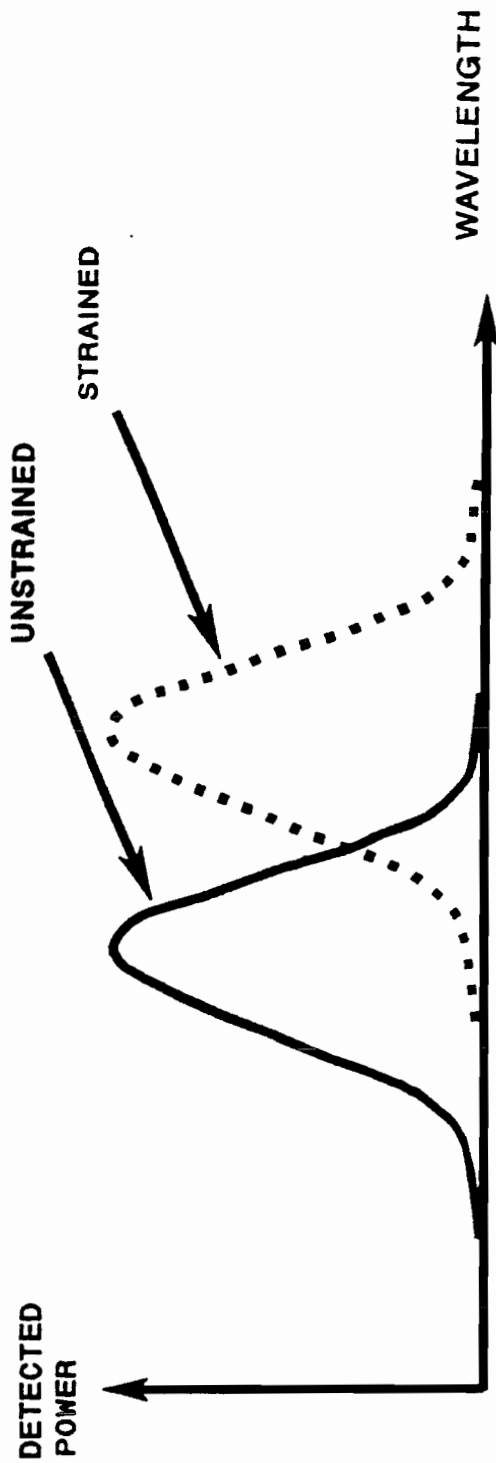
Effect of axial strain, ϵ

$$\frac{\Delta \lambda_g}{\lambda_g} = (1 - P_e) \epsilon$$

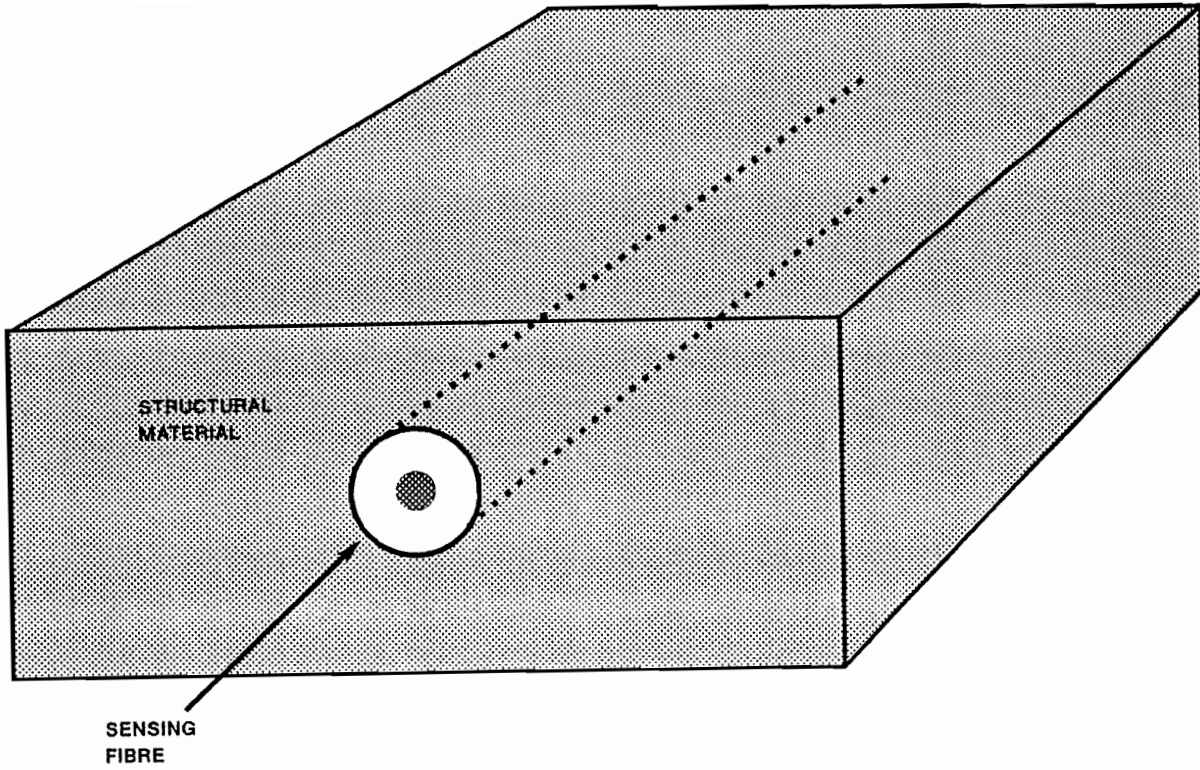
P_e = effective photoelastic coefficient



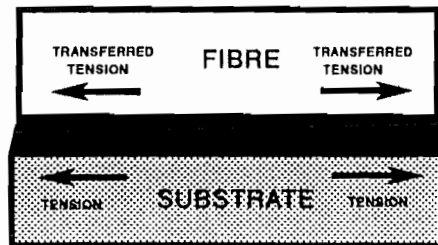
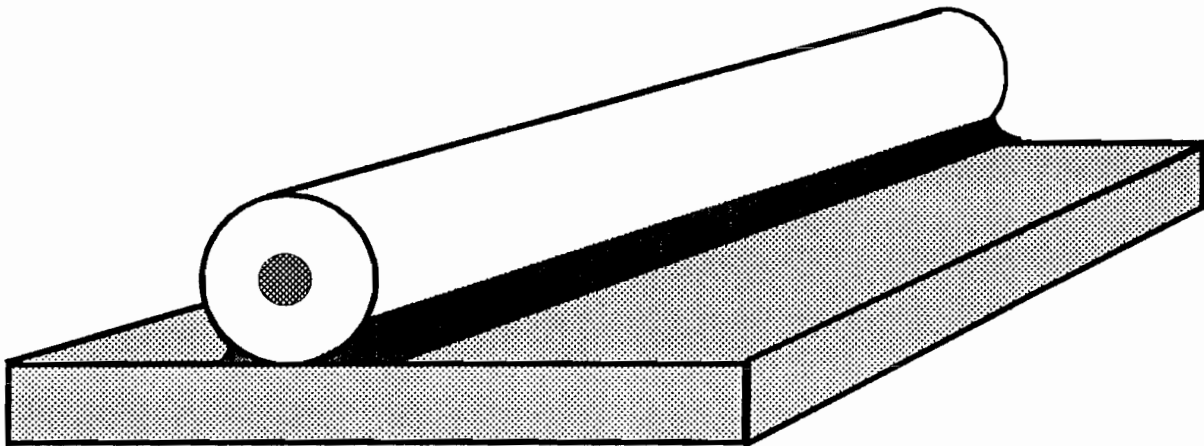
SYSTEM FOR THE INTERROGATION OF GRATING WAVELENGTH, USING SPECTROMETER



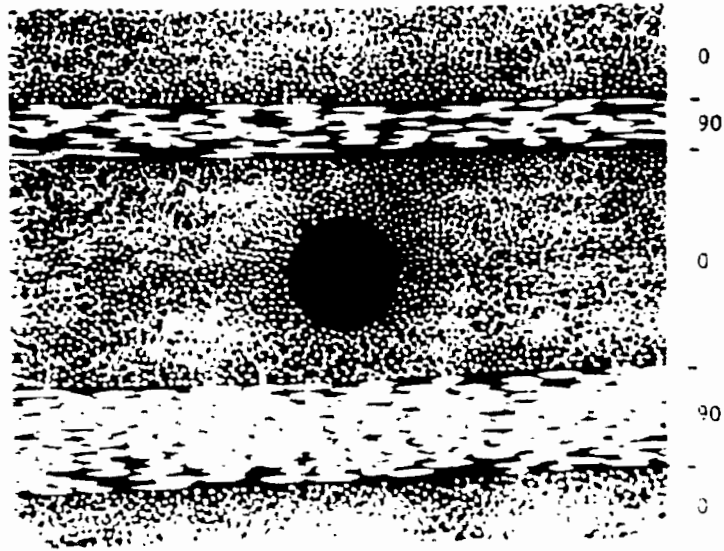
RESPONSE OF SYSTEM SHOWN IN ABOVE DIAGRAM, AS GRATING WAVELENGTH CHANGES



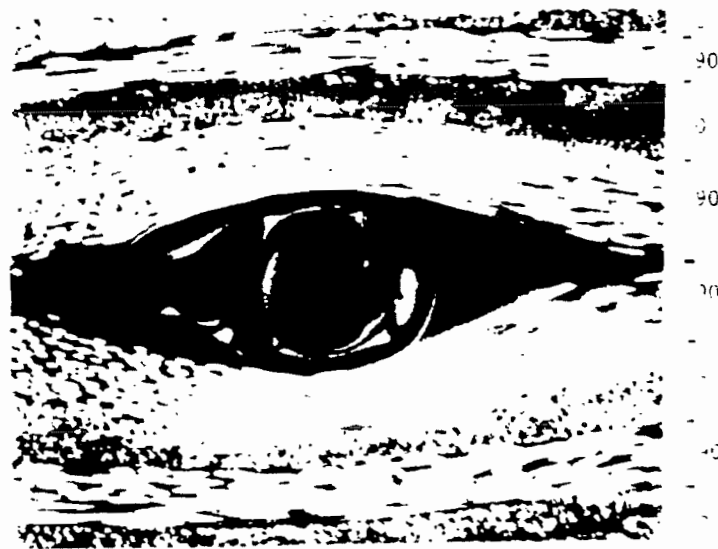
SCHEMATIC OF EMBEDDED FIBRE OPTIC STRAIN GAUGE



SCHEMATIC OF FIBRE STRAIN GAUGE BONDED TO A SURFACE



(a)

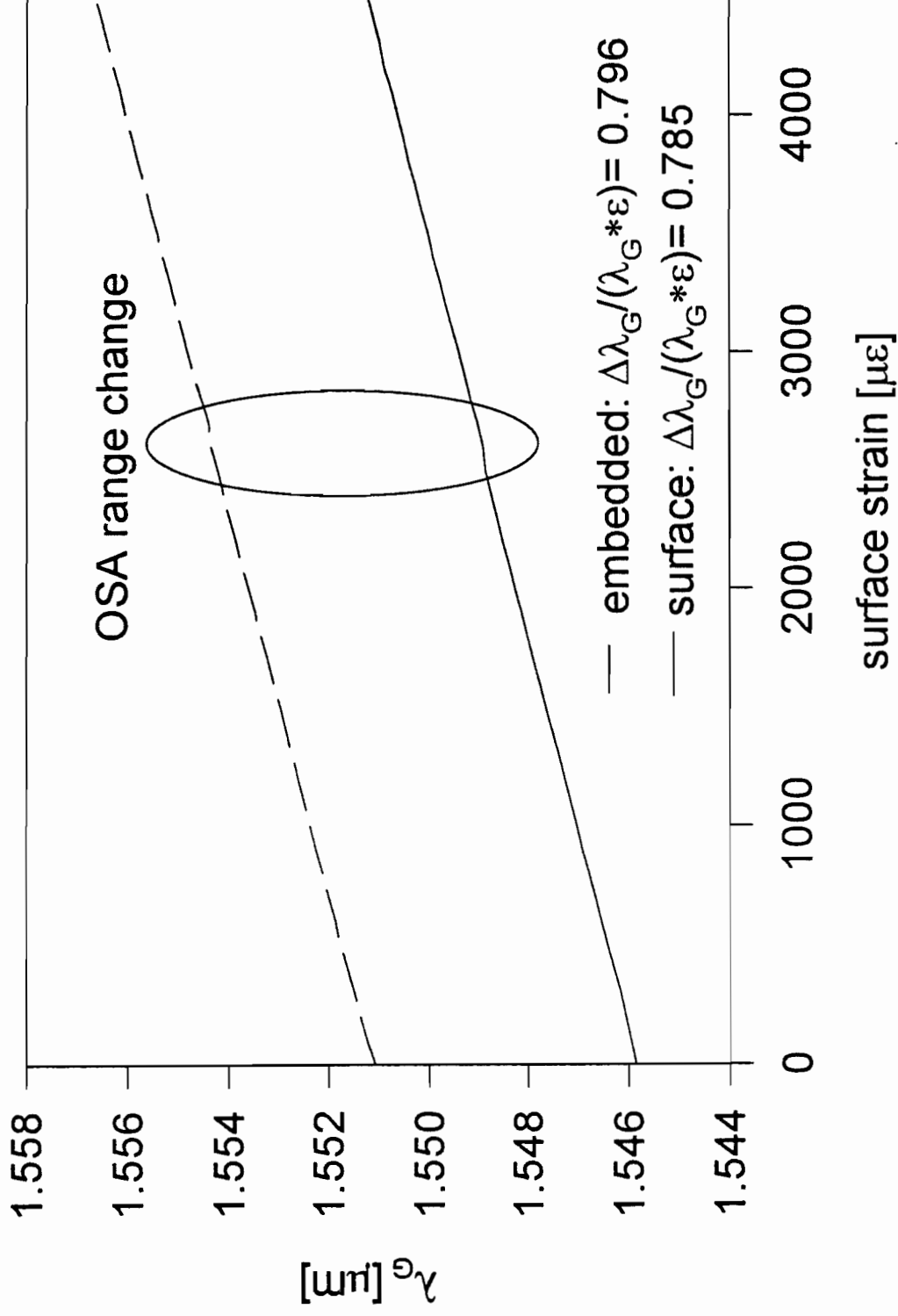


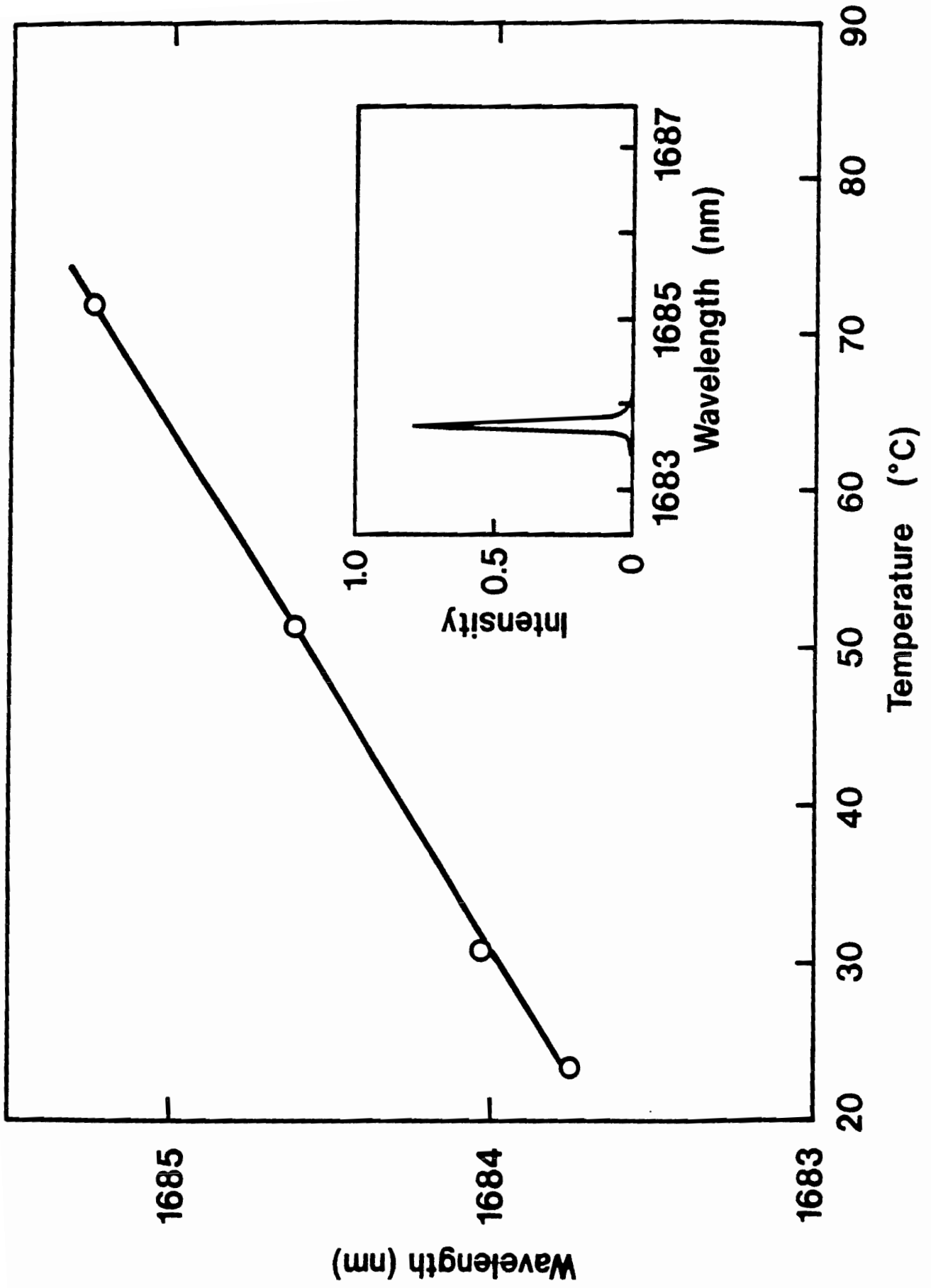
(b)

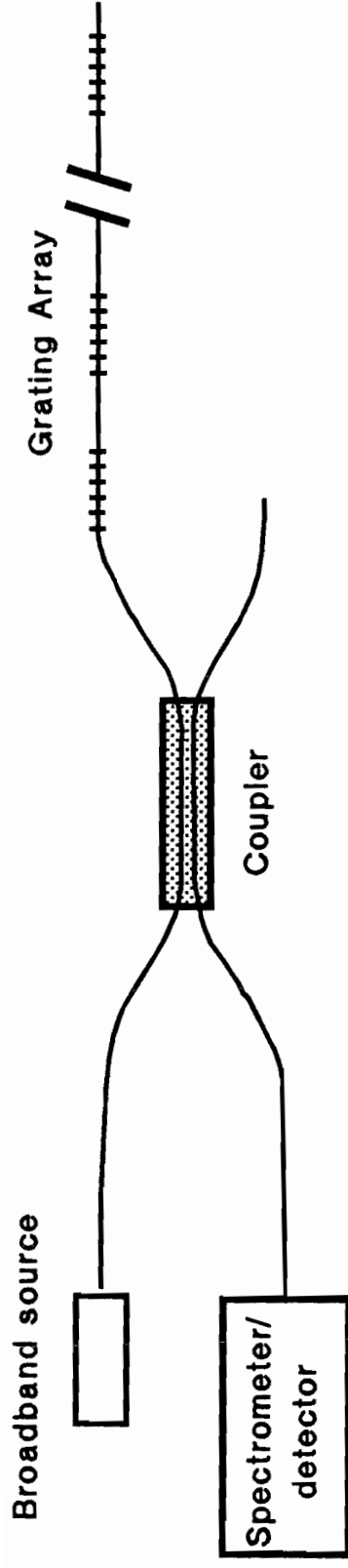
Fig. 18.7 Cross sections through typical composite materials in which optical fibres have been embedded. In (a) the fiber is parallel to the lay of the reinforcing fibers and in (b) perpendicular. Note the voids in the reinforcing structure introduced in the latter case. (Photo courtesy of UKAEA Harwell Laboratory)

THIS DRAWING IS REPRODUCED WITH THANKS FROM
"OPTICAL FIBER SENSORS" PUBLISHED BY ARTECH HOUSE.
EDITORS: J P DAKIN, B CULSHAW.
DIAGRAM TAKEN FROM CHAPTER BY B CULSHAW.

Surface-Mounted and Embedded Bragg Grating Response







Basic system using broadband source & spectrometer

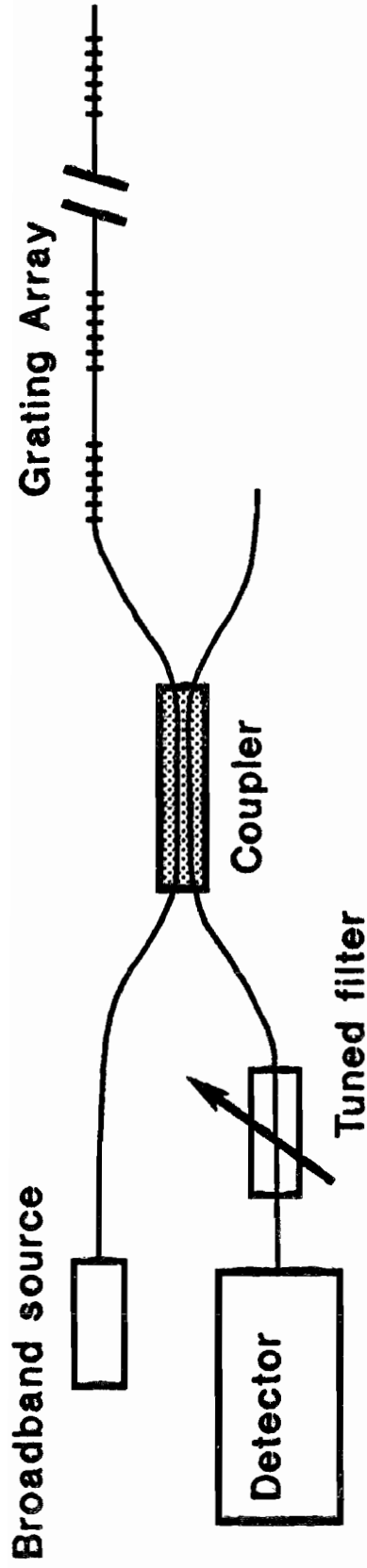
NOTES:

Most common arrangement to use CCD spectrometer

Until recently, this limited use to first fibre window (Si detector)

The pixel spacing of typical CCD devices sets resolution limit

Usually, amplitude of pixel signals are processed to find centroid



Basic system using broadband source and tuned filter

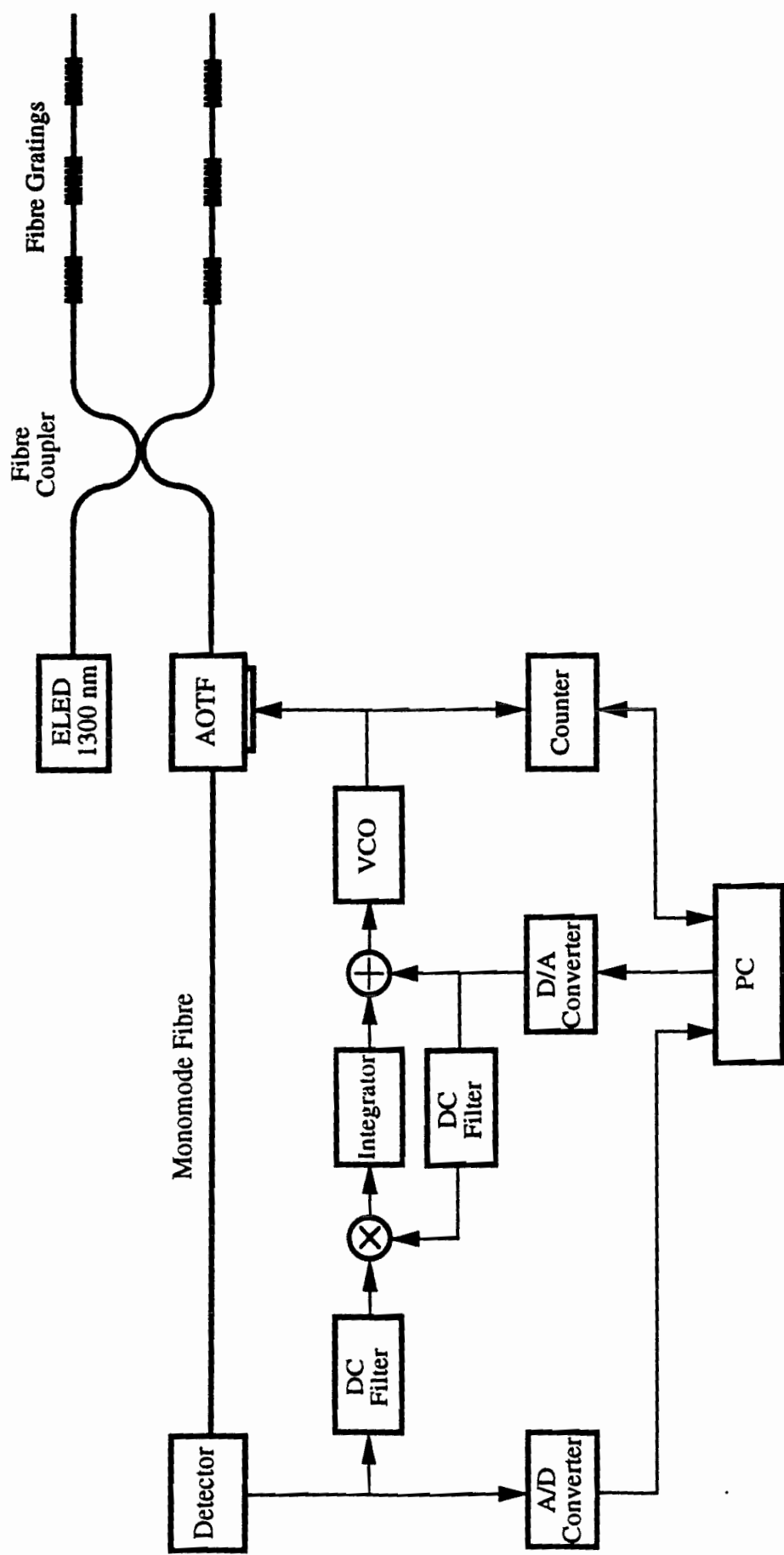
NOTES:

Most common filter types are AOTF (Dakin et Al) and micro-optics or fibre-based Fabry-Perot filters (Kersey et Al)

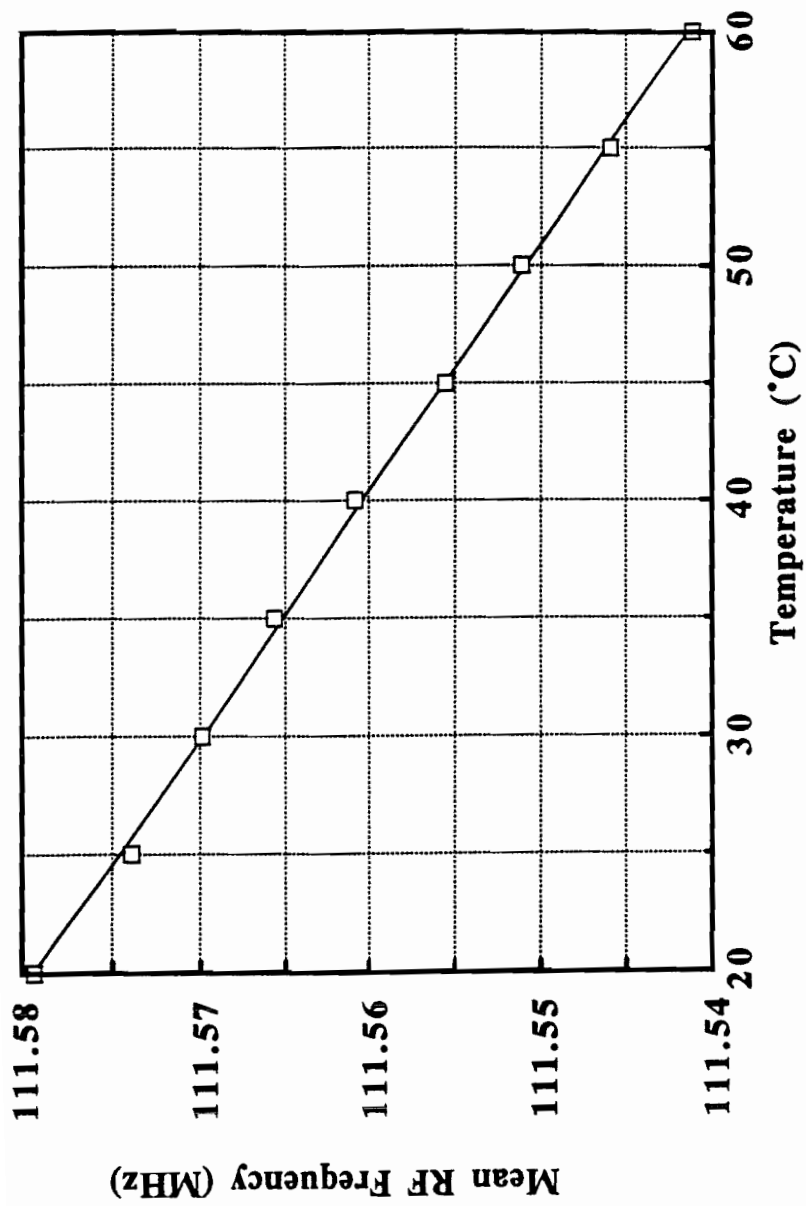
Stretched fibre gratings have also been used as filters (Jackson et Al)

Principle of AOTF Interrogation System:

- The peak transmission wavelength of an AOTF is determined solely by the frequency of an RF drive signal
- When an FSK signal is applied to the AOTF, there is normally an amplitude modulation signal. The amplitude of this is zero when the mean wavelength of the AOTF coincides with the Bragg wavelength of the grating



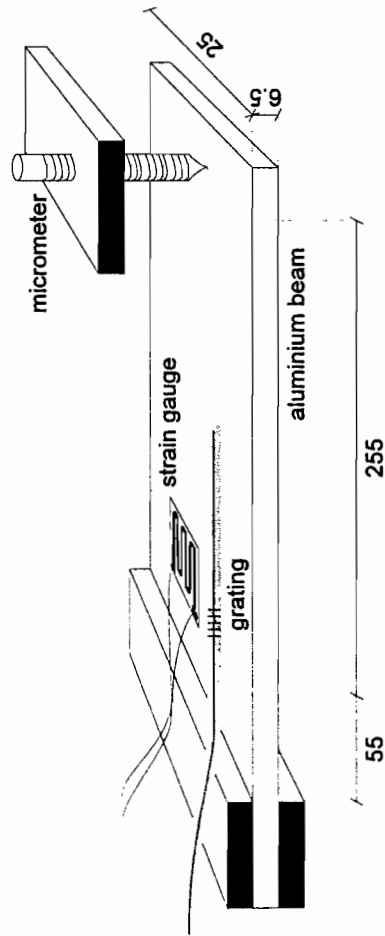
Schematic of our AOTF interrogation system



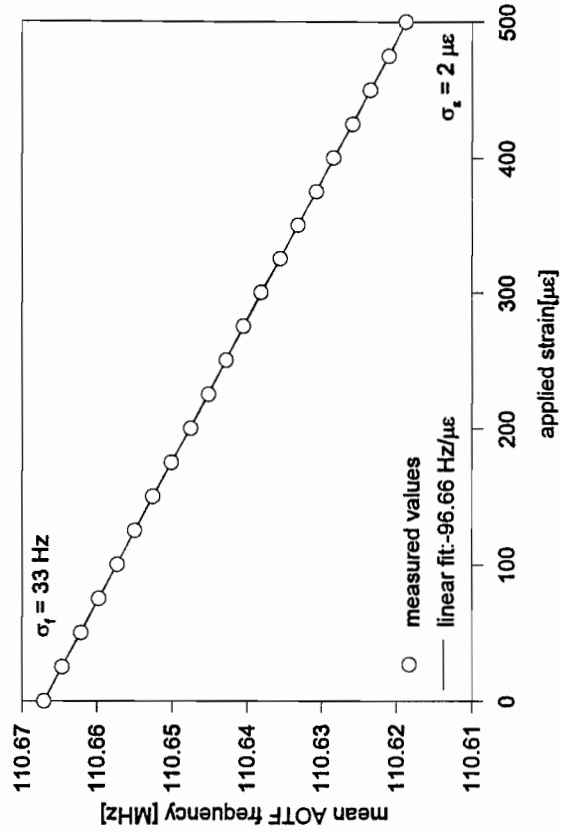
Temperature measurement using AOTF interrogation system

Surface-Mounted Grating

static loading



aluminium cantilever



system response

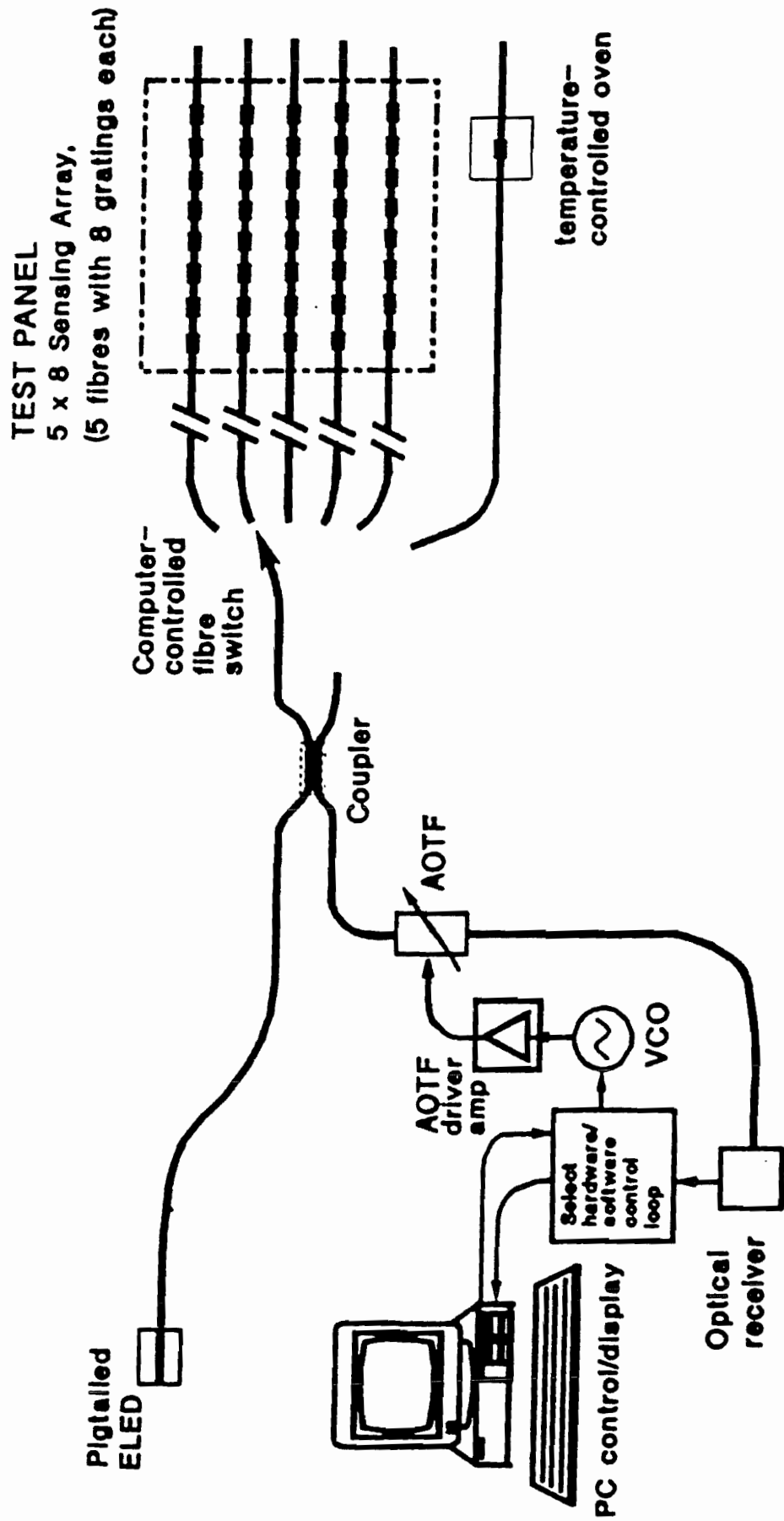
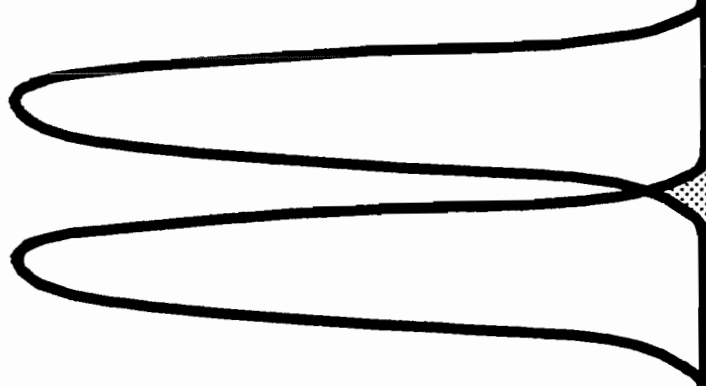
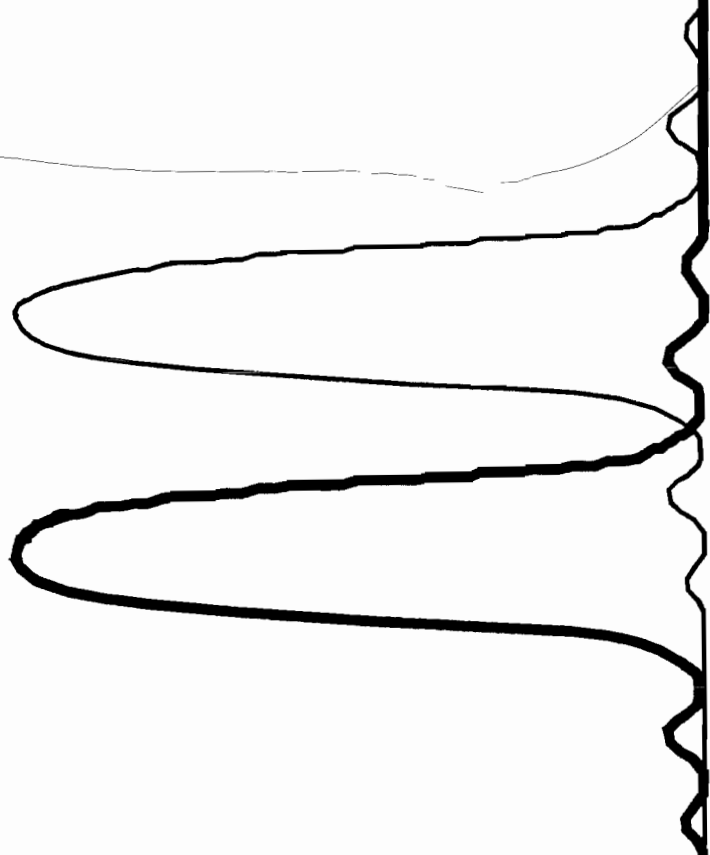


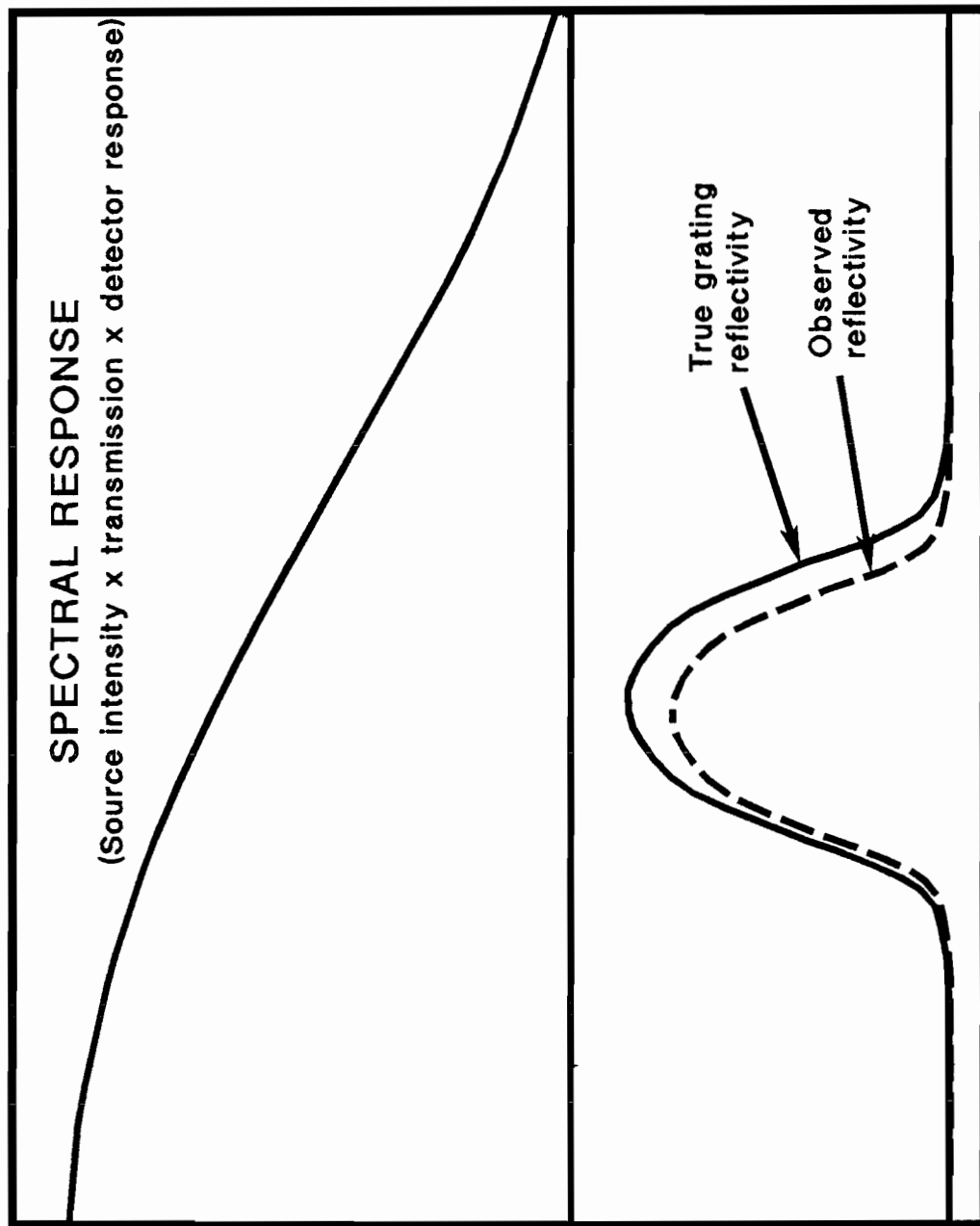
Figure 1 Multiplexed grating interrogation system using AOTF



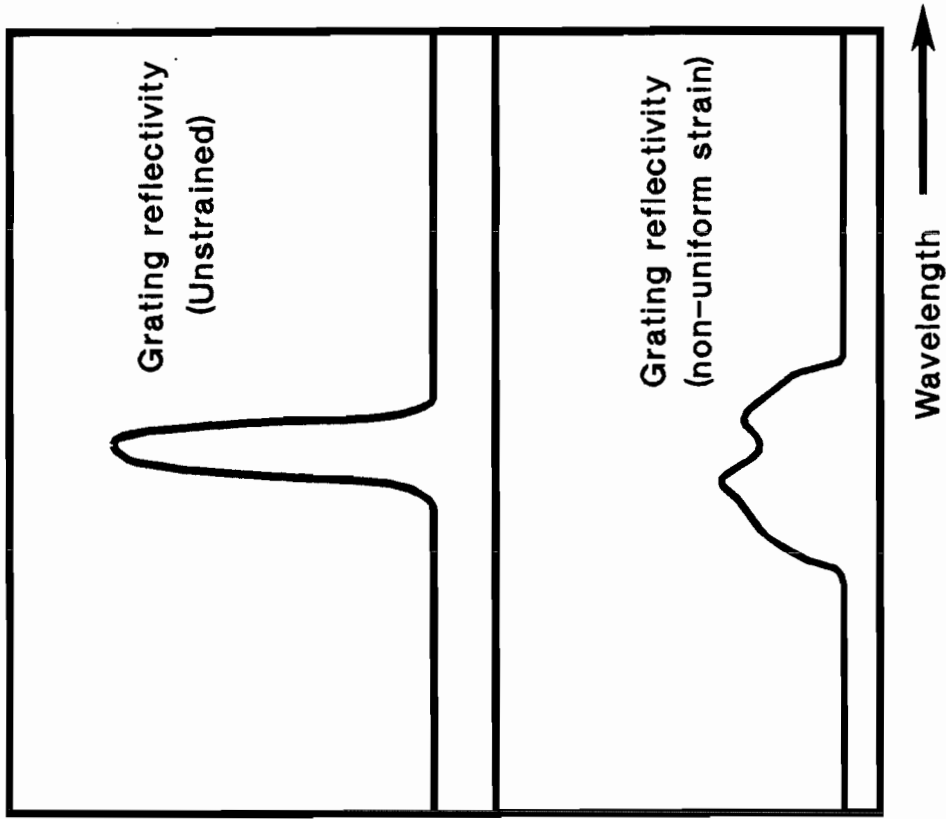
Overlap of two adjacent grating spectra. This will give errors due to shadowing and due to addition of reflected signals. "Shadowing" filters energy from the incident beam. Reflections may be single or multiple, and may add coherently.



Problems due to sidelobes in gratings or
interrogation system response.

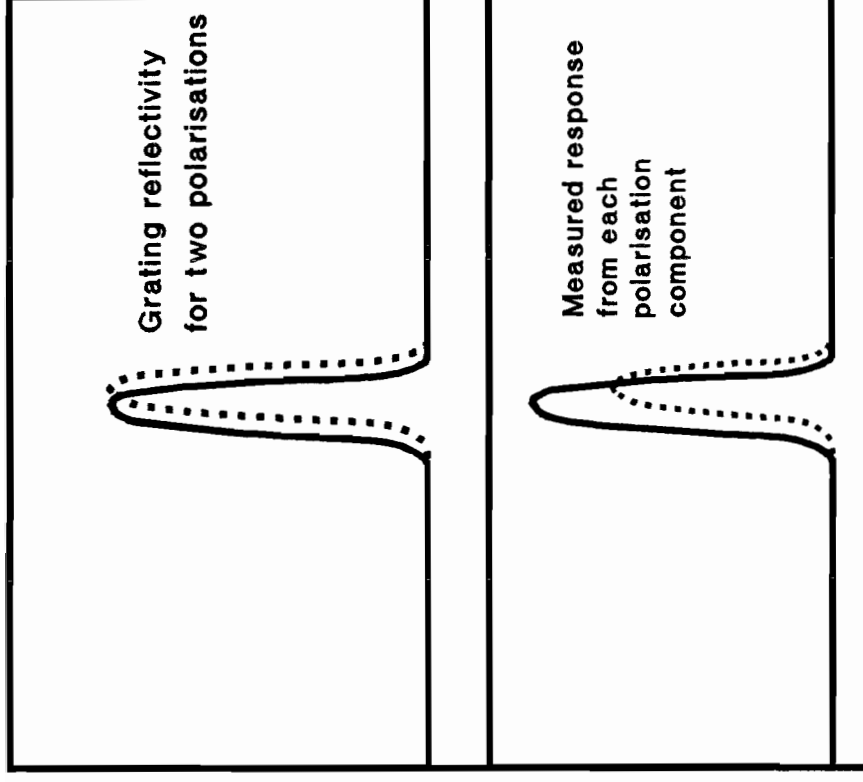


Errors in wavelength measurement due to variations in spectral response of interrogation system



Effects of non-uniform strain in gratings

NOTE: Effects are more likely to be significant in long gratings.
 Embedding of narrow-linewidth gratings requires great care.



Errors due to birefringent gratings

If the grating is birefringent (ie. birefringent fibre) then the interrogation system must measure total reflected power without any sensitivity to polarisation state, or errors will occur. Even with symmetrical fibre and gratings, embedding of sensors may induce birefringence.

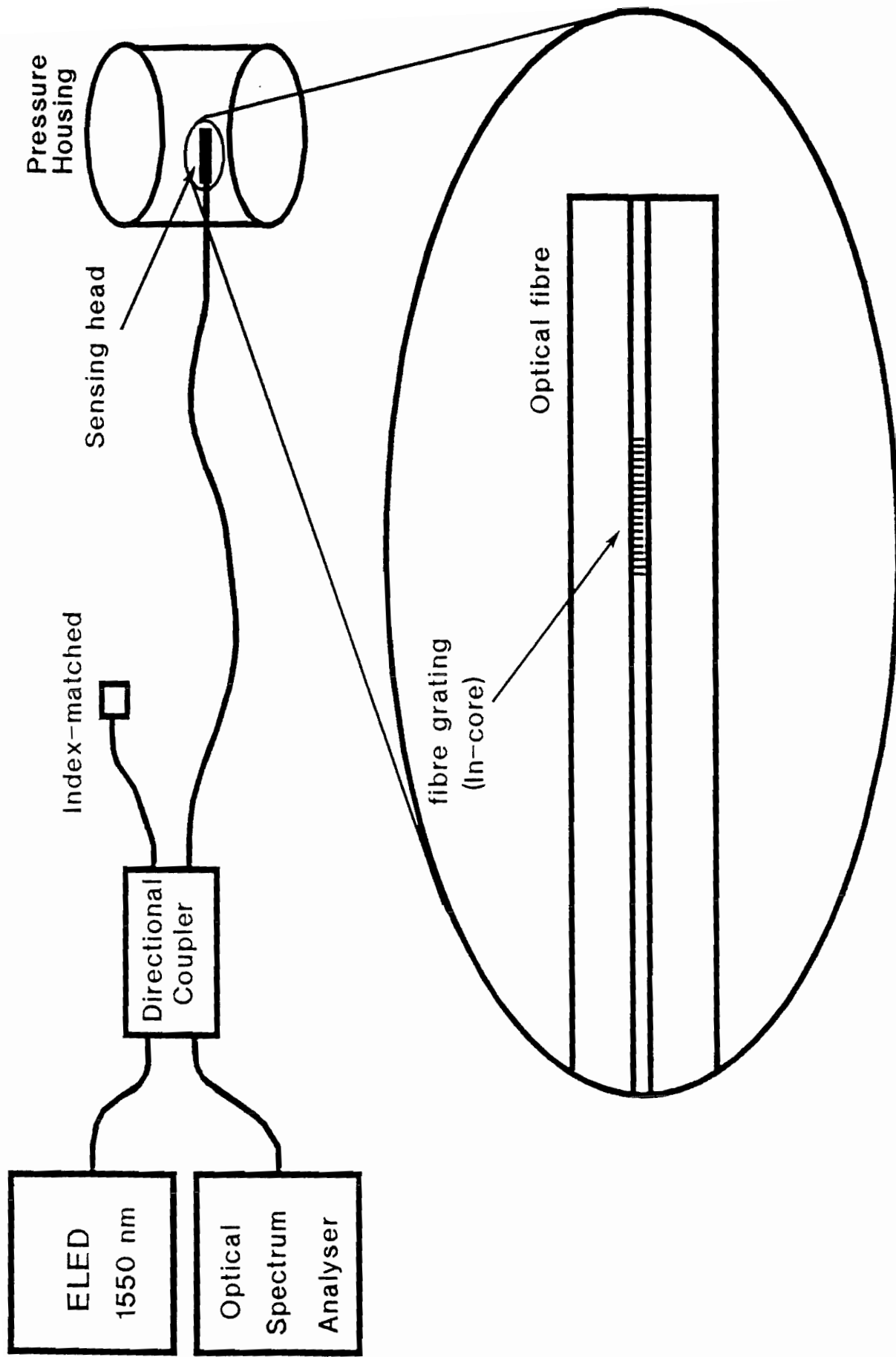


Fig 1. Schematic of the fibre grating pressure sensor

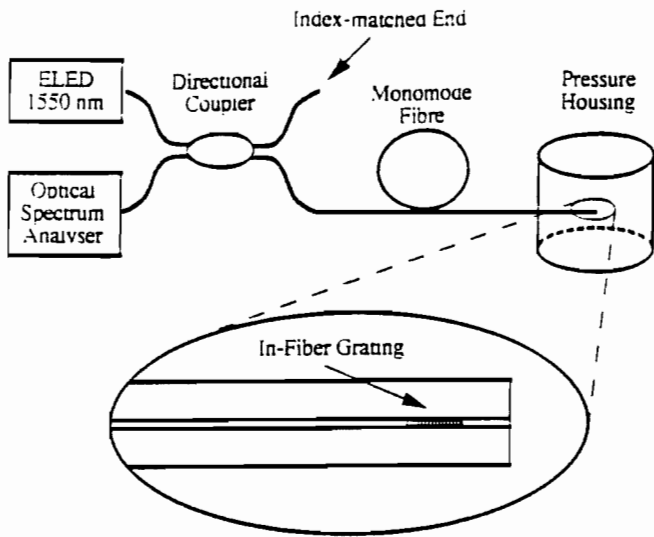


Fig.1 Schematic of In-Fibre Grating Pressure Sensor

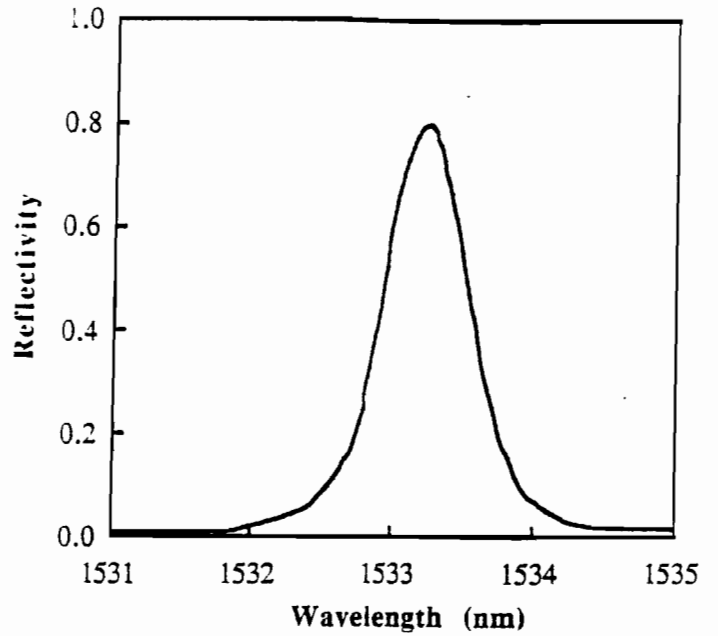


Fig.2 Reflected Spectrum From Sensing Probe

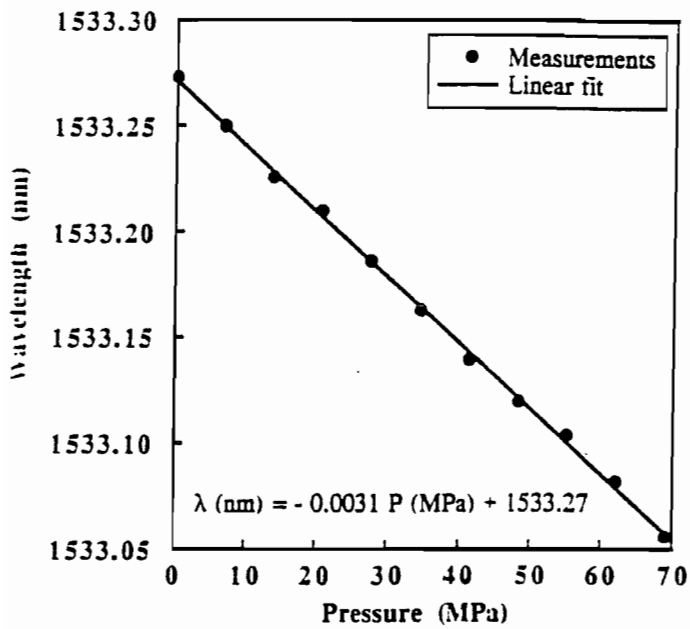


Fig.3 Pressure Response of the Sensor

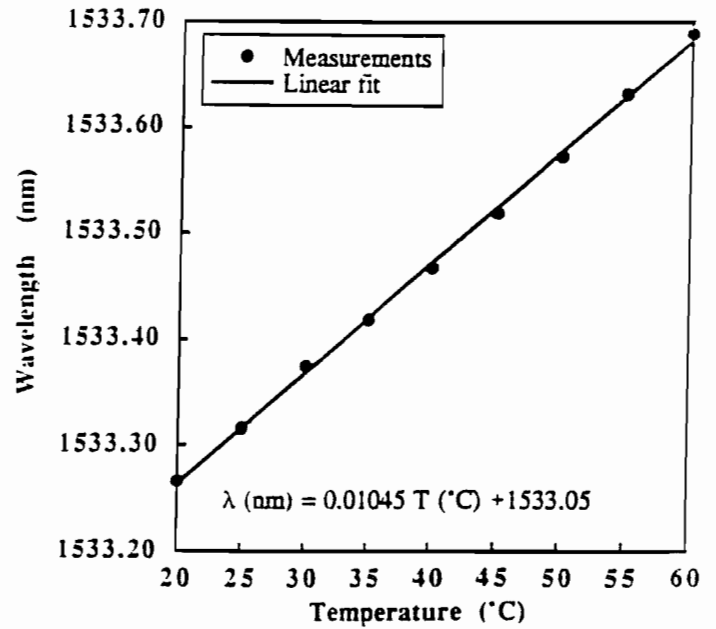
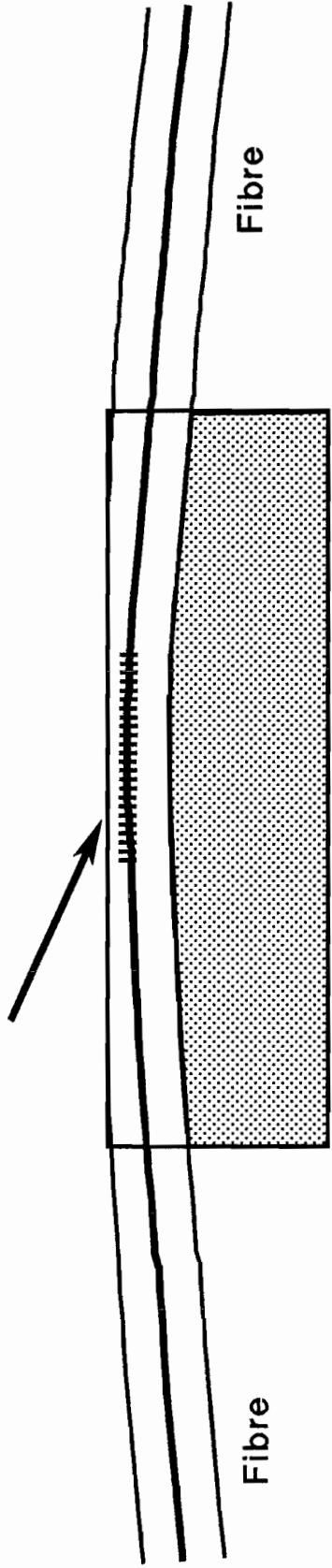


Fig.4 Temperature Response of the Sensor

In-fibre grating sensor for refractive index



Support substrate for polished fibre

Schematic of polished-half-fibre sensor in support block



Cross-sectional view of sensor in block

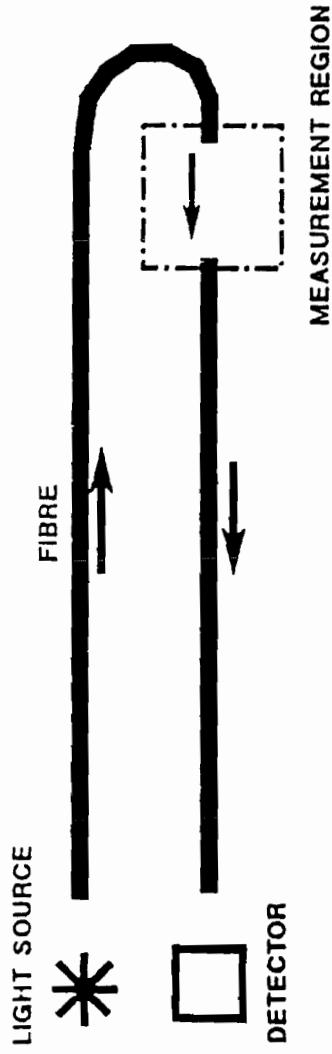
Schematic of grating sensor in support block

OPTICAL FIBER BASED REMOTE SPECTROSCOPY

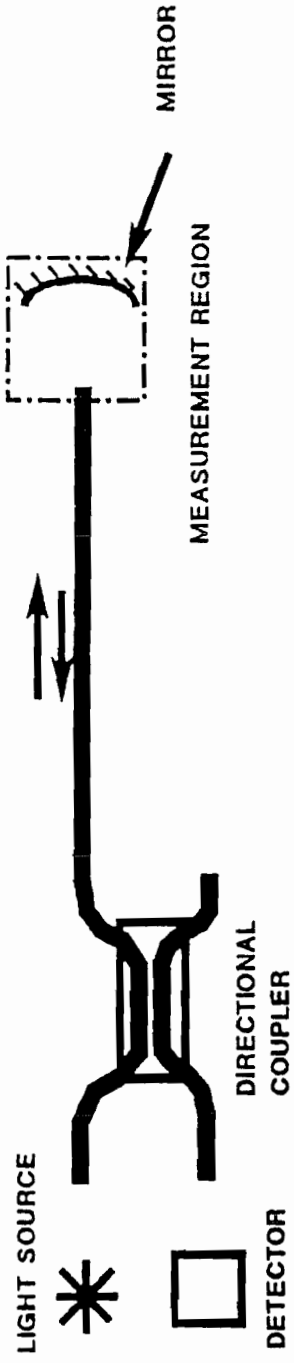
- ◆ TRANSMISSION AND REFLECTION SPECTROMETRY FROM UV (350 nm) to NIR (2200nm). FURTHER INTO IR WITH SPECIAL FIBERS.
- ◆ MEASUREMENT OF ABSORPTION, TURBIDITY, FLUORESCENCE RAMAN, NIR-REFLECTANCE, etc
- ◆ MEASUREMENT OF OPTICAL FIBERS, FIBER COMPONENTS, INTEGRATED OPTICS DEVICES & INTERFEROMETERS.
- ◆ INTERROGATION OF SPECTRAL FILTERING FIBER SENSORS, WHITE-LIGHT INTERFEROMETERS, etc.

ADVANTAGES OF FIBER-BASED SYSTEMS

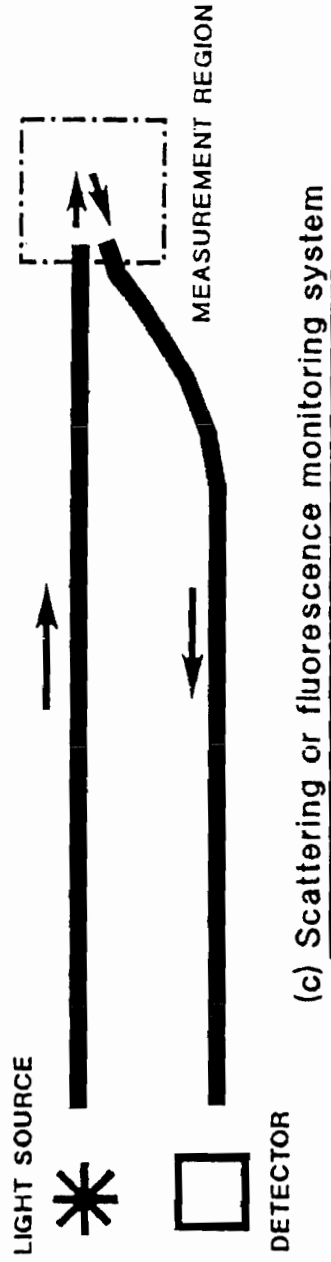
- ◆ REMOTE OPERATION
- ◆ NETWORKING AND MULTIPLEXING BECOMES PRACTICAL
- ◆ ON-LINE MONITORING IS SIMPLIFIED
- ◆ CORROSIVE AND HAZARDOUS MATERIALS ARE KEPT AWAY FROM PERSONNEL AND FROM EXPENSIVE CAPITAL EQUIPMENT.
- ◆ INSTANT RESPONSE, WITHOUT HAZARDS AND DELAYS INHERENT WHEN SAMPLING CHEMICALS.



(a) Transmissive sensor system



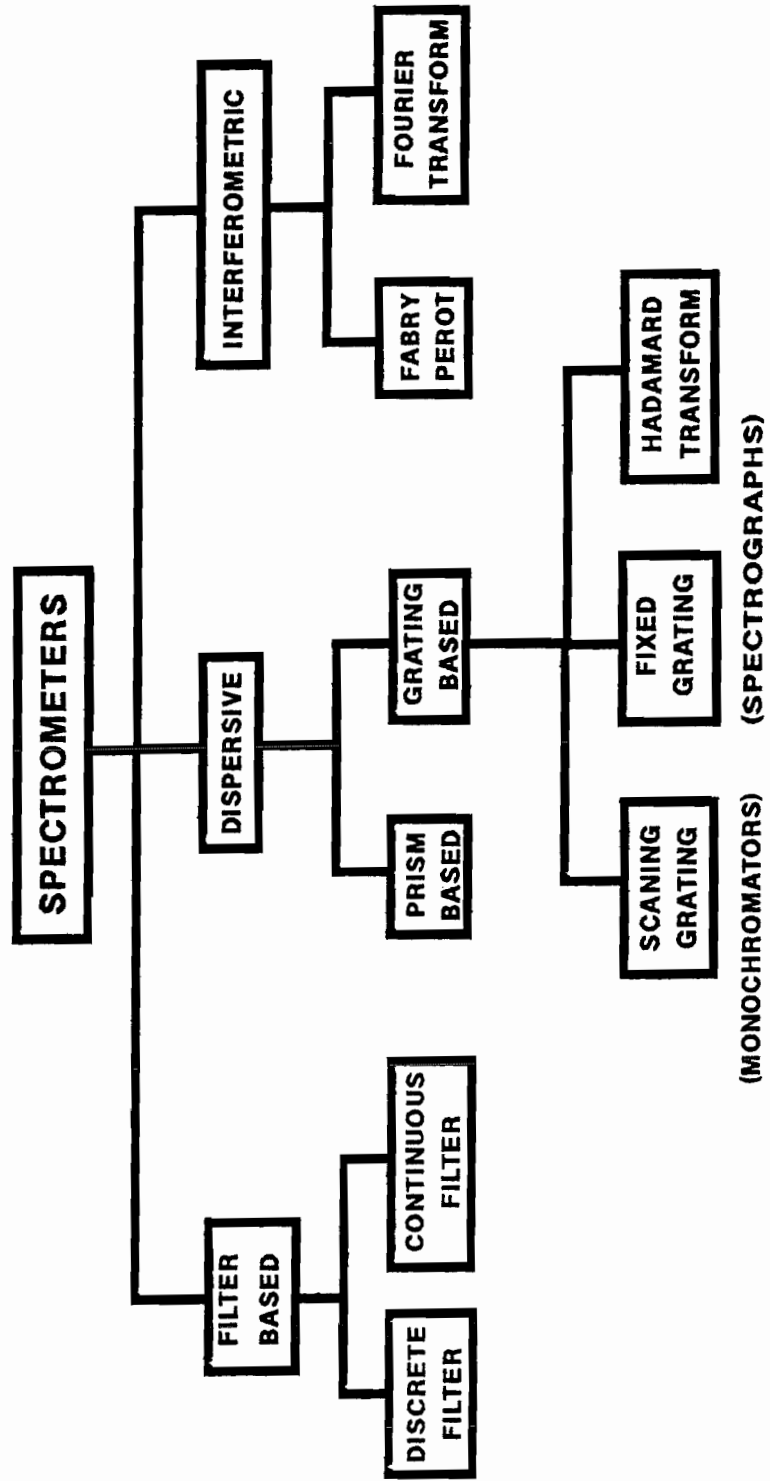
(b) Reflective sensor system

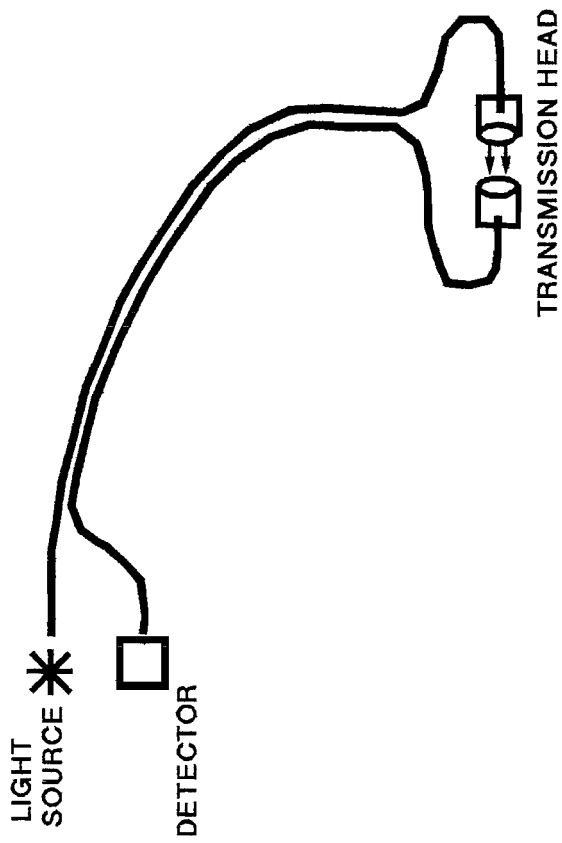


Extrinsic Fibre Optic Sensors for Spectroscopic Monitoring.

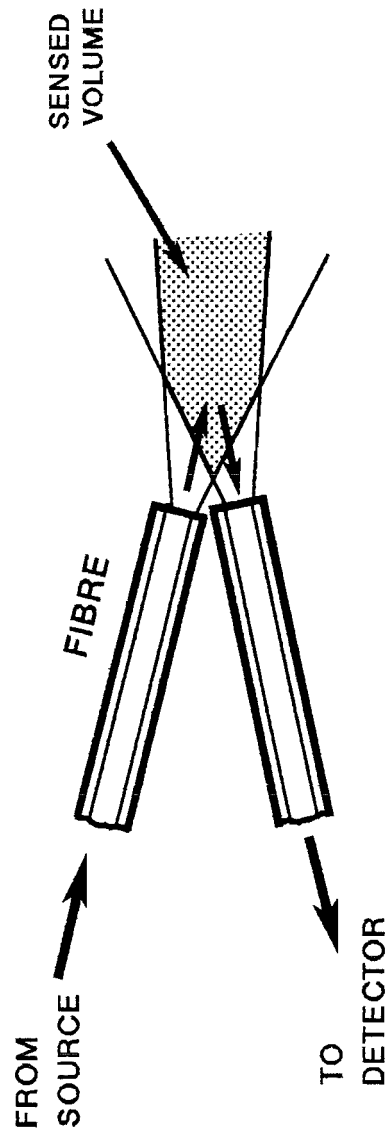


TYPES OF SPECTROMETER:



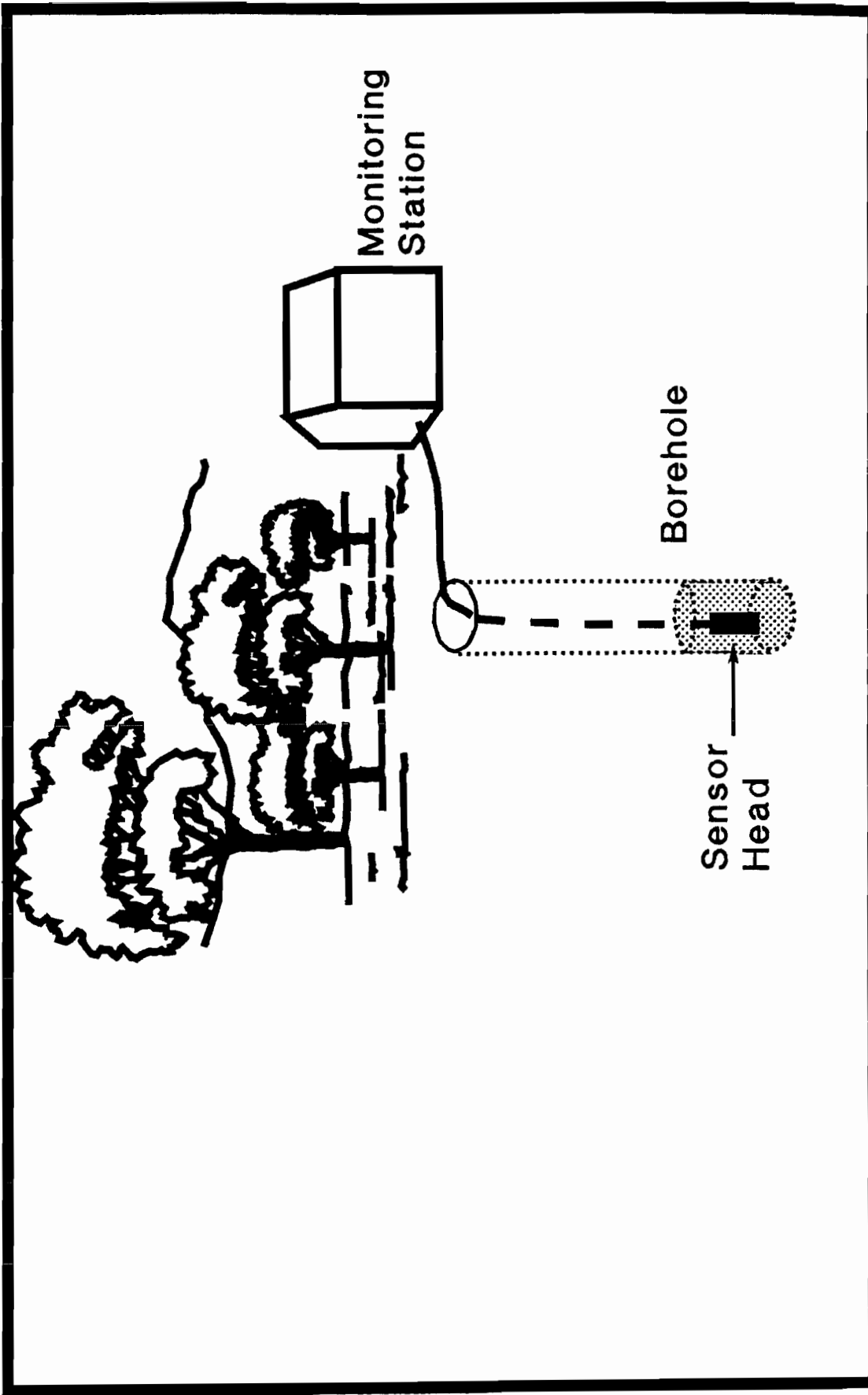


TRANSMISSION SYSTEM FOR FIBRE OPTIC SPECTROSCOPY

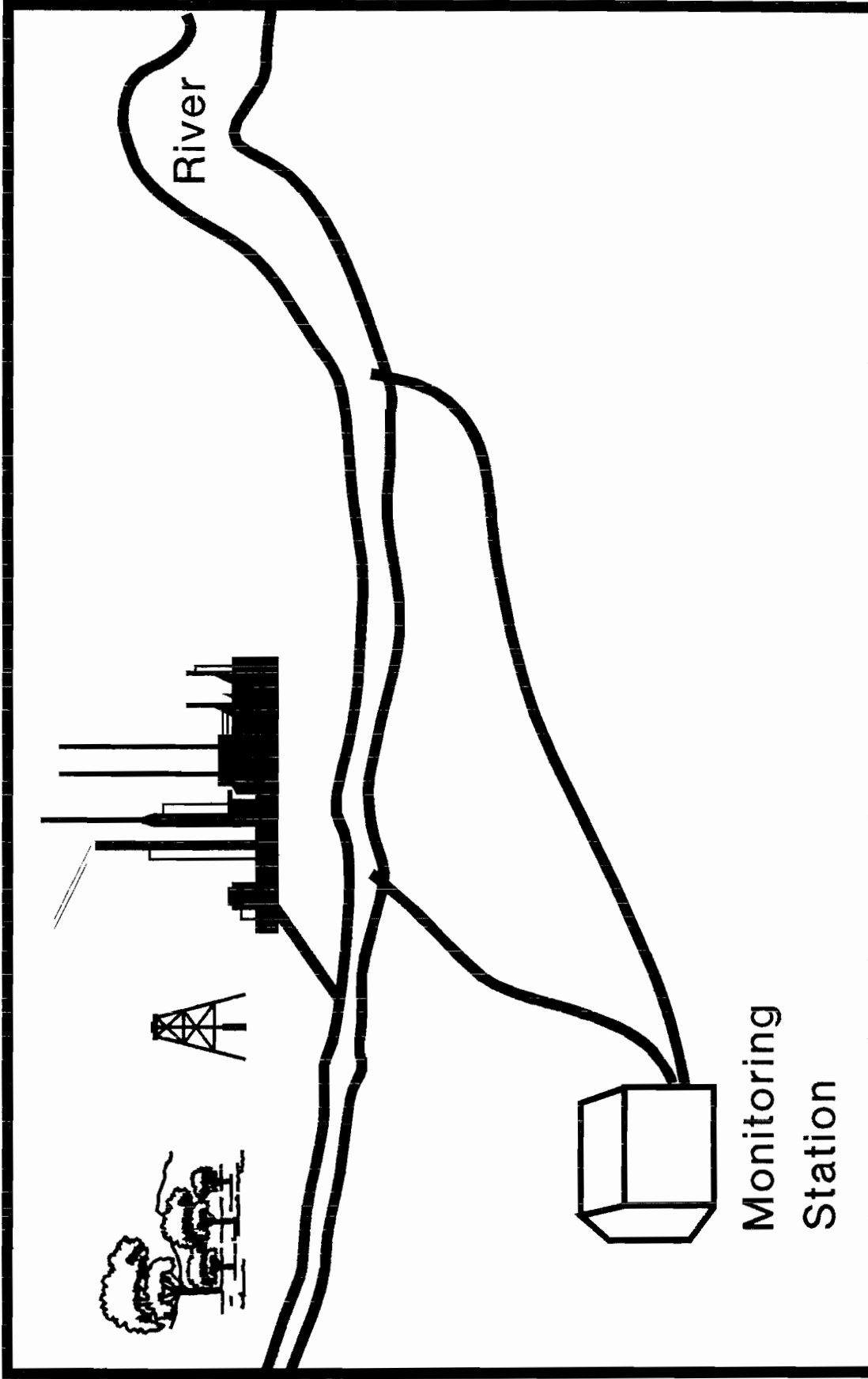


MODIFIED MEASUREMENT HEAD FOR FLUORESCENCE MONITORING

FIG 5.1 FIBRE OPTIC SPECTROSCOPY HEADS FOR REMOTE CHEMICAL SENSING

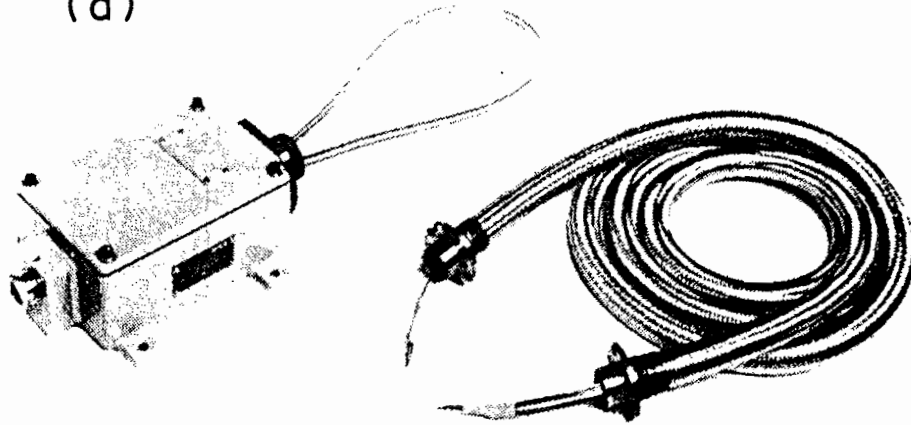
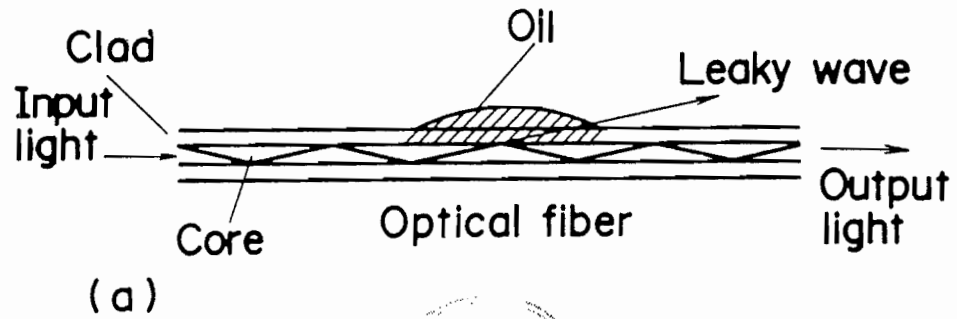


Schematic of Fibre-Remoted Pollution Monitoring Scheme for Groundwater



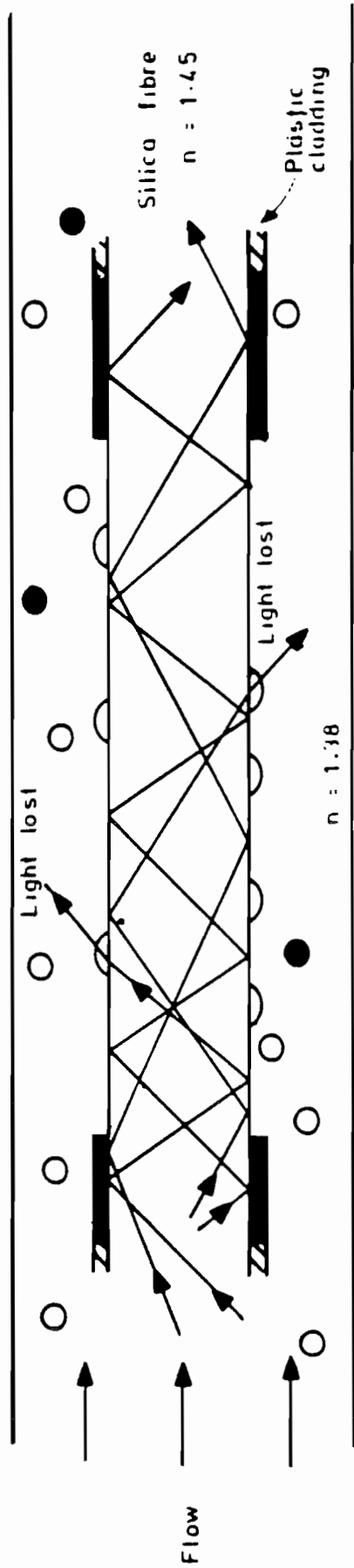
**Schematic of Fibre-Remoted Pollution
Monitoring Scheme for River**

PHYSICAL AND CHEMICAL SENSORS FOR PROCESS CONTROL



(a) Principle of operation, and (b) photograph of an oil-leak sensor using a PCS fiber as a sensing element.

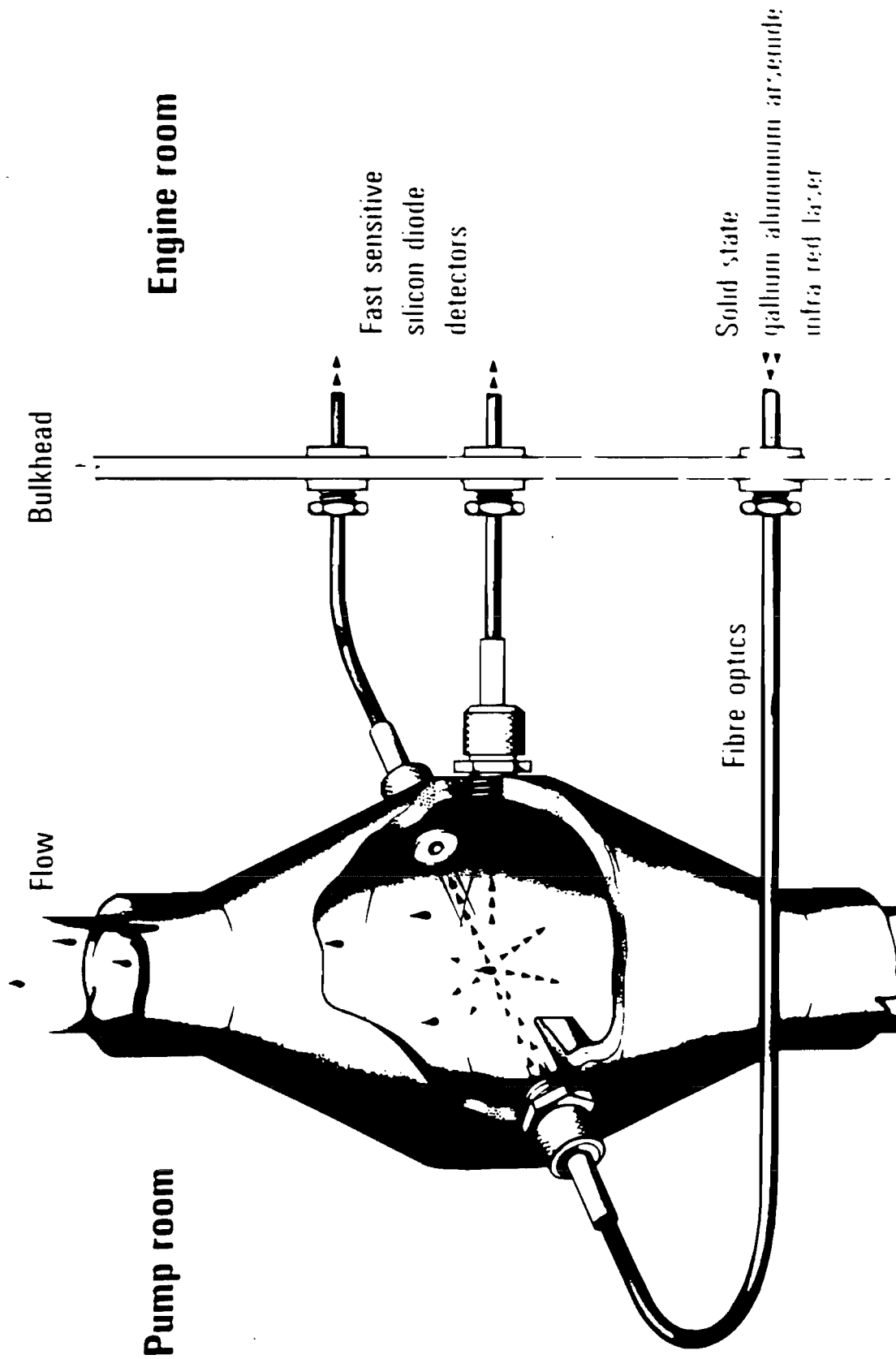
THIS DRAWING IS REPRODUCED WITH THANKS FROM
"OPTICAL FIBER SENSORS" PUBLISHED BY ARTECH HOUSE.
EDITORS: J P DAKIN, B CULSHAW.
DIAGRAM TAKEN FROM CHAPTER BY K. KYUMA



- Oil droplet
 $n = 1.40$
- Sand

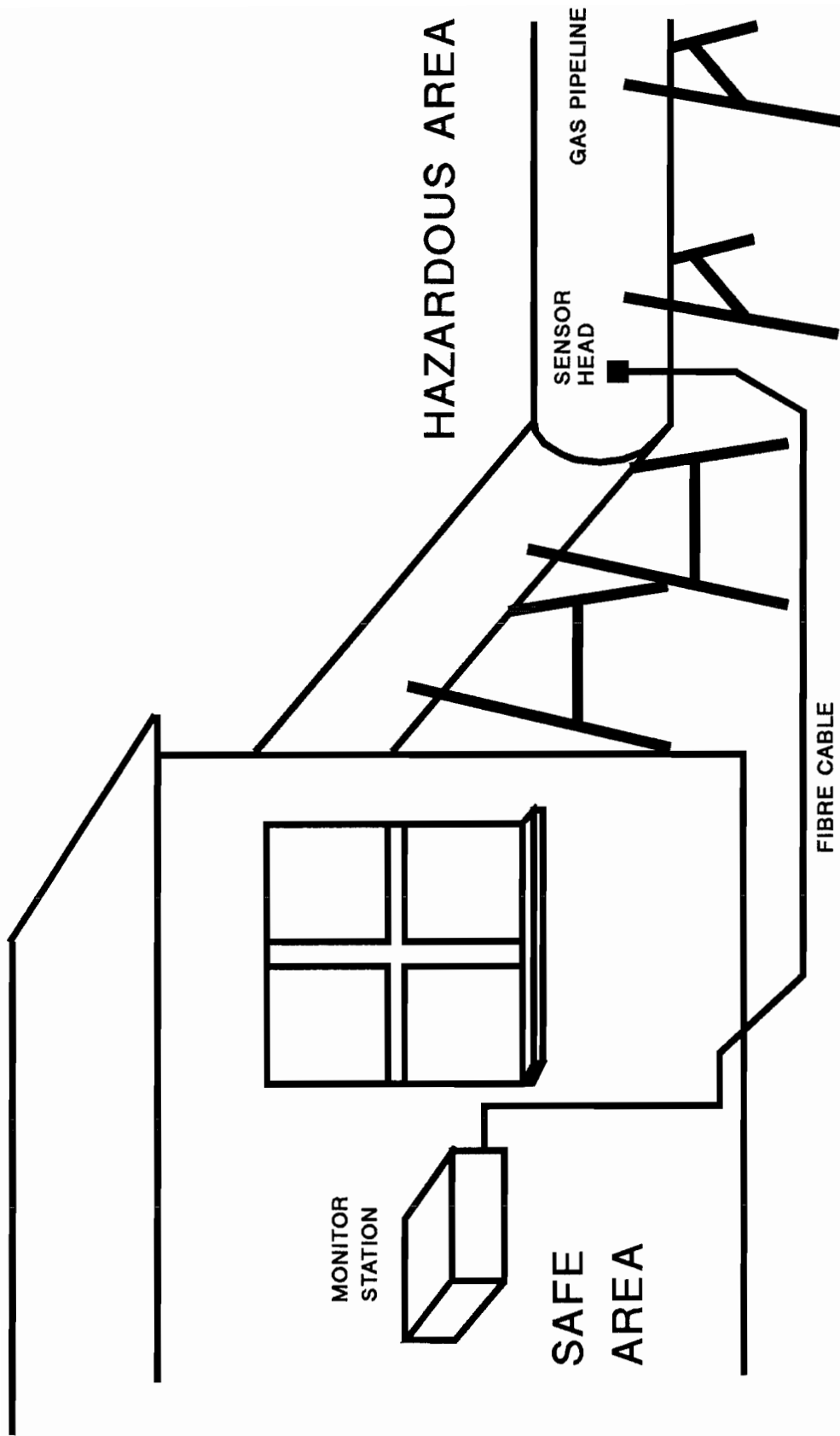
SCHEMATIC OF EARLY EXPERIMENTAL OIL SENSOR (INTRINSIC VERSION)
(OIL DROPLETS CAUSE LOSS FROM UNCLAD FIBRE SECTION)

Originator: D. PITT (Formerly STL, U.K.)



LATER, MORE SUCCESSFUL, EXTRINSIC VERSION OF OIL SENSOR

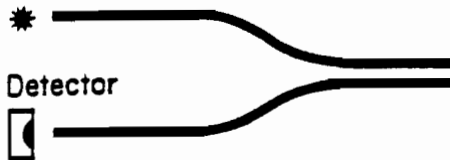
(LIGHT IS SCATTERED FROM OIL DROPLETS) Originator: D.PITT (Formerly STL, U.K.)



SCHEMATIC OF ON-LINE PROCESS MEASUREMENT
USING FIBRE-REMOVED GAS SENSOR.

LIGHT GUIDE

Source 2 Fibre probe



- REMOTE SPECTROSCOPY
- REFLECTANCE
- OXIMETRY

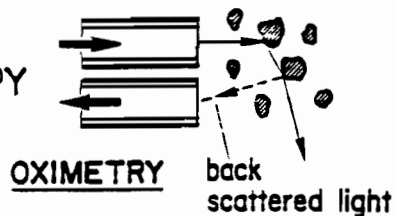
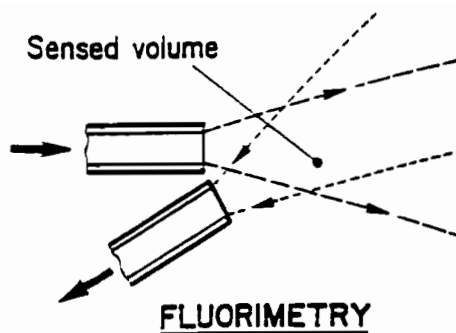
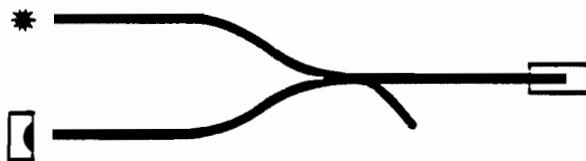


Fig. 16.1 An optical fiber as a simple light guide for chemical sensing. Two examples are illustrated: (i) a remote fluorimeter with light from one fiber exciting fluorescence which is collected by a second fiber; and (ii) an oximeter in which the second fiber collects light backscattered from blood cells. The spectral characteristics of the backscattered light gives the absorption spectra of the blood.

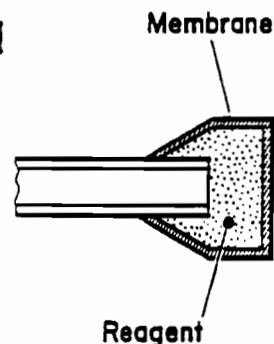
CHEMICAL REAGENT

Source



Detector

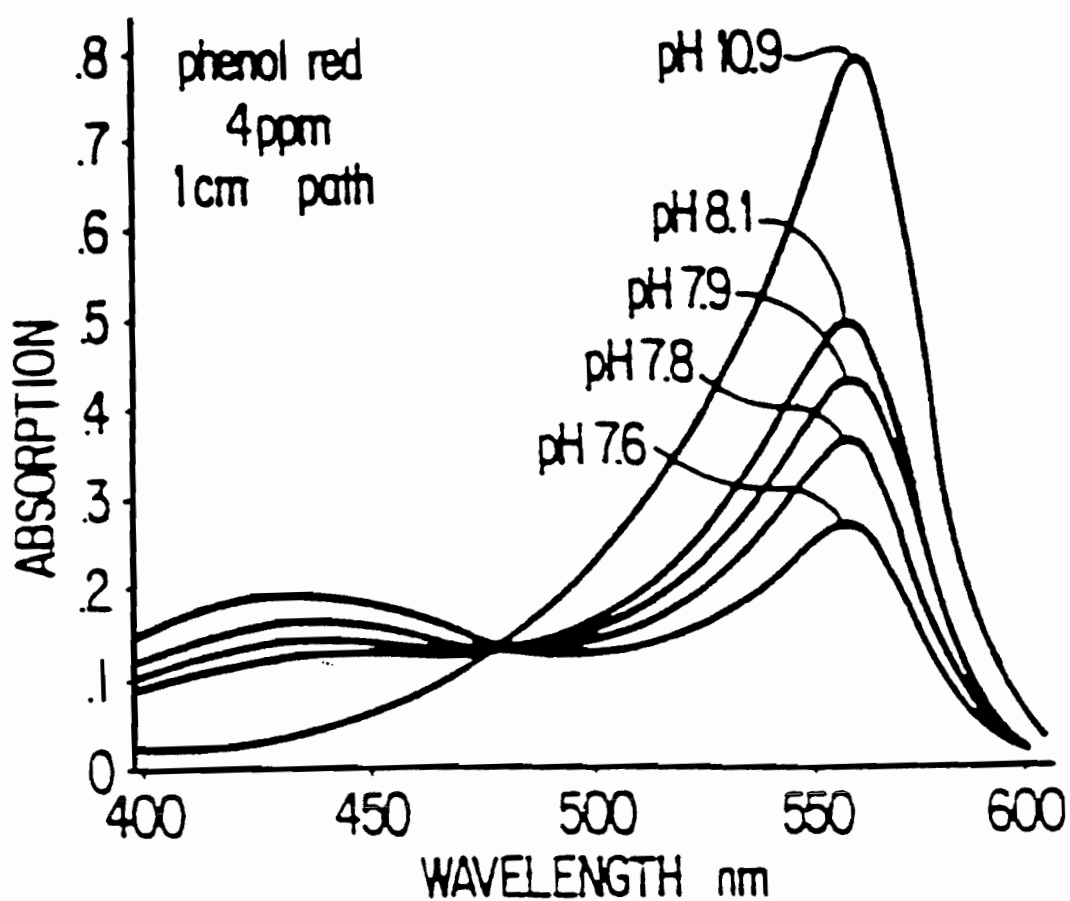
pH , pO₂ , pCO₂
CHEMICAL IONS



FLUORESCENCE QUENCHING

Fig. 16.3 Principle of chemical sensing with a chemical reagent. The reagent is enclosed and protected by an ion-permeable membrane on the end of the fiber probe. Colorimetric and fluorescence indicators are used as the reagent to measure a wide range of chemical reactions. The probe has a single optical fiber (two or more are also possible) connected to the source and detector by a 3 dB coupler (shown schematically).

THIS DRAWING IS REPRODUCED WITH THANKS FROM
"OPTICAL FIBER SENSORS" PUBLISHED BY ARTECH HOUSE.
EDITORS: J P DAKIN, B CULSHAW.
DIAGRAM TAKEN FROM CHAPTER BY A. HARMER, A-M SCHEGGI



(b) Absorption of phenol red for different pH values as a function of wavelength. (After Peterson *et al.*, 1980.)

Fig. 16.6 cont'd.

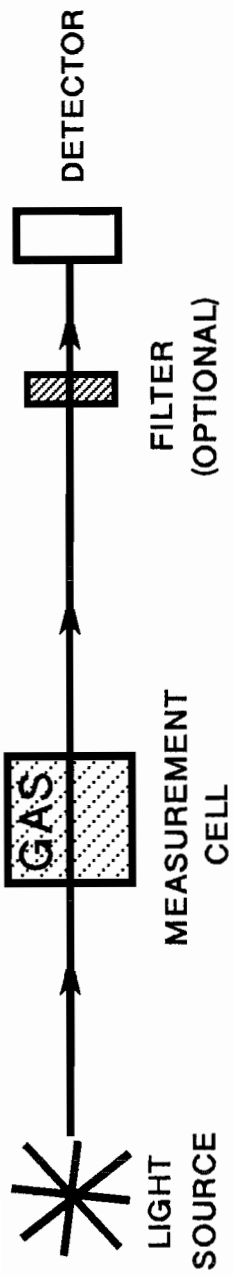
THIS DRAWING IS REPRODUCED WITH THANKS FROM
"OPTICAL FIBER SENSORS" PUBLISHED BY ARTECH HOUSE.
EDITORS: J P DAKIN, B CULSHAW.
DIAGRAM TAKEN FROM CHAPTER BY A. HARMER, A-M SCHEGGI

GAS SENSORS USING
CORRELATION SPECTROSCOPY

(COMPATIBLE WITH FIBRE-REMOVED OPERATION)

DR. J.P. DAKIN, DR. H.O. EDWARDS

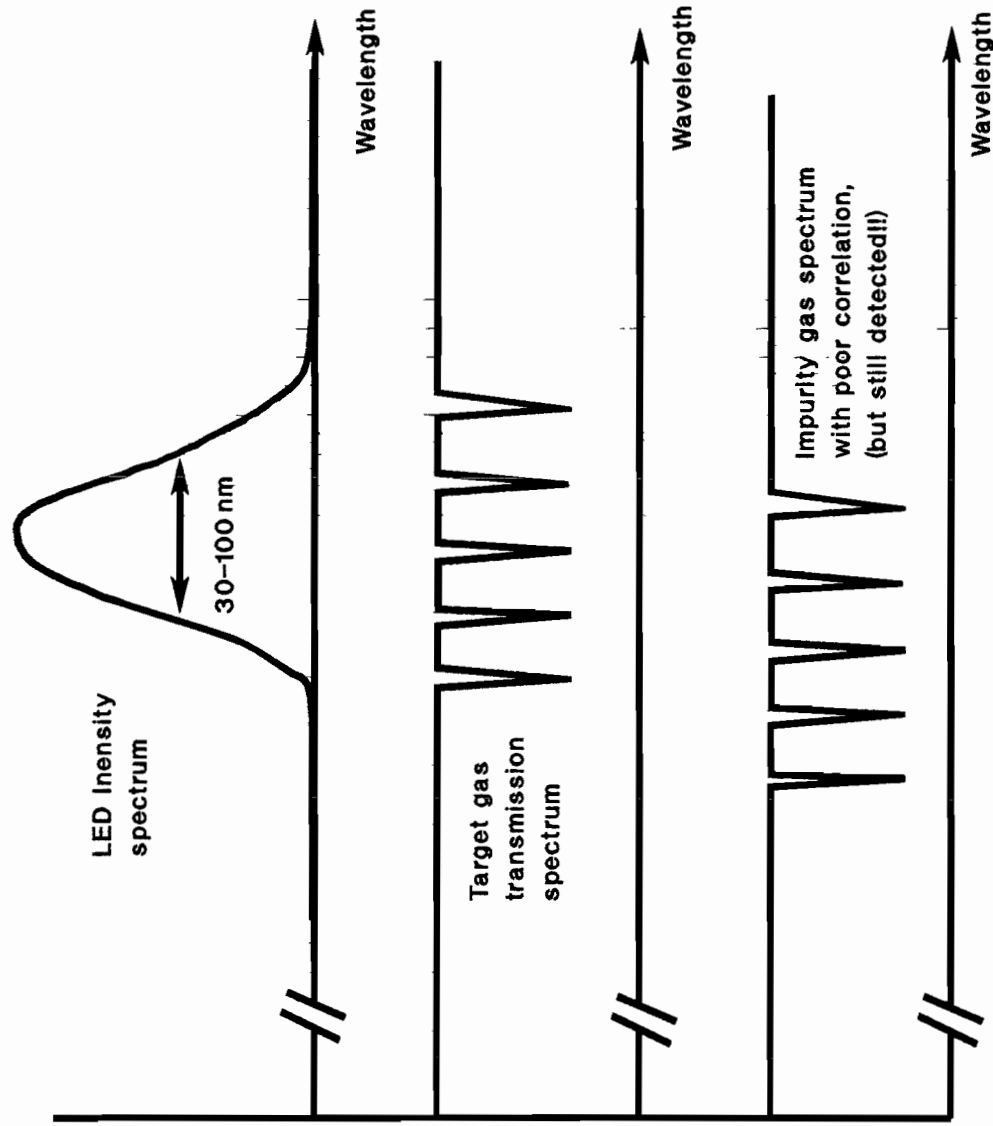
OPTOELECTRONICS RESEARCH CENTRE
UNIVERSITY OF SOUTHAMPTON,
SO9 5NH, U.K.



(a) CONVENTIONAL GAS SENSOR SYSTEM BASED ON OPTICAL ABSORPTION IN GAS

PROBLEMS WITH BROADBAND SOURCES

(eg LEDs & Filtered incandescent lamps)



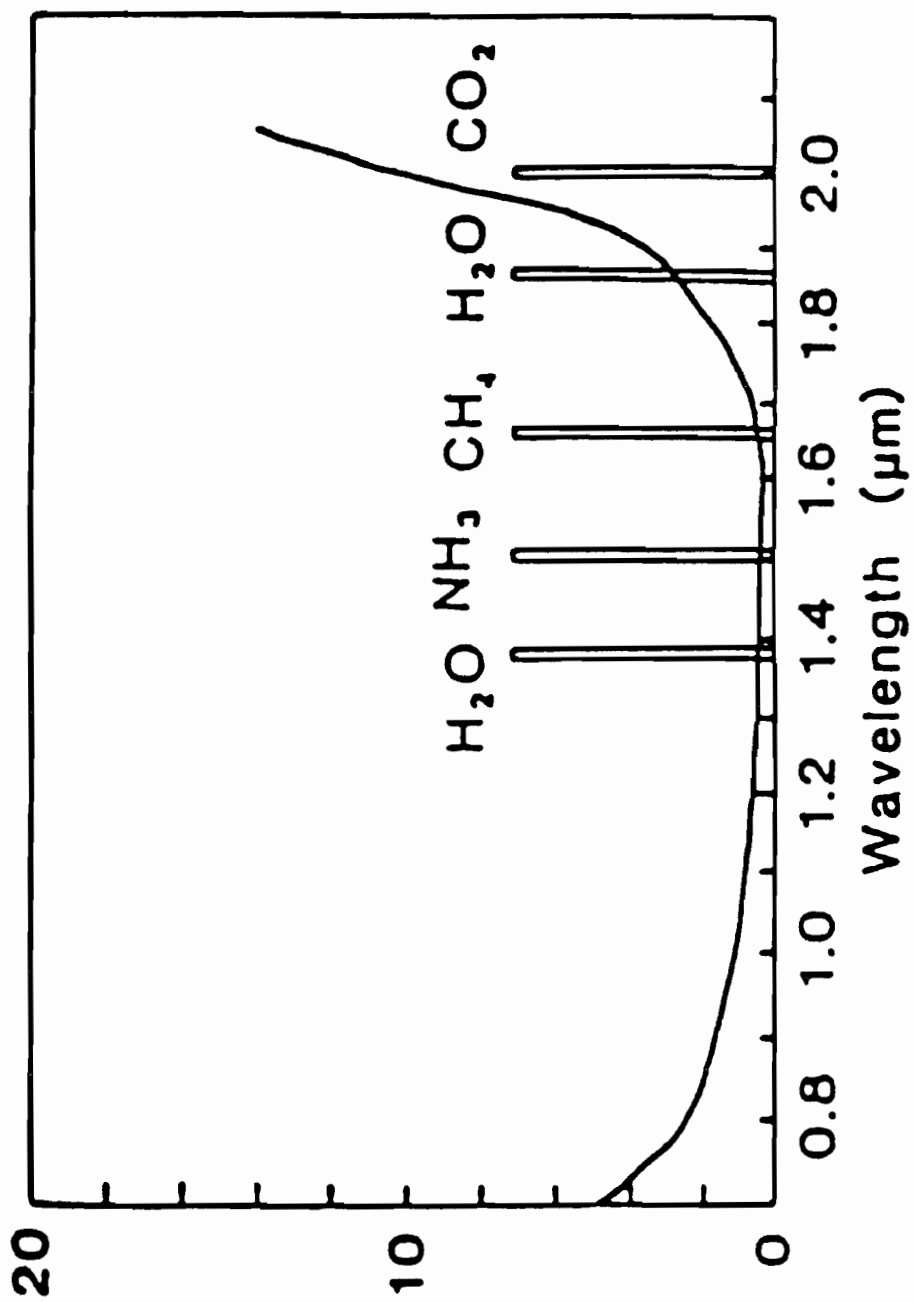


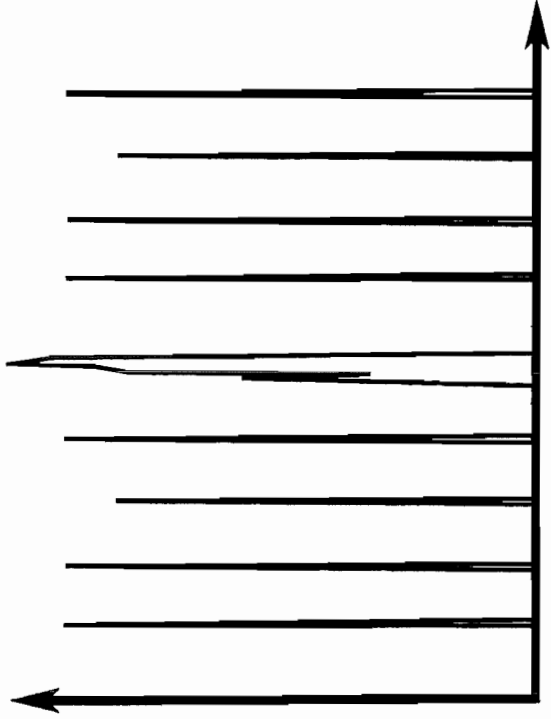
Figure 1 : Absorption bands of some common gases within the transmission window for silica fibre

OPTICAL FIBRE GAS SENSING USING CORRELATION SPECTROSCOPY

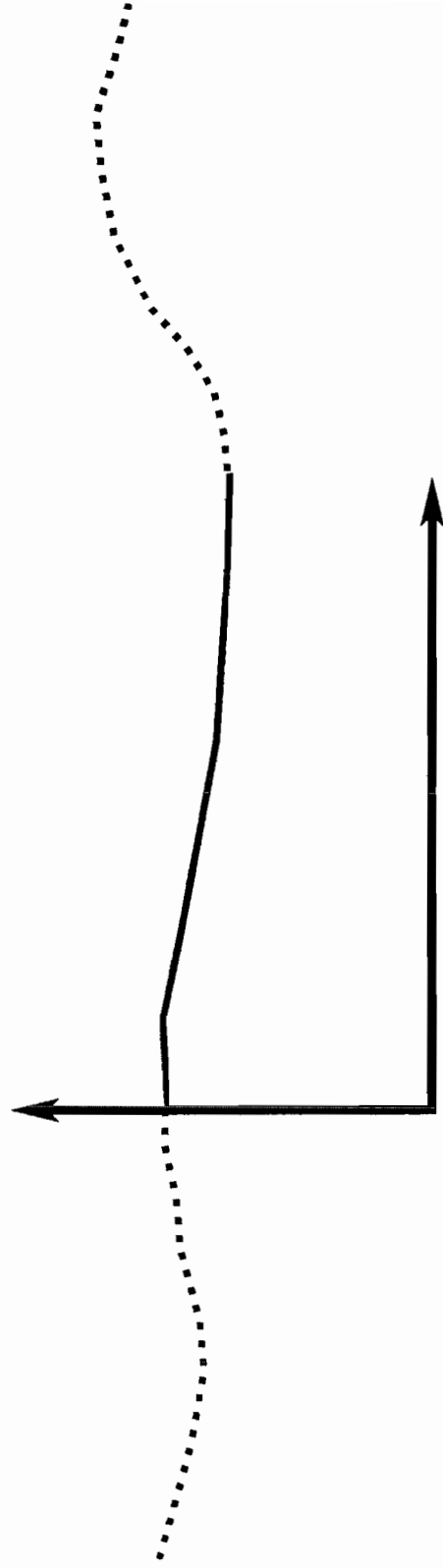
This technology involves using a sample of a gas to be detected, as a matched optical filter to recognise the same gas in a remote measurement region. The main advantage is the high selectivity.

METHODS USED:-

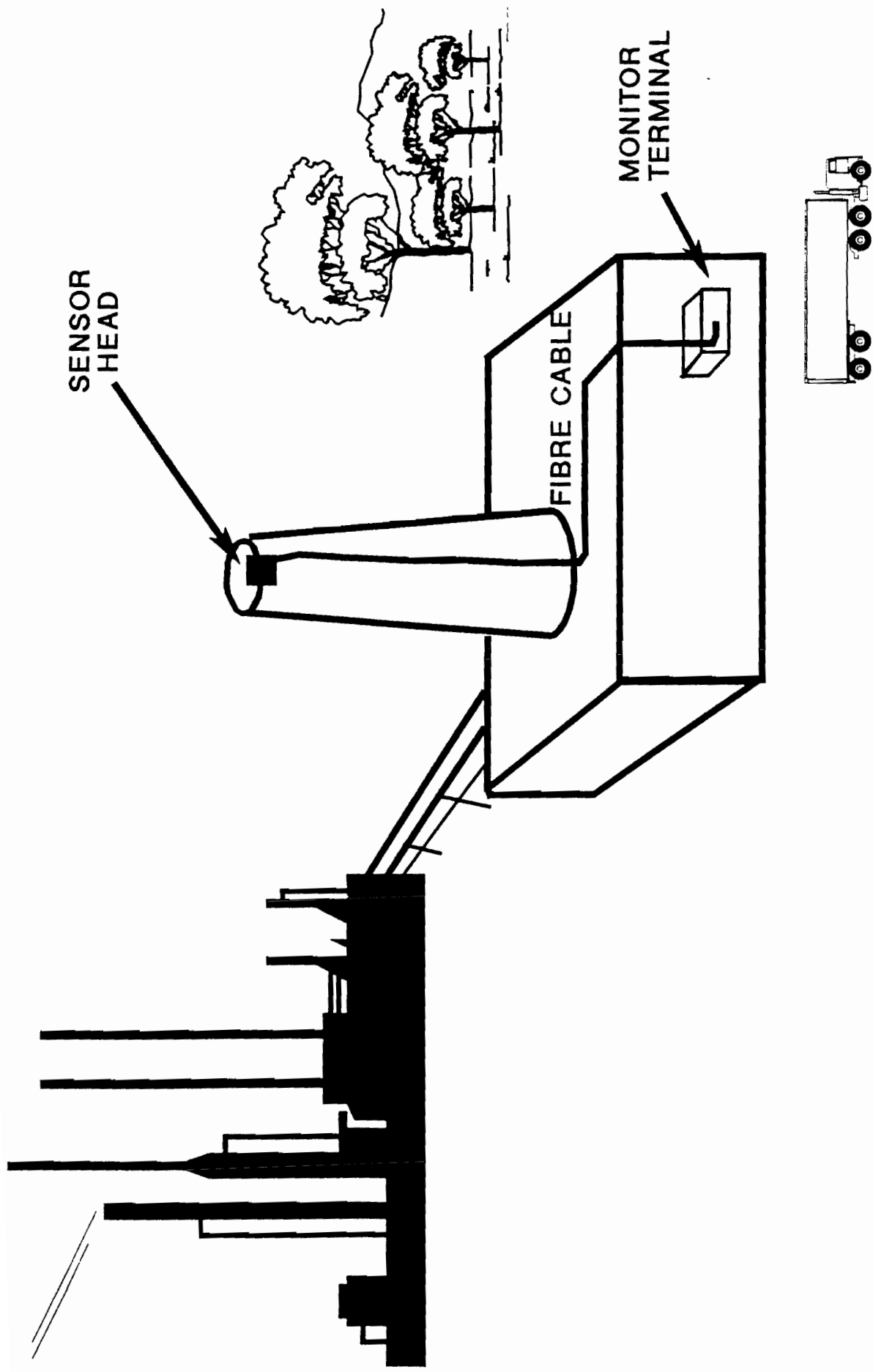
- (i) Pressure Modulation:- The gas sample is pressurised to modulate its absorption. A novel resonant acoustic cavity is used.
- (ii) Stark Modulation:- The gas is subjected to an electric field to broaden its absorption lines and modulate the degree of correlation with the remote gas sample.
- (iii) External spectral modulation:- Using an electro-optic modulator between two passive gas cells. This again modulates the correlation of the two spectra as a result of spectral broadening.



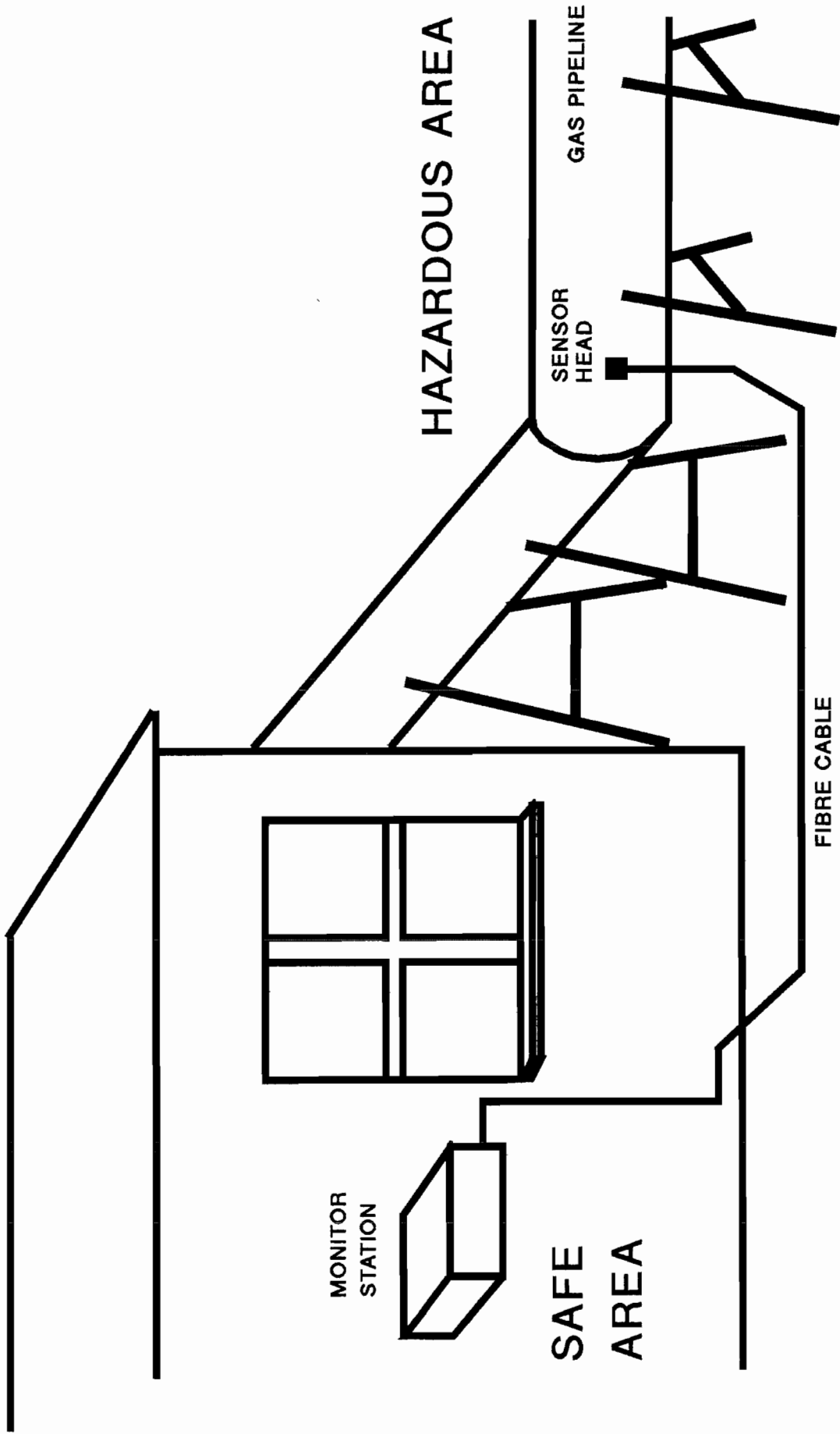
Typical absorption spectrum of simple gas



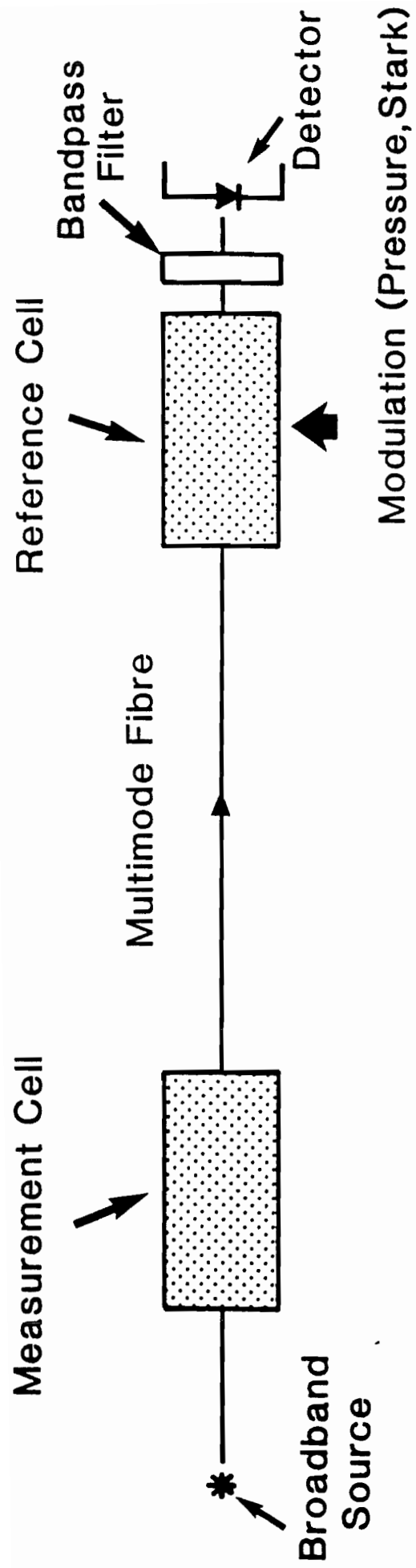
Typical absorption spectrum of liquid,
over same spectral region as gas band



SCHEMATIC OF POLLUTION MONITOR SYSTEM FOR SMOKESTACK



SCHEMATIC OF ON-LINE PROCESS MEASUREMENT
USING FIBRE-REMOVED GAS SENSOR.



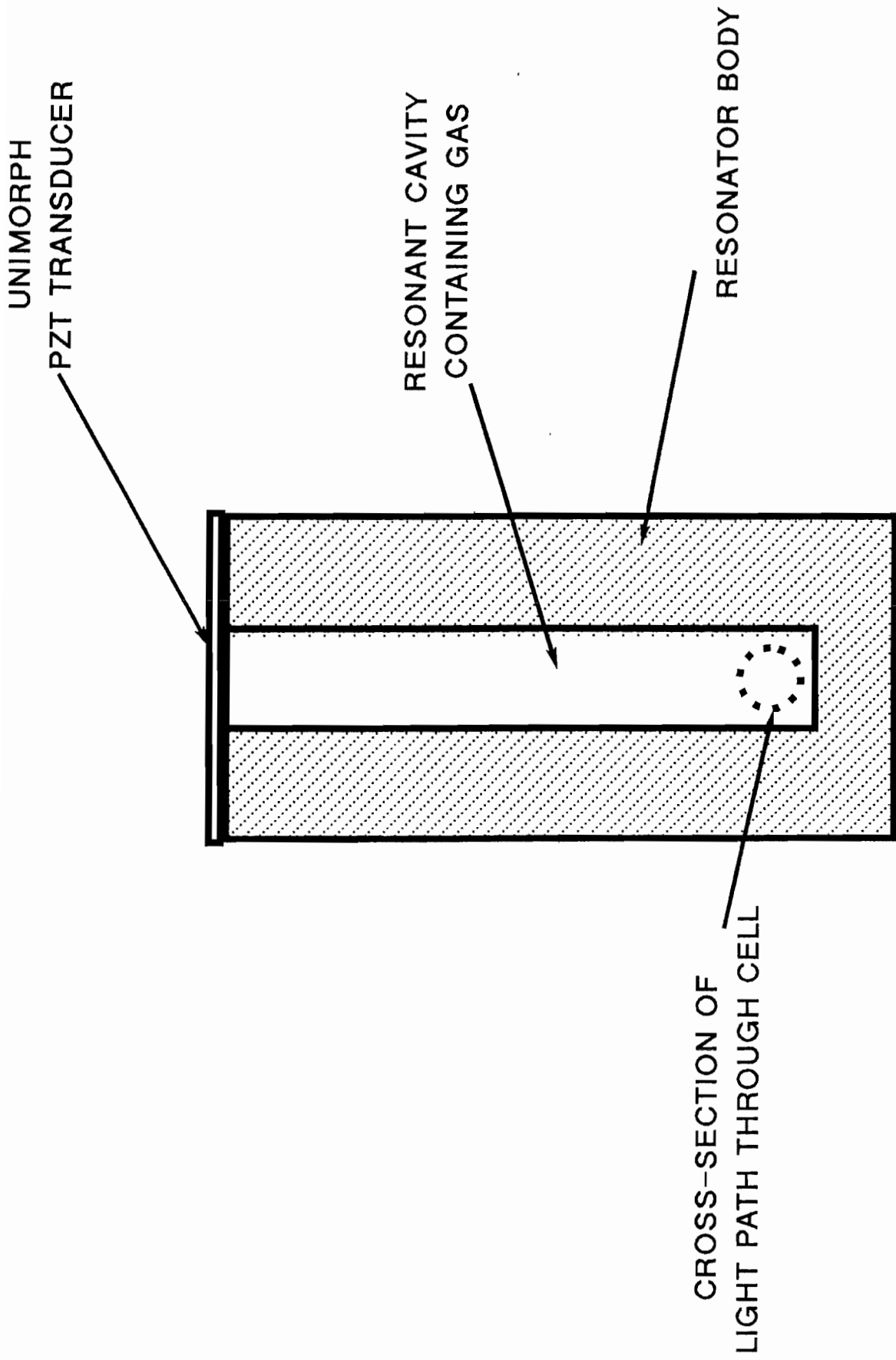
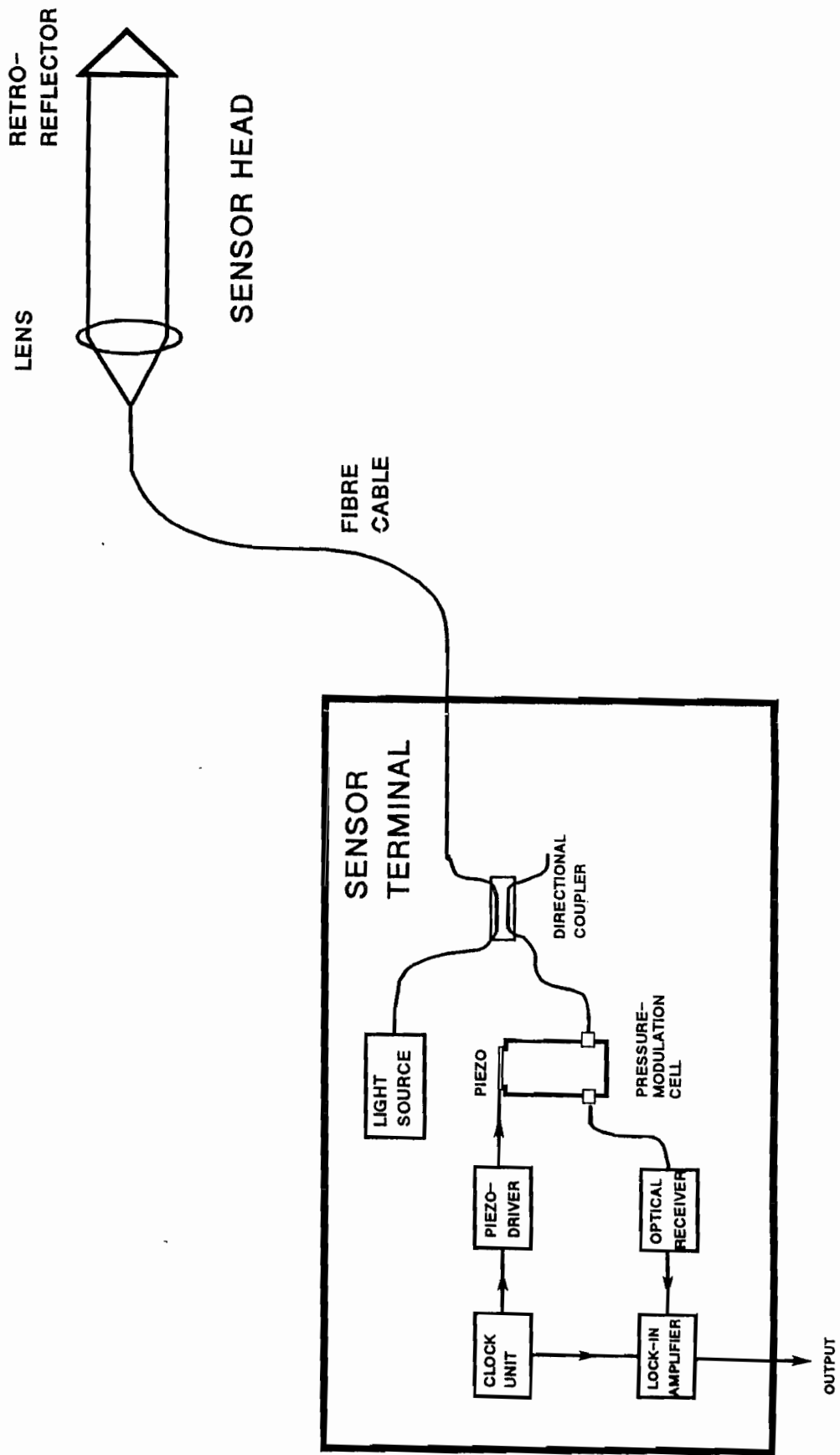
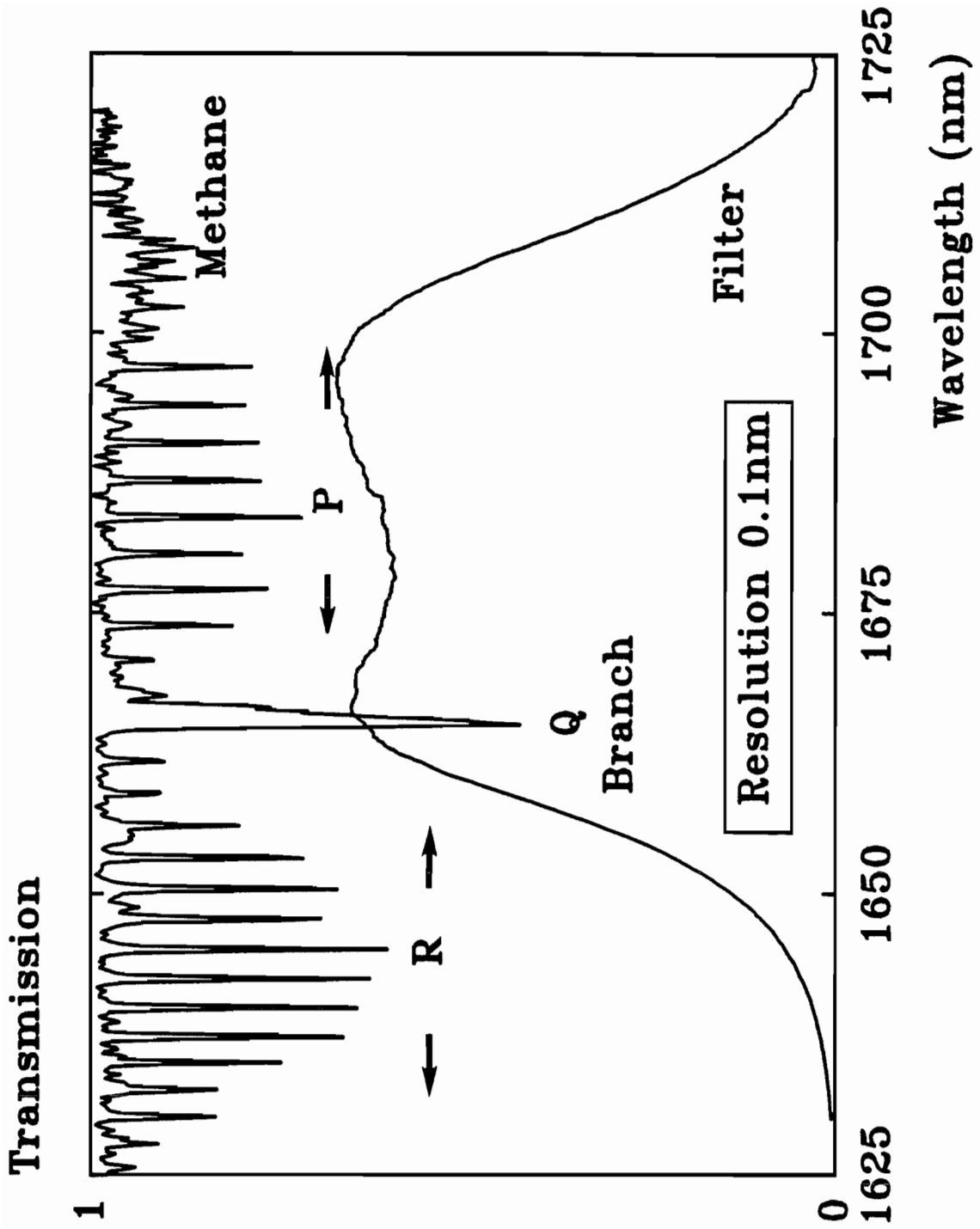


FIG 2. SCHEMATIC OF ACOUSTIC RESONATOR PRESSURE MODULATION CELL

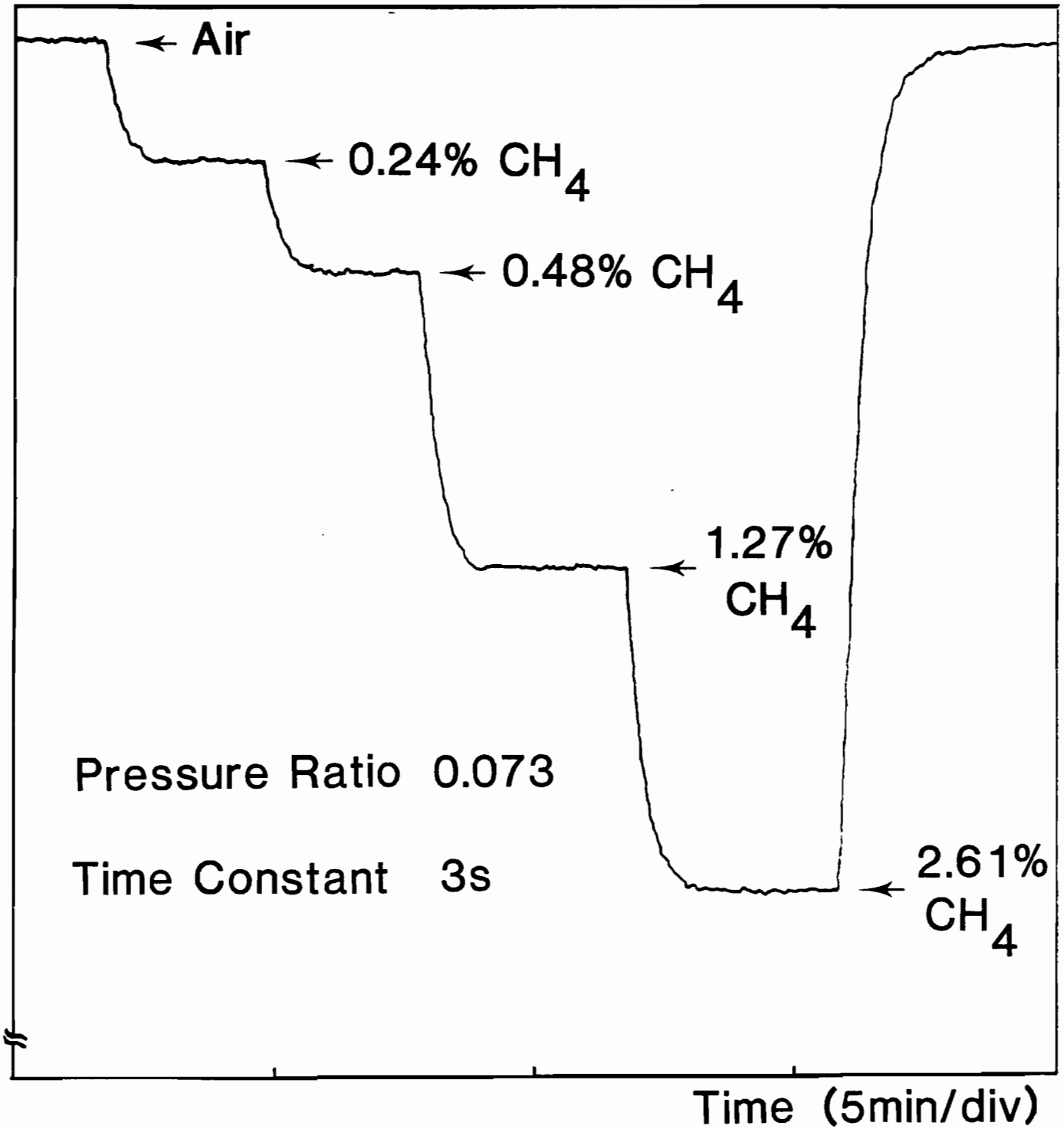


Schematic of Gas Sensor Demonstration System, Using Pressure-Modulation Method.



Pressure Modulation

Signal Amplitude



Complementary-modulated-beam approaches to correlation spectroscopy

1. Introduction to complementary-modulated-beam methods

Another approach to modulation spectroscopy avoids the need to modulate the optical properties of the reference gas by periodically switching between two light paths, one passing through and one bypassing the reference cell, before passing through the gas measurement cell. We present two different arrangements by which the light intensity in each path may be modulated. One path is arranged in free space, and sees no spectral filtering, whereas the other path contains a cell filled with the reference gas. For convenience, the system uses two separate white light sources. This has the advantage that the light intensity of each can be independently adjusted to balance the intensities, merely by changing the supply voltage. After collimation, one beam is directed through the reference cell, before joining the second collimated beam in a beam combiner. The united beams (now co-linear), are directed through the measurement cell, a filter (in our case, a monochromator) to select the gas band, and are finally incident on the detector.

Our first method is implemented using a chopper wheel, to alternately block one light path and then the other. Before entering the combiner, both beams pass through the plane of the chopper wheel, where they are alternately blocked. With the reference cell filled with the reference gas, and the monochromator set to the correct wavelength, the relative intensity in each channel was adjusted with no gas in the measurement region. This was set to the condition where the difference in detected signals was essentially cancelled. After this initial setup-procedure, to "zero" the system without gas, the measurement cell was alternately filled with sample gas and dry inert gas to demonstrate operation of the system.

It is clear that the two temporally-diplexed (i.e. time- interleaved) beam components have similar total intensity, the only difference being that one component has less energy in the narrow-spectral regions corresponding to the gas absorption lines. Thus, if the two beams pass through a medium with a flat spectral absorption, their intensities will remain the same. If, however, they pass through a gas with similar absorption bands, the component which did not initially pass through the reference cell will be more heavily attenuated (as it initially has more light energy present in the regions corresponding to the absorption lines of the gas).

Our second approach is similar, except that we intensity modulate the light sources themselves, thereby avoiding the need for moving parts (i.e. the chopper wheel). The light sources are modulated with oppositely polarised signals, the sinusoidal modulation waveform being generated by a custom-made generator, providing complementary sine wave modulation signals, with a relative phase shift of 180° . Each of the two components from the sine wave generator is used to drive a separate lamp, in combination with a D.C. bias. The two beams are combined, as before, and used to interrogate gas in the measurement cell. We shall now describe the experimental system in more detail.

2. Experimental Arrangement

2.1. Correlation gas sensor driven by alternately-chopped free-path and reference beams

Figure 8 shows the experimental setup used for the alternately-chopped path-modulation arrangement. Two separate quartz halogen lamps (6 V, 10 W) were used as light sources. The light intensity of each was independently adjustable by changing the D.C. supply voltage to each. Collimated beams were formed using silica lenses ($f=50$ mm). One beam was directed through the reference cell (pathlength was 180 mm, and the cell used silica windows), and a fraction of this was redirected to combine co-linearly with a fraction of the second beam, using a standard cube-type beam combiner. This had a nominal 50:50 (i.e. 3dB) power ratio. As described above, both beams passed through the plane of the chopper wheel, where they were alternately blocked, before reaching the combiner. The united beams passed on through the measurement cell (this had a path length of 300 mm and also had silica windows), the monochromator to select the gas absorption band, and then on to the GaInAs-photodiode detector. The latter had a responsivity of approximately 0.3 A/W between 1.5 μm and 2.0 μm . The detected signal was measured with a phase-independent lock-in amplifier (Stanford Instruments), synchronized to the chopping frequency. From measurements of the detected signal, and using the data sheet value for the responsivity of the detector, the mean detected optical power was calculated to be approximately 6.6 nW and 2.6 nW, at the principal measurement wavelength of 1.505 μm and 1.92 μm respectively. Before introducing a gas sample into the measurement cell, the relative intensity in each beam was adjusted such that the detected lock-in signals, with no gas present in the sample cell, was minimized. (*Note:* The relative intensity adjustment had to be repeated, when the wavelength was changed). After this initial setup-procedure to "zero" the system without gas in the

measurement cell, this cell was alternately filled with a test sample of gas (ammonia plus water vapour was used in our first tests) and swept with a dry inert gas (nitrogen).

For our first measurements, the reference-cell and measurement gas samples were generated by half-filling a large flask with a concentrated ammonia solution in water. The head space of the flask therefore contained a mixture of water vapour, ammonia gas, along with, after partial evacuation using a vacuum pump, a negligible fraction of residual air. This NH_3 -water vapour mixture was then present at a total pressure of 1 Bar and at room temperature. The saturated partial pressure of water vapour in the head space was estimated to be roughly 20 torr, at this temperature and hence the partial pressure of ammonia was estimated to be around 740 torr. To fill the gas cells, further gas was drawn out from the head space in the flask, allowing time for more ammonia and water vapour to escape from the solution.

This gas mixture allowed testing of the system using either water vapour or ammonia, depending on which wavelength band we selected with our monochromator filter. The monochromator was set to $\lambda=1.92 \mu\text{m}$ for water vapour measurements, and to $\lambda=1.505 \mu\text{m}$ for measuring the concentration of ammonia vapour. (The monochromator bandwidth was 20 nm).

2.2. Correlation spectroscopy using complementary (opposite-polarity) intensity modulation of light sources

We shall now describe more details of the experimental arrangement for the complementary modulated-source methods discussed above. The measurement arrangement is shown in Figure 9. In this system, the two halogen lamps (again 6 V, 10 W) were connected to a custom-made power source providing two complementary sine wave outputs, which had a phase shift of 180° to each other, in addition to providing D.C. bias for each. The intensity of each lamp was independently adjustable by changing the relative voltage of each power supply. Figure 10 shows the drive signal to each lamp.

As with the chopped-beam system, the detected signal was again fed into a phase-independent lock-in amplifier, in this case synchronised to one of the complementary sine-wave drive signals to the lamps. As before, the relative intensity in each channel was initially adjusted to minimise the detected lock-in signal, with no gas present in the measurement cell.

Similarly, for the gas detection tests, the reference cell was filled with ~740 torr ammonia, and ~20 torr water vapour, at 25°C and atmospheric pressure and the same absorption lines $1.92 \mu\text{m}$ (water vapour) and $1.505 \mu\text{m}$ (ammonia) were monitored.

2.3. Independent measurement of NIR spectrum of the gas mixture used in the measurement and reference cells

To confirm our choice of measurement bands for water vapour and ammonia, a near-IR transmission spectrum of our experimentally-used gas mixture was recorded with a Perkin-Elmer FTIR spectrometer (see Figure 11). This was measured in a slightly shorter gas cell, having a path length of 160 mm, to fit into the instrument.

2.4. Results with our complementary modulated beam gas sensor

Both the chopped-beam system and the modulated-light-source system described above were tested. In each case, results were obtained for the detection of the presence of water vapour and ammonia gas. The correlation signal was recorded consecutively at three different wavelengths; $1.505 \mu\text{m}$, $1.92 \mu\text{m}$, and $1.42 \mu\text{m}$. The latter wavelength was used to verify the correct origin of the correlation signal, as the absorptions of both H_2O vapour and NH_3 gas are insignificant at this wavelength (see Figure 11). Figure 12 shows the difference in signal, when the measurement cell was alternatively filled with sample gas (NH_3 + water vapour), and pure nitrogen, respectively, each gas mixture being at atmospheric pressure and room temperature. The signals were recorded with a lock-in integration time of 100 ms, in order to demonstrate the potential for fast response times of our gas sensor. The two curves correspond to water-vapour ($1.92 \mu\text{m}$) and ammonia vapour ($1.505 \mu\text{m}$) absorptions, depending on the wavelength range selected. Figure 13 shows an overlay of similar measurements at the same three wavelengths ($1.55 \mu\text{m}$, $1.92 \mu\text{m}$ and $1.42 \mu\text{m}$), again with the cell alternatively filled with sample gas, and pure nitrogen, but in this case the measurement was performed using the modulated-light-source method. It was found that the signal/noise was better for the latter system. (It is probable that mechanical vibration may have generated additional noise in the chopper-based system).

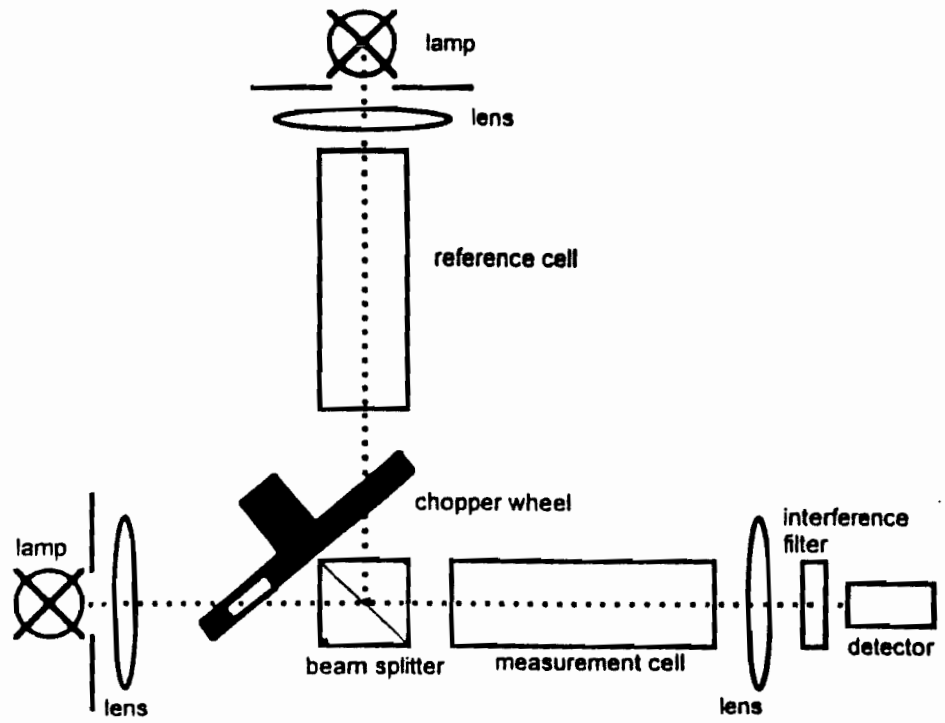


Figure 8 : Schematic diagram of the alternately-chopped-path correlation spectroscopy scheme

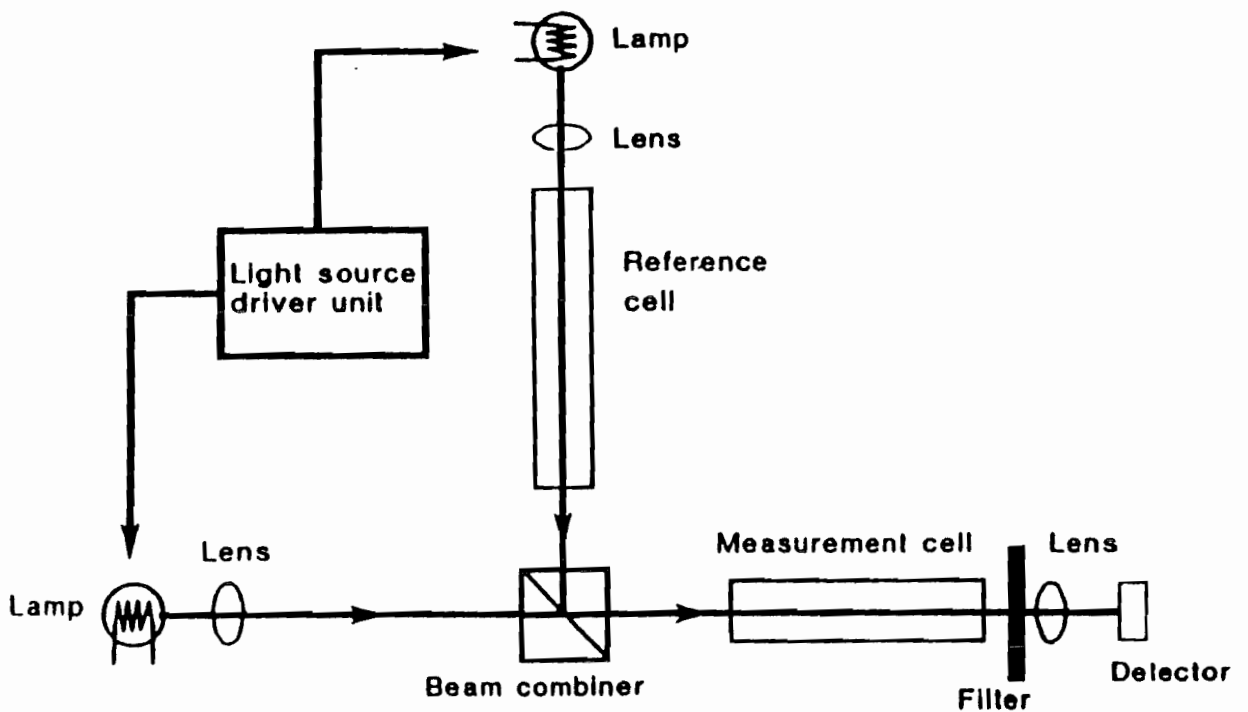


Figure 9 : Correlation-spectroscopy arrangement using complementary-modulated sources.

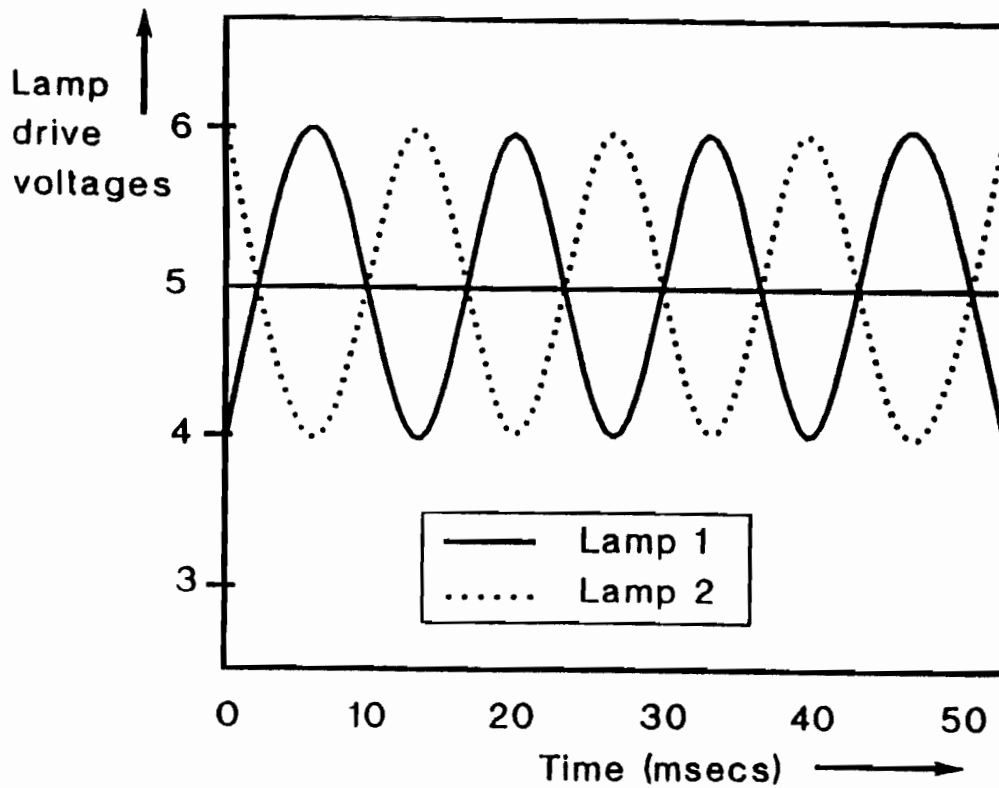


Figure 10 : Sine modulated lamp voltage for each lamp, with arrangement in fig 9.

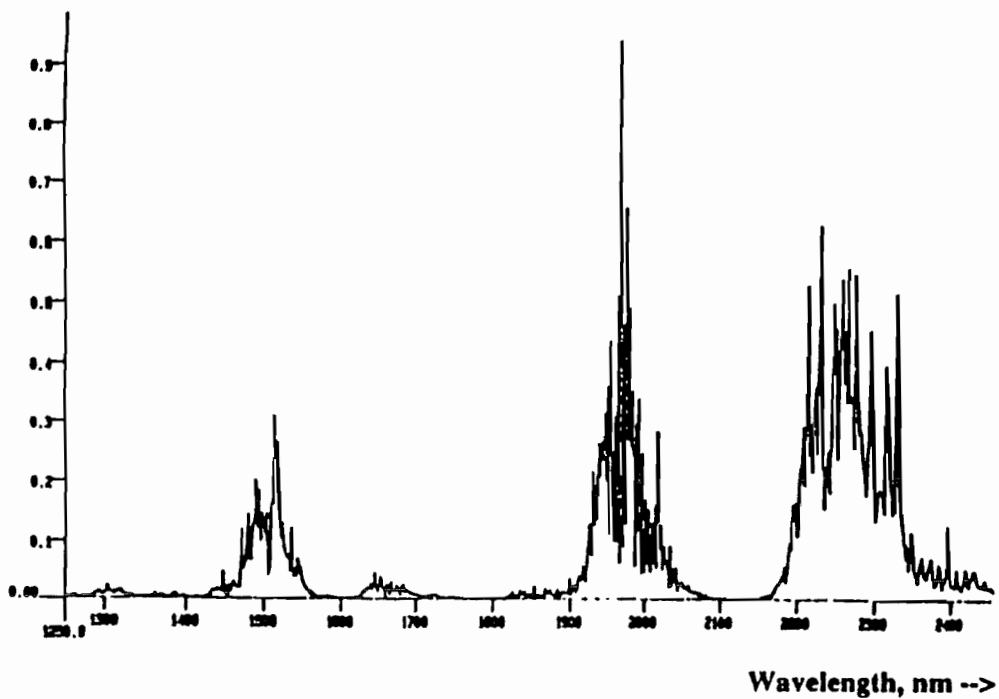


Figure 11 : Transmission spectrum of the reference/measurement test gas (ammonia and water vapour). This was measured in a Perkin-Elmer IR-Spectrometer (path length of 160 mm). The band at 1.505 μm is caused by ammonia, and that at 1.92 μm by water vapour.

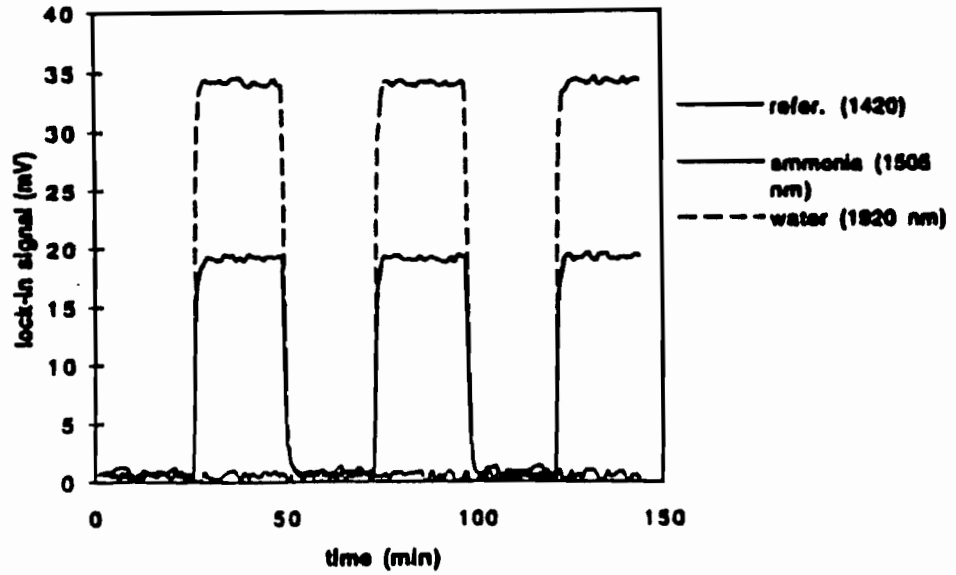


Figure 12 : Overlay of the measurements at the three wavelengths (1.505 μm , 1.92 μm and 1.42 μm) performed with the chopped-beam system of Figure 8.

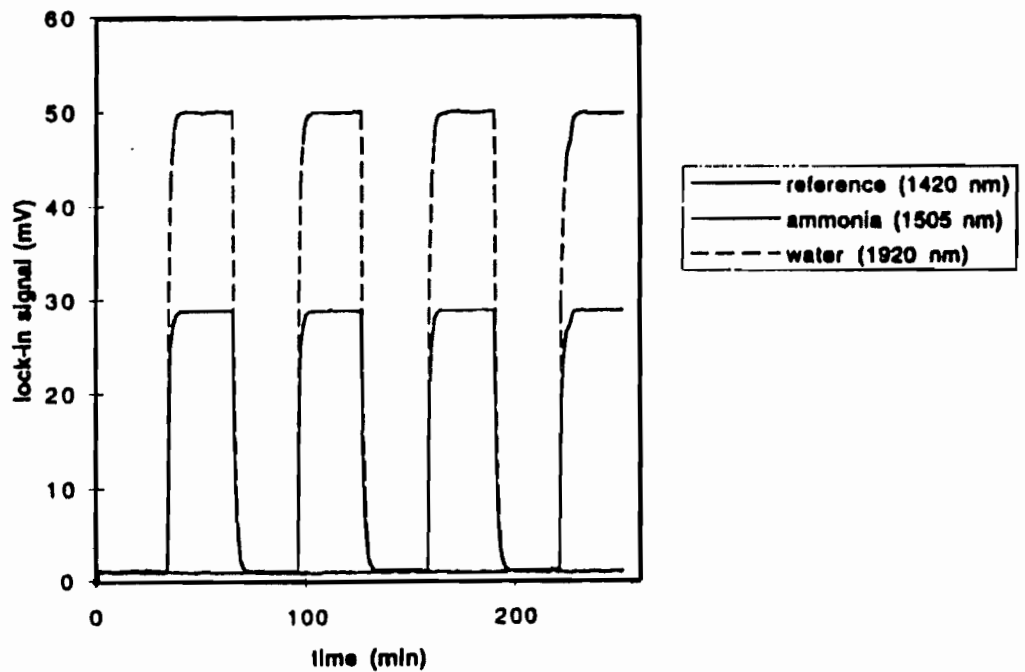
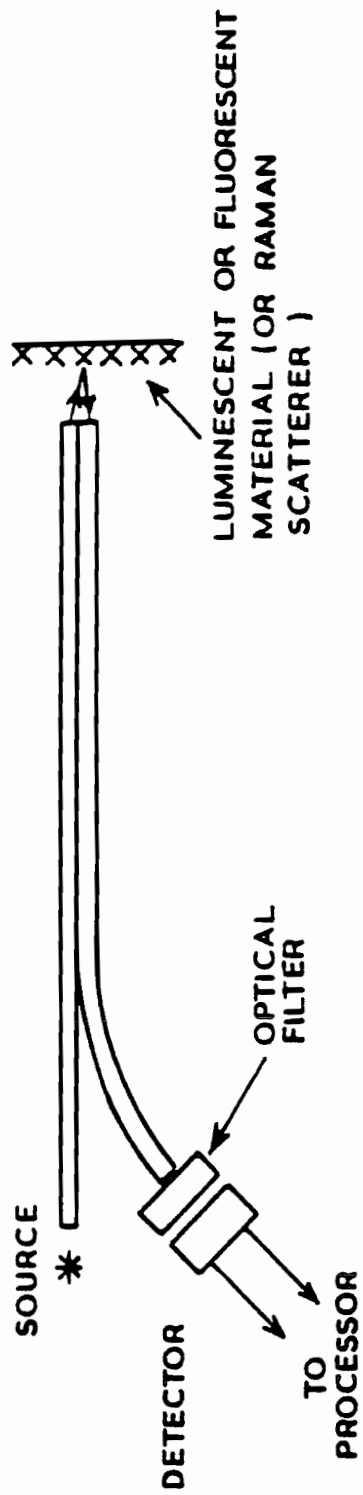


Figure 13 : Overlay of the measurements of the test gas at the three wavelengths (1.505, 1.92 and 1.42 μm), using the complementary-modulated source system of Figure 9. The measurement cell was filled alternately with sample gas, and pure nitrogen.

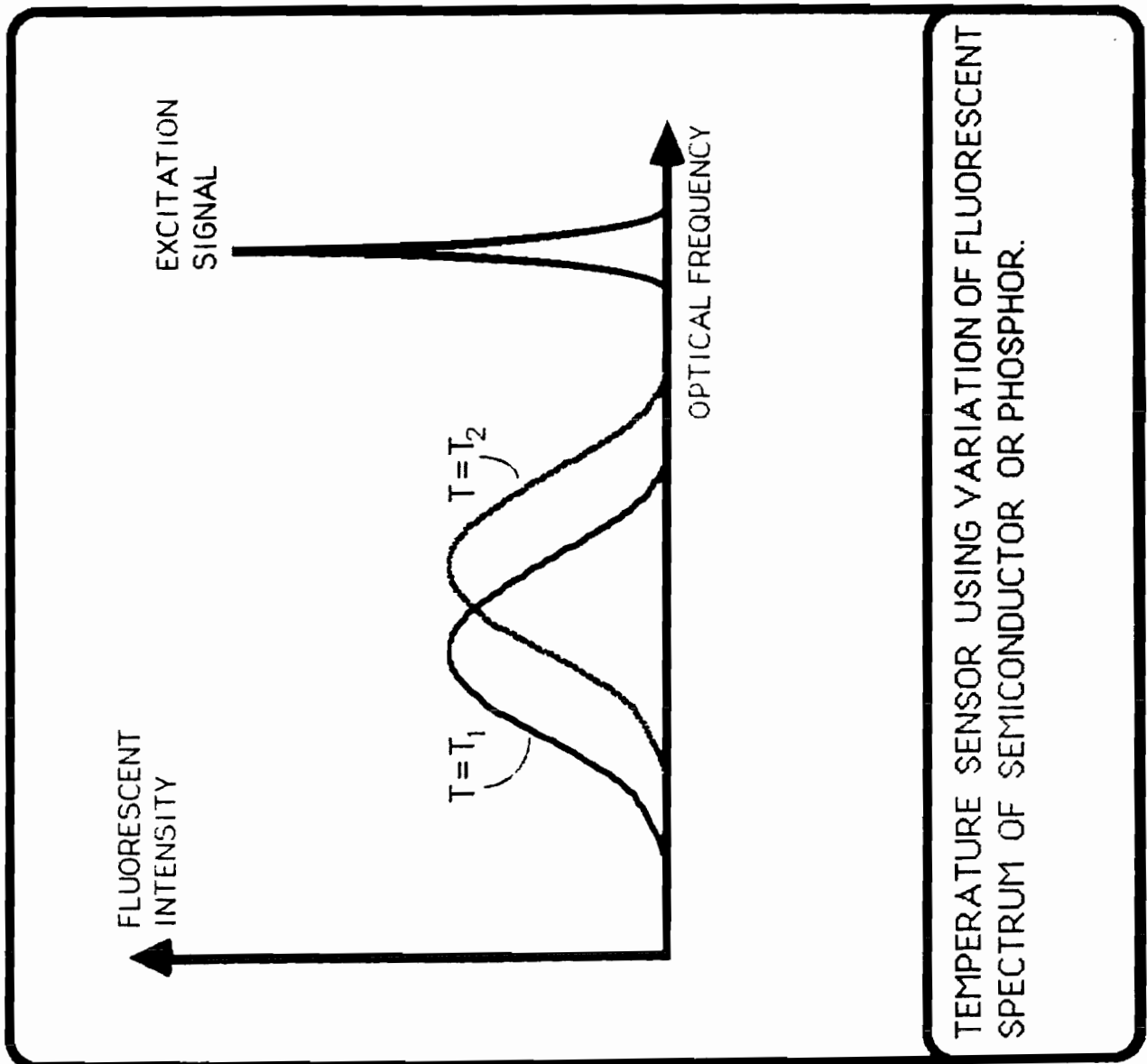
ADVANTAGES OF THE PROPOSED GAS SENSING METHODS

- APPLICABLE FOR COMBUSTION, EXHAUST OR ENVIRONMENTAL MONITORING
- SUPERIOR SELECTIVITY / INSENSITIVITY TO CONTAMINANT GASES
- INTRINSIC SAFETY IS A FEATURE OF REMOTE OPTICAL METHODS
- MAY DETECT GASES IN THE OPEN, USING AVAILABLE AMBIENT LIGHT
- MAY BE USED TO MONITOR REMOTELY OVER OPTICAL FIBRE LINKS
- CAN BE EASILY RECONFIGURED FOR ANY SUITABLE GAS OR GAS MIXTURE
- MAY BE USED TO ASSESS IGNITION RISK OF A GAS MIXTURE
- SIMPLE HARDWARE SUITABLE FOR LOW-COST PRODUCTION
- APPROPRIATE FOR USE WITH LED OR FILAMENT LAMP SOURCES
- OPTIMAL PROCESSING SCHEME, GIVING NEAR-IDEAL FILTERING, OF DESIRED GAS LINES AND BEST USE OF AVAILABLE LIGHT



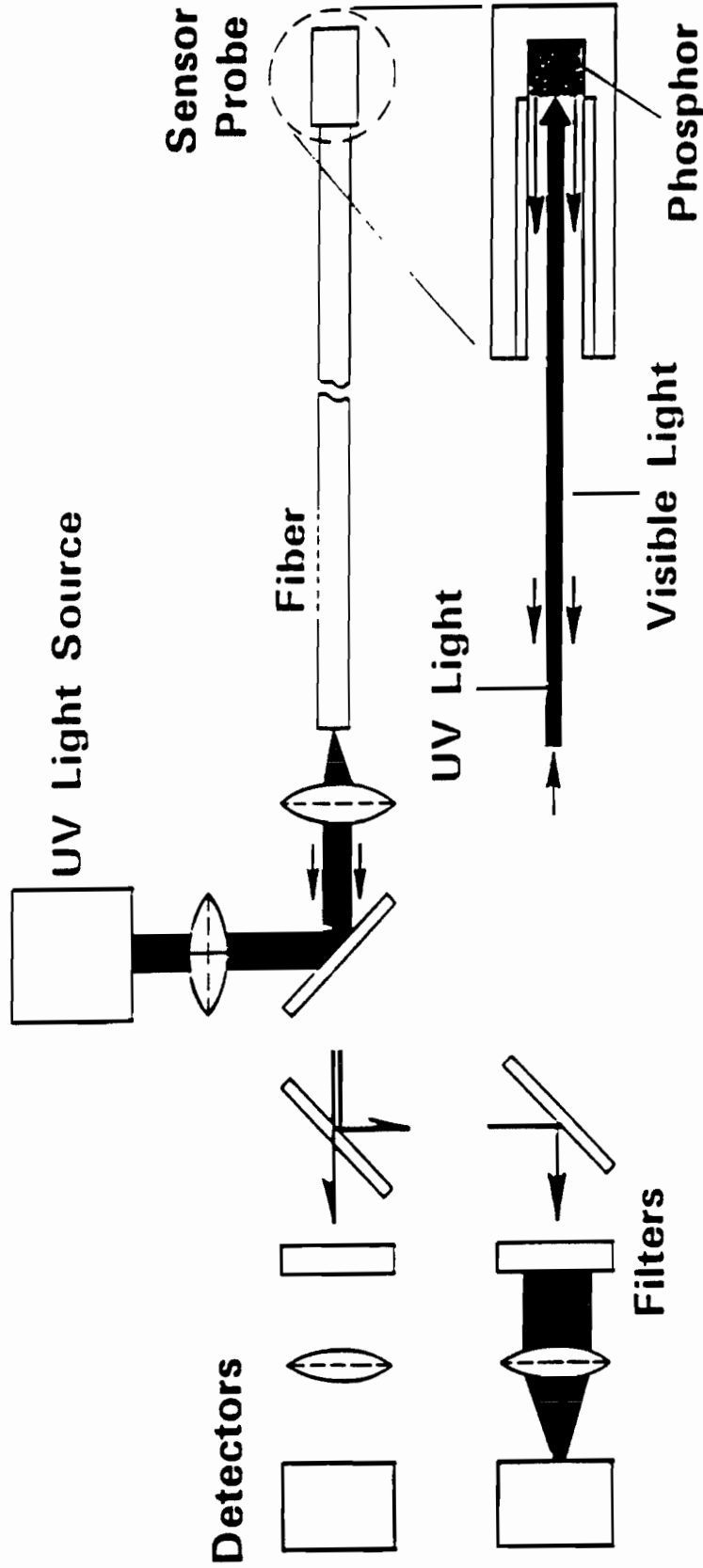
OPTICAL ENERGY LEVEL SENSOR

(may sense spectral distribution of received light or temporal variations if pulsed source is used.)

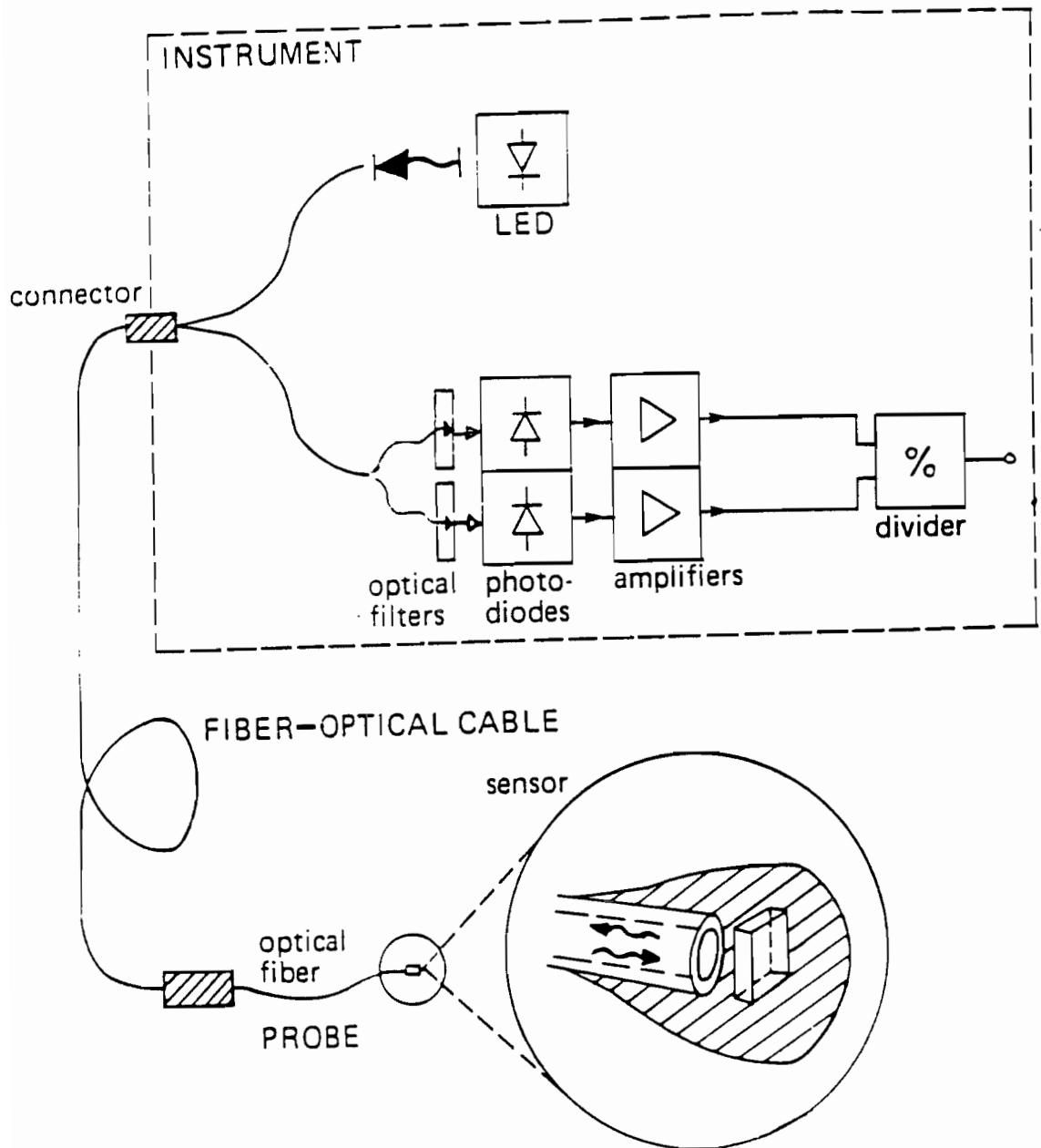


TEMPERATURE SENSOR USING VARIATION OF FLUORESCENT SPECTRUM OF SEMICONDUCTOR OR PHOSPHOR.

Temperature Probe



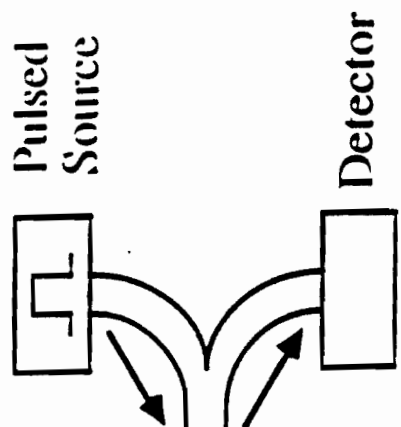
Luxtron's fiber optic thermometer relies on the temperature dependence of a phosphor's emission spectrum. Ultraviolet light excites the phosphor, causing it to fluoresce. It emits most brightly at two wavelengths—one in the yellow-green, the other in the red-orange—and the ratio of intensities at the two wavelengths varies with temperature.



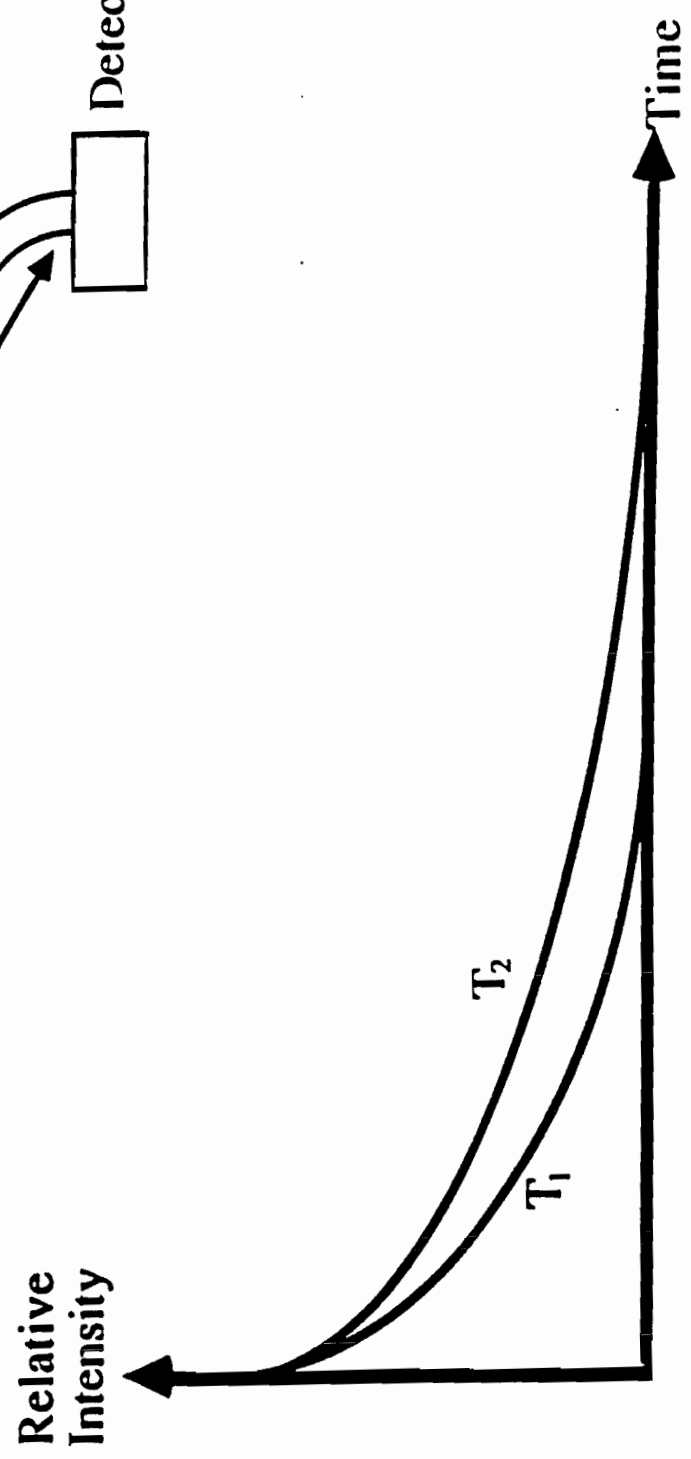
FLUORESCENT SEMICONDUCTOR

TEMPERATURE SENSOR (ASEA)

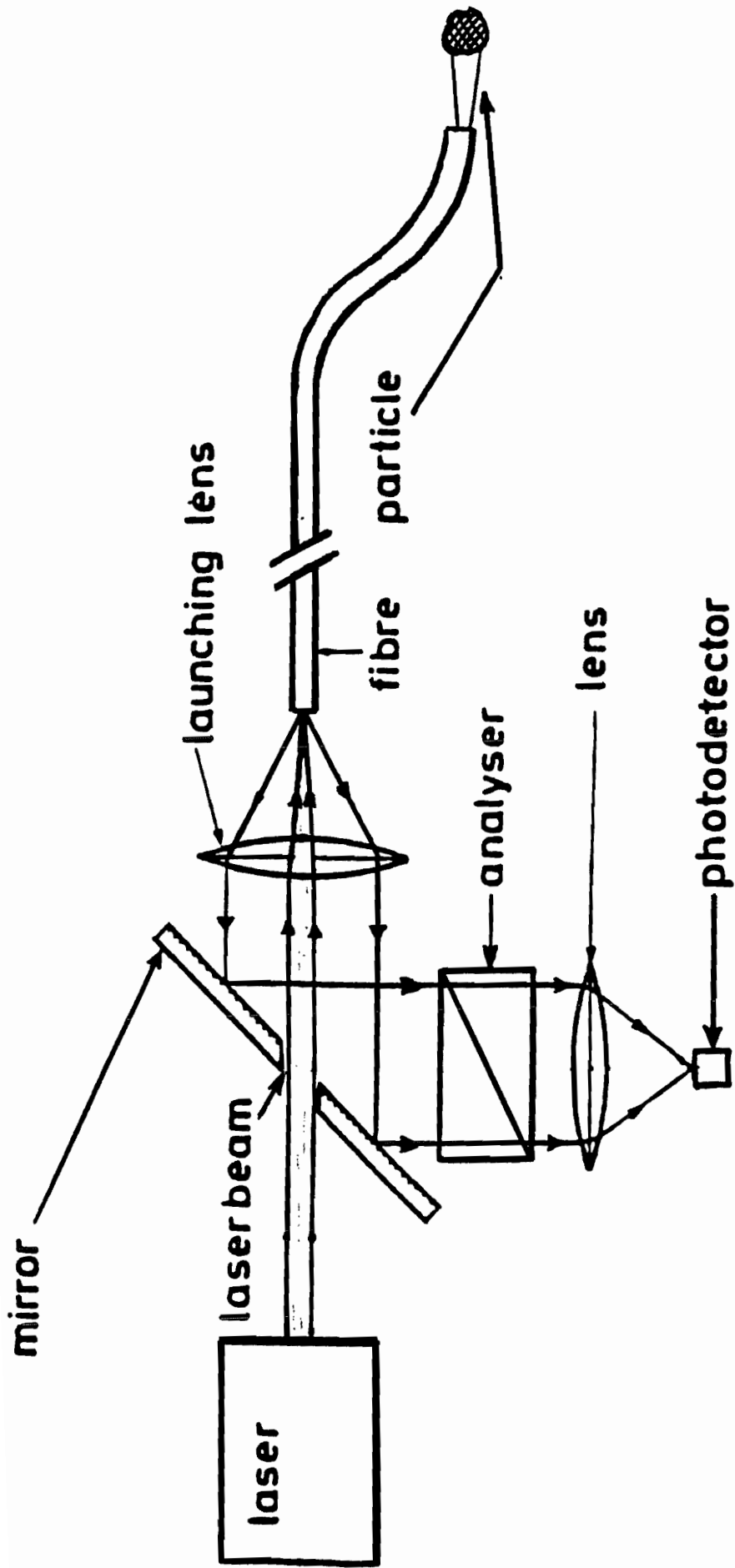
(SPECTRAL INTEROGATION FROM RATIO OF LIGHT RE-EMITTED AT TWO WAVELENGTHS)



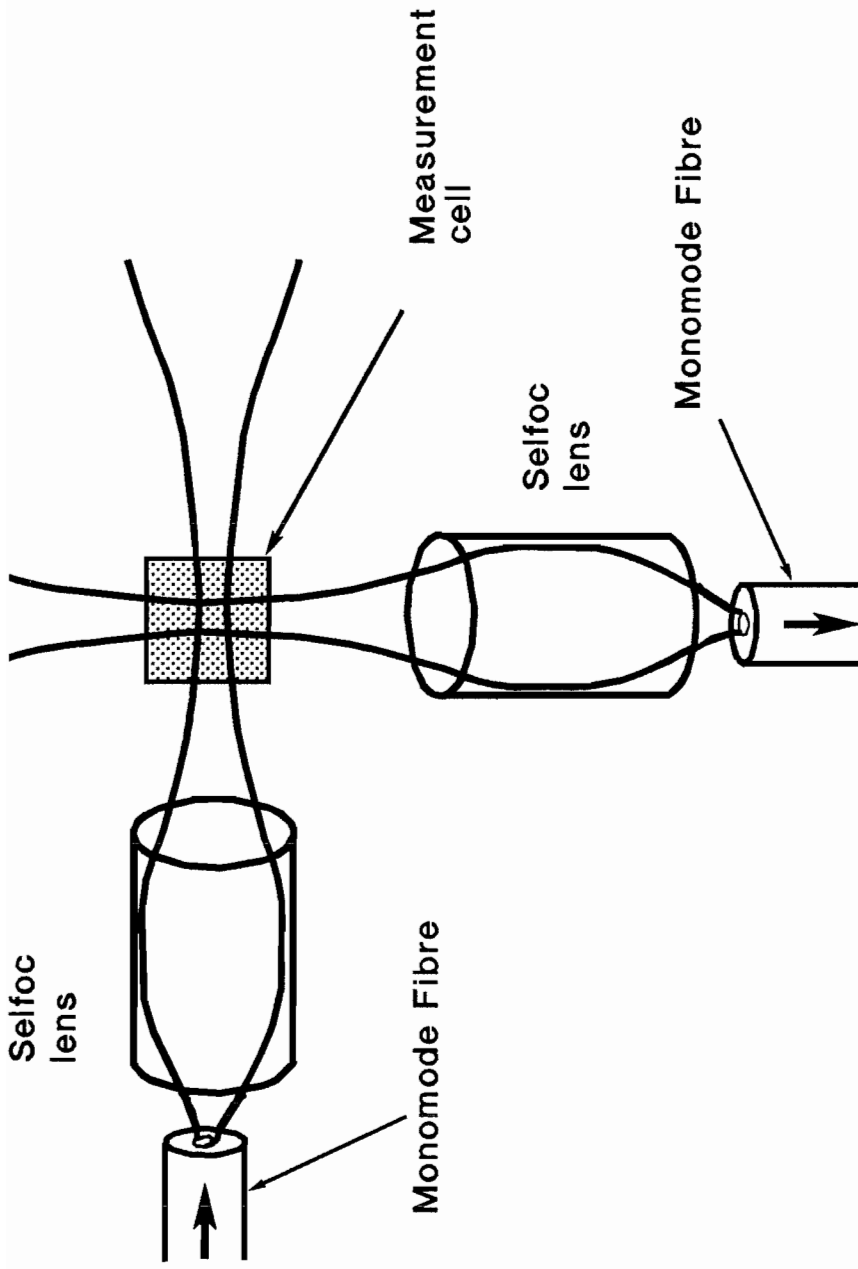
Fluorescent Probe Tip



FLUORESCENT DECAY TIME SENSOR (Cormack)

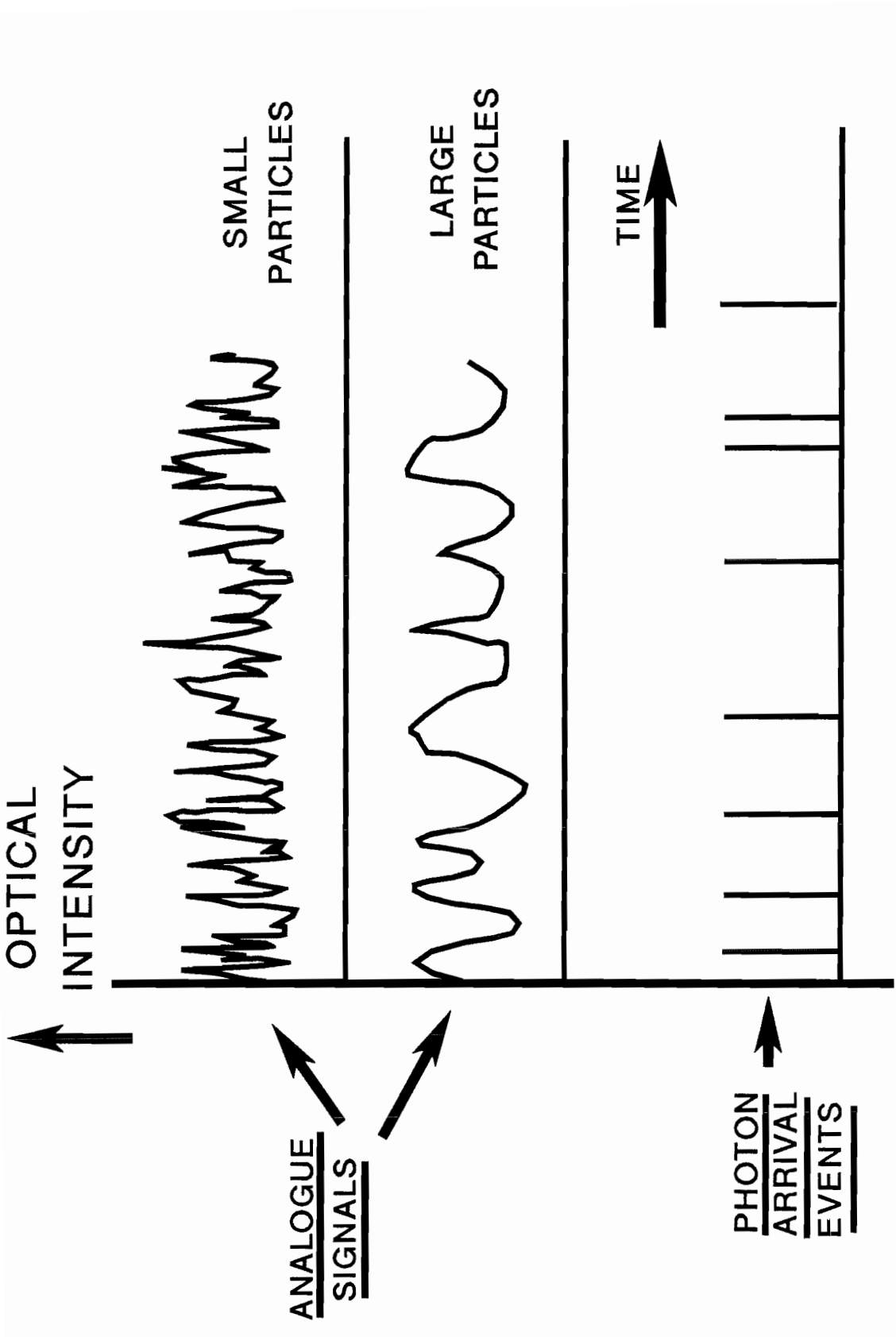


LONGITUDINAL (REFERENCE-BEAM) LASER DOPPLER VELOCIMETER VIA OPTICAL FIBRE

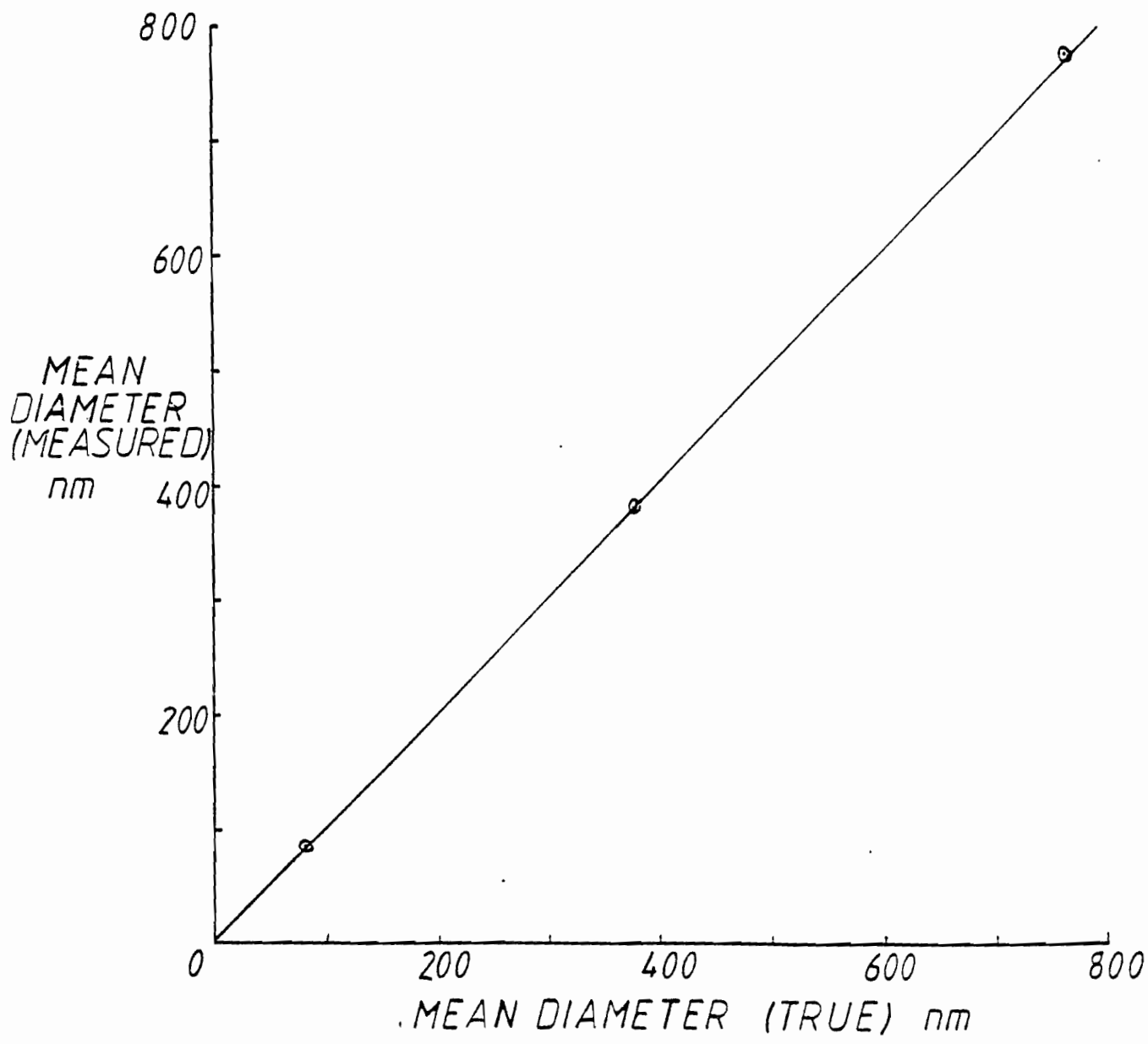


SCHEMATIC OF FIBRE-REMOTED PHOTON-CORRELATION SPECTROSCOPY SYSTEM, USING SELFOC LENSES FOR FOCUSING AND LIGHT COLLECTION.

(METHOD OF CARR ET AL, SENSOR DYNAMICS / CAMR)



OPTICAL SIGNALS WITH PHOTON CORRELATION SPECTROSCOPY



LATEX SPHERE DIAMETER
MEASURED USING
PCS

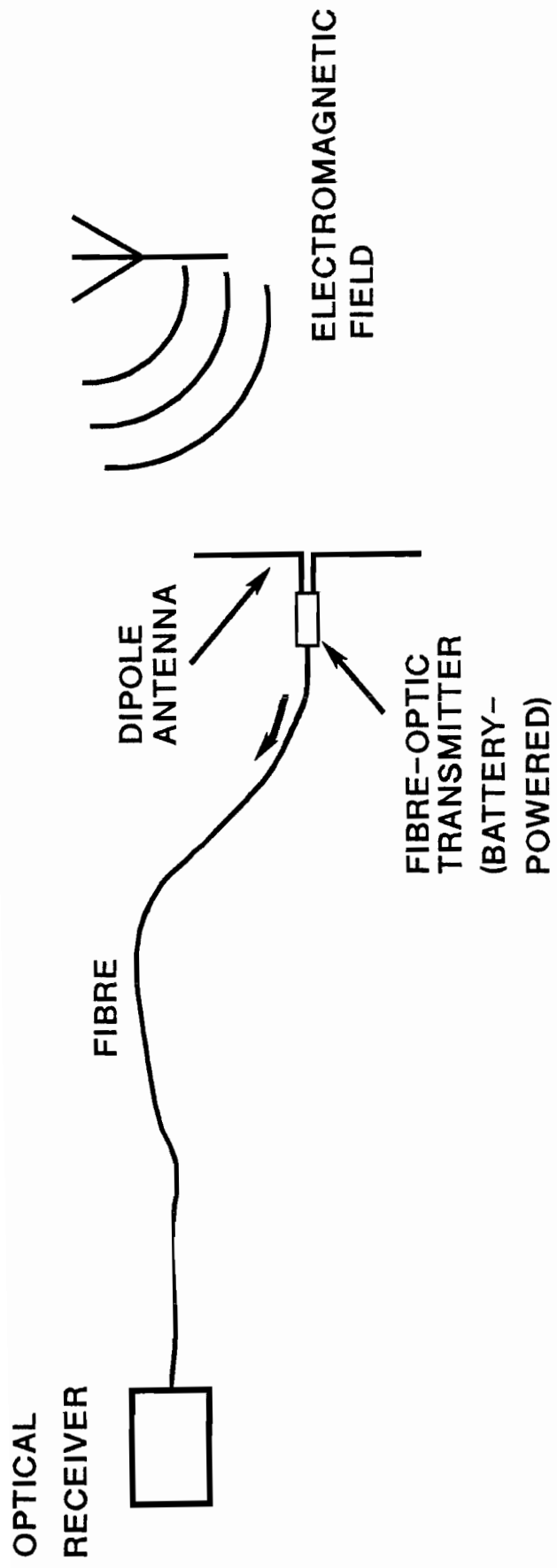


FIG 3. SCHEMATIC OF E-M FIELD SENSOR USING ANTENNA WITH TELEMETRY LINK

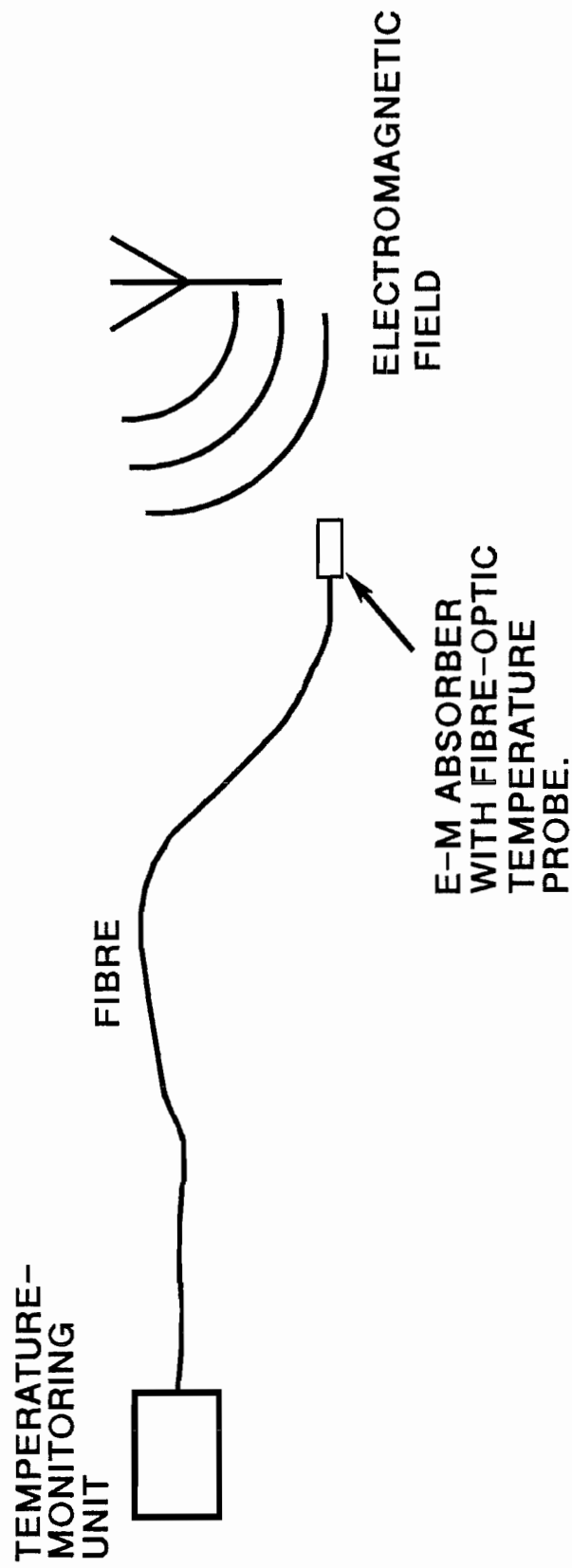


FIG 4. SCHEMATIC OF E-M FIELD SENSOR USING THERMAL METHOD

ELECTRIC FIELD-INDUCED MODULATION

The Pockels (linear electro-optic) Effect

Several crystalline materials exhibit birefringence (ie. they have a different optical wave velocity for components polarised in different directions, or polarisation states). Certain crystals (eg. LiNbO₃, ZnTe, ADP, KDP) exhibit a birefringence (or, if they are already birefringent, a change of birefringence when an electric field is applied). The electric field can be applied in either the direction of optical propagation (longitudinal electro-optic effect) or in a direction at right angles to the direction of optical propagation (Transverse electro-optic effect). If polarised light is now launched at 45° to the birefringent axes of the crystal, the state of polarisation at the output of the crystal depends on the relative phase (ie. depends on the relative optical delay) between the components of the light polarised along the direction of each axis. This is because the electric field at the output of the crystal is the vector sum of two fields at 90° to each other, with the relative phase of the two fields varying with the birefringence of the crystal. As the electric field is varied, the birefringence varies, and the polarisation state at the output varies from plane-polarised (in the 0° direction), via elliptical, clockwise circular, elliptical, plane-polarised (in the 90° direction), elliptical, anti-clockwise circular, elliptical and back to the original plane-polarised (0°) condition.

Pockels-effect Light Modulators

If the electro-optic crystal is placed between cross polarisers, a light modulator is produced which varies its transmission with applied voltage (electric field). Then the output is given by:-

$$I_o = I_{IN} \cdot A \cdot \sin^2 \left[\frac{V}{V_{\lambda/2}} \cdot \frac{\pi}{2} \right]$$

where I_{IN} is the input power, A is a transmission constant (which is always less than unity), V is the applied voltage and $V_{\lambda/2}$ is a constant for the modulator called the half-wave voltage. This is the voltage required to change the state of the modulator from 0% transmission to its maximum transmission.

Optical voltage/electric-field sensors using the Pockels effect

Pockels-cell modulators have been considered for use as voltage or electric field sensors for monitoring electric power systems. However, the biggest problem is that the crystal cannot withstand the full line voltage. If voltage dividers have to be used to reduce the voltage, more conventional metering can also then be used, so there is little advantage in using expensive new technology. In addition, reliable voltage dividers for grid and super-grid voltages are not easy to construct. Therefore electro-optical sensors have yet to find

significant practical use in 50Hz distribution systems. Optical electric field sensors have, however, been used for electric field sensors at radio-wave frequencies, where the capacitive reactance of the crystal is much lower than the resistance, thereby allowing simple free-space detection of the field. The advantage is that they can be used to monitor an RF field, for example from a transmitter antenna, with an all-dielectric fibre-coupled probe, which does not seriously disturb the field being measured.

A more frequent use for Pockel's cell modulators is for rapidly controlling the intensity of light beams with electrical input signals. These modulators normally require high voltages ($V\lambda/2$ is typically 1KVolt for bulk crystals), but this can be reduced very significantly ($V\lambda/2$ typically 10v) if narrow light guides (integrated optics) are formed in electro-optic materials, such as LiNbO₃.

MAGNETIC-FIELD-INDUCED MODULATION: The Faraday (Magneto-optic) Effect

The Faraday Effect

Most transparent materials (even many liquids, such as water) exhibit the Faraday magneto-optic effect to some extent. This effect causes a rotation in the plane of polarisation of an optical signal (which is, of course, an electromagnetic wave) due to the presence of a magnetic field in the direction of propagation. The angle of rotation, θ , of the plane of polarisation is given by:-

$$\theta = B \cdot \ell \cdot V$$

where B is the magnetic flux density, ℓ is the length of the optical path in the field region and V is a material constant called the Verdet constant.

The Faraday effect can occur in solid blocks of material such as glass (Dense glasses with a high lead oxide content, called "extra-dense-flint" glasses, exhibit a high Verdet constant), or can also conveniently occur, in guided-wave form, in optical fibres. In high-silica optical fibres, the Verdet constant is much smaller (approx five times less) than that in lead glasses, but the fibre can be wound into a long coil to ensure a longer interaction length, ℓ .

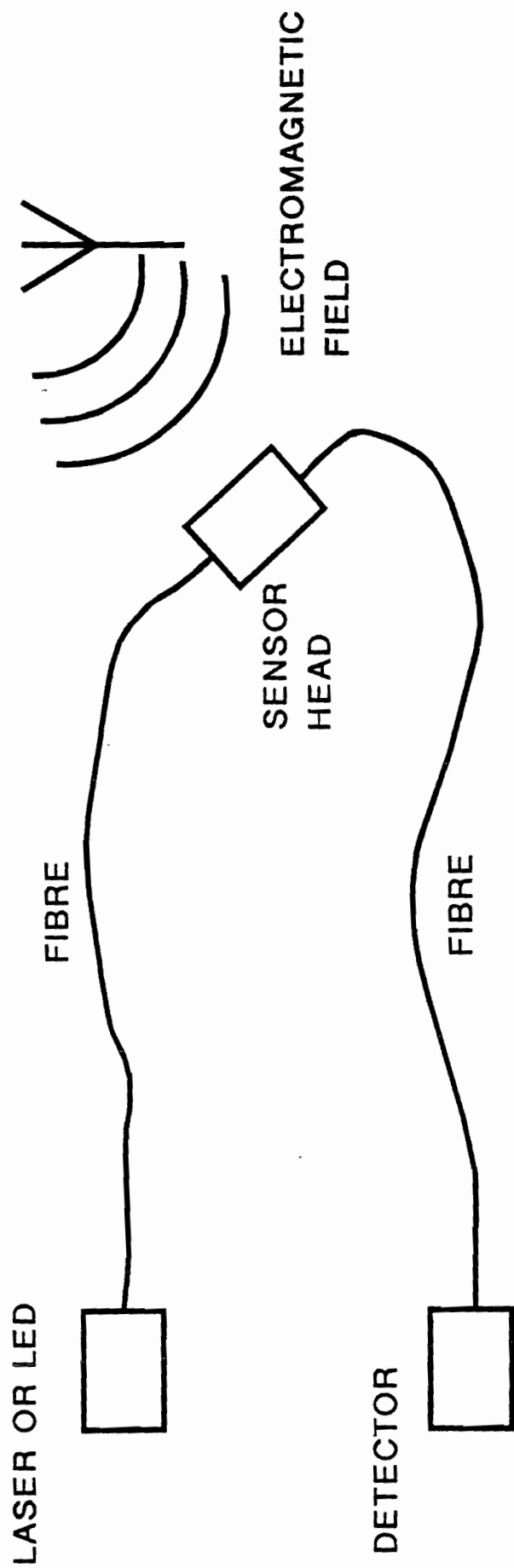
Electric current sensing the using Faraday effect

For electrical sensing, the main application of the Faraday effect is to measure electrical current. The conventional (ie. all-electrical) current transformer, used in electrical distribution systems, can convert part of the energy carried by an A.C. power-delivery line to provide a measurement signal. For use on high voltage lines, however, very high levels of insulation are required between the primary (the power line) and the secondary (measurement coil). This makes the high voltage current transformer very expensive to construct. Optical Faraday effect sensors propose to solve the insulation problem, by providing optical isolation of signals, either by directly illuminating a glass sensor on an overhead line with a ground-based laser or by coupling light energy to the measurement region via an (electrically-insulating) optical fibre. In order for it to measure current, the optical path in the glass (or glass-fibre) sensor must lie mainly in the direction of the light propagation

to modulate the light. Light is most efficiently transmitted when the current is such as to cause a 90° rotation of polarisation (ie $\theta = 90^\circ$). Then the light leaving the block is correctly aligned to pass through the output polariser without loss. The optical signal power I_o at the output of the modulator is given by:-


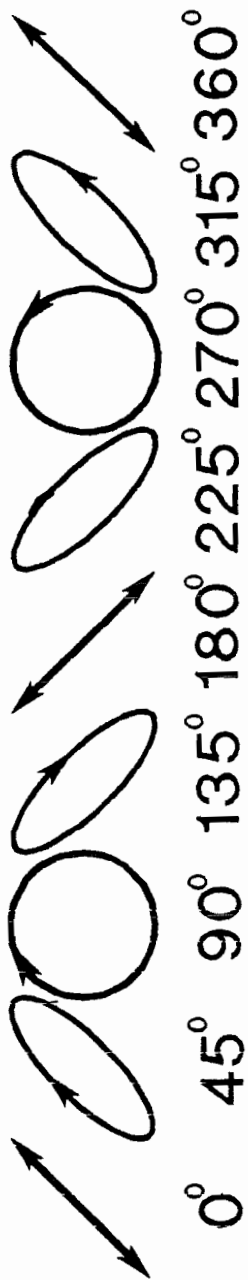
$$I_o = I_{in} \cdot K \cdot \sin^2 \theta$$
$$= I_{in} \cdot K \cdot \sin^2 [i_{coil} / i_{90^\circ}]$$

where I_{in} is the optical input power, K is a transmission constant (which is always less than unity), i_{coil} is the current in the coil and i_{90° is the current level which gives rise to a rotation of 90° .

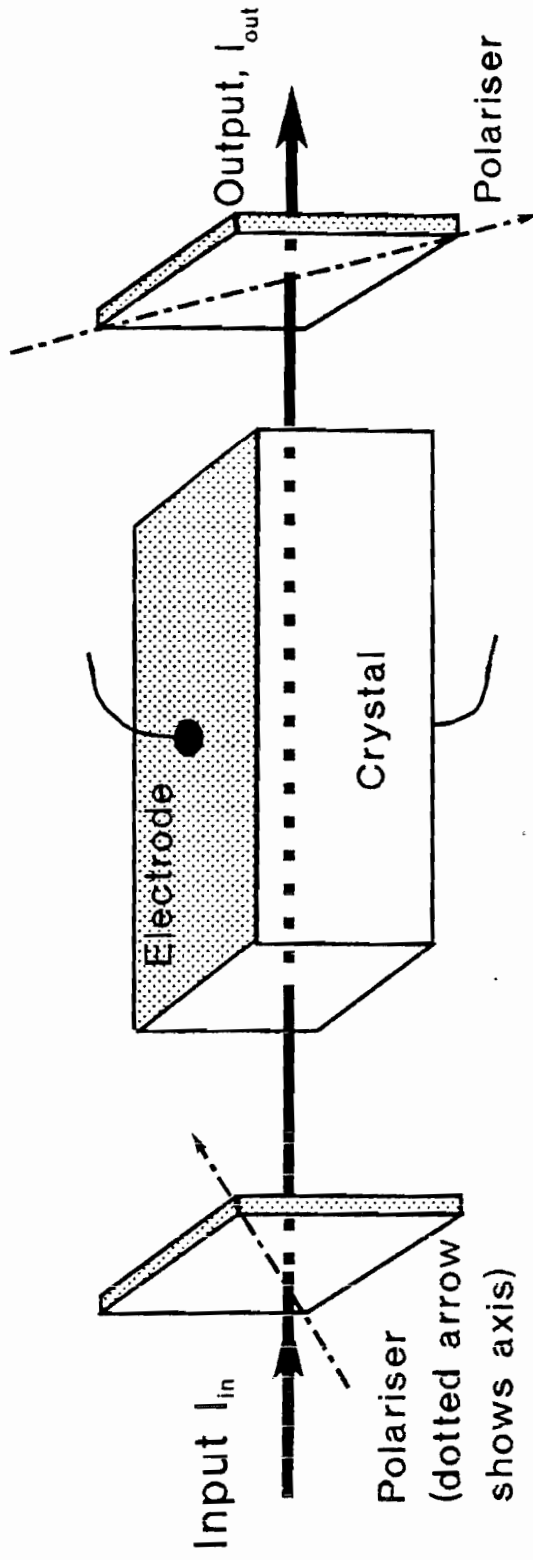


SCHEMATIC OF E-M FIELD SENSOR USING DIRECT MODULATION

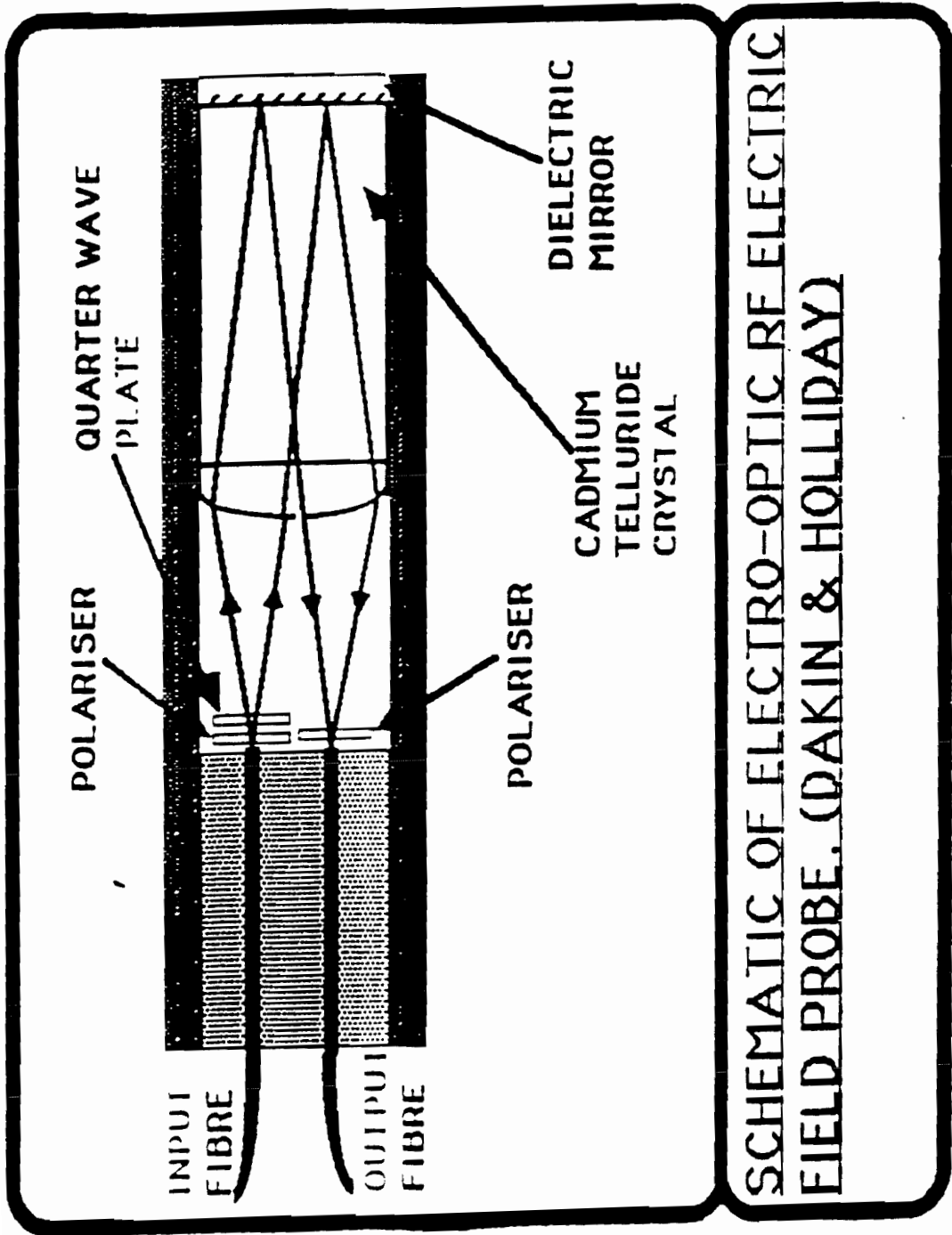
Optical axes
of crystal

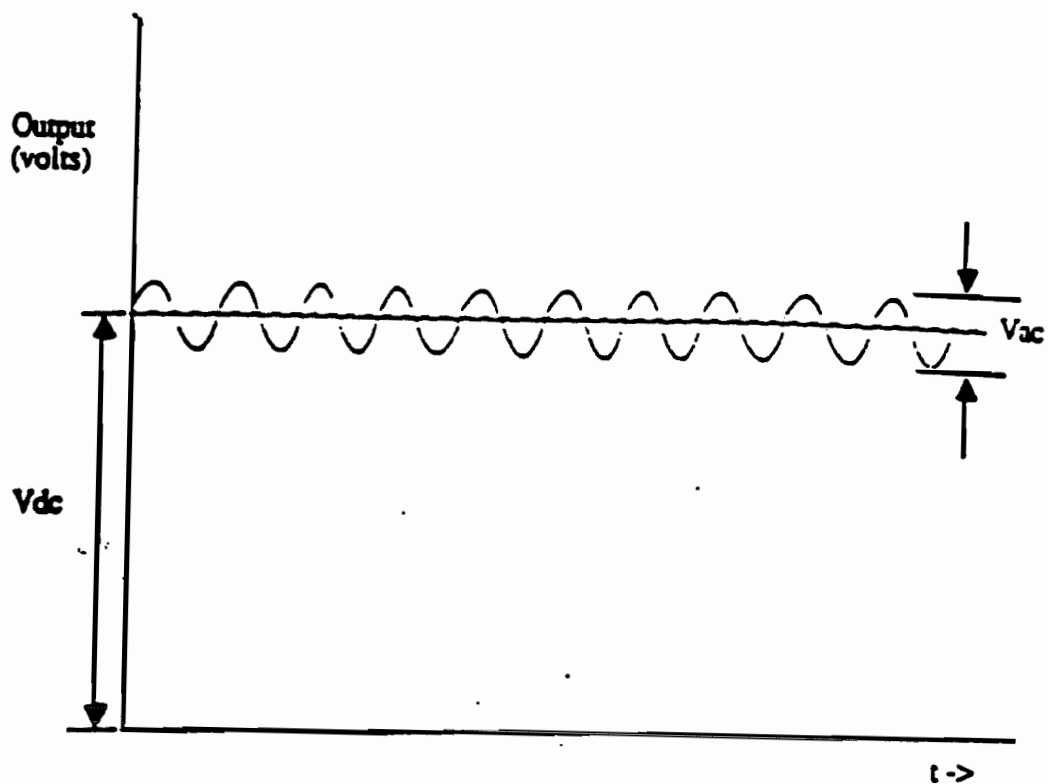



Evolution of polarisation state as birefringence varies.
(Angle shown is phase angle between orthogonal components)

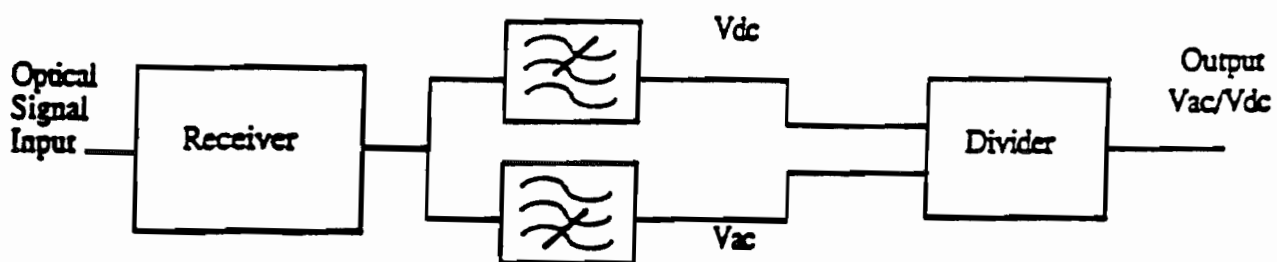


Modulator arrangement





Output of sensor with applied electric field at a single frequency



Divider circuit allowing measurement of alternating electric field independent of optical loss

V_{ac}/V_{dc} will be proportional to the field strength independent of the optical loss in the system



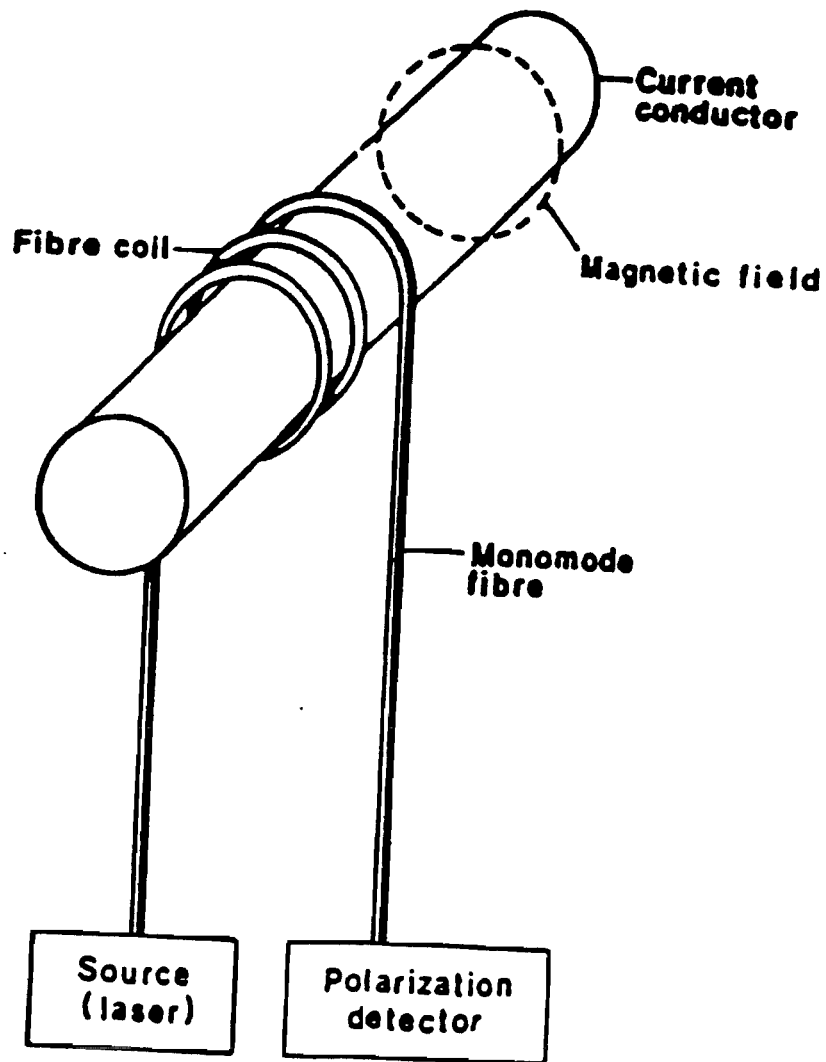
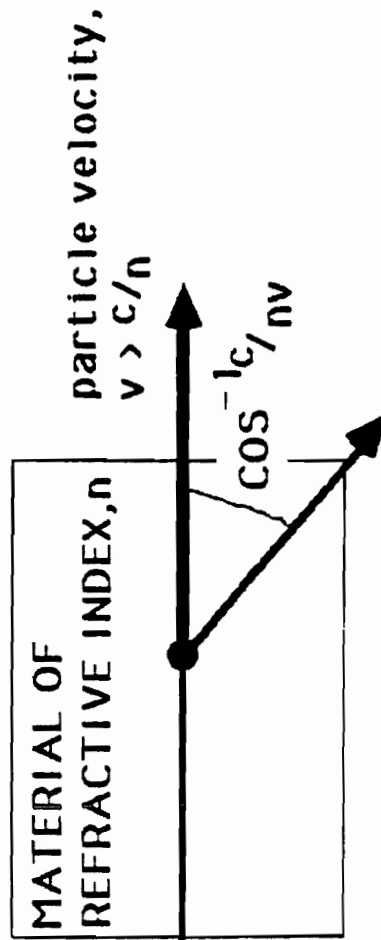


Fig. 19.22 Intrinsic fiber optic current sensor.

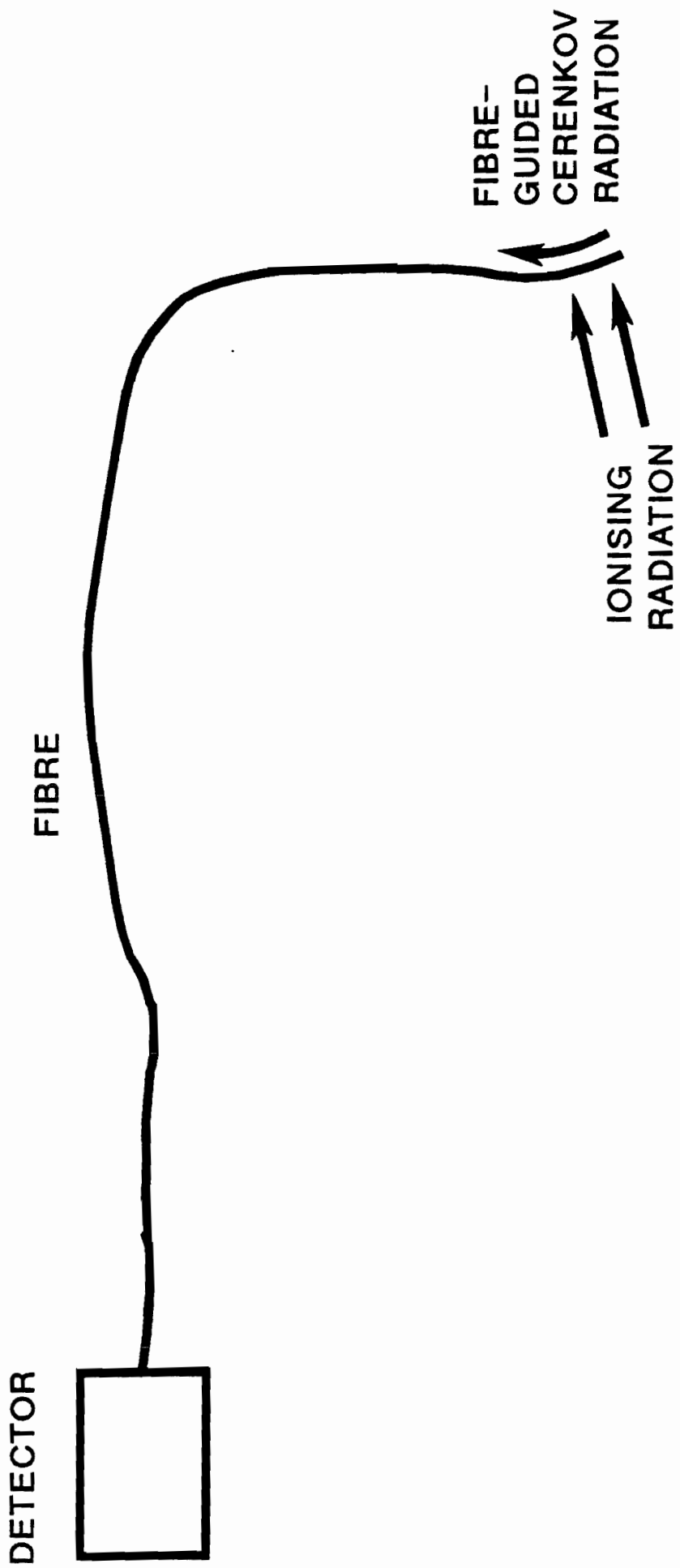
THIS DRAWING IS REPRODUCED WITH THANKS FROM
 "OPTICAL FIBER SENSORS" PUBLISHED BY ARTECH HOUSE.
 EDITORS: J P DAKIN, B CULSHAW.
 DIAGRAM TAKEN FROM CHAPTER BY A J A BRUINSMA, T M J JONGELING

CERENKOV EFFECT

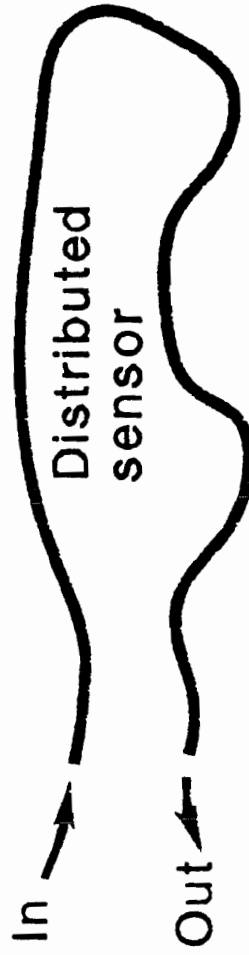
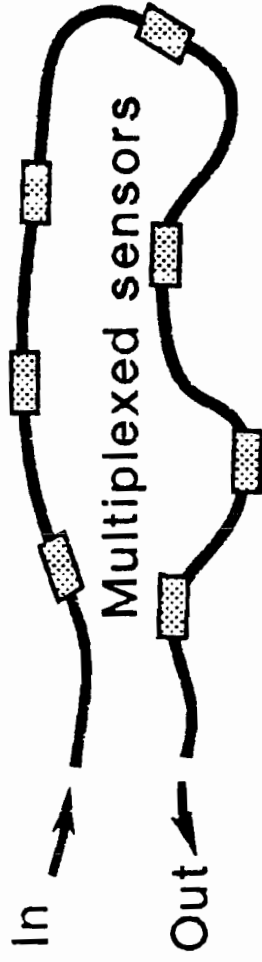
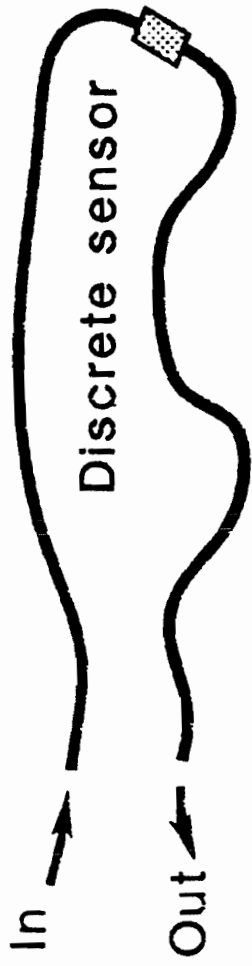
RELATIVISTIC
CHARGED
PARTICLE
TRACK



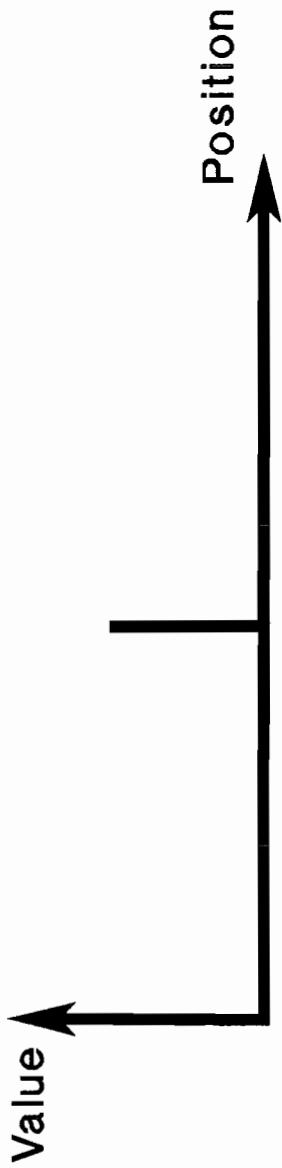
CERENKOV RADIATION IS A RELATIVISTIC EFFECT OCCURRING WHEN A CHARGED PARTICLE MOVES THROUGH A MEDIUM WITH A VELOCITY GREATER THAN THE VELOCITY OF LIGHT, C/NV , IN THE MEDIUM. A FIBRE ITSELF MAY BE USED AS A CERENKOV DETECTOR.



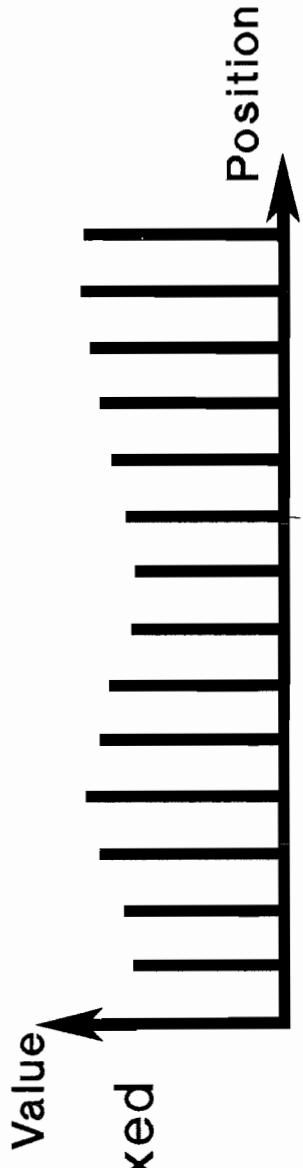
SCHEMATIC OF REMOTE RADIATION SENSOR, USING CERENKOV RADIATION GENERATED IN FIBRE CORE.



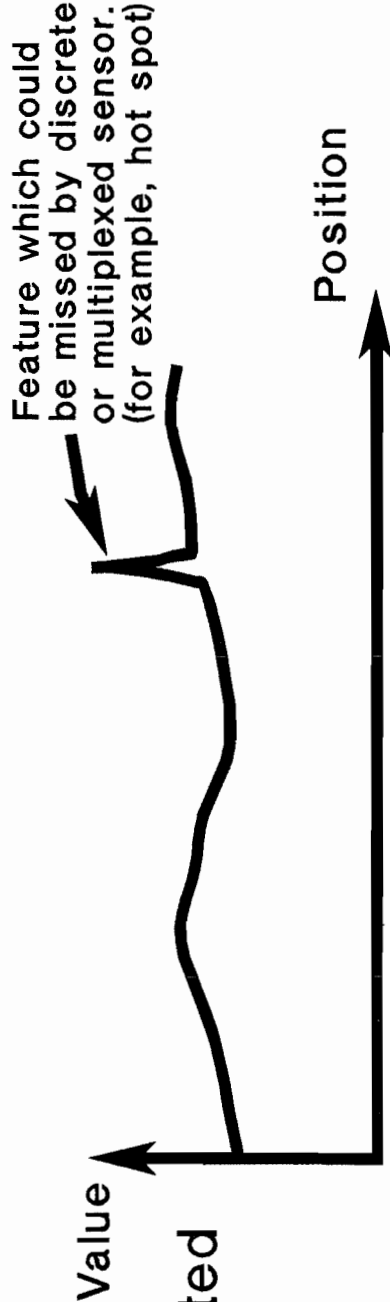
Schematic illustration of discrete, multiplexed and distributed sensors



Discrete Sensor



Multiplexed Sensor

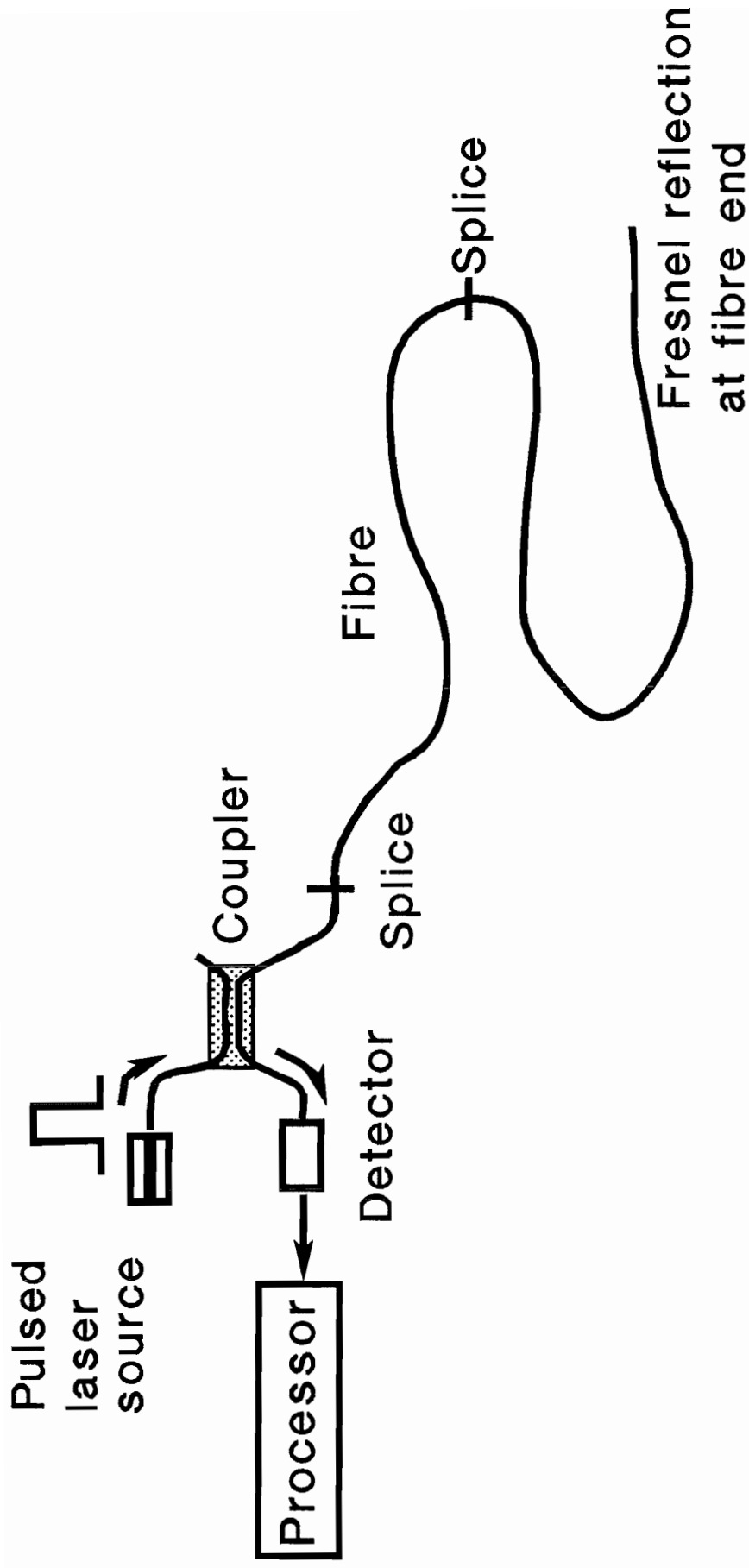


Distributed Sensor

Advantages of distributed sensors

ADVANTAGES OF DISTRIBUTED FIBRE SENSORS

- INTRINSICALLY MULTIPLEXED, WITHOUT 'GAPS' IN COVERAGE
- MORE ECONOMIC USE OF EXPENSIVE OPTOELECTRONICS
- RELIABLE COMPARISON OF MEASURAND VALUE VS LENGTH
- INOBTRUSIVE SENSOR WITH LESS CABLING



Basic arrangement of optical-time-domain reflectometer (OTDR) system.

Signal Returns from Backscatter Systems in Optical Fibre
(Return signal variation with time, for energy E launched, AFTER the coupler, into the measurement fibre).

Conventional OTDR System:-

$$P(t) = P(z) = 0.5 \cdot E \cdot S \cdot \alpha_s(z) \cdot \exp[-\alpha(z)dz]$$

P(t) is variation of return signal P with time, t

P(z) is the equivalent variation with distance, z

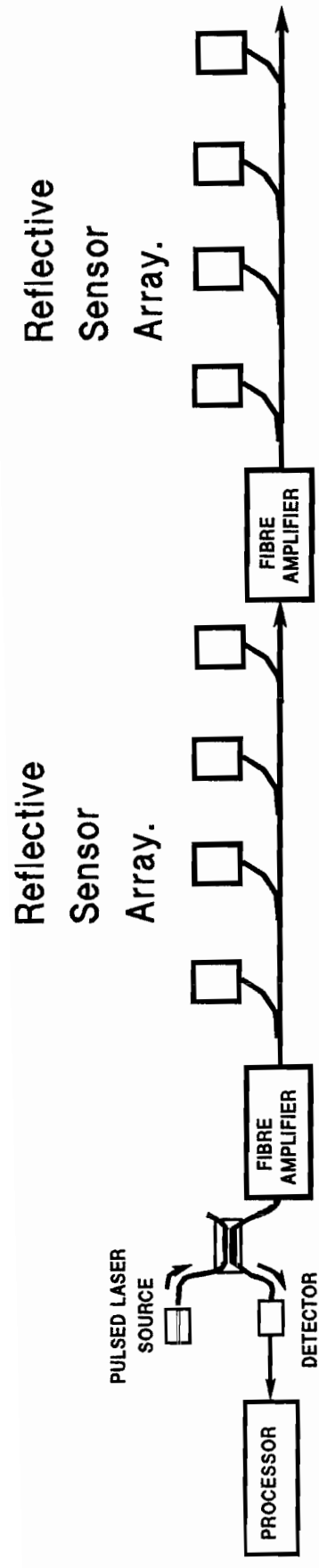
(z = v . t , where v is velocity of light in fibre)

S is fraction of scattered light coupled into backward-guided modes in fibre

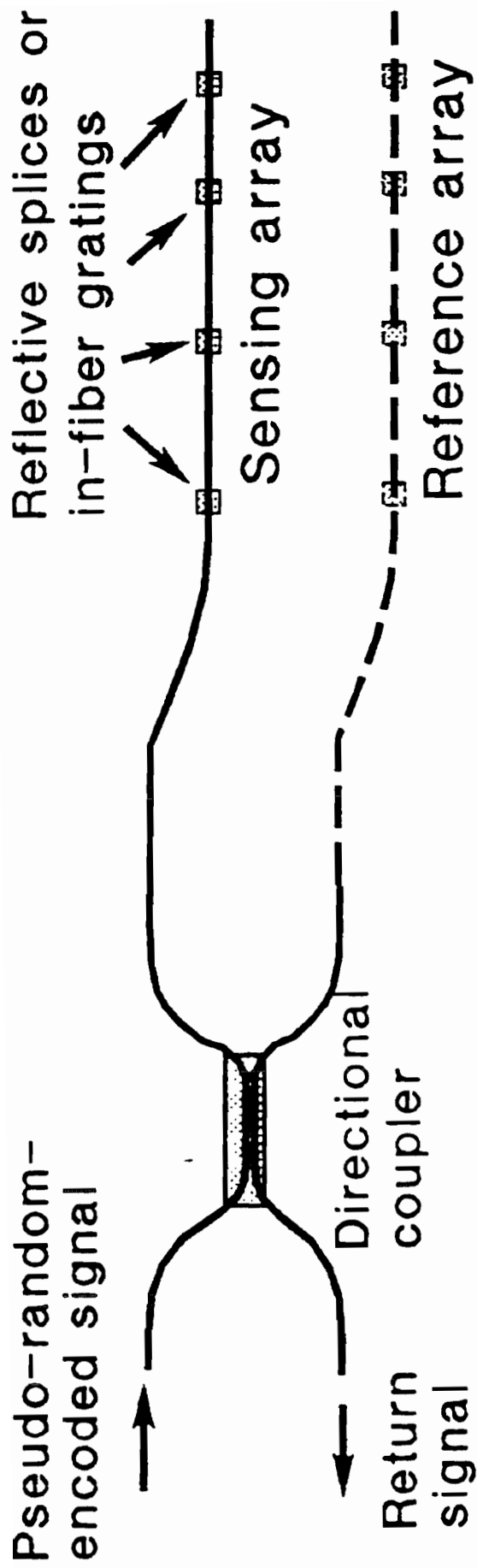
$\alpha_s(z)$ is the scattering loss coefficient of the fibre,

$\alpha(z)$ is the total attenuation coefficient of the fibre

The factor of 0.5 is included to allow for 3dB (50%) loss in the directional coupler



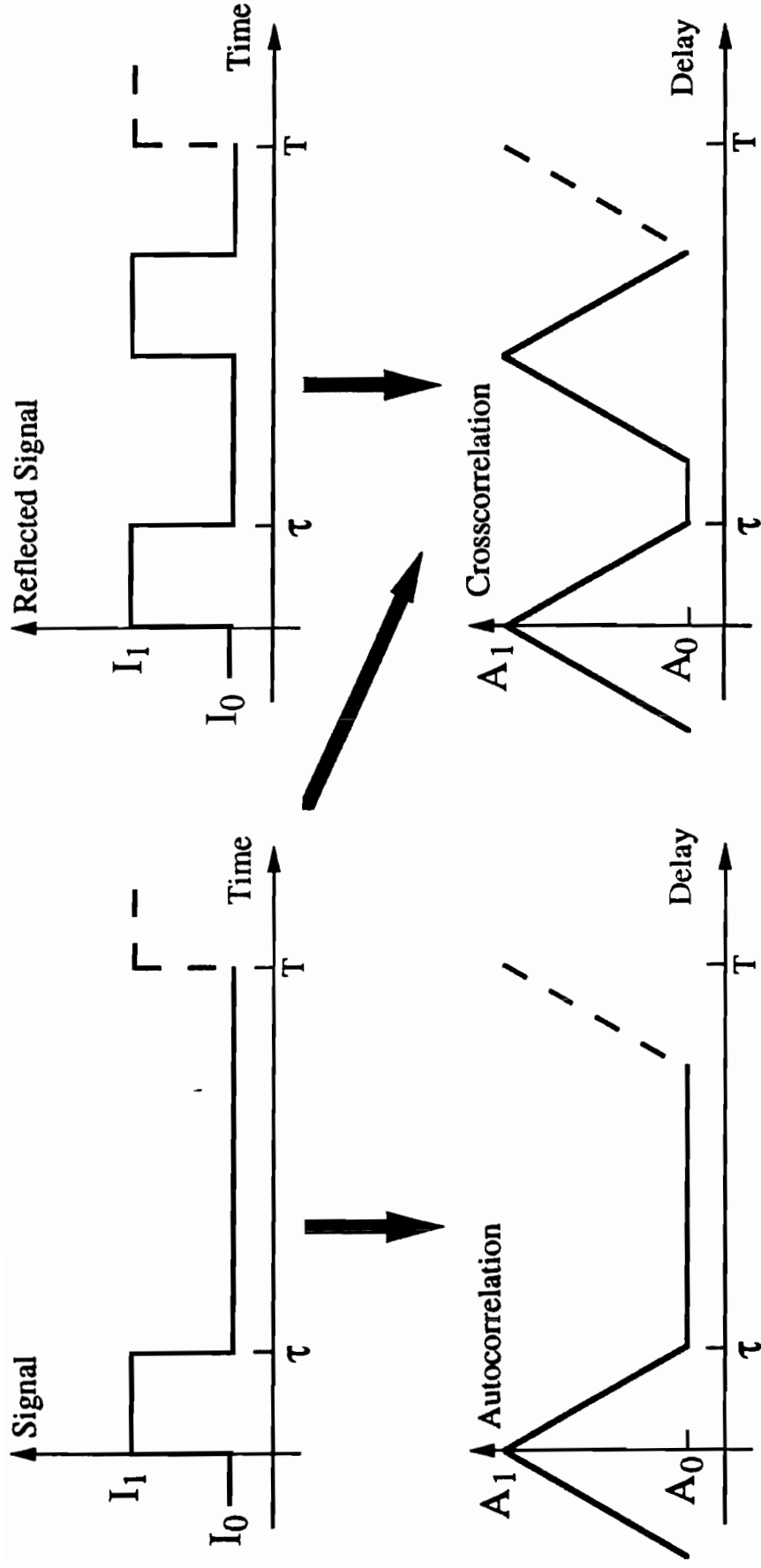
Schematic of OTDR-Addressed Array of Reflective Sensors, Using Linear Branching Highway.



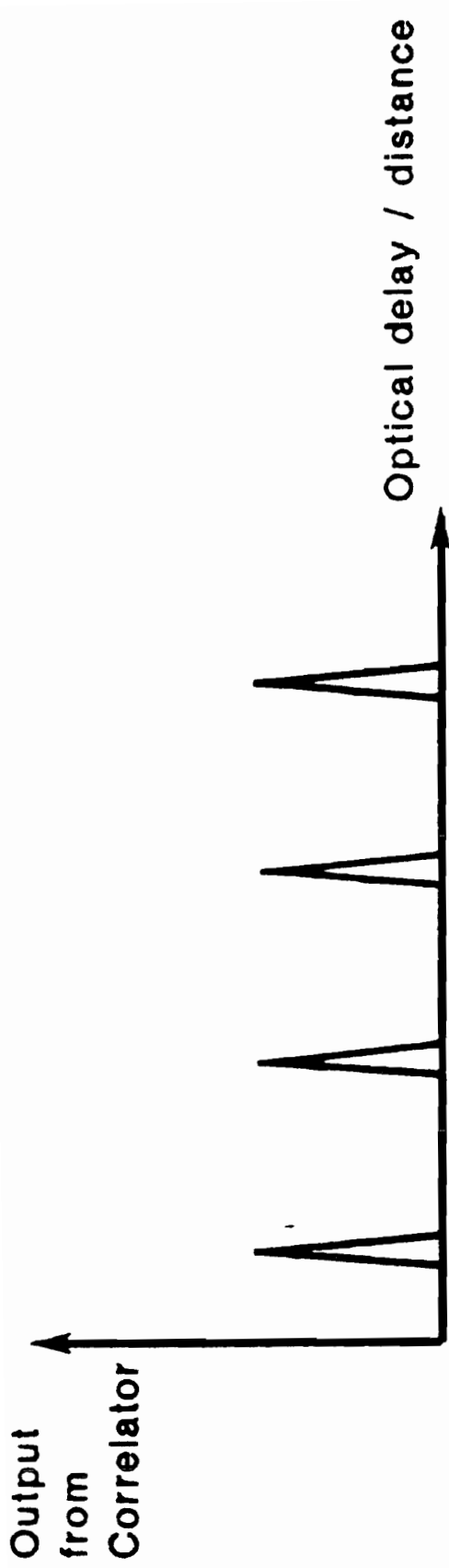
Schematic of OTDR system for precise location of reflective discontinuities. (Eg. long-gauge-length strain sensor)

Principle of Precision OTDR Interrogation System:

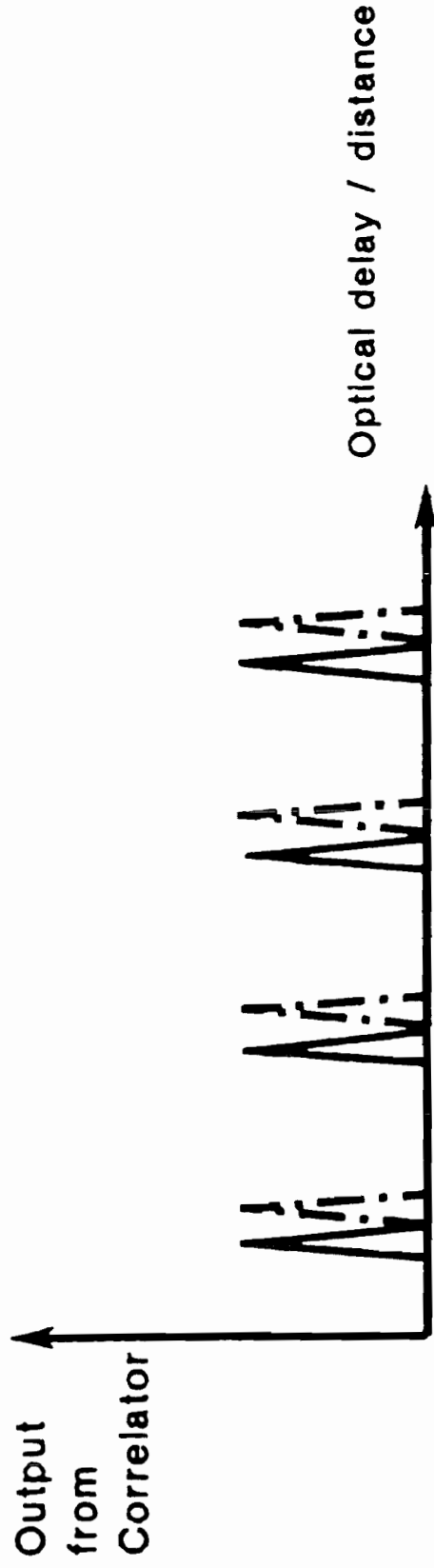
- Optical pulses are sent into the fibre and returned power is correlated with input signal.
- The correlation function can be obtained by sweeping the delay continuously. Each peak can be separately determined due to properties of pseudo-random code.
- Reflection position can be accurately determined by processing to determine precise position of each correlation peak.



Correlation of a pulse with itself (autocorrelation)
 and with two similar pulses (crosscorrelation)



(a) Correlator output signal from single-fibre reflective sensing system



(b) Correlator output signal from dual-fibre reflective sensing system.

Illustration of the correlated signal outputs

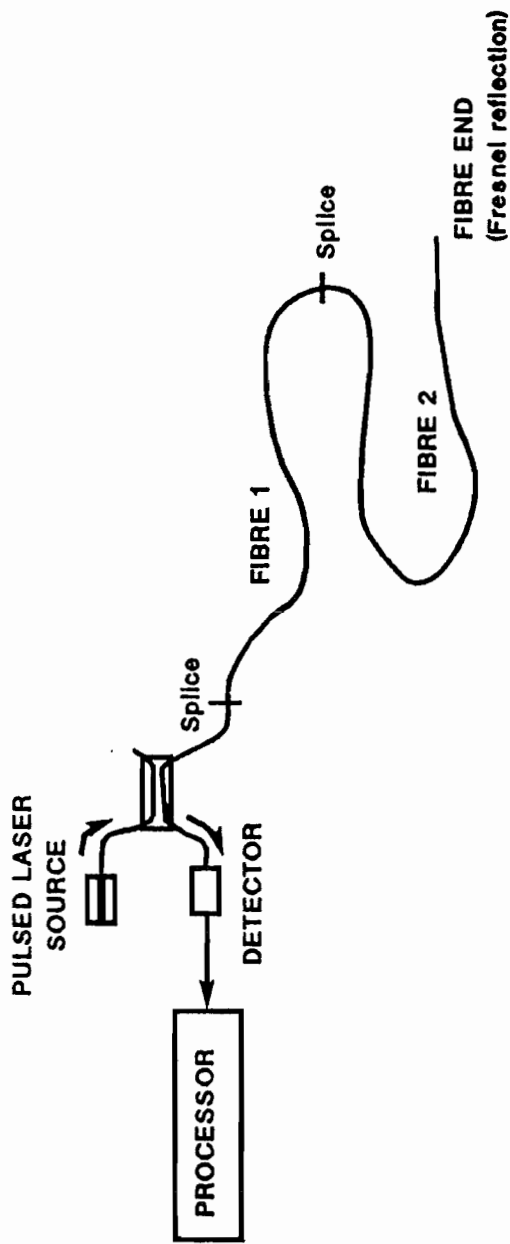
DISTRIBUTED SENSORS

e.g. *OTDR

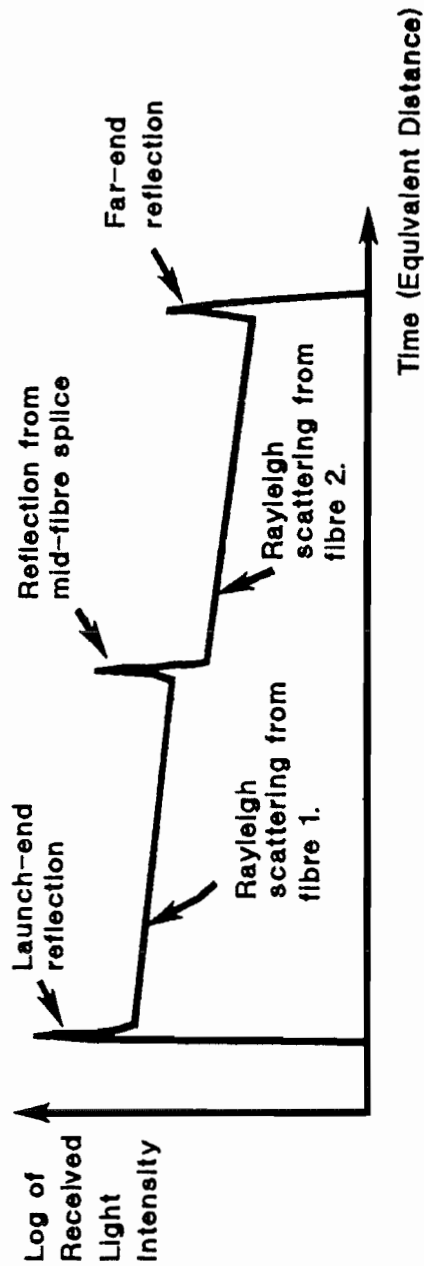
* RAMAN OTDR

* FLUORESCENT OTDR

* POLARISATION OTDR

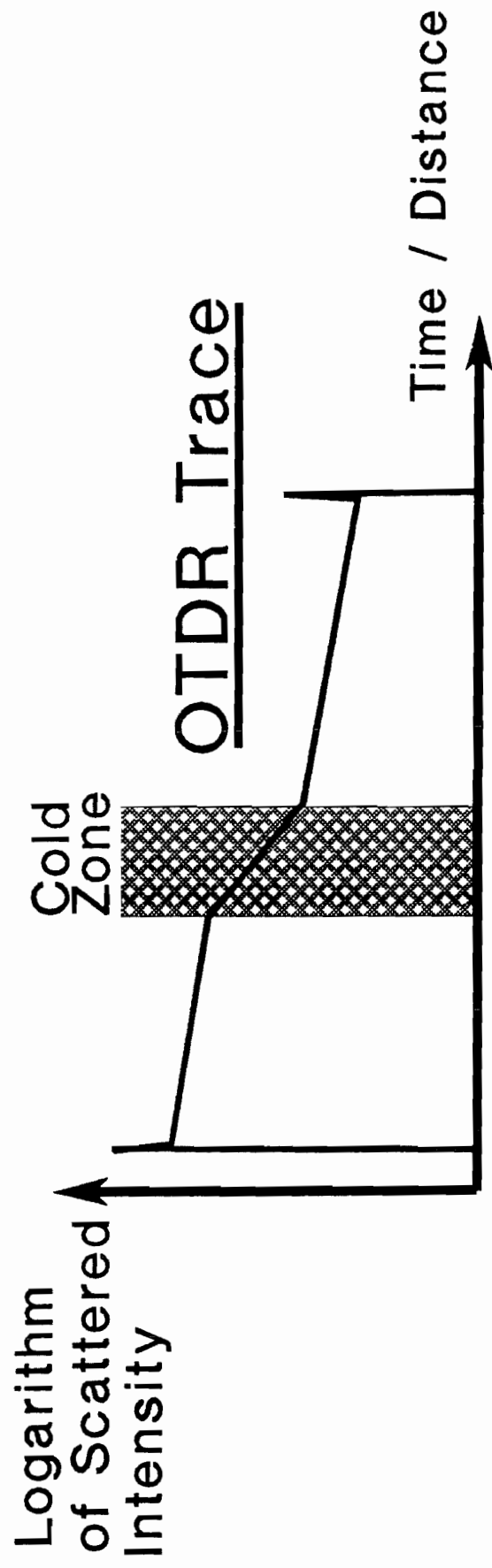
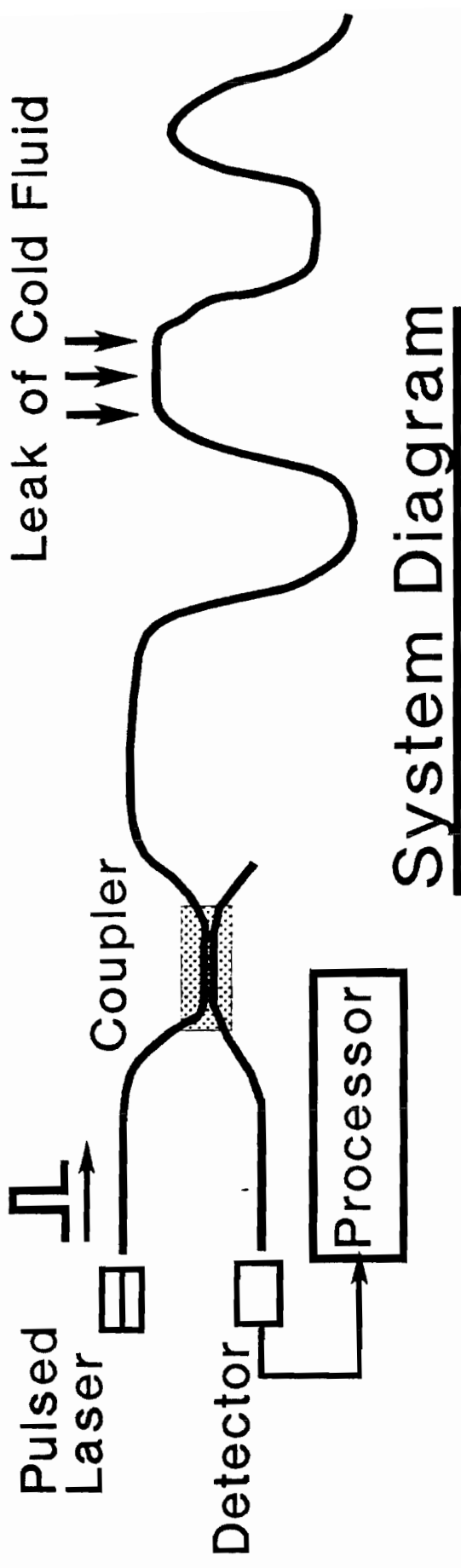


(a) BASIC OPTICAL ARRANGEMENT OF OPTICAL TIME DOMAIN REFLECTOMETER (OTDR)



(b) INTENSITY VERSUS TIME, OTDR RETURN.

CONCEPT OF THE BASIC OPTICAL TIME DOMAIN REFLECTOMETER



Concept of Distributed Sensor for Cold Spots
 (Uses a Silicone-Clad Fibre)

OTDR Systems

Advantages:-

Reliable systems already exist.

It is easy to separate signals in time domain

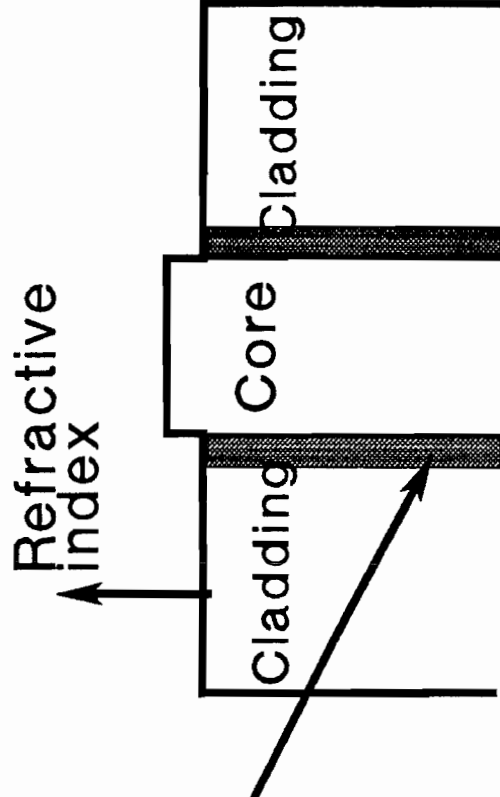
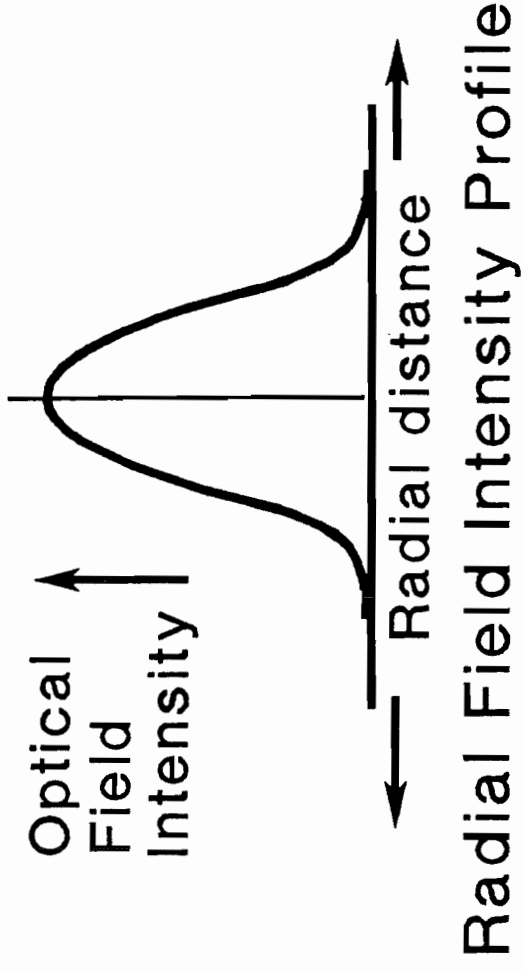
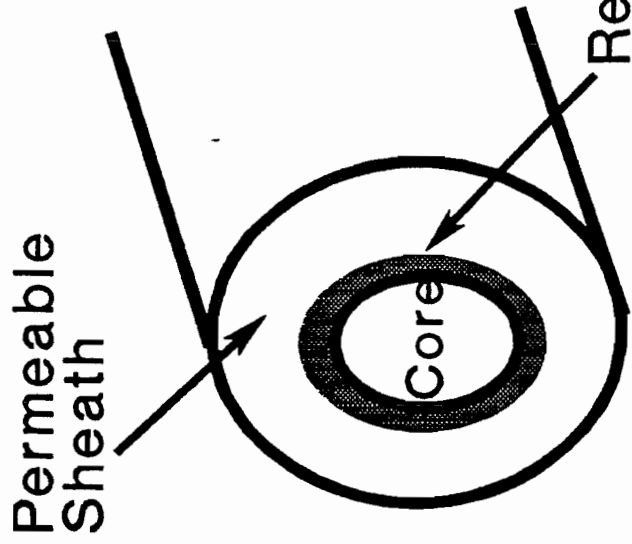
Outgoing signal and return signal can share common path

Standard fibre is usually used

Linear operation: calibration not power-level dependent

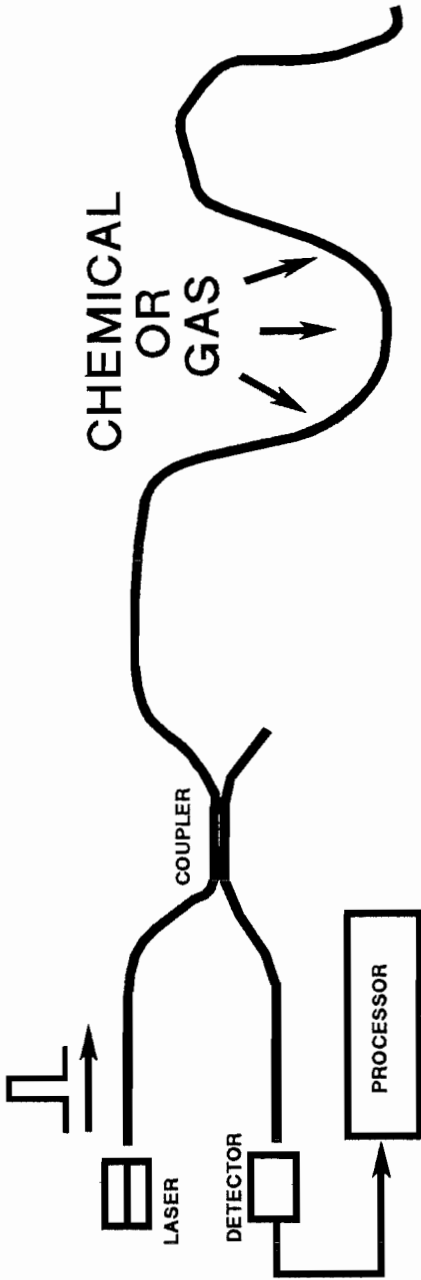
Disadvantages:-

Weak signal return, particularly with the Raman and Brillouin scattering based systems.

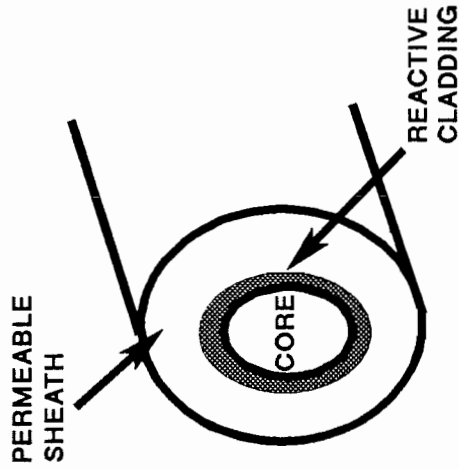


Refractive Index Profile

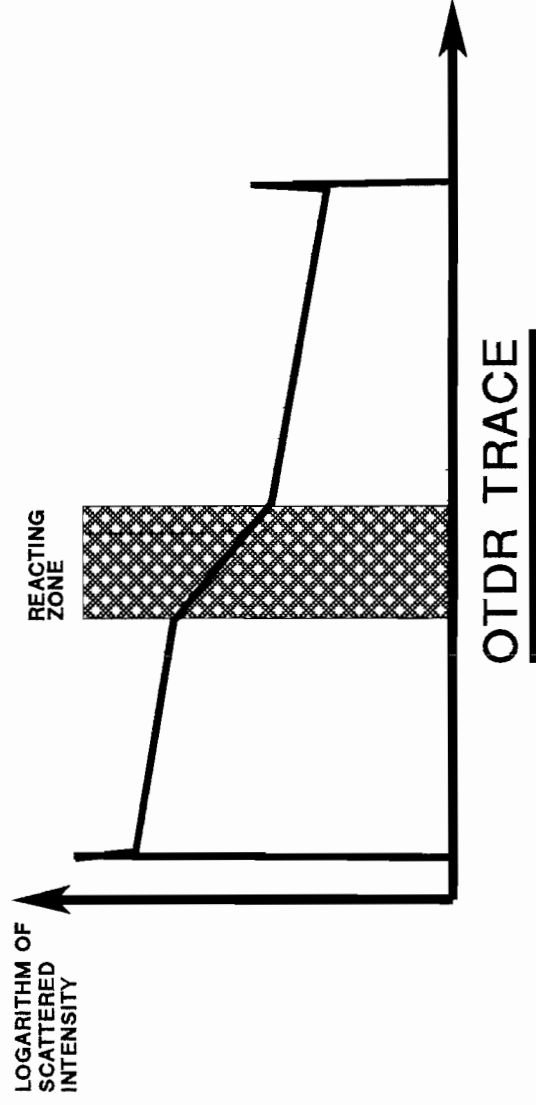
Schematic of Structure of Chemical-Sensing Fibre.
 (Also Shows Variation of Refractive Index and Optical Field Intensity)



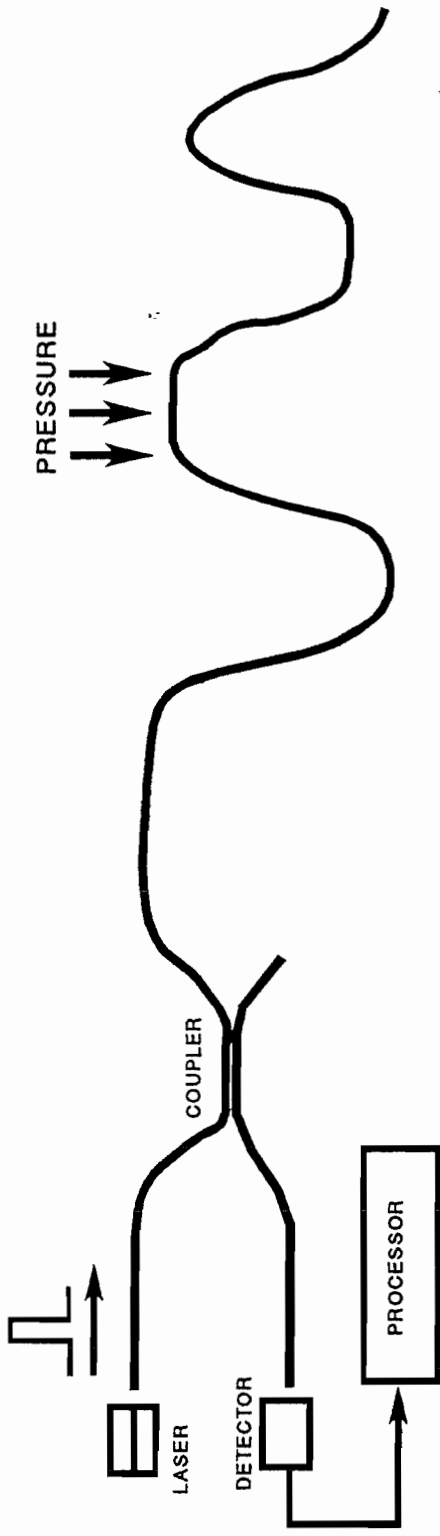
SYSTEM DIAGRAM



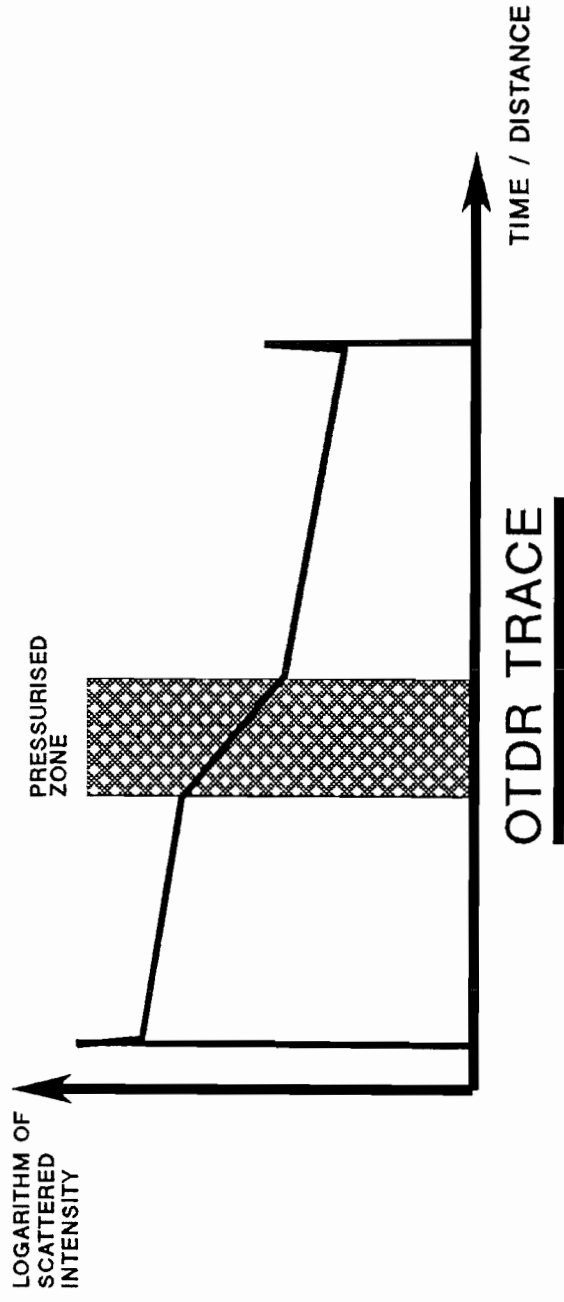
FIBRE SENSOR



CONCEPT OF THE DISTRIBUTED CHEMICAL SENSOR

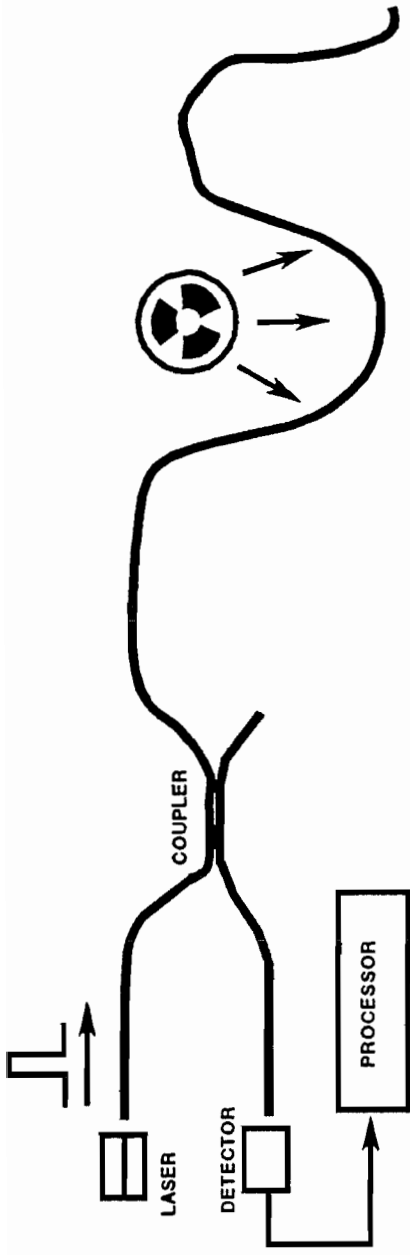


SYSTEM DIAGRAM

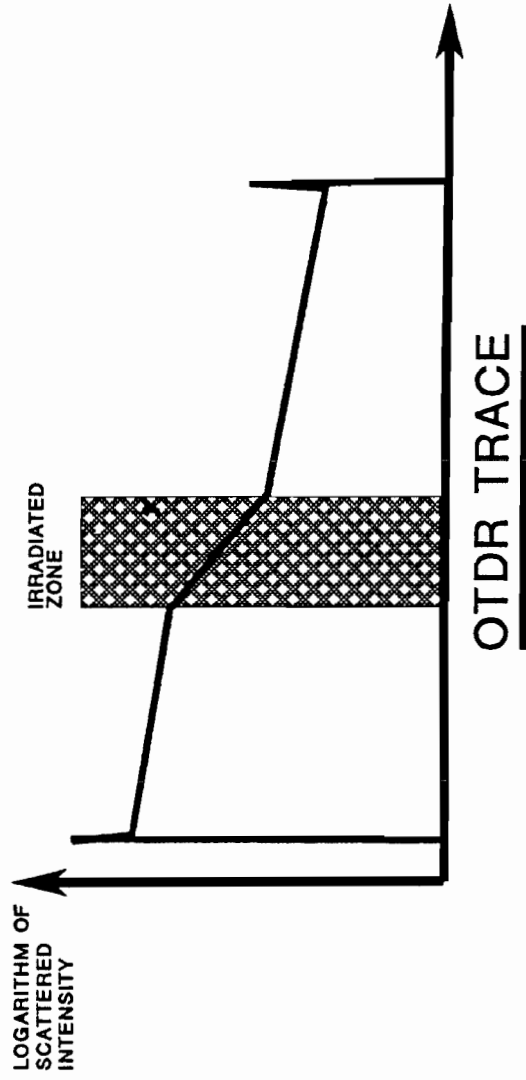


OTDR TRACE

CONCEPT OF DISTRIBUTED SENSING USING A PRESSURE-SENSITIVE CABLE

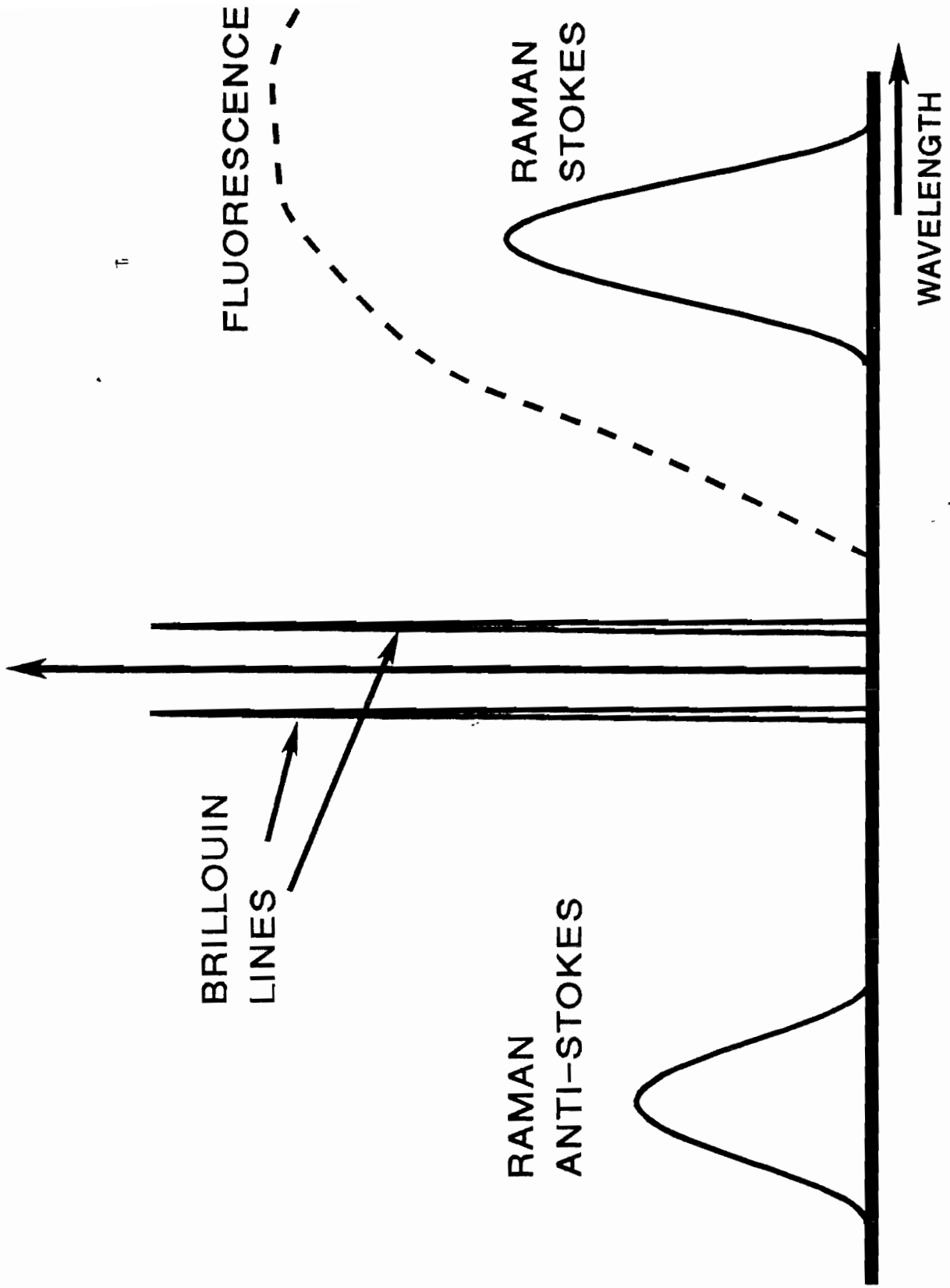


SYSTEM DIAGRAM

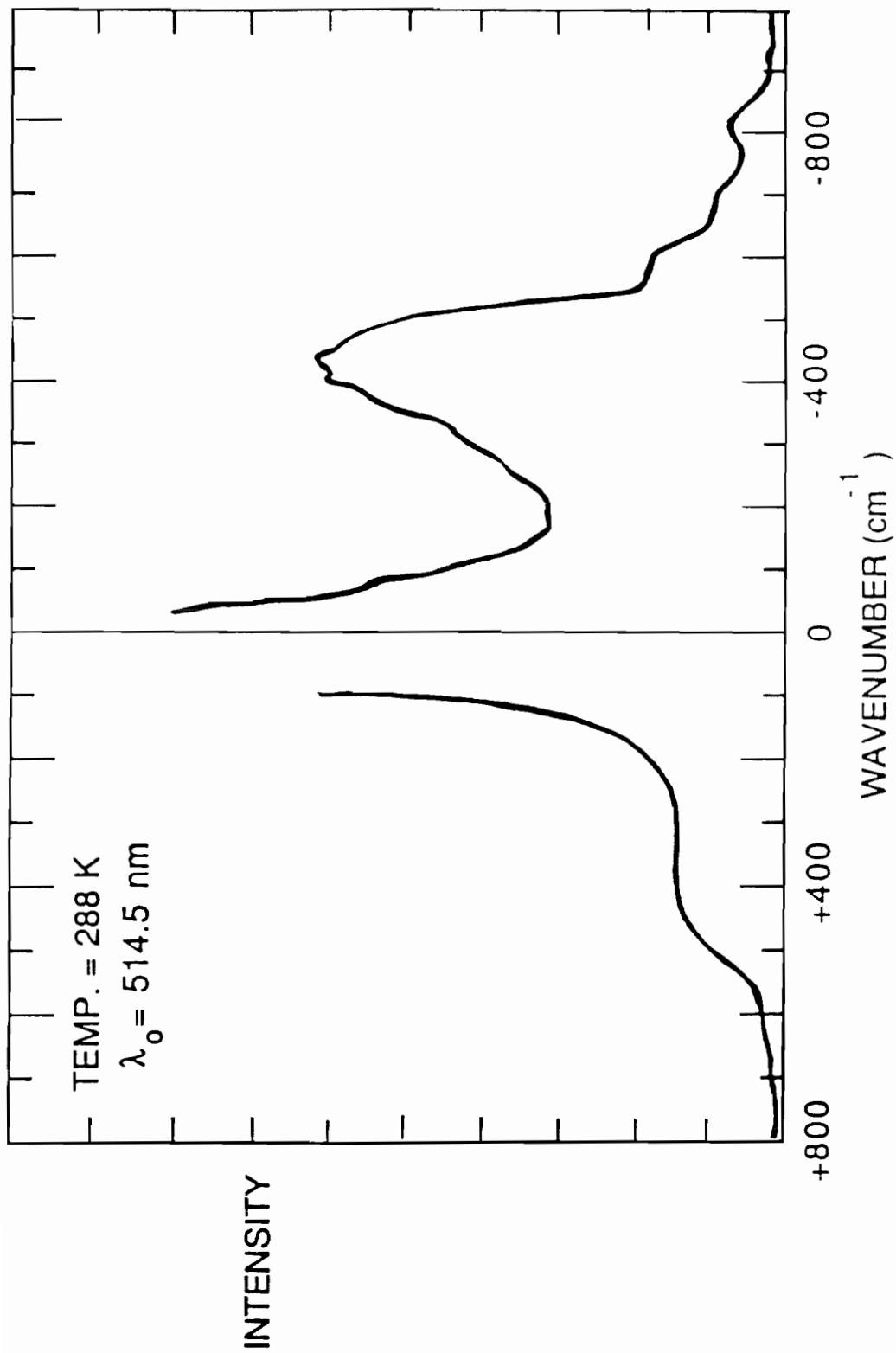


CONCEPT OF THE DISTRIBUTED RADIATION DOSIMETER
 (W. GAEBLER AND D. BRAUNIG 1983)

INCIDENT LASER WAVELENGTH



INELASTIC SCATTERING PHENOMENA USED FOR SENSING



Raman spectrum of germania-doped silica fiber

Ratio of Anti-Stokes and Stokes Backscatter Signals

$$\frac{P_{\text{Anti-Stokes}}}{P_{\text{Stokes}}} = \left[\frac{\lambda_s}{\lambda_{a-s}} \right]^4 \exp(hc\nu/KT)$$

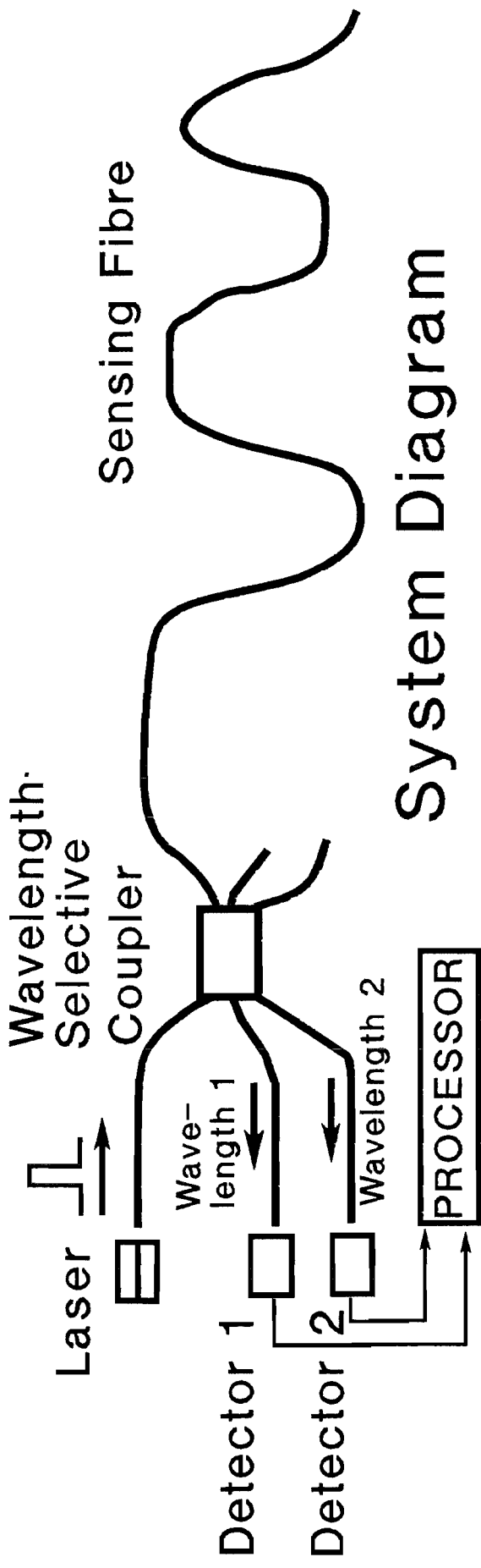
where λ_s , λ_{a-s} and Stokes and Anti-Stokes wavelength

h = Planck's constant, c = velocity of light

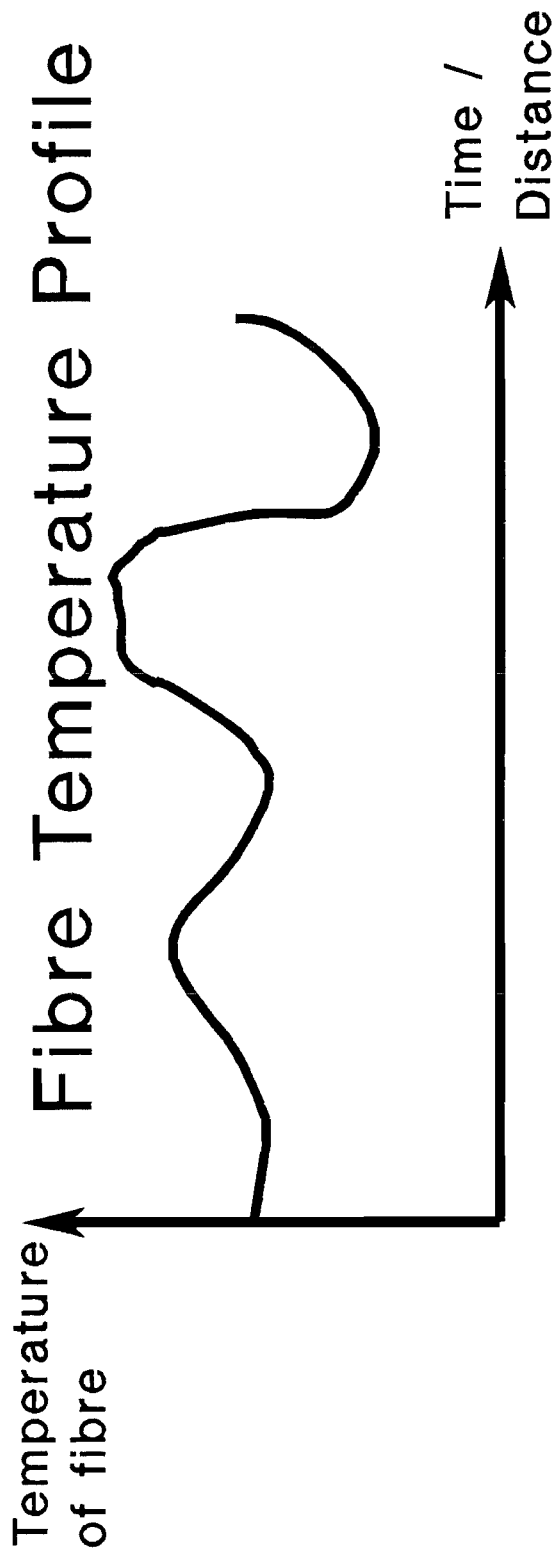
ν = frequency of incident light, K = gas constant

T = absolute temperature

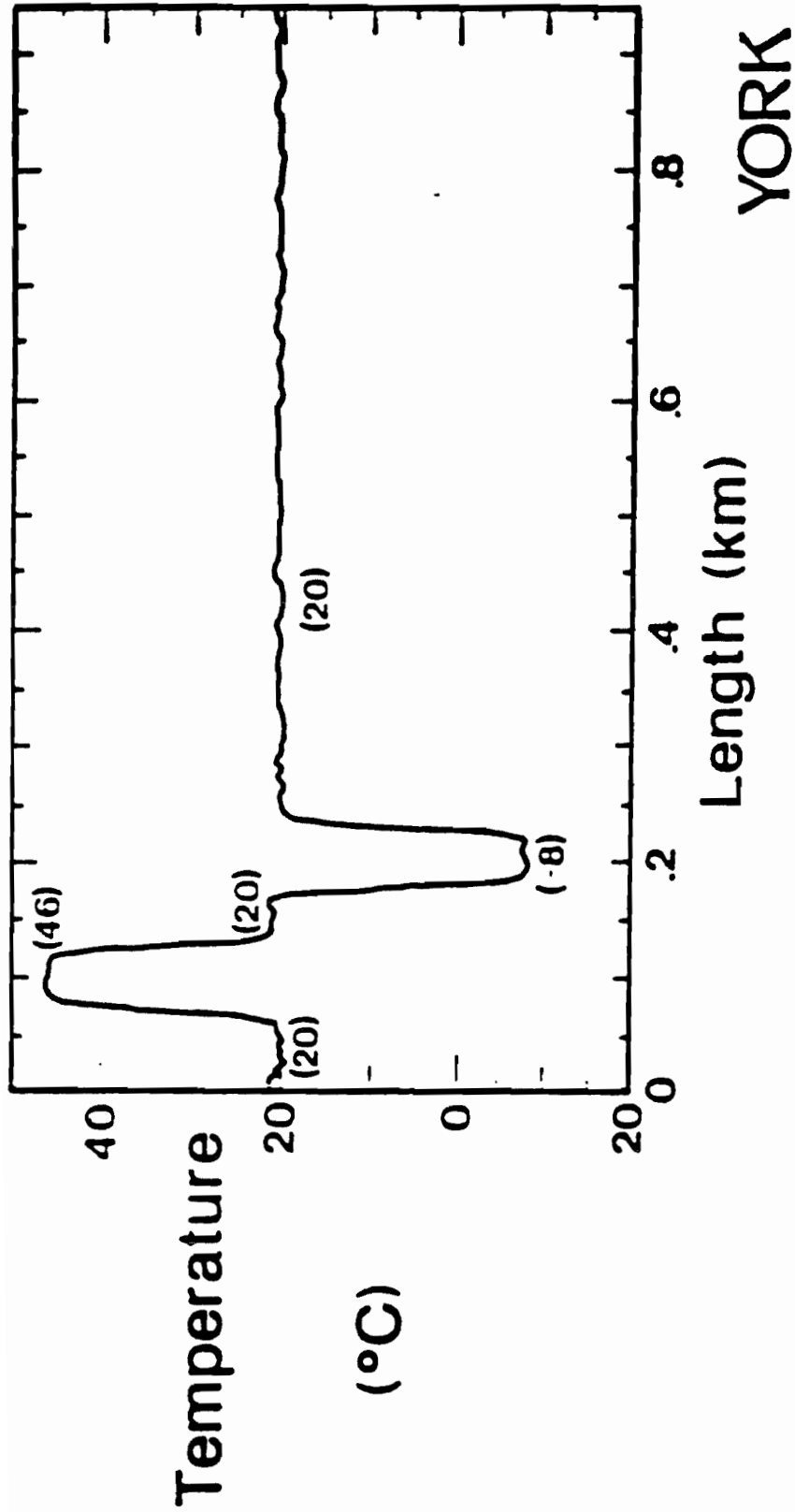
Note: Relationship is independent of the material



System Diagram



Concept of Distributed Temperature Sensing Using Raman Scattering



YORK V.S.O.P.

Plot of the temperature profile over 1km fibre, as measured using an early version of a commercial distributed sensor (Recent developments now enable ranges of up to 10km)

Signal Returns from Backscatter Systems in Optical Fibre

(Return signal variation with time, for energy E , launched into the measurement fibre)

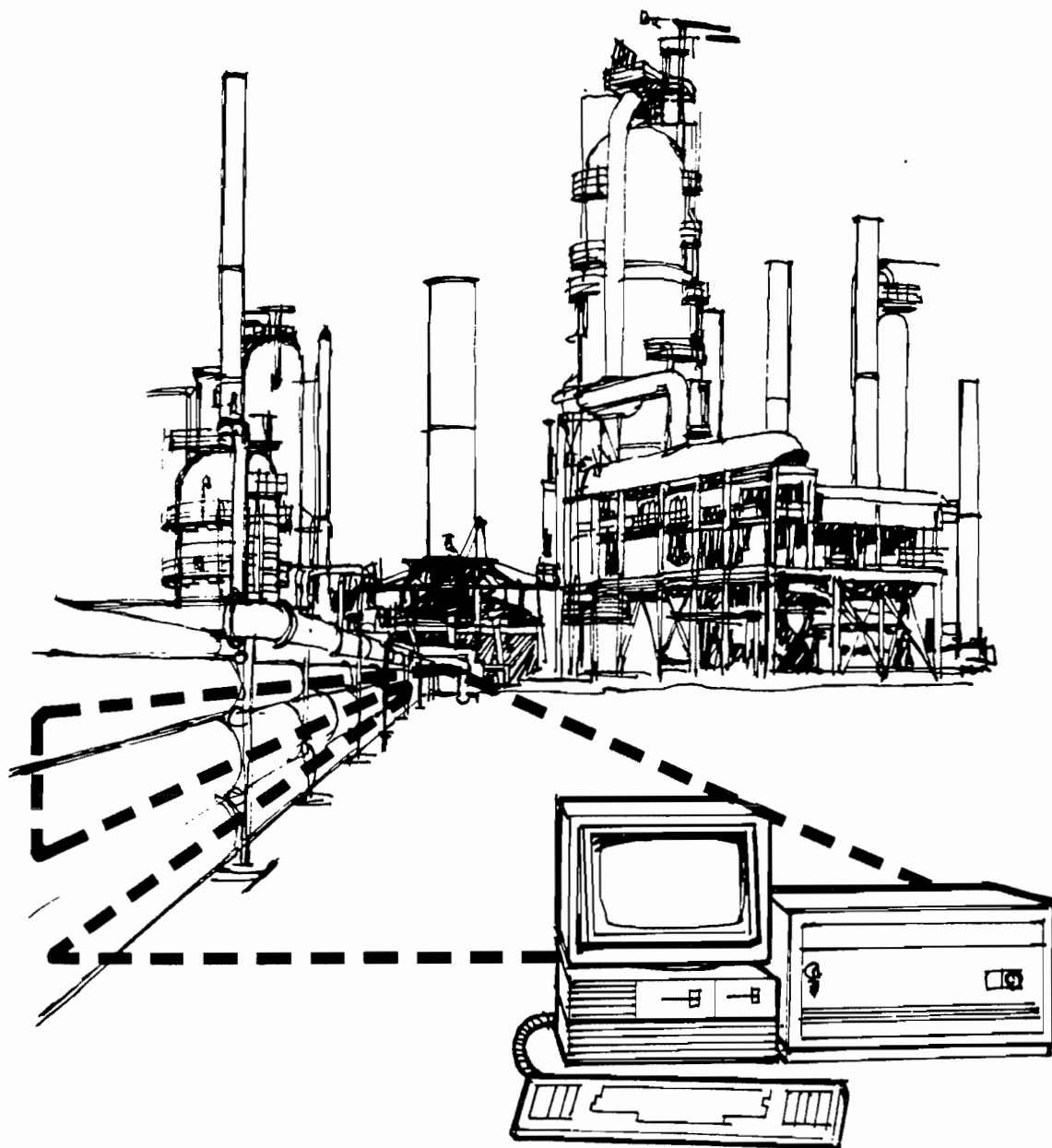
Raman QIDR System:-

$$[P(t)]_{a-s} = [P(z)]_{a-s} = E \cdot S \cdot \eta_{a-s} \alpha(z) \cdot \exp\left[-\int_0^z \alpha(z') dz'\right]$$

$$[P(t)]_s = [P(z)]_s = E \cdot S \cdot \eta_s \alpha(z) \cdot \exp\left[-\int_0^z \alpha(z') dz'\right]$$

$$\text{Ratio, } R(t), = \eta_{a-s} / \eta_s = (\lambda_s / \lambda_{a-s})^4 \cdot \exp(-hc\nu / kT)$$

where η is the quantum efficiency of the Raman process in terms of the ratio of Raman scattered photons to attenuated photons, h is Planck's constant, c is the velocity of light in vacuo, k is the gas constant, λ is the wavelength of the Raman light and ν is the frequency shift from the incident light wavelength. The subscripts $a-s$ and s correspond to anti-Stokes and Stokes Raman light, respectively.



SCHEMATIC ILLUSTRATION OF AN APPLICATION OF
OPTICAL FIBRE DISTRIBUTED TEMPERATURE SENSOR.

● — YORK

APPLICATIONS FOR DTS

DRYER PROFILING

PROCESS CONTROL OVENS

COOLING EFFICIENCY

BUILDING ENERGY MANAGEMENT

MINE SHAFT MONITORING

AIR TEMPERATURE GRADIENTS

FIRE ALARMS

LEAK DETECTION

TRANSFORMER HOTPOINTS

LARGE CHEMICAL REACTORS

FOOD PROCESSING AND STORAGE

GAS AND CHEMICAL STORAGE

PIPELINE TEMPERATURE PROFILES

MACHINERY DIAGNOSTICS

TEMPERATURE STRATIFICATION

TUNNEL MONITORING

OCEAN TEMPERATURE GRADIENT

ROAD SURFACE TEMPERATURE

MOTOR WEAR

LIQUID LEVEL MONITORING

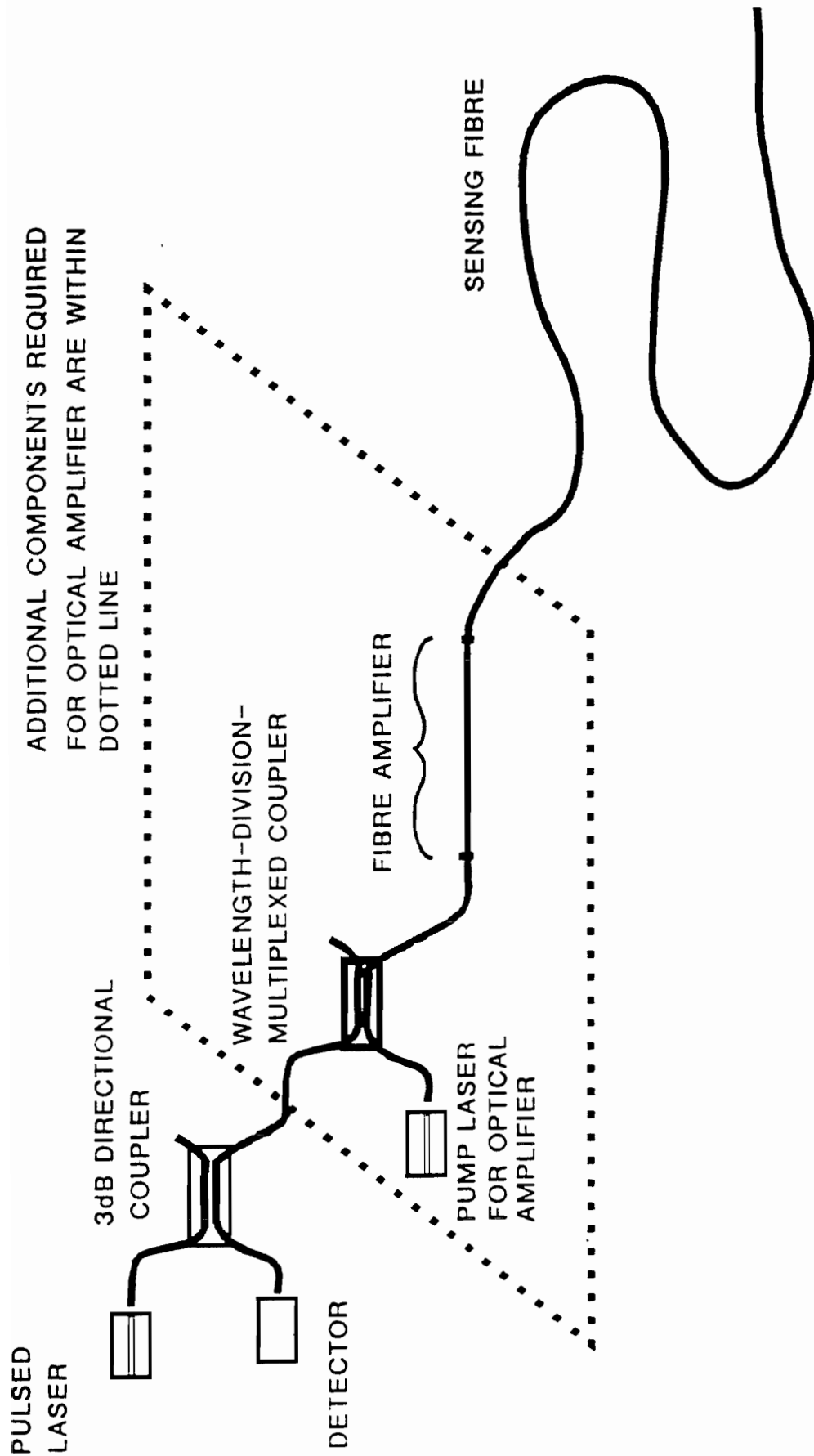
POWER PLANT MONITORING

AIRCRAFT AND SHIPS

OIL MONITORING

Optical Amplifiers in Distributed Sensors

- **Can boost outgoing signal from pulsed laser**
- **Can give signal/noise improvement as optical preamplifier, but only when bandwidth of signal is very high**
- **Advantages are greatest in high-resolution (i.e. high bandwidth) systems**
- **Care must be taken to avoid oscillation (i.e. lasing action)**



Use of optical amplifier to enhance OTDR

BRILLOUIN SCATTERING FOR STRAIN MEASUREMENT

Brillouin frequency shift, f_B is given by: $f_B = \frac{n \cdot V_s}{\lambda}$

n = refractive index, V_s = sound velocity, λ = optical wavelength

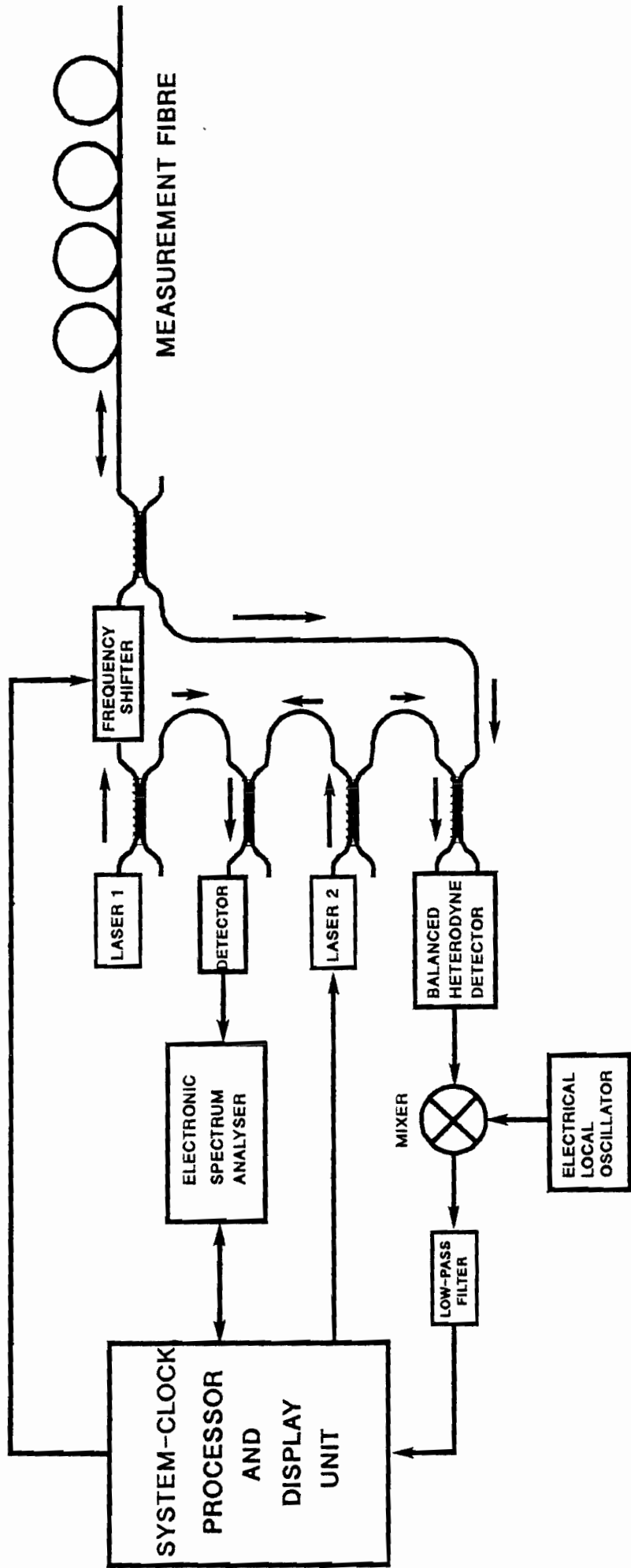
For vitreous silica:-

f_B is of the order of 12 GHz, and varies with temperature and strain with the following coefficients of variation:-

Temperature Coeff = 9.4×10^{-5} per degree K

Pressure Coeff = 4.6 per unit fractional strain

(Reference: Horiguchi et al, Proc O/E Fibers 92, Boston, Sept 1992)



SIMPLIFIED SCHEMATIC OF BRILLOUIN OTDR (BOTDR) SYSTEM OF HORIGUCHI et AL. (PROC "O/E FIBERS", BOSTON 1992.)

THE SYSTEM MIXES THE BACKSCATTERED BRILLOUIN SIGNAL WITH A FREQUENCY-SHIFTED OPTICAL LOCAL OSCILLATOR.

Temperature sensing using ratio of intensities of Rayleigh and Brillouin scattered light (Landau-Placzek ratio)

For a single component glass, the ratio of the Rayleigh scattered light to total Brillouin scattered light is called the Landau-Placzek ratio, R_{l-p} , and is given by:-

$$R_{l-p} = T_f / T (\rho_o v^2 \beta_T - 1)$$

Where ρ_o is the density, v is the acoustic velocity, β is the isothermal compressibility of the melt at the fictive temperature (T_f), and T is the absolute temperature. The fictive temperature is the temperature at which thermodynamic density fluctuations in the glass melt are frozen into the glass (and give rise to Rayleigh scattering)

For multi-component glasses, the equation is of similar form, but the Rayleigh component is increased by compositional fluctuations.

Further Reading

Optical Fiber Sensors Vols I & II (NOW ALSO
Vols III & IV)

Edited by: J.P. Dakin and B. Culshaw. Published by Artech House

Fiber Optic Smart Structures

Edited by: E. Udd. Published by John Wiley & Sons